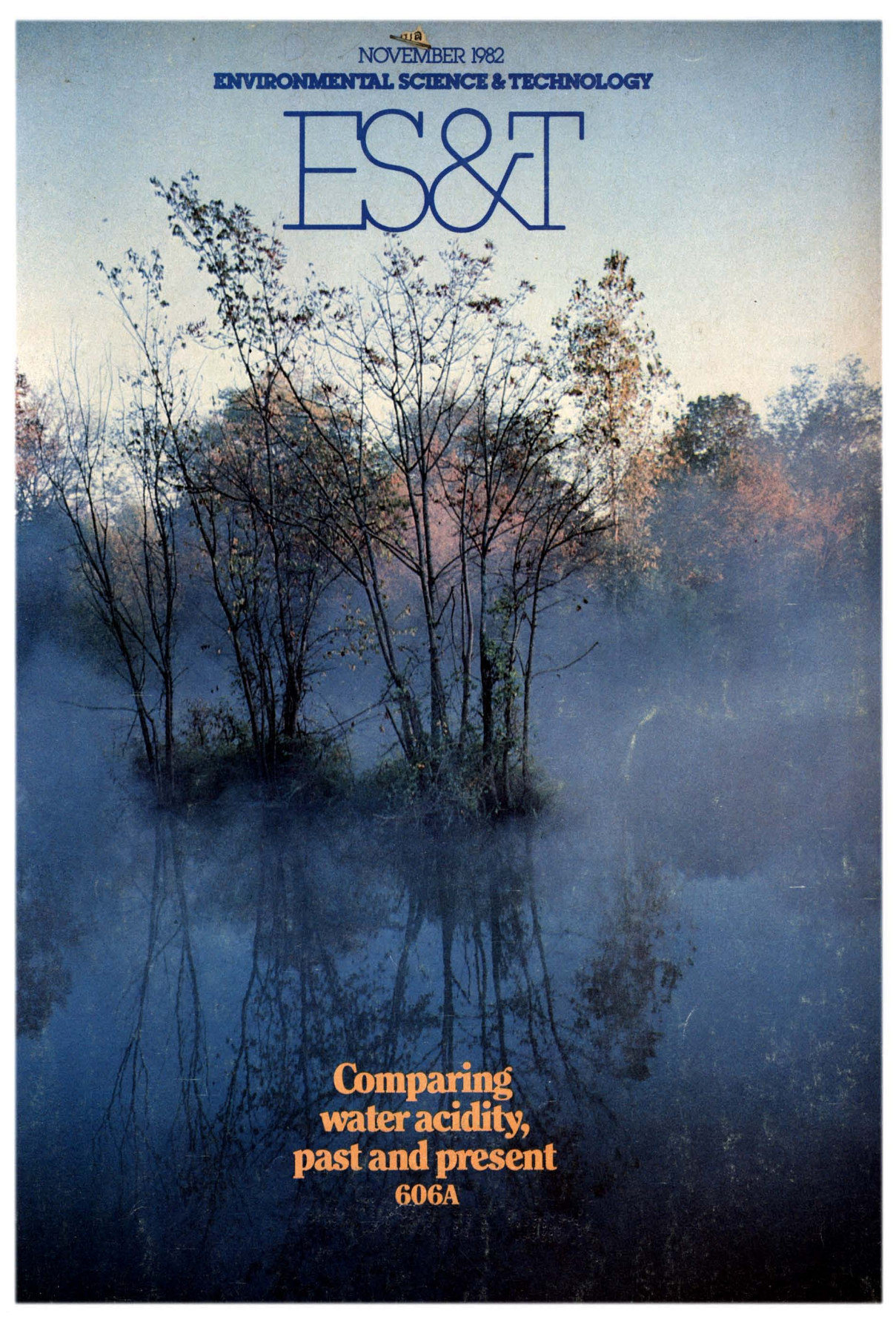




NOVEMBER 1982

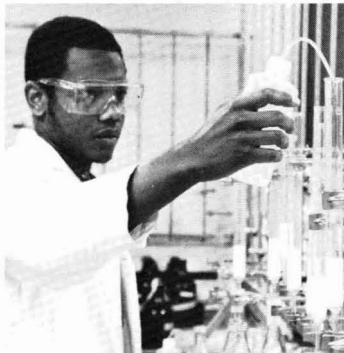
**ENVIRONMENTAL SCIENCE & TECHNOLOGY**

ES&T



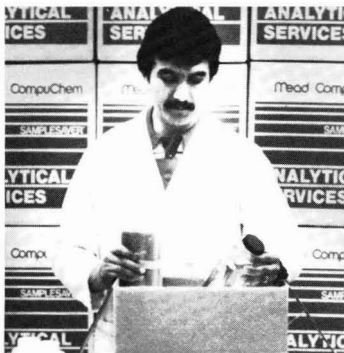
**Comparing  
water acidity,  
past and present**

**606A**



Mead CompuChem<sup>®</sup>, the nation's largest, most experienced gas chromatography/mass spectrometry (GC/MS) laboratory offers you trace level analysis for:

- Hazardous Waste
- Priority Pollutants
- Toxicology
- Organics In Air
- Quality Control
- Product Evaluation



Two laboratories in Research Triangle Park, N.C. and Cary, Illinois (Chicago) provide you with rapid data turnaround and lower cost because of high capacity and specialization.

Organic and inorganic analyses are performed on a variety of matrices and a strict Quality Assurance Program ensures the highest quality data available.

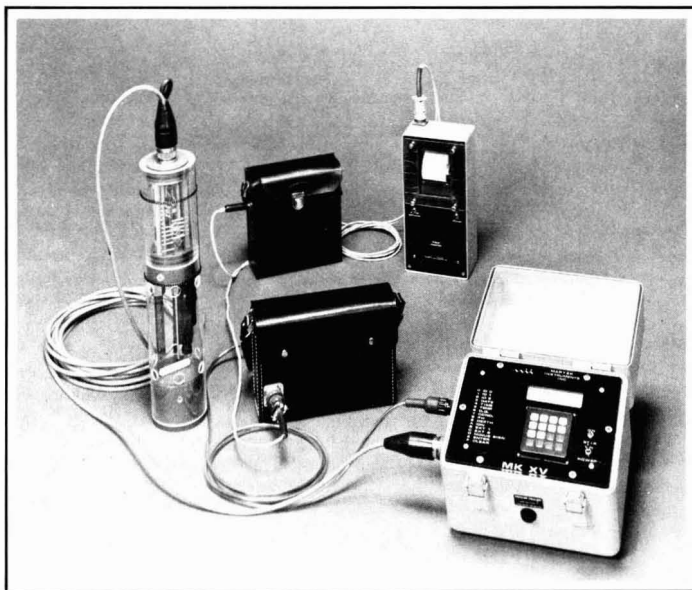


For more information on how we can meet your specific analytical requirements, please call our toll-free number: 1-800-334-8525.

**Mead  
CompuChem<sup>®</sup>**



# Fingertip Convenience . . . Microprocessor Performance



The new Mark XV Water Quality Microprocessor combines the sophistication of digital measurement with the simplicity of rugged field instruments. Designed for direct *in situ* measurement of seven parameters—temperature, salinity or temperature-corrected conductivity, depth, dissolved oxygen, pH, and specific ions—the Mark XV's microprocessor-controlled functions make it the ideal vehicle for operation in remote field environments or in the laboratory.

Housed in a water-tight case, the system's control and readout

module features keyboard data entry and low-power alphanumeric display. Digital calibration and temperature compensation require minimum operator experience and auto-ranging of conductivity simplifies shifting from freshwater to salt-water solutions. The Martek-designed sensors yield laboratory-accurate data.

The Mark XV power pack is external to the readout module and has its own vinyl carrying case with shoulder strap. While the standard configuration is a digital one, an option for onboard cassette data logging or hard-

copy output to the Model AFP Alphanumeric Field Printer is available. The Mark XV is also compatible with computer peripheral equipment.

The combination of easy-to-read digital data, simple operation, and accurate measurement make the Mark XV the microprocessor of choice in water quality monitoring. If you are involved in water quality analysis, whether in lab or field, fresh water or sea water, you owe it to yourself to find out more about the new system from Martek.

ห้องสมุดกรมวิทยาศาสตร์บริการ

๐๘.๑๓.๒๕๒๕



**MARTEK INSTRUMENTS, INC.**

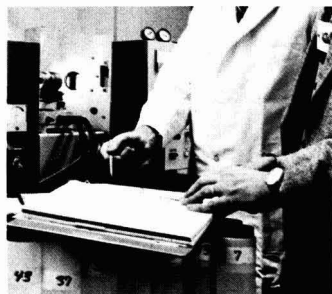
17302 Daimler St. • P.O. Box 16487 • Irvine, CA 92713 • (714) 540-4435 • Telex 692-317

CIRCLE 8 ON READER SERVICE CARD

# ES&T

## CONTENTS

Volume 16, Number 11, November 1982



601A

# Cl<sub>2</sub>

616A

### OUTLOOK

**601A ACS meeting.** Fate of pollutants, analysis of organic air pollutants, and biological modification of wastes—a report on the environmental symposia at the Kansas City meeting in September.

### REGULATORY FOCUS

**605A Managing the environment.** Mike DeLand comments on EPA's new management approach, which involves setting goals and managing programs so as to achieve them.

### FEATURES

**606A Acidification of aquatic systems:** comparing historical water quality data with recent data. James Kramer, McMaster University, Canada, and André Tessier, Université du Québec, Canada

**616A Water chemicals codex.** A compilation of specifications for the purity of chemicals used to treat drinking water. Robert Rehwoldt, National Research Council, Washington, D.C.

### RESEARCH

**735 Binding of DDT to dissolved humic materials.** Charles W. Carter\* and Irwin H. Suffet  
Dialysis techniques are used to present quantitative measurements of the extent of humic material-hydrophobic pollutant binding.

**741 Organic carbon removal by advanced waste water treatment processes.** Foppe B. DeWalle,\* William G. Light, and Edward S. K. Chian

In this study of 14 physical-chemical processes, the largest organic carbon removal was obtained with reverse osmosis at an 85% product water recovery.

**746 Sludge disposal in Southern California basins.** George A. Jackson

A one-dimensional model was developed to project environmental responses to different disposal strategies.

**757 Initial sedimentation of waste particulates discharged from ocean outfalls.** Robert C. Y. Koh

The model presented could be used to assess the environmental consequences of alternate strategies for ocean sludge disposal in Southern California.

#### Environmental Science & Technology

© Copyright 1982 by the American Chemical Society

"Environmental Science & Technology ES&T (ISSN 0013-936X) is published monthly by the American Chemical Society at 1155 16th Street, N.W., Washington, D.C. 20036. Second-class postage paid at Washington, D.C. and at additional mailing offices. POSTMASTER: Send address changes to Membership & Subscription Services, PO Box 3337, Columbus, OH, 43210."

**SUBSCRIPTION PRICES 1982:** Members, \$19 per year; nonmembers (for personal use), \$23 per year; institutions, \$94 per year. Foreign postage, \$8 additional per year/Air freight add \$30; multiple year rates available on request. Single issues \$8.00 for current year; \$9.00 for prior years. Back volumes \$96. Rates above do not apply to nonmember subscribers in Japan, who must enter subscription orders with Maruzen Company Ltd., 3-10 Nihon bashi 2-chome, Chuo-ku, Tokyo 103, Japan. Tel: (03) 272-7211.

**SUBSCRIPTION SERVICE:** Orders for new subscriptions, single issues, back volumes, and microfiche and microform editions should be sent with payment to Office of the Treasurer, Financial Operations, ACS, 1155 16th St., N.W., Washington, D.C. 20036. Phone orders may be placed, using Visa or Master Card, by calling toll free (800) 424-6747 from anywhere in the continental U.S. Changes of address, subscription renewals, claims for missing issues, and inquiries concerning records and accounts should be directed to Manager, Membership and Subscription Services, ACS, P.O. Box 3337, Columbus, Ohio 43210. Changes of address should allow six weeks and be accompanied by old and new addresses and a recent mailing label. Claims for missing issues will not be allowed if loss was due to: insufficient notice of change of address, if claim is dated more than 90 days after the issue date for North American subscribers or more than one year for foreign subscribers, or if the reason given is "missing from files."

The American Chemical Society assumes no responsibility for statements and opinions advanced by contributors to the publication. Views expressed in editorials are those of the author and do not necessarily represent an official position of the society.

Permission of the American Chemical Society is granted for libraries and other users to make reprographic copies for use beyond that permitted by Sections 107 or 108 of the U.S. Copyright Law, provided that, for all articles bearing an article code, the copying organization pay the stated appropriate per-copy fee through the Copyright Clearance Center, Inc., 21 Congress St., Salem, MA 01970. Educational institutions are generally granted permissions to copy upon application to Copyright Administrator, Books & Journals Division, at the ACS Washington address.

Cover: Uniphoto, Washington, D.C.

**Characterization of fluorocarbon-film bags as smog chambers.**

Nelson A. Kelly

Results show that the bags are suitable for sunlight irradiation of urban air without extensive conditioning but are unsuitable for rural air.

771 ■

**Acid precipitation and lake susceptibility in the central Washington Cascades.** Richard M. Logan, John C. Derby, and L. Clint Duncan\*

All of the lakes tested were found to be susceptible but not acidic, with alkalinities ranging from 4 to 190  $\mu\text{equiv/L}$ .

776

**Mineral matter and trace-element vaporization in a laboratory-pulverized coal combustion system.** Richard J. Quann, Matthew Neville, Morteza Janghorbani, Charles A. Mims, and Adel F. Sarofim\*

The composition and size distribution of fly ash produced by burning a Montana lignite at two temperatures were determined.

781

**Analysis of organic vapor emissions near industrial and chemical waste disposal sites.** Edo D. Pellizzari\*

The multipollutant capability of the sorbent cartridge capillary gas chromatography/mass spectrometry/computer-based method is discussed.

785

**Factors affecting the amperometric determination of trace quantities of total residual chlorine in seawater.** George T. F. Wong

This paper examines the problems encountered when applying the "standard method" to samples with lower and lower concentrations.

791

**Chlorination of estuarine water: the occurrence and magnitude of carbon oxidation and its impact on trace-metal transport.** James G. Sanders

Results indicate that the quantity of carbon oxidized is small in comparison to the total complexation capacity of estuarine waters.

796

**Synthesis and analysis of crystalline silica.** Frank H. Chung

The integrated intensities, flush constants, and detection limits for the three forms of crystalline silica are presented.

800

**Persistent organic chemicals in sewage effluents. 2. Quantitative determinations of nonylphenols and nonylphenol ethoxylates by glass capillary gas chromatography.** Euripides Stephanou and Walter Giger\*

The quantitative determinations of these pollutants in secondary effluents of mechanical-biological sewage treatment plants are presented.

805

**Determination of naphtho[2,1,8-*qra*]naphthacene in soots.** Akio Yasuhara,\* Masatoshi Morita, and Keiichiro Fuwa

A strongly carcinogenic PAH, naphtho[2,1,8-*qra*]naphthacene, was detected in soots by GC/MS and HPLC/FLS.

808

**Removal and recovery of arsenious oxide from flue gases. A pilot study of the activated carbon process.** Roger L. Player and Hubert J. Wouterlood\*

Arsenic content of flue gas was reduced by 99.4% without cooling the gas, thereby confirming previous laboratory results.

815

**Development and evaluation of sunlight actinometers.** David Dulin and Theodore Mill\*

The two binary chemical actinometers studied were kinetically well behaved and had quantum yields invariant within 313 to 366 nm.

820

**Entrapment of zinc and other trace elements in a rapidly flushed industrialized harbor.** Scott A. Sinex and George R. Helz\*

This study presents geochemical data on harbor sediments with zinc used as an indicator of where contaminated materials are being deposited.

## NOTES

826

**Mutagenicity of SRC-II coal liquefaction wastewater treatment residues.** Georg Keleti,\* Joseph Bern, Maurice A. Shapiro, William P. Gullledge, and George T. Moore

The Ames *Salmonella* histidine-reversion system was used to determine the mutagenic activity of SRC-II coal liquefaction wastewater treatment residues.

## CORRECTION

830

**Toxaphene Residues in Fish: Identification, Quantification, and Confirmation at Part per Billion Levels.** Michael A. Ribick,\* George R. Dubay, Jimmie D. Petty, David L. Stallings, and Christopher J. Schmitt

\* To whom correspondence should be addressed.

■ This article contains supplementary material in microform. See ordering instructions at end of paper.

## DEPARTMENTS

- 594A Editorial
- 595A Letters
- 597A Currents
- 620A Products
- 625A Literature
- 628A Books
- 629A Meetings
- 630A Classified
- 631A Consulting Services

Editor: Russell F. Christman  
Associate Editor: Charles R. O'Melia  
Associate Editor: John H. Seinfeld

WASHINGTON EDITORIAL STAFF  
Managing Editor: Stanton S. Miller  
Associate Editor: Julian Josephson  
Assistant Editor: Bette Jo Hileman

MANUSCRIPT REVIEWING  
Manager: Katherine I. Biggs  
Associate Editor: Janice L. Fleming  
Assistant Editor: Monica Creamer  
Editorial Assistant: Yvonne D. Curry

MANUSCRIPT EDITING  
Assistant Manager: Mary E. Scanlan  
Staff Editor: James Cooper  
Copy Editor: Gail Mortenson

GRAPHICS AND PRODUCTION  
Production Manager: Leroy L. Corcoran  
Art Director: Alan Kahan  
Artist: Linda Mattingly

Advisory Board: Julian B. Andelman, Kenneth L. Demerjian, William H. Glaze, Robert L. Harris, Jr., Glenn R. Hilst, Michael R. Hoffmann, Roger A. Minear, Francois M. M. Morel, Leonard Newman, R. Rhodes Trussell

Published by the  
AMERICAN CHEMICAL SOCIETY  
1155 16th Street, N.W.  
Washington, D.C. 20036  
(202) 872-4600

BOOKS AND JOURNALS DIVISION  
Director: D. H. Michael Bowen

Head, Journals Department: Charles R. Bertsch  
Head, Production Department: Elmer M. Pusey  
Head, Research and Development Department: Seldon W. Terrant  
Head, Marketing and Sales Department: Claud K. Robinson

Manager, Circulation Development: Cynthia Smith  
Associate, Circulation Development: Mary-Ellen Kirkbride

## ADVERTISING MANAGEMENT

Centcom, Ltd.  
For officers and advertisers, see page 632A. Please send research manuscripts to Manuscript Reviewing, feature manuscripts to Managing Editor. For author's guide and editorial policy, see the January 1982 issue, page 78A, or write Katherine I. Biggs, Manuscript Reviewing Office, *ES&T*. A sample copyright transfer form, which may be copied, appears on the inside back cover of the January 1982 issue.

## GC/MS criteria revisited

In March of 1982 I addressed in this space the editorial problems surrounding proliferation of manuscripts claiming identification of organic chemical structures via GC/MS. In the Letters section of this issue, it is my pleasure to share with you a selection of responses we have received from experts in this field. This problem has been in need of attention, and I am grateful for this exchange of opinion, which should be of great assistance to future users of the *ES&T* Current Research section.

I would first like to comment on several of the issues raised by these respondents, and then outline the editorial position *ES&T* will take on the matter. The March 1982 effort at policy definition was strictly focused on the applicability of GC/MS data *alone* to the problem of structural identification of components of mixtures. In this sense, many of the comments offered by Alford-Stevens, Budde, and Stevens stray from the central point. The editorial addressed the need to classify degrees of confidence in GC/MS data and proposed the use of descriptive terms to reflect degrees of confidence.

As the correspondents argue, other techniques such as LC or GC with alternative detectors are used for mixture component identification. However, with the exception of certain validated standard methods, such as the purge-and-trap technique for chloroform analysis alluded to by Stevens, GC/MS methods are generally accepted as the most definitive available at this time. The proposed terminology to reflect confidence only in GC/MS data seems reasonable, therefore.

Alford-Stevens and Budde point out quite correctly that MS data beyond EI spectra do not always provide additional significant structural information. The proposed policy does not imply that it does, and in this event such data would not warrant employing the "confident assignment" term.

Another point raised by one of the correspondents refers to the use of GC/MS data by nonchemist professionals and raises the question of why we should be concerned about confidence in such data. Surely, it is our unique responsibility in the public use of scientific results to see that the data are reliable and confident. Should public policies regarding the presence of individual chemicals be based on anything other than "confirmed structural assignments"?

I am sensitive to the need to avoid unnecessary reliance on new descriptive terms and the respondents' comments on this are well taken. Of fundamental importance is the need to properly document the level of confidence in structural assignments, and as the respondents note, this responsibility can be shared by authors, reviewers, and editors. It seems most appropriate, therefore, to amend *ES&T*'s guidelines to reviewers and not to adjust the formal editorial policy statement at this time. In addition, I will bring the entire matter before the Editorial Advisory Board at its early 1983 meeting.

*R.F. Christman*

# ES&T LETTERS

## Guidelines

Dear Sir: In response to your March 1982 editorial, "Guidelines for GC/MS identification," we submit the following comments and recommendations. We concur that improved quality control is needed for journal article statements about organic compound identifications. Frequently, authors list organic compounds as "identified" in environmental samples but fail to provide adequate supporting evidence. The problem, however, is not restricted to identifications based on gas chromatography/mass spectrometry (GC/MS). In fact, the widespread application of GC/MS to environmental samples during the past few years has significantly improved the reliability of reported pollutant identifications, many of which previously were based on much less evidence than is routinely acquired now with GC/MS procedures.

Establishing arbitrary quality descriptors (such as tentative, confident, and confirmed) for identifications based on GC/MS data does not adequately address the quality control problem; MS is only one analytical technique used to provide evidence for structural assignments. Quality control is also desirable for identifications based on GC with conventional detectors, high-performance liquid chromatography, GC/Fourier transform infrared spectrometry, and other types of MS data.

The level of confidence associated with an identification varies with several factors, only one of which is the type of MS data obtained. MS data in addition to an electron ionization (EI) spectrum do not always provide a higher level of confidence than EI data alone. For example, the proposed second-level quality category, "confident structure assignment," assumes that a chemical ionization (CI) spectrum or accurate mass measurement (HRMS) will always provide additional structural information. In the case of polycyclic aromatic hydrocarbons having the same empirical formula, neither CIMS nor HRMS would validate a tentative identification based on electron ionization MS data.

We suggest that the best approach to solving the problem is through an improved peer review system. Re-

viewers should be specifically requested to evaluate critically all of the evidence presented to support structural assignments and, for each manuscript, to determine if the author's statements are appropriate. Journal editors should be charged with the responsibility of selecting reviewers competent in the areas of analytical chemistry pertinent to a particular manuscript. When a qualified reviewer thinks that reported identifications are not accompanied by sufficient supporting data, the author would have the option of providing more data or revising statements to describe more accurately the probability of valid identification. The primary concern is not adjective selection but inclusion of supporting data.

If authors are forced to be more careful to document statements about identifications—or not be published—journal article quality will improve. The reader, both now and in the future, must judge the probability of valid identifications, considering the evidence provided in the light of contemporary technology and practice. Setting arbitrary adjective descriptors of confidence now will contribute to confusion in the future, because current criteria will undoubtedly require modification as analytical technology evolves and new techniques are developed.

We hope these comments will be useful and will at least promote further dialogue on this subject.

**Ann Alford-Stevens**, research chemist  
**William L. Budde**, chief  
Advanced Instrumentation Section  
U.S. EPA  
Environmental Monitoring and Support  
Laboratory  
Cincinnati, Ohio 45268

## GC/MS identification

Dear Sir: Your proposed criteria for an identification by GC/MS are good. In essence, the suggestion is that the electron impact and chemical ionization mass spectra and the GC retention time agree with the authentic compound. My only quibble is that the chemical ionization spectrum frequently is not available, either because of instrumental difficulties or, more importantly, the compound simply does not ionize under simple chemical

ionization conditions. Therefore, the insertion of the phrase "where possible" preceding chemical ionization would be a useful caveat.

I think it is also important to stress that an identification by GC/MS should be put in the context of the problem at hand. Is the identification plausible for the situation in which the compound was found? The classic example of this kind of problem is the identification of azulene (an isomer of naphthalene) by the EPA in several drinking water samples. Because of the similarity of the mass spectra and gas chromatographic retention times of azulene and naphthalene, there is no reason to suspect the identification is in error. However, we should ask ourselves: Is the presence of azulene plausible and reasonable in drinking water? Is the absence of naphthalene plausible and reasonable in drinking water? The answer is "no," and we become suspicious of this identification. Therefore, I suggest the addition of such considerations of plausibility and reasonableness to the list of GC/MS identification criteria.

**Ronald A. Hites**, Professor  
Indiana University  
Bloomington, Ind. 47405

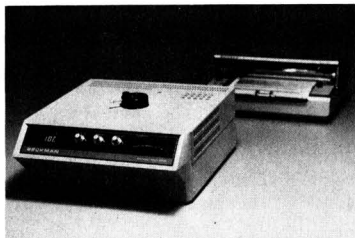
## More on GC/MS identification

Dear Sir: I have reexamined your editorial statement on GC/MS (*ES&T*, Vol. 16, No. 3, 1982, p. 143A) after our conversation in Miami Beach, and I want to document my comments regarding your proposed policy. I fully agree with the need for better documentation of criteria used by an investigator to assign structure to a compound found in an environmental sample. To simply state "confirmed by GC/MS" is far from enough. To this point I support the thrust of your editorial.

I do not believe, however, that *ES&T* should attempt to "cast in bronze" (or concrete) *standardized adjective* descriptions of degree of confidence of structural assignments. I reach this conclusion mainly for the following reasons:

- GC/MS is a powerful tool but not unique in its ability to provide structural information. Will the use of the

## Now You Can Rapidly Assess The Toxicity of Waste Material, Leachate or Effluent Samples.



In minutes, the Microtox™ Toxicity Analyzer can:

- Quantitate the relative toxicity of hazardous waste samples
- Monitor clean-up efficiency at waste or chemical spill sites
- Determine toxicity of leachates from and test well samples surrounding dump sites
- Establish toxicity of industrial and municipal WWTP effluents
- Protect WWTP from toxic shock
- Save time and money by quickly identifying samples which require further analysis

The Microtox™ Toxicity Analyzer provides toxicity information in less than 30 minutes utilizing a simple but highly effective biological test technique. This test is particularly useful for establishing the toxicity of complex samples whose individual components are present in non-toxic levels, but in combination are acutely toxic.

Beckman's rapid test uses a specially selected strain of luminescent bacteria. Upon exposure to toxic material the light output of these bacteria diminish in direct proportion to the concentration of toxicants present. Sensitivity is similar to conventional bioassays, but test results are obtained in minutes, not days. The test procedure is simple, cost effective and reproducible.

Microtox™ users include state environmental and U.S. EPA Labs where applications include hazardous waste monitoring and effluent monitoring.

For more information, including application data specific to hazardous waste materials or effluent monitoring, write: Beckman Instruments, Inc., 6200 El Camino Real, Carlsbad, CA 92008.

**BECKMAN**  
CIRCLE 2 ON READER SERVICE CARD

terms "tentative," "confident," and "confirmed" be allowed to describe degrees of confidence when other techniques are used or other non-GC/MS data are available? Will this lead to confusion?

• Frequently, knowledge of the source of the sample, historical data, physical/chemical characteristics (acid-base solubility, volatility, etc.) of the compound, and other information are available to the analyst to lend considerable credibility to "confirmation" by EI (electron ionization) only data. For example, I don't see any need for CI (chemical ionization) and accurate mass measurements to "confirm" that chloroform is the major peak on a purge-and-trap-generated chromatogram of a chlorine-disinfected drinking water sample when the EI spectrum matches a library reference and the retention time matches the standard. In fact "identification" is routinely accepted from a Hall detector response only.

• Singling out GC/MS (as opposed to other methods) for establishing standardized definitions of reliability of structural assignments may reduce the confidence of nonchemist professionals (lawyers or engineers) in GC/MS results reported and interpreted by competent analytical chemists. Will these individuals accept anything other than "confirmed" in the future?

• The degree of confidence of assignment is related to the subject compound, not just the combination of analytical procedures used. For example, I might have more confidence in an assignment for benzene from a purge-and-trap GC analysis with accompanying EI data only ("tentative") than I would for a specific alkyl-PAH isomer when given all of the data required for "confirmed" status. CI and accurate mass measurements do not necessarily give more structural information than EI spectra, especially when isomers are involved.

I believe that *ES&T* should require complete documentation of procedures leading to data that support a structural assignment but should leave it to the author, reviewers, and the readers to decide upon the appropriateness of the adjective description of degree of confidence of structural assignment. This is consistent with good scientific reporting procedures, allowing for peer acceptance or rejection of conclusions derived from the data presented. A special nomenclature for GC/MS is not needed.

Alan A. Stevens  
Cincinnati, Ohio

Note: See the editorial on page 594A of this issue for the editor's response to the preceding letters.

### Air pollutant baselines from glacial studies

Dear Sir: I appreciate the opportunity to comment on the excellent article by Julian Josephson entitled "Air pollutant baselines from glacial studies," (*ES&T*, Vol. 16, No. 8, 1982, p. 437A). The article was well researched, well written, and informative. I am particularly pleased that you published an article on the importance of baseline pollutant measurements. I feel these studies are extremely valuable, yet it can be difficult to get funding for them because of the perceived long pay-back time.

I have been doing research on pollutant levels in remote wilderness areas (U.S. National Parks) for six years now. Dr. Cliff Davidson has collaborated with me on these studies. Based on this experience, I have a few specific comments to make on the article:

• We feel baseline studies should also be carried out in nonglacial sites.

• We also ran into the problem of melt/freeze on glaciers in Olympic National Park. The problem precludes any significant coring. However, surface snow samples seemed to indicate significant trace element contamination. But, enrichment factors—calculated from soil samples taken on the lateral moraine—indicate that virtually all the detected "contamination" was merely resuspended material from the surrounding area.

• I was particularly interested in the difficulties of obtaining uncontaminated samples from glacier ice. We have faced this same problem in setting well points in remote valleys. We finally have had some success with a hand-powered, pneumatic drill rig. The drilling depth is, of course, limited to ~30–40 ft.

• Finally, I found the discussion of Patterson's work very interesting. Our air data from Olympic National Park showed average lead concentrations of 2 ng/m<sup>3</sup> of air. Based on enrichment factor calculations, using both average crustal values or measured values from park soils, we estimated that this lead level, as low as it is, is 125 to 150 times higher than could be expected from natural crustal/soil sources.

G. B. Wiersma, Manager  
Earth & Life Sciences  
EG&G  
Idaho Falls, Idaho 83415



# ES&T CURRENTS

## INTERNATIONAL

**Environment Canada, the Canadian equivalent of EPA, claims that EPA did not have enough information to conclude in its report that Love Canal is no longer a threat to the Niagara River.** Love Canal may now be contaminating or will in the future contaminate the bedrock aquifer that feeds into the Niagara River, the Canadian agency commented. It also criticized one of the report's main conclusions—that there is no statistical difference between levels of contaminants in the "declaration zone" of the Love Canal area and other sites in the Niagara River area. More control samples were needed to establish this conclusively, Environment Canada said.

**What is reputed to be the largest commercial solar-powered steam production system** has started up at the Tapud food processing plant at Sha'ar Hanegev, Israel. Developed by Luz International Company (Jerusalem), the system uses parabolic solar collectors to generate about 2.5 MW of power. Luz claims that under the right conditions, its solar energy system might replace up to 20% of Israel's industrial consumption of energy from other sources.

## WASHINGTON

**According to an interim report prepared by the Office of Technology Assessment,** sulfate particulate air pollution may have caused 51 000 deaths in the U.S. and Canada in 1980, and, if emissions remain constant, 57 000 deaths could result annually by the end of the century. A 30% reduction in SO<sub>2</sub> emissions could reduce the deaths to 40 000 a year. The health-damage function used to derive these estimates was essentially a compilation of expert opinion about the relationship between sulfate pollution and prema-

ture mortality such as that which results when sulfate pollution aggravates preexisting respiratory or cardiac problems. Sulfate pollution resulting from SO<sub>2</sub> emissions is one of the primary causes of acid rain.



*Ocean disposal banned*

**A two-year ban on the disposal of low-level nuclear wastes in the oceans** was approved by the House. At the end of the two-year period, a comprehensive environmental assessment would be required before a permit for ocean disposal of such wastes could be issued. This bill was opposed by the Reagan Administration, which would like to use the ocean for disposal of low-level wastes such as outdated nuclear submarines and contaminated soil. Since 1970, no radioactive wastes have been dumped in the ocean. The bill also imposes new demands on EPA for the ocean dumping of nonradioactive wastes. EPA would be required to perform detailed analyses on proposed ocean disposal sites and to monitor these sites.

**Boilers that burn hazardous waste as a fuel** (at an average combustion efficiency of 97%) emit 1.2 million tons of hazardous emissions annually in contrast to regulated boilers (99.99% combustion efficiency), which emit 4000 tons annually.

Boilers that burn hazardous waste as a fuel are not regulated by the Resource Conservation and Recovery Act. Consequently, about 68% of the U.S. population, 147 million people, is exposed to potentially hazardous emissions. These conclusions were reached in a new report prepared by Fred C. Hart Associates, Inc. The study recommended that the existing regulatory loophole be closed.

**Any development near a national park, either on private or public lands,** that might harm the park's environment must be identified by the Department of the Interior, according to a bill passed by the House. Findings of environmental threats would also have to be reported to other federal agencies having any jurisdiction over the development. Almost as many Republicans as Democrats sponsored the bill. It does not increase the Interior secretary's authority to block mineral or industrial development near national parks, but it does ensure that Congress and appropriate agencies are notified of any possible threat to the parks.

**House-Senate conferees rejected the Reagan Administration's EPA budget proposal** for fiscal year 1983 and increased EPA funding in several areas. Salaries and expenses were increased \$10.5 million, research and development \$10 million, abatement, control, and compliance \$58 million, and construction grants \$30 million. Only the Superfund program was funded at a level less than the Administration's proposal. It was decreased by \$20 million.

**The Reagan Administration is encouraging localities to scale back sewage treatment plants,** according to a General Accounting Office study. This cutback would increase the flow of organic pollutants into rivers and coastal waters. The study states that EPA expects to

receive as many as 800 applications to permit the discharge of incompletely treated sewage. Municipalities are allowed to seek exemptions enabling them to remove as little as 25% of the biological material from sewage. Previous Administrations required 85% removal. If the permits are granted, they will save \$4-10 billion in construction and operating costs. The Reagan Administration is requiring secondary sewage treatment facilities only when the partially treated sewage causes the pollution level of the water to grow higher than the standard set in the Clean Water Act.

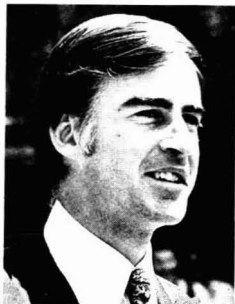
## STATES

**Three more nuclear reactors have been canceled by the Tennessee Valley Authority.** This is nearly one-fourth of what was planned to be the nation's largest nuclear power system. The reactor at the Phipps Bend plant site in northeast Tennessee and two of the four units at the Hartsville site near Nashville, Tenn., will be abandoned. Thus far, \$1.85 billion has been spent on the unfinished reactors. The loss will be written off over 10 years.

**The Clinch River breeder reactor at Oak Ridge, Tenn., could cost about \$8 billion** in contrast to the Energy Department's estimate of \$3.2 billion, a study prepared by the General Accounting Office (GAO) has concluded. The report claims that the Energy Department used false assumptions involving fuel costs and construction expenses when preparing its estimates. Energy Department officials strongly disputed the GAO cost analysis, saying they believed that cost factors not usually considered in government-financed research and development projects have been included. The Clinch River breeder reactor was almost halted by a Senate vote recently. By a vote of 48-49 the Senate failed to cut off funds for the reactor. Experts estimate that breeders will not be economical until the year 2030 or beyond.

**The nation's largest estuary, the Chesapeake Bay, is slowly deteriorating** from pollutants, according to an EPA report. Many aquatic grasses necessary at the end of the estuary's food chain have disappeared and certain freshwater fish have declined. Canvasback, red-

head, and goldeneye ducks have also decreased in number. DDT, fertilizers, and farmland sediment as well as heavy metals and other toxic materials have been added to the bay. Fertilizers cause excessive algae growth that removes oxygen from the water.



*Brown: Long-term health insurance*

**California Gov. Edmund G. Brown, Jr., proposed a statewide ban on land disposal of highly toxic chemical wastes.** If adopted, the landfill restrictions will be phased in over a two-year period, beginning in March 1983, and will make California the first state in the nation to ban land disposal of hazardous wastes. Wastes to be prohibited from landfills include cyanides, toxic metals, strong acids, PCBs, halogenated compounds, and all other wastes that the state classifies as "extremely hazardous." In announcing the proposed rules, Brown said, "These regulations are long-term health insurance for every person in California." Senator Gary Hart of Colorado has proposed national legislation similar to California's toxic waste program.

## SCIENCE

**A simple, inexpensive way to split water into hydrogen and oxygen** by using energy from sunlight has been discovered by researchers at the University of California's Lawrence Berkeley Laboratory. Iron oxide, one of the most abundant compounds in the earth's crust, is used as a catalyst for the reaction, which is carried out at room temperature under very simple conditions with no external source of electricity required. Previous methods have required expensive materials and extreme conditions. Iron oxide is formed into polycrystalline pressed discs, with silicon added to one disc to produce an anode and magnesium added to the other to

produce a cathode. The discs are connected with a wire, and the assembly is immersed in a water solution of sodium sulfate. When illuminated with visible light, a photocurrent is produced and hydrogen is generated.

**A continuous means of collecting and analyzing air samples for hydrocarbons** is a better approach than that of collecting air samples in containers for future laboratory analysis, according to Radian Corporation (Austin, Tex.). The company says that its 110A computer-controlled dual gas chromatograph (GC) monitoring system makes possible the continuous sampling, analysis, and hourly reporting of up to 38 hydrocarbon compounds containing from two to nine carbon atoms. One of the approaches enabling capture and concentration of the compounds—usually at parts-per-billion concentrations—is a multicomponent sorbent trap with provision for atmospheric moisture exclusion.

**Can mutagenic biodegradation products be formed from crude oil?** Apparently yes, say Sumner Morrison and Bruce Cummings of Colorado State University in a report prepared for EPA (Corvallis, Ore.). They tested Alaska crude with naturally occurring freshwater microbes. Prior to the tests, the crude showed no mutagenic activity. After microbe incubation and testing, base-pair substitution and frameshifts were found, seemingly causing reductions in viable numbers of bacteria in test strains of *Escherichia coli* K-12. Mutagenic activity was at its high after one week's microbial growth at 20 °C or 3-4 weeks' growth at 4 °C. Mutagenesis appeared in biologically degraded whole crude, but not in fractions of the oil.

**The chemical composition of groundwater influences its ability to transport plutonium**, according to Jess Cleveland et al. of the U.S. Geological Survey (USGS, Lakewood, Colo.). Plutonium is least soluble and, therefore, least transportable in shale groundwater; this water has high sulfate, but low fluoride, concentrations. Cleveland told the Kansas City ACS Meeting. On the other hand, in a basalt groundwater sample, with high fluoride levels, plutonium was completely soluble. Fluid from tuff and granite, with intermediate fluoride

concentrations, had intermediate solubility effects. Enhanced solubility might be attributed to fluorine complex formation with plutonium, whereas sulfates may form colloidal species.

**A giant "yo-yo" is being used by scientists from Harvard University** to measure atomic oxygen in the stratosphere, and from these measurements to determine ozone levels. In the first test of this equipment, a large balloon, 100 times the size of a Goodyear blimp, was elevated to a height of about 200 miles over Texas. A capsule of instruments was lowered seven and a half miles and hauled back up again, while the instruments made continuous measurements. A special, very light, synthetic line, which is 10 times stronger than steel, was used to lower and raise the capsule.

## TECHNOLOGY

**Recovery of 99,999% of silver from liquid photographic wastes** may be possible with a process developed at Oak Ridge National Laboratory (ORNL, Oak Ridge, Tenn.). The silver-bearing effluent is pumped into a vessel containing excess hypochlorite. Under careful pH control, thiosulfate is oxidized in the reaction vessel with the effluent; this results in precipitation of silver chloride. Sodium dithionate is then added to convert silver chloride to metallic silver. Under Tennessee law, silver ions in effluent are limited to 0.05 mg/L. On a pilot-plant basis, ORNL recovers about 400 g of silver from each 550 L of photographic or photocopier wastes.

**Conversion of cellulose to 200-proof ethanol**, sellable at under 70¢/gal wholesale, is said to be possible by Power Alcohol Inc. (Upper Montclair, N.J.). The company says that any cellulosic feedstock—sawdust, corn cobs, municipal waste fractions—can be converted to glucose, and that conversion and extraction of the glucose for subsequent fermentation to ethanol can be done in less than one hour. Apparently, breakup of cellulose to glucose is greatly accelerated by a calcium chloride catalyst. This process is exothermic, according to the firm, which estimates that one ton of waste cellulose should yield about 360 gal of 200-proof ethanol and 1000 lb of carbon dioxide.

**An alternative SO<sub>x</sub>/NO<sub>x</sub> removal approach** could consist of using ozone, along with various alkenes. For instance, propene, ozone, and water vapor together with SO<sub>2</sub> form "Criegee intermediates" that combine almost immediately with the SO<sub>2</sub>, according to the National Bureau of Standards, patentee of the process. As a "bonus," NO<sub>x</sub> is removed in secondary reactions. End products are sulfuric and nitric acid mists that are recoverable, for example, as commercial fertilizer feedstocks. Another product is a recoverable or combustible sulfur-free organic compound. NBS researchers caution that certain unknowns should be resolved before there is any attempt to commercialize the process.

**Standardization in computer models for evaluating movement of chemicals in the environment** after a spillage is the task of the American Society for Testing and Materials (ASTM) Committee E-47 on Biological Effects and Chemical Fate. The ASTM committee has joined with EPA to write a standard that would establish minimum requirements for acceptable models. Charles Coutant of Oak Ridge National Laboratory notes that the group is dealing only with *standard evaluation procedures* for the models, not with development of the models themselves. Criteria for development and use of models to integrate knowledge of partitioning, transformation, and transport used in chemical risk assessment are covered.

## INDUSTRY

**Workers are being injured at non-hazardous waste management facilities** and the environment is threatened because present EPA rules allow industries producing up to 1.1 ton/month of hazardous wastes to hide such wastes in containers of regular trash. So says Charles Johnson, technical director of the National Solid Wastes Management Association. He noted that a waste-to-energy plant in a major U.S. city blew up because small quantities of hazardous wastes were included among conventional trash. Johnson also mentioned other instances of fires and of workers being burned by chemicals. He called for eliminating provisions of the law exempting small quantities of hazardous wastes

from normally required waste management procedures.

**Use of up to 3% methanol in unleaded "gas"** either alone or together with other alcohols has been recommended to EPA by the Du Pont Company. Du Pont's director of methanol products, R. A. Darby, said that tests demonstrate methanol blends of 3% cause no emissions problems, nor do they affect conventional vehicle driveability or components. He noted that in Europe, gasoline/methanol blends continue to gain acceptance and now account for about 20% of the West German market, for example. Darby added that by the 1990s, either methanol blends or methanol itself could power a significant portion of the U.S. automobile fleet.

**Regulatory impact analysis must normally play a role in the issuance** of certain classes of federal regulations, says President Reagan's Executive Order 12 291 of February 1982. The aim is to select options that offer the greatest benefits at the least societal costs, René Zentner of Shell Oil Company points out. He stated the Chemical Manufacturers Association's (CMA) position that these analyses should not try to place a dollar value on life, health effects, and aesthetics, since this would be undesirable and unacceptable to society. Rather, CMA calls for the use of quantitative risk assessments as a basis for issuing regulations, as well as peer review of scientific data and their interpretations.

**How many compounds will emerge from chemical obscurity to reach registered pesticide status?** In 1977, the number was about one in 12 000; by 1997, that figure will probably be one in 80 000, said Jack Plimmer of the U.S. Department of Agriculture at the ACS Kansas City meeting. Over the short term, pesticide scientists and manufacturers will have to come up with more efficient ways to screen old and new pesticide components, he noted. But in the future, the industry will probably have to concentrate on learning how chemicals control insect behavior, development, and reproduction, and on tailoring compounds that interfere with insect life functions, Plimmer predicted. He added that knowledge of insect genetic codes is extremely important.

**The project may be over, but  
your responsibility still continues.**

**The Professional Liability Plan  
for Chemists helps you meet  
that responsibility.**

No matter how carefully you perform your professional duties, things can — and sometimes do — go wrong . . . exposing you to the possibility of legal action.

The Professional Liability Plan, sponsored by the Board of Trustees, Group Insurance Plans for ACS Members, can help provide the financial backing you would need to defend your reputation as a chemist. The plan offers ACS members and non-members alike up to \$1,000,000 of coverage. It covers claims that occur while your policy is in force — regardless of when first reported — whether you are acting as an industrial chemist, a teacher, or a consultant. To receive a plan brochure, which includes a rate chart, and an application, mail in the coupon or call American Professional Agency, Inc. collect at (516) 691-6400.

**American Professional Agency, Inc.  
Administrator  
Professional Liability Plan  
95 Broadway  
Amityville, NY 11701**

Send me information on the Professional Liability Plan sponsored by the Board of Trustees, Group Insurance Plans for ACS Members.

Name \_\_\_\_\_

Street \_\_\_\_\_

City \_\_\_\_\_

State \_\_\_\_\_ Zip \_\_\_\_\_

82179

Underwritten by:

National Union Fire Insurance Company  
of Pittsburgh, PA



A Member Company of  
American International Group

CIRCLE 4 ON READER SERVICE CARD

## Report from the fall ACS meeting

Five symposia at the Kansas City meeting addressed the environmental chemistry related to pressing problems. Symposia topics included:

- the environmental fate of anthropogenic organic pollutants;
- the identification and analysis of organic pollutants in air;
- processes for the biological modification of wastes;
- safety and health considerations at hazardous waste sites; and
- chlorinated dioxins and dibenzofurans in the environment.

This report describes the first three symposia.

### Fate of pollutants

Fugacity works. In a session on the environmental fates of anthropogenic organic pollutants, Donald Mackay and A. Bobra of the University of Toronto reported on a study in which they designed, constructed, and operated a completely controlled microecosystem of air, water, soil, sediment, and biota. They introduced a pulse of toxic substance into the system and measured the kinetics and "relaxation" toward equilibrium distribution. These microcosms were maintained in the dark under nearly bacteria-free conditions at 20° C and allowed to come to equilibrium for 96 h before a compound was introduced into the system. Samples from the microcosm were analyzed by gas or liquid chromatography. The correspondence between the experimental and calculated data was judged to be satisfactory, thus lending support to the use of the fugacity modeling approach for predicting the environmental behavior of chemicals.

Michael R. Hoffmann and Marianna Plastourgou of Caltech recently developed a simple, mass transport model to predict the relative degree of hydrolysis of parathion in a two-layered flow system. Trace metal cat-

alysts are present in one layer and a reactant (such as parathion) is present in the other density-stratified layer. This simplified model for interdiffusion provides a useful starting point for more elaborate models of transport with chemical reaction in a layered flow system.

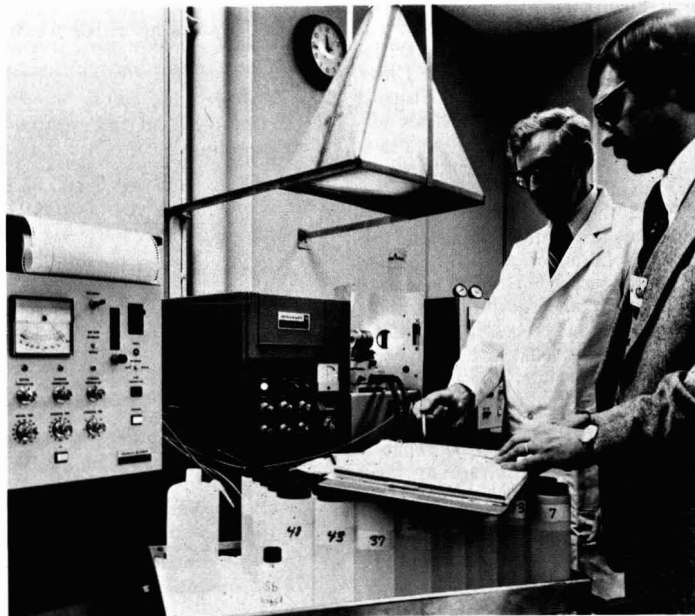
For many years, sediments were considered to be permanent sinks for hydrophobic pollutants of low water solubility, polychlorinated biphenyls (PCBs), for example. However, Steven J. Eisenreich and colleagues at the University of Minnesota presented recent data suggesting biotic recycling and sediment resuspension.

The transport and fate of high molecular weight organics in the atmosphere is, to a large extent, controlled by volatility. Terry F. Bidleman and

W. Neil Billings of the University of South Carolina summarized five years of research on the atmospheric transport and removal of chlorinated pesticides and PCBs in continental, coastal, and open-ocean environments.

### Hazardous materials in fish

Since 1974, the Environmental Research Laboratory in Duluth, Minn., has been involved in gas chromatography/mass spectrometry (GC/MS) exploratory studies of synthetic organic chemicals in fish from the Great Lakes and other major U.S. watersheds. D.W. Kuehl and colleagues at the EPA Environmental Research Laboratory in Duluth reported that the data are subjected to a pattern recognition approach in order



*Analytical results. Scientists review data on trace metals in river water samples*

to interpret those obtained from high-resolution gas chromatography. The output of this pattern recognition shows a detailed postanalysis report of the compound results. The output can be given in tabular form or as a multicolor histogram that shows both the original sample chromatograph and a chromatogram of the calculated mixture of PCBs present.

The origin of many of these chemicals often remains unknown. But polychlorinated styrenes comprise one class of compounds that has been observed in fish from the Great Lakes since 1974. This class of compounds has also been found in fish and birds in Europe.

### Organics in dump sites

Another current environmental problem is the spread of pollution from chemical dump sites. Ronald A. Hites and Ray Kaminsky of Indiana University measured the spread of chemical pollution from dumps of the city of Niagara, N.Y., into the Niagara River and downstream in Ontario. Analyses of sediment cores and grab samples from Lake Ontario have revealed a variety of halogenated organic compounds that appear to be accumulating in increasingly large quantities. The analytical technique that worked best was NCI GC/MS, negative chemical ionization mass spectrometry combined with fused silica, capillary column gas chromatography.

Other sources of naturally occurring organics are aquatic humic materials from decaying leaves and other decaying organic matter. These materials represent an important fraction of the organic content of streams. D. L. Norwood and colleagues at the University of North Carolina at Chapel Hill reported quantitative yields of more than 30 by-products from a reaction of an aquatic fulvic acid with aqueous chlorine.

Furthermore, synthetic organic chemicals in aquatic systems tend to sorb to solid materials such as sediments and suspended solids. Once absorbed, they undergo transport and transformation processes different from those they would have undergone in the dissolved state.

The role of such partitioning reactions is of concern in the process of bioaccumulation, in which hydrophobic pollutants concentrate at the highest levels of the food chain. T. C. Voice and colleagues at the University of Michigan in Ann Arbor performed laboratory, isotherm experiments using four hydrophobic organic compounds with varying octanol-water partition coefficients and three sedi-

ments collected from Lake Michigan, with solids concentrations ranging from 10 mg/L to 400 mg/L. The data suggest that the experiments conducted at high solids levels for the sake of analytical simplicity may substantially underpredict environmental partitioning.

### Visibility studies

In a study of the visibility and air quality relationships in St. Louis, Edward S. Macias of Washington University and Lih-Ching Chu of the Illinois State Water Survey said that particle size, shape, and refractive index are the most important parameters for relating the concentration of particles to their optical properties. According to the current understanding, the size distribution of atmospheric aerosol mass is generally bimodal, and light scattering and particle-related light absorption are usually dominated by fine mode aerosol. The significance of the carbonaceous compounds' contribution to visibility, especially scattering, is not well understood. No obvious relationship between humidity and light scattering due to different chemical species has been found in this work.

In summary, the relative contributions to visibility impairment in St. Louis are 49% from the scattering of sulfates, 14% from the absorption of elemental carbon, 6% from the scattering of elemental carbon, 11% from the scattering of organic carbon, and 12% from the scattering of the remainder of the fine mass. About 20% of the visibility reduction in St. Louis was caused by elemental carbon, which

accounts for only 6% of the fine mass.

### Biological monitoring

An international pilot study, sponsored by the World Health Organization, the United Nations Environment Programme, and the EPA aims to assess the baseline body burden levels of two metals, cadmium and lead. Ten countries including the U.S. are participating in the study of a nonoccupationally exposed population—school teachers in metropolitan areas. First, a questionnaire was used to collect basic demographic and medical information on possible sources of exposure to these metals. These data will be useful for examining possible correlations between body burden and exposure.

Another element of the study was the collection of kidney cortex specimens. The scientific literature indicates that the kidney is the site of lifetime cadmium accumulations. Earlier studies on the human blood levels of lead and cadmium and the cortex level of cadmium had been performed, but none had been attempted on an international level.

The U.S. phase of this international study was conducted in Baltimore, Md. Some 224 questionnaires were mailed, and 180 teachers submitted to a chemical analysis of their blood for the levels of cadmium and lead. Preliminary results are shown in the table.

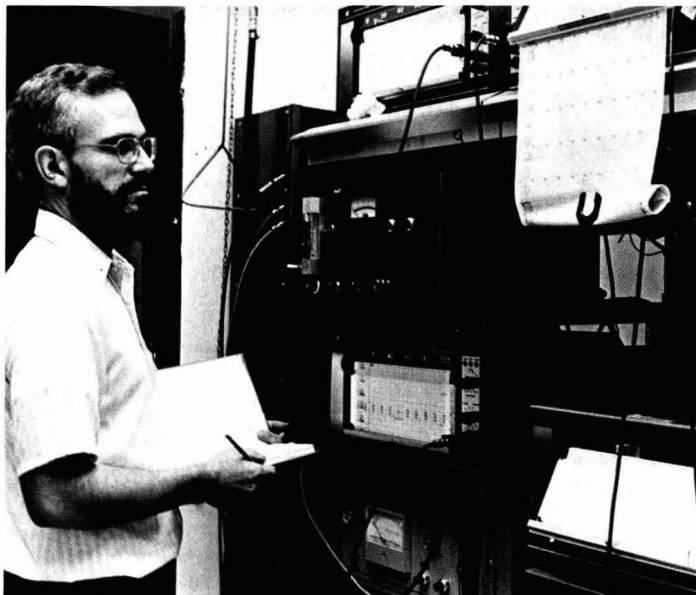
### Organic pollutants in the air

Thomas R. Hauser, director of the EPA Environmental Monitoring Sys-

TABLE  
Estimated lead and cadmium concentrations in selected subgroups

	Estimated mean ( $\mu\text{g/L}$ )		Sample No.
	Pb	Cd	
Stratum of city			
Northwest	81.8	0.83	41
Northeast	83.8	1.10	45
South	74.6	0.72	93
Sex			
Female	71.6	0.74	124
Male	102.3	1.16	55
Race			
Black	77.8	0.84	99
Nonblack	81.0	0.85	80
Smoking habits			
Current smoker	87.4	1.17	59
Former smoker	86.3	0.88	32
Never smoked	69.8	0.58	88

Source: Paper by F. W. Kutz et al., U.S. EPA, Washington, D.C.



**Gathering data.** Analyst is developing instrumentation for on-site performance audits

tems Laboratory at Research Triangle Park, N.C., gave an overview of the agency's air monitoring activities. They were divided into four categories; the procedures and techniques differed for each. The four areas were inorganic, organic, particulate matter, and gases. Hauser also mentioned the air quality assurance program. He commented on the Love Canal story and said that no air pollutants were found in the air monitoring carried out in the Love Canal area. His group was looking specifically for organic gases and liquids.

The most widely used methods for sampling gas and vapor contaminants in air are either to draw a known volume of air through a suitable solid adsorbent such as porous charcoal or porous polymer or, if the contaminant is reactive, to let the air sample be absorbed in a solution contained in a bubbler or impinger.

In recent years, passive samplers have come into play, since they obviate the use of an air pump, which is expensive. The passive device works by gaseous diffusion or by permeation. It offers a simple means of measuring time-weighted average concentrations of gases and vapors in the working area of factory workers. However, diffusional sampling has not been well accepted because of the lack of adequate backup data and the poor design of the samplers. Diffusion samplers do not require pumps. Each substance has a unique diffusion coefficient in air; however, a considerable data base is required for broad use of diffusional

samplers. Also, there are active samplers, which require battery-operated personal sampling pumps.

#### **Personal monitors**

One such personal monitoring device is the Ames vapor sampling system (AVSS). Analytical results from the use of the AVSS are comparable to those obtained with the use of the more complicated source assessment sampling system (SASS) and the EPA Method-5 sampler. Over the past three years, the AVSS has been applied to the solution of several environmental monitoring problems. It has also been used to monitor indoor and outdoor air.

#### **Adsorbents and PAHs**

Tenax-GC is usually recommended for sampling combustion gases because it has a greater thermal stability than XAD-2. Also, mutagenic degradation products have never been detected from Tenax-GC after either heat or NO<sub>2</sub> treatment.

The materials that have been used to sample organics in air include polystyrene resins, Tenax-GC, graphitized carbon black, and others. There is a need for sorbents with higher selectivities, lower background, and higher stability. For example, B. A. Demian and colleagues from the Research Triangle Institute made and tested 61 polyimides as sorbents for air sampling.

Some polynuclear aromatic hydrocarbons (PAHs) such as benzo(*a*)-pyrene are recognized carcinogens.

Assessments of PAH levels in ambient air are usually performed with high-volume air sampling using glass fiber filters. With this technique, however, many vapor-phase components are lost. But the use of polyurethane foam (PUF) extends the sampling method to vapor-phase PAHs.

Most of the 3- to 4-ring PAHs passed through the filter and were retained by the PUF trap. Data indicate that substantial portions of the lower molecular weight PAHs are lost when sampling is done with a glass fiber filter alone.

The analysis of (PAHs) in combustion emissions is not only important in determining the total burden of carcinogenic substances in the environment, but also in identifying the origin of pollutants.

The National Bureau of Standards has recently issued a standard reference material, SRM 1649, certified for concentrations of a number of PAHs.

#### **Hydrocarbons in air**

Kenneth Lee and the people from Radian Corporation said that the "fingerprinting" technique has been expanded and improved to include emissions from both waste ponds and landfill waste sites. In their work, a modification of the Bellar-Lichtenberg purge-and-trap apparatus was necessary to eliminate the water from the water-saturated purge gas into the cryogenic concentrator.

Traditionally the analysis of organic (C<sub>2</sub>-C<sub>10</sub>) hydrocarbons was accomplished by off-line techniques. Samples were collected and transported to the laboratory for analysis by gas chromatography. Radian scientist Larry D. Ogle described the development of gas chromatographic procedures for the "continuous" on-site analysis of hydrocarbons in ambient air. The procedures employ preconcentration techniques and multiple-column chromatography, and enable a wide variety of hydrocarbons to be analyzed with a sensitivity of 1 to 2 ppb. The analytical techniques were evaluated with Radian 110A chromatograph systems in a six-month field monitoring program conducted in Houston, Tex. Analytical conditions were established for the analysis of 38 C<sub>2</sub>-C<sub>9</sub> hydrocarbons, which were believed to make up 50-70% of the hydrocarbon burden of Houston ambient air. The combination of Tenax and Carbosieve retained all compounds except ethylene and acetylene, which were retained on the molecular sieve. The average trapping efficiency for all compounds was excellent.

Norman Taylor and colleagues of the University of Leeds, U.K., reported that the polarographic reduction potentials of a large number of PAHs provide the basis for the recognition of different structural types. He said that a microprocessor-based, polarographic instrument offered advantages over instruments used earlier.

Some other organics in the air are dialkyl phthalates that are commonly used as plasticizers. Scott J. Selover and colleagues of SRI International developed methods to measure airborne levels of each phthalate (mixtures of isomeric alkyl portions, weight averaged C<sub>6</sub>, C<sub>9</sub>, and C<sub>10</sub>) ranging from 0.1 to 10 µg/m<sup>3</sup>.

Airborne diisopropyl sulfate is a toxic chemical, a "suspect" carcinogen, and is produced when isopropanol is made by the acid process using propene and sulfuric acid. The airborne material can be collected on Chromosorb 102 in a sorbent tube. The diisopropyl sulfate is extracted with carbon tetrachloride and the extract analyzed by GC, using a flame photometric detector operating in the sulfur mode.

#### Other organics

Other organics in air are pesticides. T. A. Wehner et al. of the University of California reported that sampling and analytical procedures should be designed for multiresidue determination of pesticides in the air. They employed XAD-4 macroreticular resin for collecting and concentrating pesticide vapors from the air, using high- and low-volume air samplers.

T. Vo-Dinh of the Oak Ridge National Laboratory reported that analytical methods have been used in an integrated screening procedure for monitoring complex multimedia samples. These procedures include two luminescence techniques—synchronous luminescence and room-temperature phosphorescence.

John G. Windsor, Jr., et al. of Northrop Services, Inc. (Research Triangle Park, N.C.) prepared standards for solid sorbent cartridges. At present, there are two approaches. The first is to inject the cartridge with a headspace sample of a pure compound or with an aliquot of a solution standard and then drive off the solvent carrier. The other approach is to combine gas dilution systems with diffusion tubes or permeation devices that deliver a gas stream containing volatile organics to the cartridge.

Volatile organic compounds contained in diffusion tubes are used to generate known concentrations of volatile organics in the carrier gas stream. But permeation tubes cali-

brated by the manufacturer at elevated temperatures were found to have insufficient output rates at ambient temperature. For this reason, only diffusion tubes are now routinely used in the system.

Over the past two years, Northrop Services researchers made more than 2000 headspace injections of volatile compounds into a GC or GC/MS and onto cartridges that were thermally desorbed into a GC or GC/MS. These researchers have also found an alternative to the syringe pump; it involves a "static dilution bottle" that maintains a known concentration of a volatile species in the headspace of a flask. The other method is flash vaporization. In preliminary studies, they obtained results comparable to those obtained with the syringe pump method and at lower cost.

#### Emissions of organics

J. S. Stanley and colleagues at Midwest Research Institute reported on a quality assurance program that has been implemented for a nationwide study of organic emissions from coal-fired utility boilers. It includes data on inputs and emissions from seven coal-fired power plants and five sites of sampling—fuel, flue gas, ash from the control device, ash from the boiler, and plant background air.

What are the emissions from the incineration of hazardous wastes? The EPA regulation on this was published in the *Federal Register* on Jan. 23, 1981. The regulation stipulates destruction removal efficiency of greater than or equal to 99.99%. Detailed sampling analysis procedures have recently been published by A. D. Little under an EPA contract.

Input and emission samples were collected and analyzed from seven coal-fired utility boilers as a part of a nationwide survey of combustion source emissions. The primary compounds of interest include PAHs and the dibenzodioxins and dibenzofurans.

A paper by Jacob D. Paz, an environmental consultant in New York City, suggested mechanisms for the recognized health hazard effects of operating room employees. For example, high energy releasing and radio frequency devices are capable of generating high concentrations of NO, NO<sub>2</sub>, and NO<sub>x</sub>. Various disinfecting compounds in the operating room can interact with these oxides of nitrogen to produce a harmful "photochemical smog."

#### Biological modification of wastes

A number of processes for biological modification of wastes were described

at the Kansas City meeting. G. F. Payne of the University of Michigan described preliminary studies to determine the feasibility of microbial degradation of nitrogen-deficient phenolic resin wastes containing phenol, formaldehyde, and methanol. The *Azotobacter* culture used in this study was selected from soil and water samples.

Roy A. Ackerman of ASTRE (Charlottesville, Va.) looked at five strains of microorganisms (*Arthrobacter* and *Pseudomonad*), species that have mutated and stabilized to ensure their degradation of phenolics, acrolein, and acrylonitrile. To degrade satisfactorily, a waste stream containing a variety of phenolics, acrolein, and acrylonitrile needs five strains of bacteria that are grown separately. Removing organic sulfur from coal is one of the major problems in microbial desulfurization. Organisms capable of oxidizing dibenzothiophene, a refractory cyclic organic sulfur compound in coal, have been used to remove a substantial amount of organic sulfur. In addition to complete removal of inorganic sulfur, approximately 70% of initial organic sulfur has been removed from coal samples.

M. L. Shuler of Cornell University determined the feasibility of using an aerobic, biological, waste treatment system in a closed ecological life-support system such as that used for manned space missions of long duration, i.e., 5–10 years. In this closed system, food would be grown on board; the food would be consumed by the human crew; and a waste treatment module would break down human metabolic wastes and inedible plant residues into a mineral solution suitable for plant growth and into CO<sub>2</sub>. The permeate from this system is clear but colored, and contains less than 2% of the total suspended solids in the feed and less than 8% of the total soluble or colloidal organic carbon. A perfectly clear effluent can be achieved with a 2000 molecular weight cut-off membrane.

B. E. Jones and W. J. Weber, Jr., of the University of Michigan were interested in evaluating the effectiveness of adding powdered activated carbon to activated sludge systems for enhanced removal of specific toxic organic compounds. Preliminary results indicate that the addition of powdered carbon can effectively reduce the concentration of the less volatile compounds in water effluents and the concentrations of the more volatile compounds in both air and water effluents.

—Stanton Miller



# EPA's new management approach



Michael R. Deland

"Managing for environmental results," recently espoused by EPA Administrator Anne M. Gorsuch, is a refrain increasingly echoed by managers throughout the agency. The approach directs managers to use environmental-quality data to set goals for each program and then manage their programs to achieve those goals. This means that no longer will managers be evaluated by traditional "bean counting" methods, such as the number of inspections made or specific actions taken, but rather by how effectively their actions serve to protect the environment. The concept itself is not new but EPA's heightened interest and solicitation of state participation are.

The three main facets of the approach are an accountability system, "indicators" of environmental results, and "environmental management reports." The accountability system, which was established last fall, is the basic managerial framework requiring the establishment of goals, standards, and program objectives by which performance can be judged. The indicators and management reports, now being implemented, are key to whether a meaningful managerial change will in fact occur.

## Indicators of environmental results

EPA is evaluating responses from its regional offices and the states to a set of "possible indicators" for each medium that was circulated last month.

The range of indicators by which environmental results can be measured runs from "programmatic" or administrative indicators (surrogates based on the assumption that certain actions will result in improved environmental quality) to "ultimate impact" indicators.

Examples of programmatic indicators would be actions taken by the state or EPA, such as the issuance of permits or revisions to state implementation plans. Ultimate impact indicators include such measures as reduced incidence of pollution-related disease or return of certain species of fish to formerly polluted streams.

While the agency ideally would like to rely on ultimate impact data, it recognizes that such data are not yet widely available and that it must therefore use "the best combination of existing ambient, pollutant removal, or compliance data" to judge whether a program is meeting its environmental objectives.

The agency plans to use several of the more important indicators immediately and to further refine and implement others in the coming months. For example, an air quality indicator that can be immediately used is the "change over time in the number, extent and location of non-attainment areas." A "promising" air indicator "requiring further work" is the "population exposed to air quality standards violations."

## Management reports

Environmental indicators will ultimately serve as the basis for "state of the environment" assessments or "environmental management reports" (EMRs), which each regional EPA office will be required to submit by March 1983 and on a regular basis thereafter. The regions are now working with the states to develop the proposed content and format for the EMR.

The EMRs are intended to describe the status of trends in environmental quality, the most significant environmental problems, and the causes associated with those problems. The EMRs also are to outline the actions the region has taken or plans to take to address the problems and the implications of the information for environmental strategies over the short and long terms.

## State participation

At the National Governor's Association conference in September, Administrator Gorsuch and her staff met with the governors and senior environmental officials from more than 30 states. As an outgrowth of this session, several EPA-state working groups were established on matters of mutual environmental concern. One, "Managing for Environmental Results," chaired by Leonard Ledbetter, director of the Environmental Protection Division of the Georgia Department of Natural Resources, is currently exploring how state and federal resources might be more cooperatively and efficiently harnessed. This developing federal-state relationship is critical to whether managing for environmental results does in fact become a successful management tool. Many states have long been frustrated by the "bean counting" required of them by EPA and are thus enthusiastically participating in the design of what they perceive to be a sensible program.

The initial steps now being taken by EPA to manage for environmental results, particularly given active state support, have the potential to better direct government resources toward protection of public health and the environment.

Deland writes this column monthly and is counsel to ERT, Concord, Mass.

# Acidification of aquatic systems: A critique of chemical approaches

*Lake acidification models are based on many assumptions.  
 Rigorous analytic concepts must be applied when  
 interpreting historical pH data*

---

**James Kramer**  
 Department of Geology  
 McMaster University  
 Hamilton, Ontario L8S 4M1

**André Tessier**  
 INRS-Eau  
 Université du Québec  
 Ste-Foy, Québec G1V 4C7

---

During the past five to ten years, a great deal of interest and concern regarding the effects of man-made aerosols on wide regions of the earth has developed. The probable future increase in emissions and acidic deposition due to predicted increases in coal use has heightened this concern (1, 2). In the past decade, impact assessment has been considered in some depth; in addition to many articles in the literature, reports from two international conferences (3, 4) as well as reviews and assessments by the U.S. National Academy of Sciences (1), the National Research Council of Canada (5), and the U.S.-Canada Work Group I (6) have been published.

Impact assessment is generally divided into four categories: aquatic effects, terrestrial effects, health effects, and effects on man-made structures. The study of aquatic systems has provided most of the evidence that suggests changes have occurred. This is undoubtedly because aquatic sys-

tems have shorter residence times and smaller assimilation capacities than terrestrial systems. The kinds of studies that have been carried out concern: aquatic, biological, and chemical changes; aquatic, biological, and chemical indicators of change; historical evidence for changes in aquatic systems; definitions of sensitive areas on episodic and longer-term time scales; and definitions of the assimilative capacity of aquatic systems.

Numerous studies have attempted to demonstrate changes in aquatic systems. Surface waters containing low concentrations of dissolved materials are typically found in the headwater regions of watersheds sited in igneous and metamorphic rocks with little unconsolidated surficial sediment, and these waters show the greatest sensitivity to change. Generally, aquatic chemistry (7, 8), fish extinctions (9), plankton community structures (10), and lake sediment records (11) have been examined. As is typical of historical reconstructions, the quality of old data is often in doubt. This is especially true for chemical data and in particular for measurements of pH and alkalinity that were made before stable pH meters were introduced and commonly used.

Chemical acidification models are based on the concept of inorganic geochemical weathering. This article describes the basic hypotheses that are required to develop these models and considers their suitability for predicting anthropogenic acidification. In addition, the ability to assess old

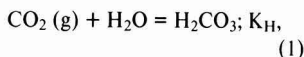
chemical data is evaluated relative to the sampling containers and the analytical techniques that were used. Historical trends are especially considered in these contexts.

## Concepts underlying aquatic models

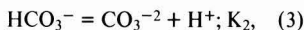
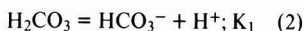
The overall chemical composition of surface water results primarily from interaction of the chemical components of precipitation with minerals and organisms in the drainage basin. Additional reactions occurring in the surface water itself also influence the composition.

Natural emissions (from sea spray, soil, vegetation, forest fires, and volcanic eruptions) and man-made emissions (from fuel combustion and smelters) are responsible for determining the chemical composition of precipitation. Atmospheric constituents, mainly nitrogen and sulfur compounds, undergo chemical changes (oxidation). These gaseous or particulate constituents are deposited on the earth's surface by various processes: by gravitational sedimentation; by turbulent transfer to the surface, followed by impaction, adhesion, sorption, or chemical reaction during dry periods; or by precipitation scavenging or gas-solution exchange during wet periods (5). Constituents of particular interest for the acid precipitation problem are the oxides of nitrogen and sulfur as well as "natural" carbon dioxide. Equilibrium between atmospheric CO<sub>2</sub> (pCO<sub>2</sub> = 10<sup>-3.52</sup> atm) and atmospheric water leads to the formation of carbonic acid:

*Feature articles in ES&T have by-lines, represent the views of the authors, and are edited by the Washington staff. If you are interested in contributing an article, contact the managing editor.*



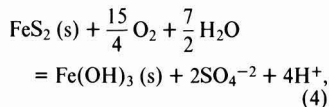
which dissociates:



giving  $[\text{H}^+] \hat{=} 10^{-5.7} \text{M}$  at 25 °C.  $K_1$  is the equilibrium constant for the first dissociation of carbonic acid and  $K_2$  is the equilibrium constant for the second. Emissions, mainly of  $\text{SO}_x$  and  $\text{NO}_x$ , and their oxidation have raised the  $\text{H}^+$  concentrations in rainwater typically to  $10^{-4}$ – $10^{-5} \text{M}$  in Scandinavia and North America. These systems can be considered an extension of the simple  $\text{CO}_2$ – $\text{H}_2\text{O}$  system, and can be analyzed by defining the system and deriving appropriate expressions with the electroneutrality function as a basis (12, 13).

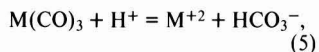
The biogeochemical interactions between the constituents of precipitation and the biotic and abiotic components of the soil include: dissolution of additional gaseous constituents; oxidation–reduction reactions; congruent and incongruent dissolution of minerals; and adsorption. During runoff, the surface water is in intimate contact with surficial soil where the gas composition may be quite different from that of the atmosphere; in particular,  $p_{\text{CO}_2}$  in soils may be higher by one or two orders of magnitude, due to biological activity (14). This may partly explain why natural waters are generally oversaturated with atmo-

spheric  $\text{CO}_2$ . Additional  $\text{H}^+$  is contributed to redox processes such as nitrification and oxidation of sulfide minerals and elemental sulfur to sulfate. For example,  $\text{FeS}_2(\text{s})$  is considered to be representative of sulfide minerals; its oxidation:



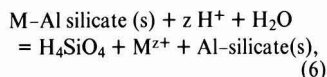
produces 4 eq.  $\text{H}^+$ /mol  $\text{FeS}_2(\text{s})$  if most of the  $\text{Fe}(\text{III})$  is precipitated. Similarly, reactions can be written to show that the oxidation of reduced nitrogen compounds produces  $\text{H}^+$  ions; for example,  $\text{NH}_4^+ + 2\text{O}_2 = \text{NO}_3^- + 2\text{H}^+ + \text{H}_2\text{O}$ . At the same time, reverse redox processes such as sulfate reduction, denitrification, and  $\text{N}_2$  fixation can consume hydrogen ions and hence product alkalinity.

Minerals in the watershed are subjected to weathering processes such as dissolution and exchange reactions that consume  $\text{H}^+$ . The congruent dissolution of calcareous minerals,

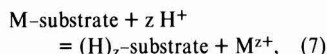


with  $\text{M}(\text{CO}_3)$  generally being  $\text{CaCO}_3$  or  $\text{CaMg}(\text{CO}_3)_2$ , is known to be highly efficient at neutralizing  $\text{H}^+$  in watersheds where these minerals are present; thus, acidification problems of surface waters would not be expected in such areas. Where only aluminosilicate minerals are present, important processes for the neutralization of  $\text{H}^+$  are

the incongruent dissolution of silicate minerals,

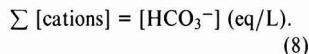


and the adsorption of protons on various substrates (organic matter, oxides, silicate minerals),



with M being typically Na, K, Ca, or Mg. Of much less importance is the congruent dissolution of oxides (Fe, Mn, Al) or silicates such as kaolinite (14).

The oxidation products of  $\text{SO}_x$  and  $\text{NO}_x$  compounds in rainwater and some redox reactions occurring in the watershed contribute an “excess” of hydrogen ions to the surface water over those acquired by dissolution of  $\text{CO}_2$  (both in soil and in cloud waters). The “excess”  $\text{H}^+$  has to be neutralized by weathering reactions such as reactions 5–7, before bicarbonate ions are produced by the so-called carbonic acid weathering (CAW); the latter may be represented by adding reaction 2 to each of reactions 5–7. Stoichiometry then requires that cations and bicarbonate ions (or alkalinity) are produced in *equivalent* amounts; that is, in the absence of any acid compound other than  $\text{H}_2\text{CO}_3$ , any weathering reaction leads to:



It should be noted that equation 8 does not hold for redox reactions.

### Existing models

Several empirical relationships have been suggested to identify lake acidification and to estimate the degree of acidification. In this section we intend to show that these models can be derived from simple chemical considerations, provided that some assumptions are made, and to discuss these assumptions.

Implicit functions are electroneutrality and alkalinity. To the extent that one can completely define the system (pH < 7), the electroneutrality condition can be written:

$$[H^+] + [NH_4^+] + 2[Ca^{+2}] + 2[Mg^{+2}] + [Na^+] + [K^+] = [HCO_3^-] + 2[SO_4^{-2}] + [Cl^-] + [NO_3^-]. \quad (9)$$

If only carbonate species are considered, total alkalinity is defined:

$$[Alk] = [HCO_3^-] + 2[CO_3^{-2}] + [OH^-] - [H^+]. \quad (10)$$

Assuming **Hypothesis (H1)** that there is no input of  $Cl^-$  from the watershed and that the composition of seawater and sea spray is the same, surface waters are generally corrected on the basis of  $[Cl^-]$  in order to remove the contribution of ions from seawater (8, 15-17). Such corrections should apply to all cations and anions; that is, electroneutrality should not be violated. Assumption **(H1)** is probably valid except when municipal and industrial waste, deicing road salts, or alkaline dust make important contributions. After adjustment for sea spray contributions and **(H2)** if nitrate and ammonium concentrations are assumed to be negligible, the electroneutrality condition becomes

$$[H^+] + 2[Ca^{+2}] + 2[Mg^{+2}] + [Na^+] + [K^+] = [HCO_3^-] + 2[SO_4^{-2}] \quad (11)$$

or

$$[H^+] + \sum z_i[M_i] = [HCO_3^-] + 2[SO_4^{-2}], \quad (12)$$

where M and z represent the cations (Ca, Mg, Na, K) and their charges, respectively.

For low-pH (<7) surface waters, equation 10 reduces to

$$[Alk] = [HCO_3^-] - [H^+]. \quad (13)$$

Combining equations 13 and 12 leads to

$$[Alk] = \sum z_i[M_i] - 2[SO_4^{-2}]. \quad (14)$$

Equation 14 is often simplified with one of the following two implicit assumptions:

$$(H3) \quad 2([Ca^{+2}] + [Mg^{+2}]) = \frac{1}{b} \sum z_i[M_i];$$

$$(H4) \quad 2[Ca^{+2}] = \frac{1}{b'} \sum z_i[M_i].$$

This leads to the expressions,

$$[Alk] = 2b([Ca^{+2}] + [Mg^{+2}]) - 2[SO_4^{-2}] \quad (15)$$

$$[Alk] = 2b'[Ca^{+2}] - 2[SO_4^{-2}], \quad (16)$$

where b and especially b' must be greater than one. The basis for assumptions **(H3)** and **(H4)** is that  $[Ca^{+2}]$  or  $[Ca^{+2}] + [Mg^{+2}]$  represent most of the cations in the weathering solution. Almer et al. suggested that since the  $[Ca^{+2}] + [Mg^{+2}]$  of lakes unaffected by acidification should result from  $H_2CO_3$  weathering, there should be an equivalence line (slope = 1; intercepts = 0) in a  $2([Ca^{+2}] + [Mg^{+2}])$  vs.  $[Alk]$  plot (7). Any deviation from the equivalence line was assumed to indicate inputs of Ca and Mg from other mechanisms; in particular, a slope lower than that of the equivalence line is interpreted as evidence of acid input (see Figure 1a). The same reasoning was employed by others (5, 18, 19).

Some comments should be made concerning the use of such graphs ( $[Alk]$  vs.  $[Ca^{+2}]$  or  $[Ca^{+2}] + [Mg^{+2}]$ ). They might be useful in cases where only  $[Alk]$  and  $[Ca^{+2}]$  or  $[Ca^{+2}]$  and  $[Mg^{+2}]$  are available, as the negative intercept would give some indication of the sulfate content of the surface water, as suggested by equations 15 and 16. It should be remembered, however, that the sulfate content thus estimated depends on the variability of b or b' for the watersheds considered. In many watersheds, the contributions of Na and K to the total cation concentration are not negligible, and they can vary greatly between watersheds even in a restricted region. When all the cations and sulfate concentrations are measured (5, 18), such graphs provide no information other than visual interest; instead graphs should be presented using all the major cations. This would probably reduce the scatter of the points due to variations in b and b' within a watershed, and particularly between watersheds. According to equation 15, a slope greater than that of the equivalence line is expected for the experimental points; however, much lower slopes are often observed (7, 19). This can be

explained if  $[Ca^{+2}] + [Mg^{+2}]$  are overestimated (or  $[HCO_3^-]$  or  $[SO_4^{-2}]$  are underestimated), or if  $[SO_4^{-2}]$  is not the same for all the waters represented in the graph, that is, high  $[Ca^{+2}] + [Mg^{+2}]$  are often associated with high  $[SO_4^{-2}]$  (8). Finally, regarding the latter point, it should be mentioned that the graphs should not include waters whose alkalinity and total cation concentrations are much higher than those typical of silicate mineral weathering ( $\leq 100 \mu eq/L$ ).

The equilibrium constant expression that results from combining equations 1 and 2 is

$$*K = K_H K_1 = \frac{[HCO_3^-][H^+]}{PCO_2}, \quad (17)$$

where  $K_H$  and  $K_1$  are the equilibrium constants for the gas phase-solution exchange of  $CO_2$  and for the first dissociation of carbonic acid, respectively. In the absence of "excess"  $[H^+]$ , CAW alone leads to equation 18:

$$\sum z_i[M_i] = [HCO_3^-]. \quad (18)$$

Combining equations 18 and 17 with either **H3** or **H4** leads to the following expressions, respectively:

$$pH = \log \sum z_i[M_i] - \log *K - \log pCO_2 \quad (19)$$

or

$$\begin{cases} pH = \log 2b([Ca^{+2}] + [Mg^{+2}]) - \log *K - \log pCO_2 \\ pH = \alpha + \log ([Ca^{+2}] + [Mg^{+2}]) \end{cases} \quad (20)$$

where

$$\alpha = \log 2b - \log *K - \log pCO_2,$$

or

$$\begin{cases} pH = \log 2b'[Ca^{+2}] - \log *K - \log pCO_2 \\ pH = \alpha' + \log [Ca^{+2}] \end{cases} \quad (21)$$

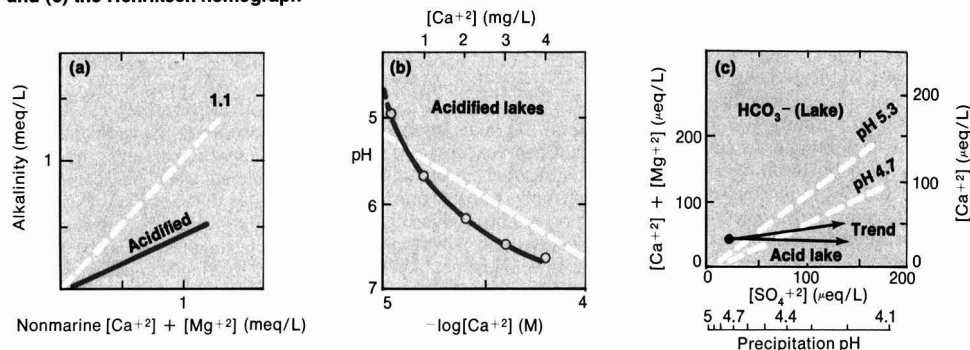
where

$$\alpha' = \log 2b' - \log *K - \log pCO_2.$$

Henriksen suggested that drawing an empirical curve of pH vs.  $[Ca^{+2}]$  could distinguish between acidified and unacidified waters positioned on the graph (Figure 1b) (16). This empirical model has been widely used (20-23); the surface waters that fall above the empirical curve are generally considered acidified. Equation 21 has the same form as the empirical Henriksen curve, but the latter does not meet the requirement of slope 1. Although such graphs may be advantageous for visual inspection, as many surface waters can be positioned on the same graph, inferring acidification or

FIGURE 1

Schematic representations of (a) Almer model, (b) Henriksen pH vs.  $[Ca^{+2}]$  model, and (c) the Henriksen nomograph\*



\*Dashed line in (b) is linearized log transform of pH vs. log  $[Ca^{+2}]$  with calcium concentration in molar units and a least-square fit of  $pH = 12 + 1.4 \log [Ca^{+2}]$ . This can be compared to equation 21 where  $\alpha' = 11.6$  when  $\log *K = -7.8$ ,  $\log pCO_2 = -3.5$ , and  $b' = 1.1$ .

not from the departure away from the empirical line seems to be without basis. Indeed, considering equation 21, the two following assumptions are implicit in the model: (H5) only acid rain is contributing to the lowered pH at a given  $[Ca^{+2}]$ ; (H6)  $\alpha'$  is the same for all the waters considered.

As mentioned previously, reactions in the watershed itself, such as redox reactions, can contribute to the departure from a CAW model. Furthermore, a high variability in  $\alpha'$  is introduced by the parameters  $b'$  and  $pCO_2$ , which vary from one surface water to the other and, to a lesser extent, by variations of  $*K$  with temperature and ionic strength. For example,  $b$  and  $b'$  vary with mineralogy, and  $pCO_2$  may vary easily by one order of magnitude from one location to another, or at the same location with time (14). If the theoretical lines for CAW are to be drawn according to equation 20 or 21, the parameters  $b$  or  $b'$  have to be estimated using such relationships as 15 and 16 for a group of nonacidified lakes of similar geology. All attempts at using these relationships have led to a negative intercept on the [Alk] axis unless the regression was forced through the origin (8, 16, 24). This emphasizes the difficulty in evaluating  $b$  or  $b'$ . If, on the other hand, the unforced regression is considered as representing the natural processes in undisturbed watersheds, then substitution of equation 13 and relationships 15 or 16 into 17 leads to, respectively,

$$pH = \log \{2b([Ca^{+2}] + [Mg^{+2}]) - 2[SO_4^{-2}] + [H^+]\} - \log *K - \log pCO_2 \quad (22)$$

or

$$pH = \log \{2b'[Ca^{+2}] - 2[SO_4^{-2}] + [H^+]\} - \log *K - \log pCO_2 \quad (23)$$

for which pH is no longer a linear function of  $\log ([Ca^{+2}] + [Mg^{+2}])$  or  $\log [Ca^{+2}]$ .

Thus, if graphs similar to that of Henriksen are to be constructed, it is suggested that pH and  $\log \sum z_i[M_i]$  be the two variables used, because the Ca, Mg, Na, and K concentrations are available most of the time. The theoretical straight line representing CAW should be drawn for a fixed  $pCO_2$ , and the pHs of the surface waters should be corrected for the variation in  $pCO_2$  according to:

$$pH(\text{corrected}) = pH(\text{actual}) - \log pCO_2(\text{fixed}) + \log pCO_2(\text{actual}), \quad (24)$$

where  $pCO_2(\text{actual})$  is calculated from pH (actual) and alkalinity using equations 13 and 17. For the points falling above the theoretical straight line, it could be inferred that sources of  $H^+$  other than  $H_2CO_3$  (not necessarily acid deposition) had contributed to the weathering processes. Points falling below might suggest that  $H^+$  neutralizing processes other than CAW, such as reduction reactions, for example, were operating in the watersheds.

Models have also been developed to predict surface water acidification (8, 15). Assuming that (H6) is valid for a given watershed and the product  $*K \cdot pCO_2$  is constant with time, equation 17 indicates that

$$[HCO_3^-][H^+] = \text{constant} = *K pCO_2 \quad (25)$$

Furthermore, with the following two assumptions (H7)  $[H^+] \ll \sum z_i[M_i]$  and (H8)  $\sum z_i[M_i]$  is constant with

time, equation 12 can be rewritten:

$$[HCO_3^-] + 2[SO_4^{-2}] = \text{constant} = \sum z_i[M_i] \quad (26)$$

Combining equations 25 and 26 leads to the following relationship, first suggested by Thompson and Bennett (15):

$$[H^+]_2 = \frac{[HCO_3^-]_1 [H^+]_1}{[HCO_3^-]_1 + 2[SO_4^{-2}]_1 - 2[SO_4^{-2}]_2} \quad (27)$$

where subscripts 1 and 2 refer to times  $t_1$  (present) and  $t_2$ , respectively.

Equation 27 might be useful in calculating the expected value of pH with change of sulfate concentration in a surface water if the actual pH,  $[SO_4^{-2}]$ , and  $[HCO_3^-]$  values are known and if the expected concentration of sulfate does not exceed the limiting value,  $[SO_4^{-2}]_L = \frac{1}{2} [HCO_3^-]_1 + [SO_4^{-2}]_1$ . Assumptions (H6) and (H8) are arguable, however. Soil microorganisms might be affected by acid deposition or by other anthropogenic activities such as deforestation, and this could conceivably affect the  $pCO_2$ . The constancy of cation concentrations in surface waters is still a debated question. Thompson and Bennett (15) and Watt et al. (25) did not find any significant increase in calcium concentration due to acid deposition. But other researchers found evidence of increased concentrations of calcium (7, 26, 27) as well as other cations (19).

With an additional assumption, (H9), that  $[SO_4^{-2}]$  measured in the surface water (and corrected for sea spray) is derived entirely from acid

deposition, equation 27 reduces to

$$[H^+]_0 = \frac{[HCO_3^-]_i [H^+]_i}{[HCO_3^-]_i + 2[SO_4^{2-}]_i}, \quad (28)$$

where  $[H^+]_0$  represents the  $[H^+]$  before the onset of acid deposition. Concerning assumption (H9), it should be mentioned that sulfide or even sulfate minerals, for example, scapolite and gypsum (probably resulting from oxidation of sulfides in igneous-metamorphic terrain), are sometimes found in watersheds sensitive to "acidification."

Another model, the Henriksen nomograph, has been suggested to predict the future acid state of a lake. Assuming a constant weathering rate (H8), together with (H9), and (H3) or (H4), the preacidification alkalinity,  $[Alk]^0$ , is written according to equation 14:

$$[Alk]^0 = \sum z_i [M_i] = 2b([Ca^{+2}] + [Mg^{+2}]) = 2b'[Ca^{+2}]. \quad (29)$$

With the additional assumption (H10), that surface waters are in equilibrium with atmospheric  $CO_2$ , combining equations 12, 25, and 29 together with  $*K = 10^{-7.8}$  and  $pCO_2 = 10^{-3.5}$  atm leads to:

$$[Alk]^0 = \frac{10^{-11.3}}{[H^+]} - [H^+] + 2[SO_4^{2-}]. \quad (30)$$

With equation 30, a theoretical pH-contour nomograph can be constructed for bicarbonate solutions (8), as suggested by Henriksen.

To test his hypothesis that the acidification of freshwaters is analogous to the titration of a bicarbonate solution with sulfuric acid, Henriksen obtained  $\{[Ca^{+2}] + [Mg^{+2}]\}$  or  $[Ca^{+2}]$  vs.  $\{\text{lakewater } [SO_4^{2-}]\}$  linear regression equations for pH 5.3 and 4.7 (Figure 1c) where actual  $[Ca^{+2}] + [Mg^{+2}]$  or  $[Ca^{+2}]$  are equated to  $[Alk]^0$ ; the validity of the hypothesis is taken as the ability of the data regressions to be equivalent to the theoretical curves for the bicarbonate solution. Such a procedure is arguable as the validity of (H8), (H9), and (H10) is questionable as is the constancy of  $b$  and  $b'$  (see above). In particular, in relation to (H10), lake water  $pCO_2$  is often greater than  $10^{-3.5}$  atm, and it varies with location or with time.

To predict changes in lake pH in response to changes in precipitation pH, Henriksen then substituted in equation 30 the two linear regressions,  $\{\text{lake water } [SO_4^{2-}]\}$  vs.  $\{\text{precipitation } [SO_4^{2-}]\}$  and  $\{\text{precipitation } [SO_4^{2-}]\}$  vs.  $\{\text{precipitation } [H^+]\}$  (see Figure 1c,

lower x-axis). It is important to realize that the complicated aerosol chemistry as well as contributions of  $SO_4^{2-}$  from sulfide and sulphate weathering are approximated by these two regressions. In the specific situation cited, however, good correlations between lake  $[SO_4^{2-}]$  and precipitation  $[H^+]$  were noted.

In general, there are probably no unambiguous approaches to an atmospheric acidification model using ionic calculations only. As noted previously, acidification can be produced by oxidation of sulfides, and in most cases the same results would be obtained when the acid is added from other sources. Good correlations may merely reflect a good approximation of electroneutrality. The fundamental question appears to be: Can lake  $[SO_4^{2-}]$  be equated to acidic aerosols; that is, do equations 14, 15, or 16 apply?

One means of assessment would be to study the  $\delta^{18}O$  and  $\delta^{34}S$  in rainfall, lakes, and runoff. Isotopic fractionation of sulfur normally occurs during reduction and possibly during oxidation reactions; similarly, fractionation of oxygen occurs as a function of environmental variables. But the oxygen ratio would probably remain quite stable in the sulfate ion. Hence, the same results for the two isotopic ratios would give strong credence to the theory that atmospheric and aquatic sulfate are correlated, whereas differences would suggest that more complicated processes involving sulfur species are occurring. This method has been proposed recently to differentiate between anthropogenic emissions of sulfate and sulfur dioxide (28).

As a final note, the use of data that do not meet the charge balance requirements of equation 11 or its modifications, such as equation 15, would also influence the way in which the results of all the above models should be interpreted.

#### Analysis of historical data

Attempts have been made to compare aquatic chemical data obtained before and after about 1960. Typically these studies have shown that there is a statistically significant difference in average pH and alkalinity values of soft-water streams and lakes for the two time periods (29-31). Furthermore, all the studies conclude that the older pH and alkalinity measurements were greater than present values; this trend has been used to imply increasing acidification over the past 20-50 y.

Other data have been used to show that rain has increased in  $H^+$  concentration. For example, Cogbill and

Likens (32) and Likens (33) found an increase in H-ion concentration for broad regions of the eastern U.S.; Herman and Gorham (34) measured an average pH of 5.7 (5.3-6.7) for precipitation at Kentville, Nova Scotia, in 1952, whereas Kerekes (35) measured an average pH of about 4.5 for both 1978 and 1979 at Kejimikujik National Park, Nova Scotia.

Many factors must be carefully considered when one compares historical with recent data. Differences in sampling methods, instrumentation, and techniques must be examined when making comparisons. For example, the pH meter with glass electrode came into common use in the period 1946-60. In addition, container materials changed at about the same time, with the introduction of common plastics. Moreover, the sampling time during the day or the year can greatly influence the observed pH and alkalinity values because in poorly buffered lakes at medium pHs, primary production can increase both pH and alkalinity, whereas respiration can decrease these parameters. Most authors recognize these problems, and many of them make corrections for different techniques; yet even after adjustments, the majority of results show a downward trend of pH and alkalinity for poorly buffered water systems.

In the following section, we focus on the sampling methods, analytical procedures, and corrections to be made in the data, as well as on the precision of the methods. The biases that would produce the decreasing pH and alkalinity trends are especially considered. Three general factors should be considered in comparing old data with recent data relative to sampling and analysis:

- the change in container material, especially the introduction of stabilized laboratory-quality plastics in about 1960;
- the development and common use of the glass electrode and the high-impedance electrometer that became significant after about 1950. Previously, color indicator comparators were used (36);
- the changes that occurred in the method for determining alkalinity.

Prior to 1960, soft glass, and, to a lesser extent, Pyrex glass were common container materials; soft glass bottles were probably used for water samples due to the difference in cost. Pyrex brand glass was never fabricated into sampling bottles although Pyrex reagent bottles could have been used for water sampling bottles (37). The sales history of laboratory plastic containers in Canada suggests that the

TABLE 1

### Summary of alkalinity and pH measurements in "Standard Methods for the Examination of Water and Sewage"

Edition	Alkalinity method, Indicator	End point	Precision/accuracy	Potentiometric	pH	Containers
7, 1933	1) Two drops MO (0.5 g/L), (erythrosine alternate for Al/Fe waters)  2) 50 or 100 mL 3) 0.02N H <sub>2</sub> SO <sub>4</sub>	"Until faintest pink coloration: that is until color is no longer pure yellow"; pH = 4.0	Not given	No	H-electrode or color comparator	No
8, 1936	Same as 1933; use reference sample for color change	Same as 1933	Not given	No	Same as 1933	No
9, 1946	Same as 1933	"yellow to pink"	Not given		1) Glass electrode pH meter preferred + calomel reference electrode 2) Special technique required for poorly buffered solutions	No
11, 1960	1) "Potentiometric preferred." "... indicators effective in these ranges will give the most reliable results." (?) 2) Fixed end point, or preferred inflection point with glass electrode 3) Use bromocresol green methyl red for pH ~ 5.0 4) Use MO for "pH 4.6-orange, or pH 4.0-pink"	1) pH = 5.1 for 0.6 meq/L  2) Double potentiometric end point if 4.5, 4.2 pH suggested 3) pH 4.5 for 10 meq/L	Precision: 20 µeq/L Accuracy: 60 µeq/L for 0.2-10 meq/L		Glass electrode and pH meter	Polyethylene or Pyrex

change toward plastic laboratory containers occurred after 1960.

Polymethyl-pentene containers were first introduced in 1958. Following initial sales growth, production more or less stabilized after 1960; however, high expense limited their use. Polypropylene was introduced in 1956, and production and sales stabilized quickly; conventional polyethylene was introduced in 1965, and sales grew and stabilized by 1967. Teflon and linear polyethylene have become more common since about 1970. The time when plastic containers were first used is further documented by the first reference to them in "Standard Methods for the Examination of Water and Sewage" (SM) in 1960 (See Table 1) (38): "For best results samples should be collected in polyethylene or Pyrex bottles." Thus one must be concerned with the earlier use of soft-glass containers, because fresh glass surfaces have been shown to contribute 20-100 µeq/L alkalinity when samples are stored for less than

12 d (Figure 2). Similarly, Bacon and Burch measured a release of alkalinity of  $137 \pm 81$  µeq/L from 11 varieties of soft-glass containers after six months of sample storage at room temperature (39). It is possible that cleansing and aging of bottles and rapid analysis reduced this effect; yet the possible increase of 20-60 µeq/L is the same magnitude as some estimates of historical change in alkalinity. It should be pointed out that glass contamination would not be a factor in some analyses done in the field immediately after sample collection, for example, New Hampshire (40).

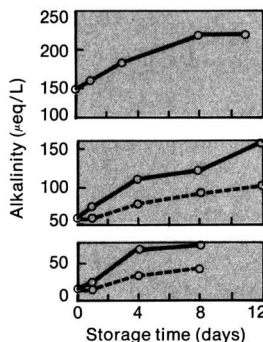
An additional container problem arises when interpreting changes in the pH of precipitation in Nova Scotia. Although Herman and Gorham used a pH meter and glass electrode to measure the pH of rain samples collected between 1952 and 1954, they collected the samples in a "... standard metal rain gauge, well weathered" (34). As noted previously, they found an average pH of 5.7 (5.3-6.7)

for the precipitation collected between 1952 and 1954 compared to a pH ~ 4.5 for samples collected between 1978 and 1979 in polyethylene containers.

We experimented with both a bright copper and a well-weathered standard copper precipitation gauge to determine the possible neutralizing effect of the container. Sulfuric acid of 41 µeq/L (pH = 4.39) was used as a model modern acid rain sample, and the pH change was examined after various periods of time up to 4 h (Figure 3). One can readily see that both the well-aged and the bright, shiny containers had a rapid neutralizing effect. Using the well-aged container resulted in a final pH of almost 5.9, up from the initial pH of 4.39. This result also can be approximated by the tenorite (CuO)-sulfuric acid ( $10^{-4.39N}$ ) equilibrium calculation, which gives a pH of 6.2 (i.e.,  $[Cu^{+2}]/[H]^2 = 10^{7.65}$  and  $2[Cu^{+2}] + [H^+] = 2[SO^{-2}_4]$ ). It should be mentioned that the reaction of a  $10^{-5.7}$  N solution of sulfuric acid with tenorite leads to a

FIGURE 2

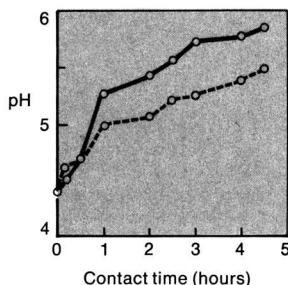
**Leaching of alkalinity over time of "Prince of Wales" soft-glass sample bottles for initial alkalinities of 142, 55, and 13  $\mu\text{eq/L}$ <sup>a</sup>**



<sup>a</sup>Samples were refrigerated (---) or not (—). (From Ontario Ministry of Environment Study, S. Villard, personal communication)

FIGURE 3

**Reaction of a  $10^{-4.39\text{N}}$   $\text{H}_2\text{SO}_4$  solution with a well-weathered (—) and a shiny (---) copper meteorological rain gauge**



calculated equilibrium pH value of 6.8. In the above experiment, we used 100 mL of acid, but the volume is probably not important because the ratio of the volume to the wetted surface of the container is constant, and, in addition, presumably all precipitation came into intimate contact with the entry funnel. It thus seems very plausible that the measured pH reflects the equilibrium pH that results from a copper oxide surface in contact with an acid solution.

Color indicator end-point titrations, pH meter end-point or multiple end-point titrations, and Gran analysis are three different basic procedures for the determination of alkalinity (see Table 1). Until about 1960, alkalinity methods were nearly the same, and often used methyl orange (MO) as an indicator. In 1960, SM suggested ambiguously that the end point be de-

termined either with a glass electrode or colorimetrically. In 1960, SM also noted that the end point would vary with the alkalinity value. It was not until after 1970 that the Gran method of analysis of the equivalence point was commonly used in North America. Today all three methods are probably still being used for the analysis of alkalinity.

The situation is even more complicated in that the recommended procedure for the MO alkalinity determination, involving the titration of 50- or 100-mL samples with 0.02 N  $\text{H}_2\text{SO}_4$ , changed with time. It was first suggested to titrate "until the faintest pink coloration appears: that is, until the color of the solution is no longer yellow" (41, 42), or "until the color changes from yellow to pink" (43). Later on, SM suggested that the operator "titrate to the proper equivalence point. The indicator changes to orange at pH 4.6 and pink at 4.0" (38).

In order to test the MO method, three operators were given the SM procedure with the "... faintest pink color..." directive and were told to experiment with the method, to define the end point by the first recognizable color change, and then to run multiple analyses on the same sample. In these experiments, both 50- and 100-mL samples were used, and the concentrations of MO and sulfuric acid recommended by SM were adopted. Titrations were effected with a 10-mL precision buret ( $\pm 0.02\text{-mL}$  precision), and an untitrated sample with MO was used to provide a reference color. A low-alkalinity sample was obtained by diluting Lake Ontario water about 10 times; the end-point pH was determined after the MO titration, and the sample was also analyzed using the Gran technique (44). The results indicated that the color end point determined independently by three different operators corresponded to a pH of  $4.04 \pm 0.10$  ( $n = 24$ ); the sample analyzed gave an alkalinity of  $244 \pm 23 \mu\text{eq/L}$  ( $n = 24$ ) by the MO method and of  $162 \pm 1$  ( $n = 4$ ) by the Gran technique. The same precision of about  $\pm 20 \mu\text{eq/L}$  as stated in SM was found for the MO technique (38). Alkalinity in this system would be

$$[\text{Alk}] \approx [\text{HCO}_3^-] - [\text{H}]$$

At the correct end point,  $[\text{H}] \approx [\text{HCO}_3^-]$ . For titration beyond the end point, the correction required is approximately equal to the excess H ion. For low-alkalinity concentrations ( $\sim 100 \mu\text{eq/L}$ ), the end-point H ion concentration ( $[\text{H}_2\text{C}^+]$ ) is about  $10^{-5}$  M

44). Therefore, the correction required on historical data should be approximately equal to  $81 \mu\text{eq/L}$ , the difference between MO end point ( $10^{-4.04}$ ) and  $[\text{H}_2\text{C}^+]$  ( $10^{-5.0}$ ). The difference in the MO alkalinity and the Gran alkalinity as measured was actually  $82 \mu\text{eq/L}$ . In reconstructing old data, many observers have either ignored the correction required or have used an incorrect value. For example, without explanation, Burns et al. used a value of  $32 \mu\text{eq/L}$  corresponding to a pH of about 4.5, but this is clearly not the  $\text{pH}_a$  for the MO technique (29).

The colorimetric comparator pH method was introduced in the early 1900s. For example, Clark stated that with care one could reproduce the pH of a well-buffered solution to within 0.1 or even 0.05 units (36). He pointed out the danger of using this technique on poorly buffered solutions, but with few exceptions this warning has apparently gone unnoticed (14, 43). A report by Zimmerman and Harvey, who noted that indicator addition will change the pH of the sample, was referred to by Hendrey et al. but they used the old colorimetric data without correction in a comparison study anyway.

The color indicator solutions are in the concentration range of  $10^{-4}$  to  $10^{-3}$  M; when using a comparator technique, they are diluted about 10 times (10 drops or about 0.5 mL in a total volume of 5, 5.5, or 10.5 mL depending on specifications), resulting in an indicator concentration of  $10^{-4}$  to  $10^{-5}$  M. Any solution with an alkalinity in this range or lower, such as soft-water lakes, will be modified by the dilution of the indicator. The pH will increase or decrease depending upon the pH of the dye compared to the actual solution pH. Table 2 gives the actual concentrations of indicators and the pK values as taken from Clark and SM. The solution recipes in SM and Clark are made by the addition of an equal molar quantity of NaOH to the acid dye; if the amount of NaOH added is quantitatively precise, one may presume a stoichiometry of the dye solution of  $[\text{NaIn}]$  with  $[\text{Na}^+] = [\text{In}^-] + [\text{HIn}]$  for the dissociated and protonated forms. To determine the correction in the H-ion concentration due to the addition of dye, we can write the protolyte charge balance for the original solution; according to equation 14:  $B = [\text{Alk}]$ , where  $B = \sum z_i[M_i] - 2[\text{SO}_4^{2-}]$  and  $[\text{Alk}]$  is the original alkalinity (eq/L). After the addition of the indicator, the electroneutrality condition can be written:

$$B' + [\text{HIn}]' = [\text{Alk}]', \quad (31)$$



TABLE 2  
Concentrations and acid dissociation constants for dyes used in pH color comparator<sup>a</sup>

Dye	Working solution Concentration <sup>b</sup> (millimolar)	-log K <sub>1</sub>
Metacresol purple	1.05	1.51
Thymol blue	0.86	1.5
Bromophenol blue	0.60	4.0
Bromocresol green	0.57	4.7
Chlorophenol red	0.95	6.0
Bromophenol red	0.78	6.2
Bromocresol purple <sup>c</sup>	0.74	6.3
Bromothymol blue <sup>c</sup>	0.64	7.1
Phenol red <sup>c</sup>	1.13 (0.57)	7.9
Cresol red <sup>c</sup>	1.05 (0.53)	8.3
Metacresol purple	1.05 (0.53)	8.3
Thymol blue <sup>c</sup>	0.86 (0.43)	8.9

<sup>a</sup> Data from "Standard Methods" (38, 41-43) and Clark (36).

<sup>b</sup> Concentration values in brackets are from "Standard Methods" recipes.

<sup>c</sup> Dyes commonly used.

where [Alk]' is the new alkalinity due to dilution and addition of HIn/In<sup>-</sup>, and B' and [HIn]' are the new values of B and [HIn] due to dilution. Making the approximation  $C_T \approx [H_2CO_3] + [HCO_3^-]$ , one can substitute in equation 31:  $B' = [Alk] V / (V + v_1)$ ,

$$[HIn]' = \frac{C_1 v_1 [H^+]_c}{(V + v_1) ([H^+]_c + K_1)}$$

and

$$[Alk]' = \frac{V}{V + v_1} \left\{ \frac{C_T K_1}{([H^+]_c + K_1)} \right\} - [H^+]_c$$

to obtain

$$[Alk] V + \frac{C_1 v_1 [H^+]_c}{[H^+]_c + K_1} = V \left\{ \frac{C_T K_1}{([H^+]_c + K_1)} \right\} - [H^+]_c (V + v_1), \quad (32)$$

where  $V$  = volume of sample (L);  $v_1$  = volume of indicator added (L);  $C_1$  = concentration of indicator solution (M);  $K_1 = [H^+] [In^-] / [HIn]$ ; and  $[H^+]_c = [H^+]$  measured with the colorimetric method.

If we assume (H11) that the total

carbonate amount is unchanged by addition of indicator, the sample of H-ion concentration ( $[H^+]_s$ ) can be obtained from rearrangement of equation 32, and substitution of

$$C_T = \frac{([Alk] + [H^+]_s) ([H^+]_s + K_1)}{K_1} \quad (33)$$

(obtained from rearrangement and substitution of  $C_T \approx [H_2CO_3^*] + [HCO_3^-]$ ,  $[Alk] \approx [HCO_3^-] - [H^+]_s$ , and  $K_1 = [H^+] [HCO_3^-] / [H_2CO_3^*]$ ), which gives

$$[H^+]_s^2 + ([Alk] + K_1) [H^+]_s - \left[ \frac{[H^+]_c + K_1}{V} \right] \left[ (V + v_1) [H^+]_c + V [Alk] - \frac{V K_1 [Alk]}{[H^+]_c + K_1} + \frac{C_1 v_1 [H^+]_c}{[H^+]_c + K_1} \right] = 0. \quad (34)$$

This can be solved as a quadratic for  $[H^+]_s$ . Assuming (H12) that  $[HCO_3^-]$  equals the alkalinity, equation 34 reduces to

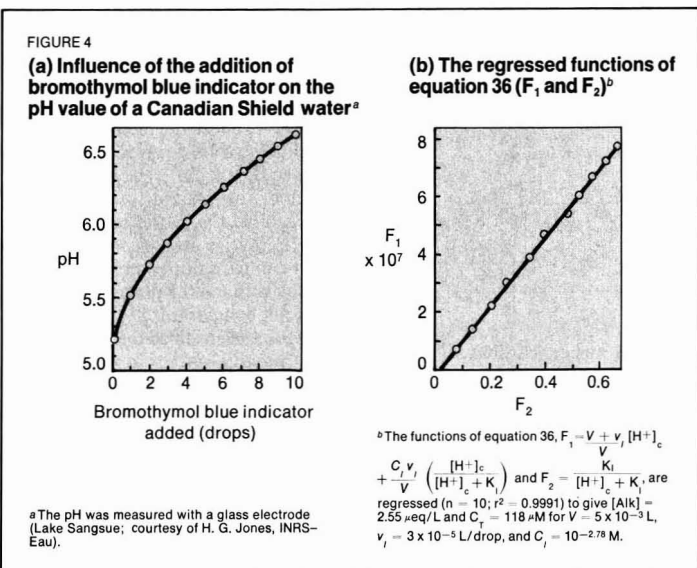
$$[H^+]_s \left[ \frac{C_1 v_1 [H^+]_c}{[H^+]_c + K_1} \right] \times \left[ \frac{[H^+]_c + K_1}{V [Alk]} \right] + [H^+]_c. \quad (35)$$

As an example, the corrections developed above can be used on published historical data. Burns et al. (29) report a MO alkalinity of 146  $\mu\text{eq/L}$  and a colorimetric pH of 6.77 for historical data of surface waters (average values) in North Carolina; the 1980 results were a pH of 6.51 and a Gran alkalinity of 80  $\mu\text{eq/L}$ . Using the experimentally determined corrections

in this paper for MO alkalinity, we obtain 65  $\mu\text{eq/L}$  for historical data, which is less than the 1980 data. Bromothymol blue was the indicator used for most colorimetric pH determinations in the 6-7 range; however, sample volumes were usually either 4.5, 5, or 10 mL. Assuming that bromothymol blue ( $C_1 = 0.64 \times 10^{-3}$  M;  $K_1 = 10^{-7.1}$ ) was used as the indicator, we calculated the original pH with equation 34 for various values of  $v_1$  and  $V$ . When the MO alkalinity value is corrected according to the present paper, one obtains pH values of 6.17 ( $v_1 = 5 \times 10^{-4}$  L;  $V = 4.5 \times 10^{-3}$  L), 6.21 ( $v_1 = 5 \times 10^{-4}$  L;  $V = 5 \times 10^{-3}$  L), and 6.40 ( $v_1 = 5 \times 10^{-4}$  L;  $V = 10^{-2}$  L), respectively; when the MO alkalinity is not corrected, one obtains pH = 6.57 ( $v_1 = 5 \times 10^{-4}$  L;  $V = 10^{-2}$  L). These values are to be compared to the recent measurements of 6.51. The New Hampshire data given in the paper cannot be adjusted without some other assumption because no alkalinity data are given. However, the historical colorimetric pH value would be reduced since bromothymol blue was the indicator used (40).

The basis of the above calculation can be tested on the data in Figure 4a, which show the change in pH of a Canadian Shield water sample, measured potentiometrically, with addition of bromothymol blue indicator. Equation 32 can be rearranged to

$$[H^+]_c + \frac{C_1 v_1}{V} \left( \frac{[H^+]_c}{[H^+]_c + K_1} \right) = -[Alk] + \left( \frac{K_1}{[H^+]_c + K_1} \right) C_T. \quad (36)$$



This function is linear with an intercept of  $-[\text{Alk}]$  and a slope of  $C_T$ ; from a least-square fit (Figure 4b), we obtain  $[\text{Alk}] = 2.55 \times 10^{-6} \text{ eq/L}$  and  $C_T = 118 \times 10^{-6} \text{ M}$  for the data sets in Figure 4a. The sample pH calculated from equations 33 is then 5.20, identical to the measurement with a glass electrode.

There does not seem to be any reason why historical color comparator pH data cannot be used if certain precautions are observed and corrections made. To make the adjustments, one must know the exact procedure used, and the alkalinity or a surrogate property must be available. Then equations 34 and 35 can be used to calculate the actual pHs.

Clark has summarized the possible errors and interferences that must be considered in measuring pH with a color comparator (36). In addition to the weak buffer correction, possible interferences from turbidity and natural color must be considered. Many low-pH and poorly buffered natural waters are colored. Precipitation would generally have a negligible interference problem from turbidity and natural color. Furthermore, for any pH value  $< 5$ , the calculation would be more straightforward, since the bicarbonate ion concentration would be negligible.

The equations for precipitation solutions with negligible  $(\text{HCO}_3^-)$  are derived as follows. For the initial sample solution,

$$[\text{H}^+]_s = A, \quad (37)$$

where A is the sum of anion charges minus the sum of cation charges; for the color comparator solution,

$$[\text{H}^+]_c + [\text{HIn}]' = A', \quad (38)$$

where A' is the new value of A due to dilution. Substitution of equation 37 into equation 38 along with other notation and rearrangement for the solution of  $[\text{H}^+]$  gives

$$[\text{H}^+]_s = \frac{Cv_1}{V} \left[ \frac{[\text{H}^+]_c}{[\text{H}^+]_c + K_i} + [\text{H}^+]_c \left[ \frac{V + v_1}{V} \right] \right], \quad (39)$$

## Summary and conclusions

This review has developed the basis for various acidification models and has shown the basis for assessment of historical pH and alkalinity data. It is not an attempt to make an argument for or against trends in atmospheric acidic deposition and change in watersheds in the past decades. Rather, the discussion has tried to define a

rigorous basis for the development of models and analysis and for the interpretation of pH and alkalinity data. We hope that this discussion will assist in a more careful and rigorous development of theory, of experimental design, and data analysis.

Acidification models are based upon the electroneutrality condition and CAW. Whenever data are available, all major ions ( $\text{Na}^+$ ,  $\text{K}^+$ ,  $\text{Ca}^{+2}$ ,  $\text{Mg}^{+2}$ ) should be considered;  $[\text{Ca}^{+2}]$  must be regarded as an approximate substitute for  $\sum z_i [\text{M}_i]$ . In such cases, only intrabasin comparisons should be made and only when it is known that the soil/lithological-water reactions are similar throughout the basin; interbasin comparisons assume a constant b value. The boundary drawn between affected (acidified) and unaffected (unacidified) media in the pH vs. log  $[\text{Ca}^{+2}]$  graphs is subjective.

Calculations in none of the models suggested so far consider oxidation-reduction protolyte reactions involving C, N, and S. The inability to obtain a zero intercept in  $\sum z_i [\text{M}_i]$ -alkalinity plots for unaffected waters suggests that other processes are in fact important. In some cases, it may be possible to define sources of sulfate through the use of stable sulfur isotope studies. Differences in  $\delta^{34}\text{S}$  and  $\delta^{18}\text{O}$  ( $\text{SO}_4^{-2}$ ) values between precipitation and water imply that complicating reactions of sulfur are occurring in a specific system.

In comparing historical water quality data with recent data, the following points should be noted. The type of sampling container must be considered because most container material available before 1960 could have contributed alkalinity to the water sample. The analytical method used to obtain the historical data must be known precisely, and experiments should be carried out on representative samples to check the method. The MO alkalinity technique gives an additional 80  $\mu\text{eq/L}$  alkalinity beyond the end point of low-alkalinity samples; the precision of the method is about  $\pm 20 \mu\text{eq/L}$ . With suitable corrections, the color comparator pH method can give results within  $\pm 0.1$  pH units. Historical color comparator pH data for precipitation seems to be the simplest and most reliable system to work with to establish trends in pH.

## Acknowledgment

Before publication, this article was read and commented on for suitability as an *ES&T* feature article by Dr. Herbert E. Allen, Department of Environmental Engineering, Illinois Institute of Technology, Chicago, Ill. 60616; Dr. S.J. Eisenreich, Department of Civil and Mineral Engi-

neering, University of Minnesota, Minneapolis, Minn. 55455; and Dr. I.H. Suffet, Department of Environmental Engineering and Science, Drexel University, Philadelphia, Pa. 19104.

## References

- (1) Committee on the Atmosphere and Biosphere. "Atmosphere-Biosphere Interactions: Toward a Better Understanding of the Ecological Consequences of Fossil Fuel Combustion"; National Academy Press: Washington, D.C., 1981.
- (2) Kramer, J. R. In "Restoration of Lakes and Inland Waters"; U.S. EPA 440/5-81-010, 1981, p. 478.
- (3) Dochinger, L. S.; Seliga, T. A. "Proceedings of the First International Symposium on Acid Precipitation and the Forest Ecosystem"; USDA Forest Service Gen. Tech. Rep. NE-23. Upper Darby, Pa., 1976.
- (4) Drablos, D.; Tollan, A., Eds. "Proc. Int. Conf. Ecol. Impact Acid Precip."; Sandfjord, Norway, 1980.
- (5) Harvey, H. H.; Pierce, R. C.; Dillon, P. J.; Kramer, J. R.; Whelpdale, R. M. "Acidification in the Canadian aquatic environment: scientific criteria for assessing the effects of acidic deposition on aquatic ecosystems"; National Research Council of Canada, Associate Committee on Scientific Criteria for Environmental Quality, NRCC No. 18475, 1981.
- (6) U.S.-Canada, Memorandum of intent on transboundary air pollution; Interim report, February 1981.
- (7) Almer, B.; Dickson, W.; Ekström, E.; Hörnström, E. In "Sulfur in the Environment, Part II. Ecological Impacts"; Nriagu, J. O., Ed.; John Wiley and Sons, Inc.: New York, 1978; p. 271.
- (8) Henriksen, A. In "Proc. Int. Conf. Ecol. Impact Acid Precip."; Drablos, D.; Tollan, A., Eds.; Sandfjord, Norway, 1980; p. 68.
- (9) Harvey, H. H. *Verh. Intern. Verein. Limnol.* **1975**, *19*, 2406.
- (10) Yan, N. D. *Water Air Soil Pollut.* **1979**, *11*, 43.
- (11) Norton, S. A.; Dubiel, R. S.; Sasseville, D. R.; Davis, R. B. *Verh. Intern. Verein. Limnol.* **1978**, *20*, 538.
- (12) Brossset, C. *Water Air Soil Pollut.* **1979**, *11*, 57.
- (13) Seymour, M.; Clayton, J. W., Jr.; Fernando, F. *Anal. Chem.* **1977**, *49*, 1429.
- (14) Stumm, W.; Morgan, J. J. "Aquatic Chemistry: An Introduction Emphasizing Chemical Equilibria in Natural Waters," 2nd ed.; John Wiley and Sons: New York, 1980.
- (15) Thompson, M. E.; Bennett, E. B. In "Restoration of Lakes and Inland Waters"; U.S. EPA 440/5-81-010, 1981.
- (16) Henriksen, A. *Nature* **1979**, *278*, 542.
- (17) Thompson, M. E., personal communication, 1981.
- (18) Dillon, P. J.; Jeffries, D. S.; Scheider, W. A.; Yan, N. D. In "Proc. Int. Conf. Ecol. Impact Acid Precip."; Drablos, D.; Tollan, A., Eds.; Sandfjord, Norway, 1980; p. 212.
- (19) Dickson, W. In "Proc. Int. Conf. Ecol. Impact Acid Precip."; Drablos, D.; Tollan, A., Eds.; Sandfjord, Norway, 1980; p. 75.
- (20) Glass, G. E. In "Proc. Int. Conf. Ecol. Impact Acid Precip."; Drablos, D.; Tollan, A., Eds.; Sandfjord, Norway, 1980; p. 112.
- (21) Jones, H. G.; Quellet, M.; Brakke, D. F. In "Proc. Int. Conf. Ecol. Impact Acid Precip."; Drablos, D.; Tollan, A., Eds.; Sandfjord, Norway, 1980; p. 226.
- (22) Wright, R. F.; Harriman, R.; Henriksen, A.; Morrison, B.; Caines, L. A. In "Proc. Int. Conf. Ecol. Impact Acid Precip."; Drablos, D.; Tollan, A., Eds.; Sandfjord, Norway, 1980; p. 248.
- (23) Drablos, D.; Sevaldrud, I. In "Proc. Int. Conf. Ecol. Impact Acid Precip."; Drablos, D.; Tollan, A., Eds.; Sandfjord, Norway, 1980; p. 354.

- (24) Thompson, M. E., personal communication, 1980.
- (25) Watt, W. D.; Scott, D.; Ray, S. *Limnol. Oceanogr.* **1979**, *24*, 1154.
- (26) Henriksen, A. *Vann* **1972**, *7*, 65.
- (27) Dillon, P. J.; Yan, N. D.; Scheider, W. A.; Conroy, N. *Archs. Hydrobiol. Ergeb. Limnol.* **1979**, *13*, 317.
- (28) Holt, B. D.; Kumar, R.; Cunningham, P. T. *Science* **1982**, *217*, 51.
- (29) Burns, D. A.; Galloway, J. N.; Hendrey, G. R. *Water Air Soil Pollut.* **1981**, *16*, 277.
- (30) Norton, S. A.; Davis, R. B.; Brakke, D. V. "Response of Northern New England Lakes to Atmospheric Inputs of Acids and Heavy Metals"; Rep. University of Maine; Orono, Land and Resource Center, 1981.
- (31) Hendrey, G. R.; Galloway, J. N.; Norton, S. A.; Schofield, C. L.; Schaffer, P. W.; Burns, D. A. "Biological and Hydrochemical Sensitivity of the Eastern United States to Acid Precipitation"; U.S. EPA Rep. EPA-600/3-80-024, 1980.
- (32) Cogbill, C. V.; Likens, G. E. *Water Resour. Res.* **1974**, *10*, 1133.
- (33) Likens, G. E. *Chem. Eng. News* **1976**, *54*, 29.
- (34) Herman, F. A.; Gorham, E. *Tellus* **1957**, *9*, 180.
- (35) Kerekes, J. J. In "Proc. Int. Conf. Ecol. Impact Acid Precip.," Drablos, D.; Tollan, A., Eds.; Sandefjord, Norway, 1980; p. 232.
- (36) Clark, W. M. "The Determination of Hydrogen Ions," 3rd ed.; Williams and Wilkins: Baltimore, 1928.
- (37) Corning Glass Works, personal communication, 1982.
- (38) APHA. "Standard Methods for the Examination of Water and Sewage," 11th ed.; American Public Health Association: New York, 1960.
- (39) Bacon, F. R.; Bureh; D. G. *J. Am. Ceram. Soc.* **1941**, *24*, 29.
- (40) New Hampshire Fish and Game Department, Survey Reports 8a, 8b, 8c; Concord, N.H., 1970, 1972, 1977.
- (41) APHA. "Standard Methods for the Examination of Water and Sewage," 7th ed.; American Public Health Association: New York, 1933.
- (42) APHA. "Standard Methods for the Examination of Water and Sewage," 8th ed.; American Public Health Association: New York, 1938.
- (43) APHA. "Standard Methods for the Examination of Water and Sewage," 9th ed.; American Public Health Association: New York, 1946.
- (44) Kramer, J. R. In "Treatise of Water Analysis"; Minear, R., Ed.; Academic Press: New York, 1982.



**James R. Kramer** is professor in the Geology Department of McMaster University, Hamilton, Ontario. He has worked on the chemistry of the Great Lakes and Precambrian Shield Lakes and is currently interested in aluminum speciation and toxicity to fish.

**André Tessier** is professor of aquatic chemistry at INRS-Eau, a research center of the Université du Québec. His main research interest is in the area of trace metal interactions with aquatic organisms.

# A World of Opportunity— FREE!



Your guide to  
new knowledge  
in your own field  
... other fields  
in chemistry ...  
management  
and commu-  
nication skills.

- 7 new courses listed for the first time.
- 55 courses to choose from — offered in Analytical Chemistry . . . Organic and Organometallic Chemistry . . . Polymer Chemistry . . . Chemical Engineering/Statistics . . . Literature Aids . . . Business and Professional Development.
- All courses developed and presented by well known experts, and include course-integrated workbooks.

Begin to benefit right away! Send for  
your FREE copy of the ACS 1982  
Audio Course Catalog today!

American Chemical Society/Education Division  
1155 16th Street, N.W.  
Washington, D.C. 20036

Please send my personal copy of the ACS 1982 Audio Course Catalog. No cost or obligation.

Name \_\_\_\_\_

Organization \_\_\_\_\_

Address \_\_\_\_\_

City \_\_\_\_\_ State \_\_\_\_\_ Zip \_\_\_\_\_

Need extra copies—for management . . . organization library . . . others? List names and addresses on separate sheet of paper and mail with this coupon.

# Water chemicals codex

*The National Academy of Sciences has recommended specifications for the purity of chemicals used to treat drinking water; the first compilation covers direct additives*

**Robert Rehwoldt**

*National Research Council  
Washington, D.C. 20418*

The availability and production of potable water are matters of great national and worldwide concern. In the U.S. alone, an estimated 1-2 billion gal of drinking water must be provided each day. To comply with health and other applicable standards for treating that amount of potable water, suppliers used more than 1.2 million tons of chemicals in 1981, according to an American Water Works Association (AWWA) report (Table 1).

Large segments of the U.S. population come in contact with chemical additives used for water disinfection, coagulation, softening, corrosion control, fluoridation, and other water treatment functions. Thus, in 1979, a memorandum of understanding was signed by the Food and Drug Administration and the Environmental Protection Agency, by which responsibility for monitoring and controlling these additives, whether direct or indirect, was vested in the EPA. Not long thereafter, in response to a request from EPA, the National Research Council, an arm of the National Academy of Sciences, undertook to recommend minimum acceptable purity specifications for such substances.

Accordingly, the Committee on Water Treatment Chemicals was formed and entrusted with the task of developing such specifications, first for direct additives, and later, as feasible, for indirect additives. After two years of deliberations, the committee produced a Water Treatment Chemicals Codex. The codex is meant to supplement existing compendia on water treatment chemicals and is confined to information on purity as it is related to health. It does not address product

performance, packaging, storage, or handling.

Analytical procedures were selected from compendia on methodology and protocol, adopted from manufacturers, or derived from methods set forth in the scientific literature. Data on toxicologic aspects were obtained from the scientific literature, from chemical manufacturers, and from the Code of Federal Regulations.

## Purity requirements

The committee recognizes that the assignment of purity requirements depends upon the toxicity of the contaminant and the use patterns of the additive. Although the interpretation of toxicological data concerning these contaminants is at times controversial and depends upon an evolving science, the toxicological data base for water treatment chemical impurities is improving steadily.

To arrive at its recommended contaminant limits, the committee met with EPA with the aim of compiling a list of priority chemicals (Table 2). This list was then categorized according to use pattern, that is, those chemicals used in coagulation and flocculation; softening, precipitation and pH control; disinfection and oxidation; and miscellaneous treatment applications. In drafting the monographs in each category, a subgroup of the committee reviewed current data on known impurities in the chemicals, grades of manufactured products, use patterns, and other variables.

The committee also developed a list of impurities to be considered. Initially, the list was identical to that of the regulated inorganic impurities specified by the National Interim Drinking Water Regulations developed in response to the Safe Drinking Water Act of 1974. This list was subsequently modified to include those substances for which there is evidence of occurrence as contaminants in water treatment chemicals. The toxicology subgroup of the committee supplied toxicological data on these substances, including information on possible genotoxic or epigenetic (nongenetic cellular damage) effects.

TABLE 1  
**Chemicals used for water treatment in 1981 (tons)**

### Coagulation and flocculation

Alum	152 801
Ferric chloride	15 583
Ferric sulfate	6 196
Polyelectrolytes	4 280
Sodium aluminate	2 650
Ferrous sulfate	1 912
Sodium silicate	1 752
Diatomaceous earth	700
Clay (bentonite)	104

### Disinfection and oxidation

Hypochlorite	440 222
Chlorine	104 477
Sodium chlorite	6 369
Ammonia gas/liquid	2 497
Potassium permanganate	793
Ammonium salts	452

### Precipitation and softening

Calcium oxide	349 312
Hydrated lime	86 313
Sodium hydroxide	49 093
Carbon dioxide	18 604
Soda ash	15 805

### Miscellaneous reagents

Fluoride compounds	37 327
Activated carbon <sup>a</sup>	9 287
Phosphates	8 891
Sodium chloride	6 369
Copper sulfate	1 051
Other chemicals	1 521

<sup>a</sup>Absorbent

Source: AWWA, "1981 Water Utility Operating Data," Denver, Colo., June 1981

# NH<sub>3</sub> FeSO<sub>4</sub> CaO Na

## Recommended maximum impurities

In general, the committee felt that it would be appropriate to utilize the maximum contaminant level (MCL) for calculating the allowable contaminant level contributed by an impurity in a water treatment chemical, unless there was no current MCL for that impurity, or where there was new information concerning either the toxicity of the contaminant or the current status of the MCL.

An MCL was thus converted to a Recommended Maximum Impurity Content (RMIC) for the additive by the following equation:

$$\text{RMIC} = \frac{\text{MCL}}{\text{Maximum dosage} \times \text{safety factor}} = \frac{\text{MCL (mg/L)} \times 10^6 \text{ mg/kg}}{\text{MD (mg/L)} \times \text{SF}}$$

where maximum dosage (MD) for the water treatment chemical was based

on maximum patterns known by the committee to be representative of water treatment practice.

The safety factor (SF) used in the calculation of the RMIC was 10, reflecting the view of the committee that no more than 10% of a given MCL value should be contributed by a given impurity in a water treatment chemical. Some may argue for a higher safety factor, but 10% was deemed reasonable by the committee in view of other uncertainties and approximations relating to the fate of impurities introduced during treatment.

A sample calculation of an RMIC is performed as follows. Contaminant mercury (Hg):

$$\text{MCL} = 0.002 \text{ mg/L}$$

Water treatment additive:

$$\text{Maximum dosage (MD)} = 500 \text{ mg/L}$$

$$\text{Safety factor} = 0.1$$

RMIC

$$= \frac{0.002 \text{ mg Hg/L} \times 10^6 \text{ mg/kg}}{500 \text{ mg additive/L} \times 0.1}$$

$$\text{RMIC} = 0.4 \text{ mg Hg/kg additive}$$

The codex contains RMIC values for impurities of concern at selected additive dose levels, which are reported to one significant figure. RMIC values defining the purity of each water treatment chemical are also contained in individual monographs and may be used as guidelines for the water works industry. At present, the codex contains 26 monographs; an additional 15 are expected to be completed by the end of this year. The user should note that if actual dosages applied exceed those upon which the monograph is based, appropriate RMIC values should be extrapolated from the table. In addition, although no documented cases were found, if a contaminant is suspected of creating additional health

## Codex format

The basic form of the codex is a series of individual monographs, each dealing with a specific compound. Each monograph contains the following information:

- chemical name and alternative acceptable names
- Chemical Abstract Service number
- chemical formula and formula weight
- physical properties
- function
- use range
- purity requirements
- bulk sampling procedures
- analytical procedures
  - a) Sample preparation—special procedures are noted where appropriate. In cases where the chemical added is not soluble in water, the analytical procedures apply to a leachate of that material as obtained under the conditions described.
  - b) Sample analysis—techniques are given either as citations of existing recognized procedures or as procedures developed specifically for the monograph.

TABLE 2

### Water treatment chemicals included in the codex

Aluminum sulfate	Carbon dioxide	Sodium chlorite
Ammonia	Chlorine	Sodium fluoride
Ammonium hydroxide	Ferric chloride	Sodium hydroxide
Ammonium sulfate	Ferric sulfate	Sodium hypochlorite
Calcium hydroxide	Ferrous sulfate	Sodium metabisulfite
Calcium hypochlorite	Fluosilicic acid	Sodium silicofluoride
Calcium oxide	Potassium permanganate	Sodium polyphosphate, glassy
Carbon, activated, granular and powder	Sodium aluminate	Sulfur dioxide
	Sodium carbonate	

concerns because of radioactivity, RMIC values must be calculated in accordance with radiation limits set forth in the Code of Federal Regulations.

The RMIC levels are based upon information available to the committee. It is impossible to recommend maximum content levels for unusual or unexpected impurities, the presence of which would depend upon the method of manufacture and the quality of raw materials used. If unusual raw materials or unusual methods of manufacture go into the preparation of a treatment chemical, the user should require appropriate certification of purity from the vendor or manufacturer, to prove that the chemical is suitable for application to the making of potable water.

#### Analytical methods

Preferred sampling, sample preparation, and analytical methods for the determination of impurities are cited. Methods that are cited or appear in the codex should be considered as the preferred analytical procedures; alternative methods may be used if they can be shown to be equivalent.

It is recognized that a contaminant

in a water treatment chemical may require special sample preparation or analysis methods, because of the nature of the chemical matrix. For such chemicals, the recommended special procedures are included in the codex.

#### Some areas of concern

Although for the most part, the committee relied on published MCLs for recommending impurity limits, there were some areas of concern. For example, the RMIC values for lead are based upon an MCL of 0.05 mg L<sup>-1</sup>.

There is considerable evidence that lead is more widespread than has been previously thought and that lead poisoning is still a serious problem in the U.S. Therefore, even though the committee finally accepted the current MCL as a basis for calculating an RMIC for lead, supporting material submitted to EPA contained a recommendation that the agency critically evaluate the existing lead standard.

Another troublesome case is that of carbon tetrachloride, which is a common contaminant in the manufacture of chlorine. The committee felt that if it made no recommendation for maximum content, it would be shirking its

duty. However, any attempt to define health risks quantitatively in terms of exposure to a carcinogen—which carbon tetrachloride is suspected of being—is extremely complex; in many cases, appropriate data do not exist. EPA has published a notice of proposed rulemaking for volatile organics; and until that process is completed, the committee has recommended, an RMIC for carbon tetrachloride in chlorine of 100 mg kg<sup>-1</sup>.

The genotoxic or epigenetic potential of water treatment chemical impurities, which can present yet another problem, was evaluated on a case-by-case basis. Appropriate data bases were investigated, and published risk assessments or other exposure models were considered.

#### Review and revision

It is expected that the codex will be reviewed continuously and that annual supplements will be issued. The supplements may contain lists of additional chemicals and revisions of the monographs contained in the present codex, as well as revisions of analytical procedures. Distribution of the codex is planned for the end of this year. Information about ordering it can be obtained from the National Academy of Sciences, Washington, D.C. 20418.

It is hoped that the Water Treatment Chemicals Codex will be used in conjunction with other existing voluntary standards, such as those developed by the American Water Works Association. It is recommended that more extensive data bases on the purity of drinking water additives be developed and that this information be used continuously to revise and update the codex.

---

#### Committee members:

William H. Glaze (chairman)  
University of Texas, Dallas  
Richardson, Tex.

Charles A. Buescher  
St. Louis County Water Company  
St. Louis, Mo.

John H. Mahon  
Calgon Corporation  
Pittsburgh, Pa.

Nina I. McClelland  
National Sanitation Foundation  
Ann Arbor, Mich.

Gerald E. Stobby, 1980-81  
Dow Chemical Company  
Midland, Mich.

Robert S. Bryant  
Stauffer Chemical Company  
Westport, Conn.

Arnold E. Greenberg  
California Department of  
Health Services  
Berkeley, Calif.

J. Carrell Morris  
Harvard University  
Cambridge, Mass.

Ronald C. Shank  
University of California  
Irvine, Calif.

R. Rhodes Trussell  
James M. Montgomery Consulting  
Engineers  
Pasadena, Calif.

In carrying out its task, the committee was greatly aided by contributions from the toxicologists and persons experienced in analytical procedures:

Frank J. Baumann  
California Department of Health  
Services  
Los Angeles, Calif.

Robert K. Hinderer  
The B.F. Goodrich Company  
Cleveland, Ohio

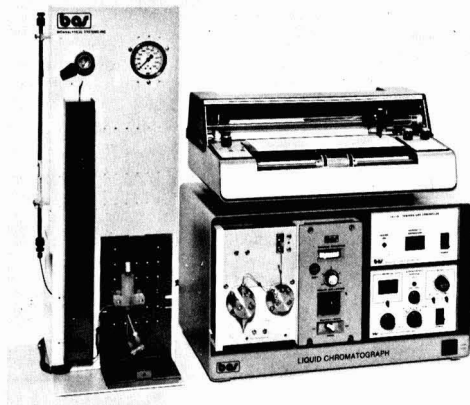
Joseph Connors  
Editor, *Standard Methods for the  
Examination of Water and  
Wastewater*  
Oakland, Calif.

Richard Larson  
University of Illinois  
Urbana, Ill.



*Robert Rehboldt is currently a senior staff officer of the National Research Council, National Academy of Sciences, in Washington, D.C. Prior to assuming his position at NRC he taught and conducted research on the toxicity of metal ions to aquatic communities. He has published a number of papers in that field and has acted as a consultant in environmental problems. He received his B.S. from Queens College in New York and a Ph.D. in analytical chemistry from Lehigh University.*

# PHENOLS AND AROMATIC AMINES?



We're the specialists in liquid chromatography for trace organic determinations. Let us know your problem. We will provide detailed applications support and a selection of instrumentation which will do your job in the most cost effective manner.

LC systems based on ultraviolet and/or electrochemical detection are tailor made for environmental analysis. Temperature control, gradient elution, automated trace enrichment, and column switching are options which may be adapted to your needs.

Circle the bingo card for general information, but if you want specific answers, write to our Environmental Services Department and tell them what you can about your samples.

**ANILINES • BENZIDINES • MOCA • PENTACHLOROPHENOL • CRESOLS • PARABENS • HYDROQUINONES**



**BIOANALYTICAL SYSTEMS INC.**

P.O. Box 2206 • W. Lafayette, IN 47906 • (317) 463-2505 • telex 276141 BAS WLAF

CIRCLE 3 ON READER SERVICE CARD

## Toxic Chemical and Explosives Facilities

Practical examples are provided on specific work practices and engineering controls for propellant and propulsion facilities, and for the production, storage, maintenance, surveillance, and demilitarization of explosives. Also included are design criteria for new university chemistry laboratories, and for the handling and transportation of toxic chemicals. ACS Symposium Series 96, 352 pages, 1979, ISBN 0-8412-0481-0, Cloth .....\$37.95

## Thermal Conversion of Solid Wastes and Biomass

Forty-nine chapters deal with the U.S. Dept. of Energy sponsored programs concerned with urban wastes and biomass; the conversion of wood to fuels, chemicals, and energy in the form of steam or electrical power; combustion processes; and the densification of solid waste and biomass to produce solid fuels with more desirable physical properties. ACS Symposium Series 130, 747 pages, 1980, ISBN 0-8412-0565-5, Cloth .....\$57.50

## ACS Titles in WASTE MANAGEMENT

### Monitoring Toxic Substances

State-of-the-art techniques for monitoring toxic substances: the Salmonella/microsome mutagenicity test, and cell-culture in-vitro assay tests; instrumental analytical techniques: liquid and gas chromatography/mass spectrometry for organic pollutants in wastewaters and drinking waters; atomic absorption and inductively coupled plasma-atomic emission spectroscopy for trace elements in environmental samples; and surface analysis techniques. ACS Symposium Series 94, 289 pages, 1979  
ISBN 0-8412-0480-2, Cloth .....\$31.95  
ISBN 0-8412-0656-2, Paper .....\$19.00

### Transplutonium Elements — Production and Recovery

This state-of-the-art volume emphasizes the continuing importance of industrial-scale production, separation, and recovery of transplutonium elements. Among the processes discussed are solvent extraction, cation exchange chromatography, precipitation, partitioning, LiCl-based anion exchange chromatography, and calcination. ACS Symposium Series 161, 302 pages, 1981, ISBN 0-8412-0638-4, Cloth .....\$37.00

### Radioactive Waste in Geologic Storage

Seventeen papers cover the DOE program for long-term isolation of radioactive waste, the biogeochemistry of actinides, ceramic forms for nuclear waste, sorption behavior studies on clay minerals, WIPP, and the consequences of radiation from sorbed transplutonium. ACS Symposium Series 100, 344 pages, 1979, ISBN 0-8412-0498-5, Cloth .....\$35.95

### Particulates in Water: Characterization, Fate, Effects, and Removal

Topics include the characterization of surface chemical properties of oxides in natural waters; redox coprecipitation mechanisms of manganese oxides; adsorption reactions of nickel species at oxide surfaces; and poliovirus adsorption on oxide surfaces. Advances in Chemistry Series 189, 401 pages, 1980, ISBN 0-8412-0499-3, Cloth .....\$59.50

CALL TOLL FREE (800) 424-6747 or Order From:

SIS Dept. 13 American Chemical Society  
1155 Sixteenth Street, N.W. Washington, D.C. 20036

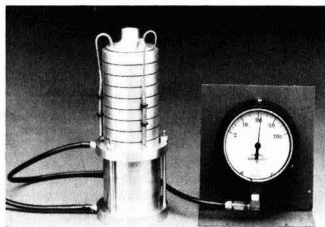
# ES&T PRODUCTS

## Hi-vol sampler

This system is suitable for size-specific sampling of inhalable particulates. It maintains an airflow rate with an accuracy of  $\pm 1$  SCFM. It is unaffected by wind speeds from 2–24 km/h or by  $\pm 20^\circ$  variations in wind direction. General Metal Works 101

## Drinking water filter

Filter, which consists of activated charcoal impregnated with silver, removes bacteria, chlorine, impurities, color, and unpleasant taste from water. According to the manufacturer, the silver additive enables the charcoal filter to make water completely bacteria-free. The filter can be mounted directly onto a faucet and is capable of filtering 5000 L of drinking water. Interag 102



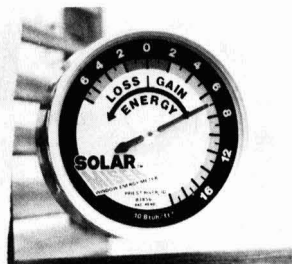
## Low-pressure impactor

Suitable for sizing ultrafine aerosols such as diesel particulates or smoke, impactor classifies particulates into 14 size ranges from 0.08–35  $\mu\text{m}$ . A pressure tap downstream of the critical orifice connected to an absolute pressure gauge allows precise control of the cut points of the low-pressure stages. Anderson Samplers 103

## Digital turbidimeter

Instrument is suitable for all types of filtration, clarification, and quality control. It covers ranges of 0–1, 0–10, and 0–200 NTU and interfaces with popular microcomputers for results analysis and automatic filtration control. Hellige 104

*Companies interested in a listing in this department should send their releases directly to Environmental Science & Technology, Attn: Products, 1155 16th St., N.W., Washington, D.C. 20036*



## Window energy meter

Meter attaches to a window and measures in Btu/h energy flow in and out of windows. The device is designed to work with any heating or cooling system to allow consumers to calculate how much energy (and consequently, energy dollars) is being lost or gained through the windows. Solar Miser 105

## Precision rain gauges

Tipping-bucket rain gauge uses two calibrated buckets with a sensitivity of 0.01 in. The tipping of the assembly causes a momentary closure of a mercury switch, which can be logged on an event recorder or an electromechanical event counter. WeatherMeasure 106

## Data logging thermometer

Hand-held thermocouple thermometer has a range of  $-148$ – $2502^\circ\text{F}$  and an accuracy of 0.1%. Both normal and relative temperature data can be automatically logged in  $^\circ\text{F}$  or  $^\circ\text{C}$  at preset intervals. At the maximum 4-h interval, the instrument will operate unattended for 5 d. Maximum and minimum readings are automatically stored for display at any time. Caspar Integrated Systems 107

## Computer interface

Device connects an Apple II computer directly to eight strain-gauge load cells or Whitston bridge pressure transducers. Eight floating input instrumentation amplifiers also provide stabilized currents to the load cells. Resolution is one part in 4000. The interface is supplied with supporting programs that allow automatic zeroing and scale adjustments to read in pounds, grams, kilograms, or millimeters Hg. Columbus 108

## Data logger

Portable data logger operates for long periods without external power supplies. The unit has a solid-state memory for up to  $20 \times 10^3$  data points. Special functions options exist for multiple thresholds, threshold-dependent scans and alarms, signal averaging, engineering unit conversion, and maximum and minimum values. The data logger is designed for a wide variety of field applications including weather monitoring and environmental and agricultural research. Crodata 109

## ac-line voltage regulators

These maintain output voltages to within  $\pm 0.5\%$  or better and are insensitive to load changes and frequency changes up to  $\pm 10\%$ . They do not introduce waveform distortion or any harmonics. Bypass circuit breakers and isolation transformers are available as options. George Kelk Ltd. 110

## Temperature monitor

Six- or 12-channel temperature monitor can be used for multipoint temperature monitoring of bearings, generator field windings, and engine exhaust and cylinder temperatures. Up to 12 points or locations can be monitored continuously with inputs consisting of RTDs, ungrounded thermocouples, or other transducers. The unit has both visual and relay alarms. Dynalco 111

## Sterile tubes

Polystyrene and polypropylene  $12 \times 75$ -mm sterile tubes have a two-position cap. With the polyethylene cap in the closed but unsealed position, samples are kept aerobic for microbiological procedures. When the cap is in the sealed position, the tubes can be used for laboratory storage, transfer, and centrifuge applications. Sarstedt 112

*Need more information about any items? If so, just circle the appropriate numbers on one of the reader service cards bound into this issue and mail in the card. No stamp is necessary.*



### Air-flow transducers

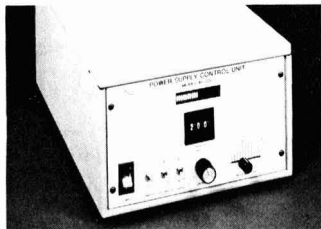
Measure air flow and velocity electronically with 20 selectable ranges from 0-12 000 ft/min and  $\pm 2\%$  full-scale accuracy. The transducers are compatible with computers, data loggers, and air monitoring systems. Sierra Instruments 113

### Emission monitor

Instrument uses glass fiber optic cables around the outside of smokestacks to measure opacity. It has a set-point alarm, a 1-6 min integrator, automatic exit correction, and an air-operated lens cleaning unit. The opacity output is displayed on a strip chart recorder or data logger. Datatest 114

### Radiometer

Designed for use in salt gradient solar ponds, this radiometer measures the energy interchange between the various thermal gradient levels. The remotely switchable modes of operation enable the instrument to measure radiant energy in the upward or downward directions, or the net balance. The unit has a flat spectral response from 0.3-2.8  $\mu\text{m}$  and is linear from 0-100 °C. Hollis Geosystems 115



### Power supply

Device delivers a dc voltage to a thermal conductivity detector or a gas density balance. Two models are available: the 40-200 hot-wire supply and the 40-400 thermistor supply. The 40-200 uses thumbwheel switches to set current and makes use of a bar readout. The 40-400 uses current control and meter readout. Both models have solid-state components. GOW-MAC Instrument 116

### Thermometer calibration cells

Fixed-point cells use the thermometric freezing points of high-purity metals (99.999%) for precise meteorological calibration of thermometers. The metal is contained in a graphite crucible that is enclosed in a quartz envelope filled with inert gas at a pressure of 1 standard atm at the freezing temperature. Freezing-point cells for the following metals are available: indium, tin, lead, zinc, aluminum, and silver. Yellow Springs Instrument 117

# TOX Plus TRihalOMETHANES

### The New Model 610 — a screening machine.

The New Model 610 TOX Analyzer is a rapidfire screening analyzer for organic halogens — plus, it can be equipped to perform the EPA's specified procedure for analysis of trihalomethanes! The screening approach can save the cost (hundreds of dollars) of detailed specific analyses on every single sample.

### Surrogate tests.

Purgeable Organic Halogen (POX) tests may be regarded as a surrogate for certain highly specific measurements, including those for trihalomethanes. Non-purgeable Organic Halogens (NPOX) can be used as a surrogate test for pesticides, PCBs, and certain other pollutants in water. Both POX and NPOX comprise TOX, and are separately measured by the Model 610. A surrogate test can be used to determine whether more specific testing is warranted. In ruling out those samples where contaminants of interest are clearly not present, the Model 610 can save a tremendous amount of money. And where trihalomethanes are not ruled out — the 610 has the capability for this key specific analysis. The combination, TOX plus trihalomethanes, makes excellent sense.

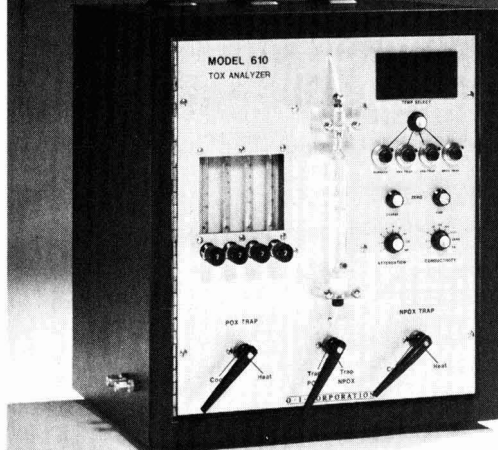
### Those "Other" Contaminants.

Chlorine may react with natural organic compounds present in water to form chlorinated humics of unknown structure. These compounds can be detected as a group by the Model 610. This feature is especially useful in making before-and-after evaluations of filtration and other purification techniques.

### Buy one.

There's nothing like it for speed. Sample goes in, result comes out. Period. Write for a detailed brochure, or call (713) 693-1711.

<sup>1</sup>"The analysis of trihalomethanes in finished water by the purge trap methods," U.S. Environmental Protection Agency, Environmental Monitoring and Support Laboratory, Cincinnati, Ohio, September 9, 1977.



The Model 610. For TOX, POX, NPOX and, as an accessory capability, trihalomethanes. An unbeatable combination.

## O·I·CORPORATION

P.O. Box 2980 College Station, Texas 77840 (713) 693-1711

CIRCLE 7 ON READER SERVICE CARD



#### X-ray microanalyzer

Instrument uses a dispersive X-ray detector in conjunction with a scanning electron and transmission electron microscope for microanalysis of all elements in the periodic table from carbon to uranium. The system consists of a console with keyboard, video display, minicomputer, dual double-density floppy disk, and high-speed printer. Kevex **118**

#### Electron beam power supply

This is a three-output, high-voltage system specifically designed for electron beam microscopy. It incorporates a high-voltage isolated coupling technique and linear conversion circuitry. Output voltages and current are controlled from the front panel or by re-

mote programming. The isolated bias supply can be operated at constant voltage or constant emission current. Bertan Associates **119**

#### Closed-loop stripper

This apparatus removes and concentrates organics from aqueous samples. It extends the range of purge-and-trap techniques to include organics that are water soluble and have low volatility. The purged organics are trapped on charcoal and eluted from the trap with a suitable solvent. An aliquot of the resulting concentrate is then injected into a GC for analysis. Tekmar **120**

#### Portable calibrator

Light-weight, self-contained unit calibrates pressure transducers, controllers, pressure gauges, and other control equipment in the field. Ranges as low as 0–50 in H<sub>2</sub>O to as high as 0–100 psi may be interchanged. The instrument operates in temperatures from –10–95 °F with an accuracy of ±0.1%. International Controls **122**

#### Spectrophotometric detector

This can be interfaced with any HPLC instrument. It allows a sample to be analyzed at eight different wave-

lengths simultaneously without interrupting the chromatographic run. A linear photodiode array and high-speed computer network permit spectral scanning without loss of chromatographic data. The detector is useful in chemical separations of components that absorb in the ultraviolet or visible spectrum. Hewlett Packard **131**

#### Digital thermocouple

Reads temperatures in the range of 25–500 °F or –32–260 °C with an accuracy of 1%. The surface, needle, or bare-tip probe is held at the side in a special holder, and the power is provided by two 9-V transistor batteries. Atkins Technical **132**

#### Bubble tubing

Extruded from clear, autoclavable polyvinyl chloride, this tubing is available in four sizes and has bubbles every 36 in. By cutting through a bubble, a female funnel is created; by cutting adjacent to a bubble, a tapered male connector is formed. Lancer **133**

#### Portable recorders

Battery-powered or ac recorders measure 6 × 9 × 11 in. and have a 4-in. vertical chart width. Up to eight days of recording is possible on one battery charge. The unit has a single channel, and can be used with either roll paper or optional fan fold paper. Linear Instruments **134**

#### Rapid kinetics instrumentation

This modular system for the study of fast reactions is composed of three basic units: sample-handling unit, spectrophotometer unit, and data capture and processing unit. The system may be purchased in its entirety or in individual components. The sample-handling device has a temperature range of –100–100 °C. Tekmar Company **135**

#### Ethylene oxide detection system

Tube system detects ethylene oxide in air from 5–50 ppm with a distinct white to brown color change. Tubes can be used without correction factors from 10–40 °C and 5–60% relative humidity. Matheson **136**

#### HPLC fraction collector

Programmable collector can be used for both preparative and analytical HPLC and can be adapted to any liquid chromatographic system. According to the manufacturer, the system has a high degree of programming flexibility for automating sample injection and selecting collection modes. ES Industries **137**

# FORMALDEHYDE

## and other hazardous vapors safely monitored with MIRAN Direct-Reading Gas Analyzers.

With the MIRAN portable gas analyzers, you will be able to conduct, with confidence, area mapping and leak detection tests for formaldehyde or other potentially-toxic materials. MIRAN analyzers continuously sample and measure vapor concentrations and can detect formaldehyde at sub-ppm levels.

Get laboratory accuracy — and industrial ruggedness — in a portable analyzer. Contact us today for complete details. Foxboro Analytical, A Division of The Foxboro Company, PO Box 5449, South Norwalk, CT 06856. (203) 853-1616 TWX: 710-468-3054.

With Foxboro, you have ambient air analysis under control.



**FOXBORO**

CIRCLE 9 ON READER SERVICE CARD

# ES&T LITERATURE

**Current detector.** Paper describes streaming current detector for measured coagulant dosage in wastewater treatment. L'eau Claire Systems

151

**Draft controls.** "Combustion Checklist" gives procedure for setting, adjusting, and testing barometric draft controls for maximum burner fuel efficiency. Field Control Division

152

**Glassware joiners.** Brochure describes a new way to join laboratory glassware that eliminates the need for grease, clamps, hooks, and springs. Wheaton Scientific

153

**Chemical safety.** Catalog, "Handling Chemicals Safely," covers books on hazardous chemicals and biohazardous materials use in laboratory and industry. Lab Safety Supply

154

**Flow meters.** Bulletin No. 46 lists flow meters and other items useful for measuring flow and pressure. Purifiers and solvents are also featured. Alltech Associates

155

**Polystyrene fractionation.** Technical paper, "Nonaqueous Reversed-Phase Liquid Chromatographic Fractionation of Polystyrene," by D. W. Armstrong and K. H. Bui (Georgetown University) is available. Whatman

156

**Geophysical instruments.** 1982-83 catalog lists instruments for meteorology, hydrology, environmental control, and other applications. WEATHERtronics

157

**Hazardous waste disposal drums.** Brochure features the HercuDrum, a bulk-corrugated drum for environmentally controlled hazardous waste disposal. It has no metal straps, hoops, or hardware and can be disposed of properly with hazardous waste. International Paper

158

**Processing microcomputers.** Brochure tells how to use microcomputers for batch or continuous processes. Artisan Industries

159

**Biochemical reagents.** Brochure, "High-Purity Biochemical Reagents," lists reagents proven through actual lot analysis, use-matched specifications, and use-testing. J.T. Baker Chemical

160

**Microminiature tubing.** Brochure describes Zeus Sub-Lite Wall tubing made of Teflon, with walls as thin as  $1.5 \times 10^{-3}$  in. Zeus Industrial Products

161

**Hazardous waste site samples.** Brochure outlines DSS (Disposal Site Screening) analysis program for analyzing hazardous waste site samples to meet analysis requirements under Superfund cleanup guidelines. Mead CompuChem

162

**Dust suppressant.** Announcement describes DUSBLOC 220, a petroleum emulsion that can prevent fugitive dust dispersion from unpaved surfaces. ARCO Chemical

163

**Separations.** Bio-Radiations 41 for June 1982 discusses high-performance liquid chromatography (HPLC), column chromatography, and other related items. Bio-Rad Laboratories

164

**Flow measurement.** Catalog describes new line of liquid flow measurement systems giving total flow, rates, and batch load capability. ELECTRO-NUMERICS

165

**Waste to energy.** Newsletter, *Bethlehem Highlights*, points out recent innovations in waste-to-energy, heat transfer, precious metals, and other areas. The Bethlehem Corp.

166

**pH test system.** Brochure includes principles and applications of indicator strips, dyes, papers, and liquid indicators for weakly buffered and unbuff-

ered solutions, and sources of error in colorimetric pH measurement. EM Science

167

**Fluid analyzers.** Bulletin 3300 describes systems that automatically monitor, measure, and control suspended solids in a waste stream for waste treatment and other applications. Gam Rad

168

**Water filter.** Bulletin describes HF automatic water filter that removes trace contaminants from plant and process waters in high-flow applications. Dover Corporation

169

**Level controls.** Bulletin highlights LCM-130 ultrasonic level controls to measure liquid or solid levels in open or closed-top tanks and vessels. Lee Industries

170

**Toxic chemicals.** Brochure announces "Handbook of Priority Pollutants and Toxic Chemicals," which sells for \$245. Complete spectra are given. Sadtler Research Laboratories

171

**Geophysical equipment.** New edition of general catalog lists equipment for radiation protection, field exploration, and many other uses. GISCO

172

**pH electrodes.** Announcement describes X-EL series of pH electrodes for applications requiring wide temperature range capabilities with fast response of silver chloride electrodes. Silver chloride precipitation is eliminated. Corning Glass

173

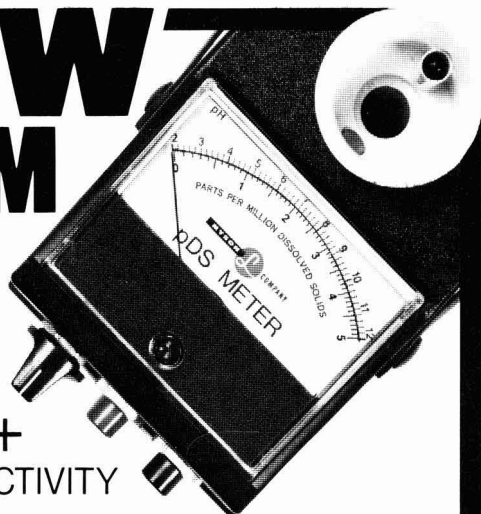
**GC/MS system.** Brochure describes gas chromatography/mass spectrometry (GC/MS) system known as MS 25/DS 55, a double-focusing magnetic sector instrument with sophisticated controls and up to 40 h of unattended operation. Kratos

174

*Companies interested in a listing in this department should send their releases directly to Environmental Science & Technology, Attn: Literature, 1155 16th St., N.W., Washington, D.C. 20036*

*Need more information about any items? If so, just circle the appropriate numbers on one of the reader service cards bound into this issue and mail in the card. No stamp is necessary.*

# THE NEW TEAM



## pH + CONDUCTIVITY

Introducing the Myron L pDS Meter - a compact, hand-held instrument that measures pH and conductivity with a single sample. Accurate, on-the-spot readings can be made quickly and easily.

The pH sensor and conductivity electrode are built-in to the cell cup for greater protection and convenience. Myron L quality is built-in too, and that means years of reliable service for you.



6231C Yarrow Drive,  
Carlsbad, CA 92008

Tel: (714) 438-2021

Tlx: 695009

Cable: MYELCO

CIRCLE 6 ON READER SERVICE CARD

## REQUEST FOR PRELIMINARY PROPOSALS FOR A PLAN ON AN ACID DEPOSITION FIELD PROGRAM

EPA plans to sponsor a large-scale, long duration acid deposition field program designed to understand the nature of processes contributing to acidification on a regional scale and to supply reliable data for model testing and verification.

A major goal of the program is to examine the transport of acid and acid precursor pollutants and to specify source/receptor relationships over local to regional scales.

The National Center for Intermedia Transport Research (NCITR) is soliciting on behalf of EPA preliminary proposals to develop a scientifically sound comprehensive technical plan for the regional acid deposition field program.

The proposals will be submitted in two stages. Initially short preliminary proposals will be submitted.

Examples of topics to be included in the preliminary proposals follow. However, topics covered need not be limited to these examples.

1. Methods of collection and measurement of acid producing pollutants.
2. Wet deposition.
3. Dry deposition.
4. Source/receptor relationships.
5. Climatic effects on pollutant transport.
6. Tracer selection and tracer methods.
7. Fog, mist, and cloud sampling.
8. Pollutant mass balances.
9. Quality assessment and control.

The preliminary proposal should be no longer than five typewritten pages to which material should be appended documenting the qualifications of the group to perform the work. Preliminary proposals are due at NCITR by January 31, 1983.

Five to ten of the most promising preliminary proposals will be selected by March 15, 1983. From this group, detailed proposals for the experimental plan will be requested by June 15, 1983; out of which a selection will be made, by July 31, 1983, of a single proposal that will be awarded the task of preparing the EPA comprehensive acid deposition field program.

Additional details may be obtained from:

Professor Chaim Gutfinger  
National Center for Intermedia Transport Research (NCITR)  
University of California, Los Angeles, 5531 Boelter Hall (ADP)  
Los Angeles, California 90024 (213) 825-9741 or (213) 206-8123

CIRCLE 11 ON READER SERVICE CARD

**Liquids/solids separation.** Bulletin 32-7 describes anionic polyelectrolytes used as primary coagulants or coagulant aids in conjunction with inorganic primary coagulants. Used for sedimentation and centrifugation, among other applications. Calgon 175

**Elemental analyzer.** Announcement describes Model 1106 CHN-O/S elemental analyzer, which can do C, H, and N analyses in 10 min each and O and S analyses in less than 6 min each. Keeps track of up to 50 samples. ERBA Instruments 176

**Ion chromatography (IC).** Announcement with sample analysis readout describes Anion/HS columns for high-speed IC. Adaptable to  $Cl^-$ ,  $Br^-$ ,  $SO_4^{2-}$ , and many others. Detection limits below 0.5 ppm for direct injection; below 10 ppb with sample preconcentration. Wescan Instruments 177

**Personal O<sub>2</sub> monitor.** Announcement describes Model 50 personal oxygen (O<sub>2</sub>) monitor, which gives *true percent* O<sub>2</sub>, unaffected by weather changes or elevation; O<sub>2</sub> changes by air diluents are read. Size is 6½ × 3½ × 1½ in. No adjustments needed prior to use. Sierra Monitor 178

**Chromatography.** 1982 catalog lists line of chemicals and accessories for gas, liquid, and thin-layer chromatography. Analabs/Foxboro 179

**Temperature recorders.** Brochure describes full line of Rustrak galvanometric temperature recorders. Can monitor range of -75 to 1700 °C (-100 to 3000 °F). Simultaneous recording of up to three temperatures is possible. Gulon Industries 180

**Air cleaner.** Literature describes portable room-size air cleaner, the EA 400, for large and small particle removal and neutralization of more than 270 kinds of odors. Can do six air changes/h in a 12 × 12 ft room. Ecology Tech 181

**Aerosol counter.** Brochure announces Model 4000 laser aerosol counter. Sensitivity to 0.3 μm at 1-cfm sample flow rate. HIAC/ROYCO 182

**Environmental chambers.** Minicatalog lists line of environmental chambers, freezers, washers, ovens, and laboratory furniture. Baths and test chambers also included. Forma Scientific 183

**Technical PR.** Brochure describes firm's capability in technical public relations (PR) counseling and activities; the company has worked with the American Water Works Association and the Water Quality Association. Services from writing to media contacts. DXM 184

**Reactor simulation.** Predictive computer code, described in announcement, can calculate behavior of a nuclear power plant in "off-normal" conditions. EG&G Idaho 185

**Clarification enhancement.** "3 Footer" brochure tells how tube settlers enhance clarification by protecting settling solids from crosscurrents, so settling is disturbed much less. Envirofax 186

**Temperature controllers.** Catalog ED-1 lists full line of temperature controllers with modular, plug-in 1/4 DIN design for thermocouple or RTD input. Ranges from -100 to 2500 °F. Burling Instrument 187

**Level gauges.** Bulletin 15.10/Am lists line of electronic level gauges, level alarms, and level controls. Oil-water separation is one of many applications. AMPRODUX 188

**Aerial photography.** Publication M-29 addresses aerial films, processing equipment, chemicals, papers, and many other related items and topics. Eastman Kodak 189

**Low-leakage valve.** Bulletin 51.6:8510 describes eccentric disc control valve, suited for liquid and gas applications requiring extremely low leakage. Fisher Controls International 190

**Specialty gases.** Buying guide lists specialty gases in purity grades ranging from 99.0-99.9999%. Scott Specialty Gases 191

**Odor masking.** Bulletin 30D describes advantages of Dizene emulsifiable orthodichlorobenzene as an industrial-strength odor-masking agent and solvent. Chemical properties and health precautions are listed. PPG Industries 192

**Particulate sampling training.** Brochure describes training program for those to be involved in particulate sampling; the program is for inexperienced people and as a refresher course. ASA Consultants 193

**Pressure instrument protectors.** Bulletin describes pressure instrument protectors that prevent liquids from clogging or corroding delicate pressure instruments, such as gauges, switches, and the like. Dover Corp. 194

**Calibrated gas leaks.** Brochure lists line of calibrated gas leaks used with gas analyzers, leak detectors, and the like. Standard gases and system connection fittings are also listed. Vacuum Instrument 195

**Nuclear engineering.** Brochure lists full range of nuclear engineering services for establishing and maintaining nuclear power plants. Wyle Laboratories

**Water purification.** Brochure describes company's services for the production of ultrapure water and discusses features of various water purification systems. HYDRO

**Wastewater treatment.** Brochure describes complete mix basin for the aeration and clarification of wastewater in one place. It qualifies for share-costed EPA funds. Mixing Equipment

**Refinery wastewater.** "Refinery Wastewater Priority Pollutant Study—Sample Analysis and Evaluation of Data" shows how wastewater treatment systems reduce toxic organics below detectable limits (cost of report, \$4.40). American Petroleum Institute Publications and Distribution Dept., 2101 L St., N.W., Washington, D.C. 20037. Ask for Order No. 84143460 (write direct)

**Nuclear science.** Brochure lists public policy statements and books available. American Nuclear Society, 555 North Kensington Ave., LaGrange Park, Ill. 60525 (write direct)

**Refinery effluent analysis.** Trace substances in aqueous refinery effluents analyzed. CONCAWE Report 6/82 of June 1982. CONCAWE, Babylon Kantoren A, Koningin Julianaplein 30-9, 2595 AA Den Haag, The Netherlands (write direct)

**Passive solar energy.** Passive solar is explained by the booklet, "Living With The Sun." Cost, \$1. PPG Industries, One Gateway Center, 10 North, Pittsburgh, Pa. 15222 (write direct)

**WATER ANALYSIS**

SULFIDE    SULFITE  
COPPER    HARDNESS  
CHLORIDE    CHLORINE  
AMMONIA    NITROGEN  
DISSOLVED OXYGEN

Our test kits are different!

Ordinary kits are complicated to use, but ours are simple. In most cases you don't have to measure the sample or even handle a reagent because the testing is done with disposable, self-filling, evacuated ampoules.

The pre-measured reagent is sealed inside, so they're safe, simple, fast and extremely dependable.

SO SIMPLE TO USE, TESTS MAY BE PERFORMED BY NONTECHNICAL PERSONNEL

(1) Snap the tip of the self-filling ampoule in your water sample.

(2) Compare the filled ampoules with liquid color standards for fast, accurate results.

COMPACT KITS ARE AVAILABLE FOR:

- Dissolved Oxygen • Phenols • Chlorine
- Copper • Iron • Ammonia • Phosphate • Amines
- Sulfide • Chloride • Hardness • Sulfite
- Hydrazine • Hydrogen Peroxide

**CHEMetrics, Inc.**

WRITE FOR FREE BROCHURE

MILL RUN DRIVE, WARRENTON, VA. 22186  
(703) 788-4100

CIRCLE 5 ON READER SERVICE CARD

**Residue Reviews: Residues of Pesticides and Other Contaminants in the Total Environment.** Francis A. and Jane Davies Gunther, Eds. Vol. 83. viii + 174 pages. Springer-Verlag New York, Inc., 175 Fifth Ave., New York, N.Y. 10010. 1982. \$24.80, hardcover.

This volume of reviews examines the properties, effects, residues, and analysis of the insecticide Endosulfan. Among topics discussed are metabolites, toxicity, environmental behavior, effects on arthropods, tolerances, and crop protection.

**Electromagnetism and Life.** Robert O. Becker, Andrew A. Marino. xiii + 211 pages. State University of New York Press, State University Plaza, Albany, N.Y. 12246. 1982. \$10.95, paper.

Electromagnetic energy plays a role in the regulation of life processes, and that is one of several topics discussed in this work. Others are the adaptability of organisms to electromagnetic energy, effects on various physiological systems and functions, and health effects, as well as the field of electrobiology in general.

**Solar Heating and Cooling of Buildings.** Joe J. Harrell, Jr. xii + 365 pages. Van Nostrand Reinhold Company, Inc., 135 West 50th St., New York, N.Y. 10020. 1982. \$22.95, hardcover.

This book is devoted mainly to design techniques for sizing solar system components; descriptions of how solar energy system components function; and economics of specific system designs. Life cycle strategies, data processing methods, tax incentives, government assistance, and pertinent meteorological information are also covered.

**The Environment of the Deep Sea.** W. G. Ernst, J. G. Morin, Eds. x + 371 pages. Prentice-Hall, Inc., Englewood Cliffs, N.J. 07632. 1982. \$36.95, hardcover.

This book examines the physical and chemical as well as the biological environment of the deep sea. Among its topics are changing environments over time, N<sub>2</sub>O in the sea, the chemistry of biogenic matter, bacterial ecology, and many different benthic communities. The manganese cycle is also covered. The book is Vol. II of a series dedicated to the memory of distinguished geologist W. W. Rubey (1898-1974).

**Research for Small Farms: Proceedings of the Special Symposium.** Howard W. Kerr, Jr., Lloyd Knutson, Eds. 300 pages. Superintendent of Documents, U.S. Government Printing Office, Washington, D.C. 20402. 1982. \$7.50 (\$9.40 outside U.S.), paper. When ordering, also specify MP1422.

This U.S. Department of Agriculture publication is aimed at those wishing to engage in small-scale farming, either as a business or for family needs. Among many topics covered concerning horticulture and raising livestock are raising yields, combating diseases and pests, marketing, and organic waste and residue management.

**Atmospheric Biogenic Hydrocarbons.** Joseph J. Bufalini, Robert R. Arnst, Eds. Vols. 1 and 2, 181 and 230 pages, respectively. Ann Arbor Science Publishers Inc., P.O. Box 1425, Ann Arbor, Mich. 48106. 1981. \$45/set, hardcover.

Vol. 1 covers emissions; Vol. 2 discusses ambient concentrations and atmospheric chemistry. By biogenic hydrocarbons, the editors mean those generated by biota in nature, not by humans.

**Examination of Water for Pollution Control.** Michael J. Suess, Ed. Vols. 1, 2, 3, xxi + 360, 555, and 531 pages, respectively. Pergamon Press, Inc., Maxwell House, Fairview Park, Elmsford, N.Y. 10523. 1982. \$350/set, hardcover.

Each volume examines a different aspect of water pollution and its control in detail. Vol. 1 discusses sampling, data analysis, and laboratory equipment; Vol. 2 looks at physical, chemical, and radiological examination; Vol. 3 covers biology, bacteriology, and virology.

**Energy and Environment in the Developing Countries.** Manas Chatterji, Ed. xii + 357 pages. John Wiley & Sons, Inc., 605 Third Ave., New York, N.Y. 10016. 1982. \$47.95, hardcover.

In this work, energy and environment problems of so-called Third World nations are examined. Options such as ethanol fuel, pesticide alternatives, renewable energy, and waste briquetting are considered. Economics and capital formation are discussed, and case studies of several countries are presented.

**Insects, Experts, and the Insecticide Crisis.** John H. Perkins, xviii + 304 pages. Plenum Press, 233 Spring St., New York, N.Y. 10013. 1982. \$29.50, hardcover.

This book details the quest for new pest management strategies. It starts with the evolution of chemical pesticides, discusses hazards to other, particularly useful species of pests' natural enemies, and examines policy problems involving insecticides. The search for alternatives (integrated pest management and others) is discussed in detail, as is entomology in its cultural context.

**Acid Rain Information Book.** Frank A. Record et al. 228 pages. Noyes Data Corporation, Mill Road at Grand Avenue, Park Ridge, N.J. 07656. 1982. \$24, hardcover.

This book is based principally on a study by GCA Corporation for the Department of Energy. It discusses acid precipitation and its measurement, discovery of the phenomenon, sources, transport and deposition, and adverse and beneficial effects. Mitigative strategies and current and proposed research are also covered.

# ES&T MEETINGS

**Nov. 20-21** New York, N.Y.  
**7th Annual International Conference on Toxic Substance and Hazardous Waste Management.** Chinese-American Academic & Professional Association

*Write:* K. T. Lin, P.O. Box 1168, Piscataway, N.J. 08854; (201) 932-9039

**Nov. 29-Dec. 1** Washington, D.C.  
**3rd National Conference and Exhibition on Management of Uncontrolled Hazardous Waste Sites.** Hazardous Materials Control Research Institute

*Write:* HMCRI, 9300 Columbia Blvd., Silver Spring, Md. 20910; (301) 587-9390

**Dec. 1-2** Arlington, Va.  
**Fundamental Research Needs for Water and Wastewater Systems.** Association of Environmental Engineering Professors, National Science Foundation, and EPA Office of R&D

*Write:* Francis A. DiGiano, Environmental Sciences and Engineering (ESE), University of North Carolina, Chapel Hill, N.C. 27514; (919) 966-2488

**Dec. 5-9** San Antonio, Tex.  
**Aromatic Hydrocarbons and Related Chemicals.** D-16 Committee, ASTM  
*Write:* Alice C. Cavallaro, ASTM, 1916 Race St., Philadelphia, Pa. 19103; (215) 299-5486

**Dec. 6-8** Baltimore, Md.  
**2nd International Symposium on High-Performance Liquid Chromatography (HPLC) of Proteins, Peptides, and Polynucleotides.** Varian Associates Inc.

Fee: \$195. *Write:* Shirley E. Schlessinger, Symposium Manager, Second International Symposium on HPLC of Proteins, Peptides, and Polynucleotides, 400 East Randolph, Chicago, Ill. 60601; (312) 527-2011

**Dec. 6-8** Phoenix, Ariz.  
**ASTM Meeting on Soil and Rock.** D-18 Committee, ASTM

*Write:* Ken Pearson, ASTM, 1619 Race St., Philadelphia, Pa. 19103; (215) 299-5520

**Dec. 9** Phoenix, Ariz.  
**Use of Fuel Combustion Solid By-Products.** Committee E-38.06.03, ASTM

*Write:* Jim Thomas, ASTM, 1916 Race St., Philadelphia, Pa. 19103; (215) 299-5498

**Dec. 13-15** Miami, Fla.  
**5th International Conference on Alternative Energy Sources.** Clean Energy Research Institute at the University of Miami

*Write:* David L. Coffin, EPA, Mail Drop 70, Research Triangle Park, N.C. 27711; 919-541-2909

**Jan. 20-21** Palo Alto, Calif.  
**12th Annual National Measurement Science Conference and Exhibition.** California State Polytech University and others

*Write:* Bob Weber, Lockheed Missile & Space Corp., Sunnyvale, Calif. 94046; (408) 742-2957

## COURSES

**Dec. 13-17** Madison, Wis.  
**Wastewater Treatment—Part I.** University of Wisconsin—Madison

Fee: \$660. *Write:* John T. Quigley, Program Director, Department of Engineering, University of Wisconsin Extension, 432 North Lake St., Madison, Wis. 53706; (608) 262-2061

**Jan. 10-14** Las Vegas, Nev.  
**Water Quality Modeling.** Desert Research Institute

*Write:* Water Resources Center, Desert Research Institute, P.O. Box 60220, Reno, Nev. 89506; (702) 673-7361

**Jan. 24-27** Houston, Tex.  
**Industrial Waste Incineration Technology.** The Center for Professional Advancement

Fee: \$895. *Write:* The Center for Professional Advancement, Dept. NR, P.O. Box H, East Brunswick, N.J. 08816; (201) 249-1400

## CALL FOR PAPERS

**Nov. 30 deadline**  
**Source Control to Effects of Power Generating Stations on Receiving Streams**

The meeting will be Oct. 31-Nov. 4, 1983, in Washington, D.C. *Write:* Robert W. Peters, Environmental Engineering, School of Civil Engineering, Purdue University, West Lafayette, Ind. 47907; (317) 494-2191

**Dec. 15 deadline**  
**38th Annual Meeting of the Soil Conservation Society of America**

The meeting will be July 31-Aug. 3, 1983, in Hartford, Conn. *Write:* Marion F. Baumgardner, Program Chairman, Soil Conservation Society of America, 7515 N.E. Ankeny Rd., Ankeny, Iowa 50021-9764

**Dec. 15 deadline**  
**Fugitive Dust Issue in the Coal Cycle**

The conference will be April 11-13, 1983, in Pittsburgh, Pa. *Write:* Richard L. Kerch, Consolidation Coal Co., Consol Plaza, Pittsburgh, Pa. 15241; (412) 831-4527

**Dec. 20 deadline**  
**1983 National Conference on Environmental Engineering**

The conference will be July 6-8, 1983, in Boulder, Colo. *Write:* Allen J. Medine, Conference Chairman, 1983 National Conference on Environmental Engineering, Civil and Environmental Engineering, Campus Box 428, University of Colorado, Boulder, Colo. 80309

**Dec. 31 deadline**  
**International Symposium on Sources, Transport Pathways, Properties, and Effects of Highway Pollution.** Middlesex Polytechnic

Symposium to be held Sept. 6-8, 1983, in London. *Write:* Ron Hamilton, Urban Pollution Research Centre, Middlesex Polytechnic, Queensway, Enfield, Middlesex, EN3 4SF, U.K.

# Chief Environmental Scientist

Battelle Project Management Division's Office of Nuclear Waste Isolation (ONWI) is seeking a qualified professional for the position of *Chief Environmental Scientist*. This is a highly visible position in the Site Exploration Functional Office requiring immediate and important contributions and excellent communication skills. The requirements are for an environmental scientist/manager with experience in directing multidisciplinary groups of environmental scientists and socioeconomic specialists.

The candidate should possess a doctorate or equivalent combination of education and experience, and a record of proven leadership.

The successful candidate will offer a background that reflects ability to plan and implement environmental siting and licensing programs including experience in interacting with regulatory and licensing agencies. The candidate should have demonstrated expertise in the physical and environmental sciences and socioeconomic, with a minimum of 10 years of environmental siting and licensing experience, particularly with large energy related projects and nuclear-power facilities.

ONWI has a strategic role in the Department of Energy's National Waste Terminal Storage Program developing appropriate environmental analyses and assessments, and in the management of subcontractor activities leading to the siting and licensing of nuclear waste repositories.

The Site Exploration Functional Office includes active project-management teams of engineers, geologists, geochemists, hydrologists, environmental scientists and socioeconomic specialists working on a wide range of siting and licensing objectives.

We offer a comprehensive benefits package and an excellent salary commensurate with your background and experience. Send resume in confidence to:

**Box EST-1182**



**Battelle Project Management Division  
Office of Nuclear Waste Isolation (ONWI)  
Columbus, Ohio**  
an equal opportunity employer

**UNIVERSITY OF COLORADO—  
VISITING FACULTY AND  
POSTDOCTORAL FELLOWSHIPS (1983-84)  
FOR RESEARCH IN ATMOSPHERIC AND CLIMATE DYNAMICS,  
ATMOSPHERIC CHEMISTRY, ANALYTICAL CHEMISTRY, AND  
ENVIRONMENTAL CHEMISTRY, BIOCHEMISTRY AND  
GEOCHEMISTRY at the Cooperative Institute for Research in  
Environmental Sciences (CIRES)**

Five competitive fellowships will be awarded to recent Ph.D. recipients and to senior scientists, including those on sabbatical leave. Selection of awardees is made in part on the likelihood of active interaction with CIRES scientists and other research groups in Boulder. Senior CIRES-affiliated scientists working in these fields include Roger Barry, John Birks, R. Ray Fall, Fred Fehsenfeld, Richard Gammon, Murray Johnston, Uwe Radok, Robert Sani, Robert Sievers, and Harold Walton. Stipend is scaled to experience and accomplishments. Apply to **Prof. R. Sievers, Director of CIRES, University of Colorado, Campus Box 449, Boulder, Colorado 80309.**

Include vitae, publications list, and brief outline of proposed research. Also request that three persons familiar with your qualifications send letters of recommendation. First consideration will be given to applications received by December 1. Final application deadline is February 15. The University of Colorado is an affirmative action/equal opportunity employer.

## ENVIRONMENTAL MANAGER

Specialty Chemicals

Ensure that corporate activities are performed in a manner consistent with existing and foreseeable environmental control regulations.

A background in negotiating permits from state and federal environmental agencies is required. BS Environmental Sciences or equivalent CH or CE with at least 3-5 years' experience in chemical process industry necessary.

We offer competitive salary and excellent benefits package. Principal candidates only are requested to send their resumes to: Jeanne Fauer, Human Resources, M&T Chemicals Inc., P.O. Box 1104, Rahway, New Jersey 07065. An equal Opportunity Employer M/F/V/H. Second party responses will be considered on a deferred basis.



University of Miami, Dept. of Civil Engineering, is seeking applications for the position of Chairperson starting Fall semester 1983. Candidates should have a Ph.D. in Civil Engineering, and a distinguished teaching and research record. Desirable qualifications include professional experience and administrative ability. The department has 16 full-time faculty members, 350 undergraduate and 50 graduate students. Undergraduate and graduate specialty areas include Structural, Environmental, Geotechnical, Transportation and Architectural Engineering. Applications with resumes, or nominations should be received by December 15, 1982. Send to **Thomas Walte, Chairman, Search Committee, Dept. of Civil Engineering, University of Miami, P.O. Box 248294, Coral Gables, Florida 33124.** Affirmative action/equal opportunity employer.

## ENVIRONMENTAL SCIENTIST

State Attorney General seeks concerned scientist to join five person technical team to plan, undertake and supervise environmental field sampling with special emphasis on toxic materials in groundwater, to interpret varied environmental data sets, and to provide professional guidance to legal staff. Candidate must demonstrate public interest motivation and adequate education and experience in geology, chemistry, and field operations to carry out such tasks effectively. Advanced degree preferred. Salary, mid to upper twenties. Contact **Peter Skinner, P.E. Room 239, Justice Building, The Capitol, Albany, NY 12224.**

The University of Pennsylvania is seeking applications for a tenure-track faculty position at the level of Assistant Professor in the area of Environmental and Resources Engineering. The candidate should have a Ph.D. and professional experience is desirable. Duties will include: Teaching undergraduate and graduate courses in environmental engineering, and participation in and development of research activities. We are seeking an individual who has experimental research interests in water and wastewater engineering with a specialty in an area such as aquatic chemistry, process chemistry or treatment systems. Reply with credentials to: **Dr. John D. Keenan, Chairman of Search Committee, Department of Civil and Urban Engineering, Towne Building D/3, University of Pennsylvania, Philadelphia, PA. 19104.** The University of Pennsylvania is an equal opportunity/affirmative action employer.

### CLASSIFIED ADVERTISING RATES

Rate based on number of insertions used within 12 months from date of first insertion and not on the number of inches used. Space in classified advertising cannot be combined for frequency with ROP advertising. Classified advertising accepted in inch multiples only.

Unit	1-T	3-T	6-T	12-T	24-T
1 inch	\$90	\$85	\$82	\$79	\$77

(Check Classified Advertising Department for rates if advertisement is larger than 10")  
SHIPPING INSTRUCTIONS: Send all material to

**Environmental Science & Technology  
Classified Advertising Department  
25 Sylvan Rd. South, Westport, CT. 06881  
(203) 226-7131**

USE  
THE  
CLASSIFIED  
SECTION



# professional consulting services directory



## FIREMAN'S FUND RISK MANAGEMENT SERVICES, INC.

CONSULTING SERVICES IN:

- ENVIRONMENTAL LABORATORY
- WATER POLLUTION
- HAZARDOUS WASTE
- AIR POLLUTION
- INDUSTRIAL HYGIENE
- OCCUPATIONAL HEALTH

Offices in Principal Cities

Contact: Dr. Peter Russell, P.E.  
1600 Los Gatos Drive  
San Rafael, CA 94911  
(415) 929-2706



## A.F. Meyer and Associates, Inc.

Environmental, System Safety,  
and Occupational Health  
Consultants

Free Brochure Upon Request

1317 Vincent Place • McLean, VA 22101  
703/734-9093

## ENVIROPLAN

One of the Largest and Most  
Experienced Environmental  
Consulting Companies  
Specializing in Air Quality  
and Meteorological Studies

- Air Quality Modeling
- Air Quality and Stack Emissions Monitoring
- Multidisciplinary Studies
- New Source Reviews
- Regulatory Strategies
- Special Field Studies

CORPORATE HEADQUARTERS WESTERN REGIONAL OFFICE  
WEST ORANGE, NJ DENVER, CO  
(201) 325-1544 (303) 989-5061

**Environmental Planning and Problem Solving for Industry and Government**

• AIR • WATER • SOLIDS • NOISE • ODOR

• MEASUREMENT • IMPACT ASSESSMENT  
• CONTROL • INFORMATION SYSTEMS  
• MODELING • PERMIT PLANNING

800 Connecticut Blvd., E. Hartford, CT 06108  
(203) 289-8631

• EAST HARTFORD • DENVER • SAN DIEGO

## Scott Environmental Technology, Inc.

The Air Pollution Specialists

- Research and Consulting
- Source Emissions Testing
- Control Device Efficiency
- Continuous Source Monitoring
- Ambient Monitoring
- Fuel Additive & Automotive Testing

Route 611, Plumsteadville, PA 18949  
215-766-8861  
2600 Cajon Blvd., San Bernardino, CA 92411  
714-887-2571  
1290 Combermere St., Troy, MI 48084  
313-589-2950

## Woodward-Clyde Consultants

- Site Selection Studies
- Impact Assessment Evaluation
- Decision and Risk Analyses
- Environmental Field and Laboratory Studies

San Francisco • Denver • Houston • Chicago  
New York • Anchorage • Kansas City  
Wayne, NJ • Plymouth Meeting, PA

## Your Full Service Independent Laboratory

- Comprehensive Analytical Services
- EPA Priority pollutants
- Drinking water—SDWA
- Hazardous wastes—RCRA
- NPDES permits testing
- Gas Chromatography/Mass Spectroscopy

**United States Testing Co., Inc.**  
1415 Park Avenue, Hoboken, NJ 07030  
(201) 792-2400



## ACOUSTIC TECHNOLOGY, INC.

ACOUSTIC CONSULTANTS

- Environmental Noise Impact Assessment
- Ambient Noise Monitoring
- Computerized Acoustic Modeling and Analysis

240 Commercial Street, Boston, MA 02109 Telephone: (617) 367-0164



## Dames & Moore

- Environmental Impact Assessment
- Geotechnical and Environmental Engineering
- Meteorology and Air Quality Monitoring
- Water Pollution Control Engineering
- Modelling and Numerical Analyses
- Permitting and Licensing Consultation
- Solid and Hazardous Waste Management

San Francisco • Denver • Chicago  
Cincinnati • Atlanta

Offices in Principal Cities  
Throughout the World

## SIRRIE

ENGINEERS • ARCHITECTS • PLANNERS

- Permit Assistance
- Air & Water Quality Modeling
- Site Selection Studies
- Laboratory Analyses
- Environmental Impact Assessments
- Hazardous Solid Waste Management
- Complete Design Services
- Construction Management

Greenville, SC 29606 Houston, TX 77042  
Research Triangle Park, NC 27709

## WESTON

DESIGNERS • CONSULTANTS

HEADQUARTERS West Chester, PA 19380 • 215-692-3030  
OFFICES Atlanta, GA • Boston, MA • Camden, NJ  
Chicago, IL • Cleveland, OH • Concord, NH  
Houston, TX • Nashville, TN • New Orleans, LA  
New York, NY • Richmond, VA • St. Paul, MN  
Washington, DC • Amman, Jordan • Cairo, Egypt



## Ground Water Associates, Inc.

Water Supply Geologists and Engineers

- Quantitative and qualitative ground water evaluations
- Iron removal by VYREDOX process

P.O. Box 280 Westerville, Ohio 43081 Cranford, New Jersey  
614/882-3136 Arlington, Massachusetts

## Complete Analytical Services

SINCE 1919

- Screening of Industrial Waste for EPA Priority Pollutants using Finnigan OWA-30 GC/MS.
- NPDES & SPDES Organic & Inorganic Testing.
- Drinking Water Analysis to EPA Standards.
- Bioassay, Bioaccumulation & Toxicity Studies of Industrial Waste, Municipal Sludge & Dredge Spoils.
- Leachate Potential Studies & Analysis.
- Total Instrumental Analysis: A.A., GC/MS, G.C.I.R., TOC & TOD.
- RCRA Hazardous Waste Testing.

**NEW YORK TESTING LABORATORIES**  
81 Urban Avenue, Westbury, N.Y. 11590  
(516) 334-7770

## SpectroChem

LABORATORIES, INC.

545 Commerce St., Franklin Lakes, New Jersey 07417  
(201) 337-4774 (201) 893-3787

- Atomic Absorption
- Gas Chromatography
- Chemical
- Optical Emission
- X-ray Spectrometry
- ICP

TRACE ANALYSIS Est. 1948  
Complete Analytical Services

The Professionals

## ENTROPY

ENVIRONMENTALISTS, INC.

- Source Emissions Testing
- Continuous Emissions Monitoring
- In-Plant Air Studies
- Technical Consulting

Box 12291E • Research Triangle Park, NC 27709  
Call: 1-800-ENTROPY

# professional consulting services directory

<p>17605 Fabrica Way Cerritos, California 90701 213/921-9831 714/523-9200</p>		<p><b>Your Only FULL SERVICE Independent Laboratory</b></p>
		<p>FOR: Priority Pollutant, Pesticide, PCB, THM, PNA, and Metals Analyses. Also GC, MS, GC-MS, LC, IR, AA, DTA, TGA, and DSC.</p>
		<p>We are EPA approved, AIHA accredited, and a Calif. licensed water lab.</p>
		<p>Brochure and /or fee schedule available on request</p>

**Stearns-Roger** **COMPLETE ENVIRONMENTAL SERVICES:**

Environmental impact assessments. . . Pollutant emission, air quality & water quality monitoring. . . Dispersion estimates. . . Ecological consulting. . . Meteorological field studies & consulting services. Contact

**ENVIRONMENTAL SCIENCES DIVISION** P. O. Box 5888  
 (303) 758-1122 Denver, Colorado 80217

**BC Laboratories**

EPA Drinking Water Stds. & Priority Pollutants  
 Haloforms, PCB's—Gases, TOC, Solid Waste  
 Extractions, Heavy Metals  
**4100 Pierce Road (805) 327-4911**  
 Bakersfield, California 93308

**ETC** **MOST ADVANCED GC/MS LABORATORY**

in the nation—programs ensuring compliance with local, state & EPA requirements, including RCRA & Superfund.

Call toll-free 1-800-631-5382. In NJ, (201) 225-5600.

284 Raritan Center Pkwy, Edison, NJ 08837

ENVIRONMENTAL TESTING AND CERTIFICATION CORPORATION

USE THE  
 CONSULTANTS'  
 DIRECTORY

**HE** **Havens and Emerson**  
 Consulting Environmental Engineers

Cleveland St. Louis Atlanta Saddle Brook Boston

**DAVID KEITH TODD**  
 CONSULTING ENGINEERS, INC.

Groundwater Planning, Development,  
 Management, and Protection

2914 Domingo Avenue  
 Berkeley, California 94705 415/841-2091

## INDEX TO THE ADVERTISERS IN THIS ISSUE

Advertising Management for the  
 American Chemical Society Publications

### CENTCOM, LTD.

Thomas N. J. Koerwer, President  
 James A. Byrne, Vice President  
 Alfred L. Gregory, Vice President  
 Clay S. Holden, Vice President  
 Benjamin W. Jones, Vice President  
 Robert L. Voepel, Vice President  
 Joseph P. Stenza, Production Director

25 Sylvan Road, South  
 P.O. Box 231  
 Westport, Connecticut 06881  
 (Area Code 203) 226-7131

ADVERTISING SALES MANAGER  
 JAMES A. BYRNE

ADVERTISING PRODUCTION MANAGER  
 GERI P. ANASTASIA

### SALES REPRESENTATIVES

Philadelphia, Pa. . . . CENTCOM, LTD., GSB Building,  
 Suite 425, 1 Belmont Ave., Bala Cynwyd,  
 Pa 19004 (Area Code 215) 667-9666

New York, N.Y. . . . CENTCOM, LTD., 60 E. 42nd  
 Street, New York 10165 (Area Code 212)  
 972-9660

Westport, Ct. . . . CENTCOM, LTD., 25 Sylvan Road  
 South, P.O. Box 231, Westport, Ct 06881 (Area  
 Code 203) 226-7131

Cleveland, Oh. . . . Bruce Poorman, CENTCOM,  
 LTD., 17 Church St., Berea, OH 44017 (Area  
 Code 216) 234-1333

Chicago, Ill. . . . Bruce Poorman, CENTCOM, LTD.,  
 540 Frontage Rd., Northfield, Ill 60093 (Area  
 Code 312) 441-6383

Houston, Tx. . . . Dean A. Baldwin, CENTCOM, LTD.,  
 (Area Code 713) 667-9666

San Francisco, Ca. . . . Paul M. Butts, CENTCOM,  
 LTD., Suite 112, 1499 Bayshore Highway,  
 Burlingame, CA 90410. Telephone 415-  
 692-1218

Los Angeles, Ca. . . . Clay S. Holden, CENTCOM,  
 LTD., 3142 Pacific Coast Highway, Suite 200,  
 Torrance, CA 90505 (Area Code 213) 325-  
 1903

Boston, Ma. . . . CENTCOM, LTD. (Area Code 212)  
 972-9660

Atlanta, Ga. . . . Donald B. Davis, CENTCOM, LTD.,  
 Phone (Area Code 203) 226-7131

Denver, Co. . . . Clay S. Holden, CENTCOM, LTD.  
 (Area Code 213) 325-1903

United Kingdom:  
 Lancashire, England—Technomedia, Ltd. . . .  
 c/o Meconomics Ltd., Meconomics House,  
 31 Old Street, Ashton Under Lyne, Lan-  
 cashire, England 061-308-3025  
 Reading, England—Technomedia, Ltd. . . .  
 Wood Cottage, Shurlock Row, Reading  
 RG10 0QE, Berkshire, England 0734-343302

Continental Europe . . . Andre Jamar, Rue Maillet 1,  
 4800 Verviers, Belgium. Telephone (087)  
 22-53-85. Telex No. 49263

Tokyo, Japan . . . Shigeo Aoki, International Media  
 Representatives Ltd., 2-29, Toranomon 1-  
 Chrome, Minatoku, Tokyo 105 Japan. Tele-  
 phone: 502-0656

### CIRCLE INQUIRY NO. PAGE NO.

- 1 . . . . . AGIP GIZA (ENI Group) . . . OBC  
 Linera SPN
- 2 . . . . . Beckman Instruments . . . 596A  
 Cochran Chase, Livingston  
 & Company, Inc.
- 3 . . . . . Bioanalytical Systems,  
 Inc. . . . . 619A  
 Kissinger Advertising Assoc.
- 4 . . . . . Board of Trustees . . . . . 600A  
 ACI Designs
- 5 . . . . . CHEMetrics, Incorp. . . . . 627A  
 Kleppinger Associates
- 9 . . . . . Foxboro Analytical . . . . . 622A  
 TCI Advertising, Inc.
- 8 . . . . . Martek Instruments . . . . . 591A  
 Tekmar Marketing Service
- 10 . . . . . Mead CompuChem . . . . . IFC  
 Gilbert Design, Inc.
- 6 . . . . . Myron L. Company . . . . . 626A  
 Lak Advertising
- 11 . . . . . National Center  
 Intermedia Transport  
 Research . . . . . 626A
- 7 . . . . . O.I. Corporation . . . . . 621A  
 Marketing Idea of Texas,  
 Inc.

CLASSIFIED SECTION . . . . . 630A  
 PROFESSIONAL CONSULTING  
 SERVICES DIRECTORY . . . . . 631A-632A

## Binding of DDT to Dissolved Humic Materials

Charles W. Carter<sup>\*†</sup> and Irwin H. Suffet

Environmental Studies Institute, Drexel University, Philadelphia, Pennsylvania 19104

■ Quantitative measurements have been made by using equilibrium dialysis techniques on the extent of binding between DDT and dissolved humic materials. A significant fraction of the dissolved DDT found in natural waters may be bound to dissolved humic materials. The extent of binding depends on the source of the humic material, the pH, the calcium concentration, the ionic strength, and the concentration of humic materials.

A number of authors have demonstrated that hydrophobic pollutants can bind to dissolved humic materials (1-5). These authors have suggested that binding to dissolved humic materials could significantly affect the environmental behavior of hydrophobic organic compounds. The rate of chemical degradation, photolysis, volatilization, transfer to sediments, and biological uptake may be different for the fraction of pollutant that is bound to dissolved humic materials. If this is the case, the distribution and total mass of a pollutant in an ecosystem would depend, in part, on the extent of humic material-hydrophobic pollutant binding.

Hassett and Anderson (1) found that recoveries of cholesterol using liquid-liquid extraction were lower in the presence of dissolved humic materials. They also found that the elution behavior of cholesterol in gel permeation chromatography changed in the presence of humic materials. Wershaw et al. (2) found that the presence of high concentrations of humic materials increased the solubility of DDT. Porrier et al. (3) spiked a highly colored natural water sample with DDT. The colored colloids were removed by centrifugation and the amount of DDT in the colloids and the water was measured. The DDT was enriched by a factor of 15800 by weight in the colloids. Boehm and Quinn (4) found that the dissolved organic matter in seawater and sewage increased the rate of dissolution of the normal alkanes hexadecane and eicosane. The increase was not observed for phenanthrene. Matsuda and Schnitzer (5) found that concentrated solutions of fulvic acid caused a dramatic increase in the solubility of dialkyl phthalates.

There are a number of reports that do in fact indicate that the environmental fate of organic pollutants changes in the presence of humic materials. Zepp et al. (6) have found that the rate of photolysis of certain organic compounds changes in the presence of humic materials. Griffin and Chian (7) and Hassett (8) found that the rate of volatilization of some polychlorinated biphenyls decreases

in the presence of dissolved humic materials. Perdue (9) has measured the rate of hydrolysis of the octyl ester of 2,4-D in the presence and absence of humic materials. The rate was slower in the presence of humic materials. Perdue suggested that a fraction of the octyl ester of 2,4-D was bound to humic materials and that this fraction was unreactive. Laversee (10) found that the extent of bioaccumulation of some polynuclear aromatic hydrocarbons was changed in the presence of humic materials.

One weakness in the above discussion is the scarcity of quantitative data on the extent of humic material-hydrophobic pollutant binding. Of the authors cited above, only Porrier et al. (3) have made a quantitative measurement at realistic environmental concentrations of humic materials. Their report, however, only discusses one water sample, so it is not appropriate to extrapolate their results to other situations. This paper presents quantitative measurements of the extent of humic material-hydrophobic pollutant binding, using dialysis techniques, with *p,p'*-DDT as a model pollutant.

### Experimental Section

Spectra/Por 6 dialysis tubing from Fisher Scientific, molecular weight cutoff of 1000 daltons, is washed in distilled water, 1 M Na<sub>2</sub>CO<sub>3</sub>, twice in 1 M NaHCO<sub>3</sub>, and once in distilled water. This procedure removes the sodium benzoate preservative that the tubing is supplied with. Dialysis bags are made by tying off the ends of a length of tubing with acetone-washed cotton-coated polyester sewing thread. Before the second end is tied off, the bag is filled with a solution of either humic materials or buffered water (for controls). The volume of the dialysis bag is varied between 20 and 35 mL. A 250-mL amber glass bottle is filled with 200 mL of buffered water of varying pH, ionic strength, and calcium concentration. The bottle is spiked with a solution of radiolabeled *p,p'*-DDT (2,2-bis(4-chlorophenyl)-1,1,1-trichloroethane) in acetone. The radiolabeled DDT was obtained from New England Nuclear. The specific activity of the DDT was 6 mCi/mmol and its radiopurity greater than 98%. The bottle is poisoned with 0.5 mg of NaN<sub>3</sub>, the dialysis bag is placed in the bottle, and the bottle is shaken at 25 °C for 4 days. At the end of this period aliquots of either 10 or 25 mL are removed from both the dialysis bag and the solution outside the dialysis bag. Each is extracted in a screw top test tube with 4 mL of heptane. Eight drops of KOH (1 N) are added to each test tube to control emulsions. The test tube is shaken on a mechanical shaker for at least 30 min, and the heptane is transferred to a glass scintillation vial containing 10 mL of Beckman EP scintillation cocktail. The vials are counted on a Beckman

<sup>†</sup>To whom correspondence should be addressed at Versar Inc., 6621 Electronic Dr., Springfield, VA 22151.

LS-100C scintillation counter in the carbon-14 mode with a preset error of 5%. The above analytical technique was found to recover greater than 95% of the DDT even in the presence of 40 mg/L of humic material.

The dialysis tubing is chosen so the humic material is retained inside the bag while the DDT can diffuse freely through the bag. The extent of leakage of the humic materials has been checked by UV spectroscopy and is less than 5%. In a dialysis experiment it is assumed that the DDT inside the dialysis bag consists of two fractions. One fraction is free, truly dissolved DDT. The other fraction is bound to humic materials. Since the free DDT can diffuse through the dialysis bag, the concentration of free DDT will be the same both inside and outside the bag. The bound concentration can then be measured as the difference between the DDT concentration inside and outside the dialysis bag. A dialysis experiment, therefore, measures the amount of bound DDT as a function of the free DDT concentration.

All reagents used in this research were ACS reagent grade. All solvents were pesticide quality. The humic materials were collected and treated as follows:

**Pakim Pond Humic Acid (PPHA).** Pakim Pond is a small man-made pond located in the New Jersey Pine Barrens in Lebanon State Forest. It is highly colored during the spring and summer, with dissolved organic carbon (DOC) values ranging from 30 to 120 mg/L. Iron is usually present at about 10 mg/L, and the normal pH is between 4.0 and 4.5 (11). The sample was collected in late September of 1980. During this sampling trip it was observed that the water was quite clear and the bottom of the pond was covered with a brown flocculant material. Apparently this was the humic material that had recently been in the water column. The humic acid was collected by stirring up the water to suspend the solids and then quickly immersing a 1-gallon amber glass bottle to collect the suspended humic acids. The humic acid was redissolved by raising the pH to 11 with NaOH, and the sample was centrifuged, filtered through 0.2- $\mu$ m glass-fiber filters, and reprecipitated by lowering the pH to less than 2 with HCl. The precipitated humic acid was washed with distilled water, filtered, and desiccated.

**Boonton Reservoir Sediment Humic Acid (BSHA).** Boonton Reservoir is a drinking water reservoir located in Northern New Jersey. A sediment sample was collected in June 1980, during a low-water period. The location of the sample would normally be under about 5 m of water, but due to the low water, the sample was collected just offshore in about 0.5 m of water. The sample was extracted with 0.05 N NaOH for 24 h, centrifuged to remove most of the particles, filtered through 0.2- $\mu$ m glass-fiber filters, precipitated at a pH less than 2 with HCl, and collected on a filter. The filtered humic acid was washed with distilled water, redissolved in 0.1 N NaOH, and reprecipitated with HCl to remove some of the ash. The humic acid was again washed with distilled water and desiccated.

**Commercial Humic Acid.** Humic acid was purchased from Aldrich Chemical Co., Milwaukee, WI. The humic acid had an extremely high ash content (about 60%). To reduce the ash content, it was dissolved in 0.1 N NaOH, reprecipitated by lowering the pH with HF, redissolved in 1 N  $\text{NH}_4\text{OH}$ , and reprecipitated with HF. The precipitated humic acid was washed with distilled water and desiccated. Table I presents the percent ash and percent carbon values for the humic acids used in this research.

**Verification of Dialysis Technique for DDT.** A number of experiments were necessary to confirm that the

Table I. Carbon (%) and Ash (%) in Humic Materials

humic material	carbon <sup>a</sup>	ash <sup>b</sup>
Aldrich	54.9	35.5
BSHA <sup>c</sup>	54.3	28.8
PPHA	45.8	9.8
BFA	ND	ND
PPW	ND	ND

<sup>a</sup> Total organic carbon/total organic matter. <sup>b</sup> Percent not volatile at 650 °C. <sup>c</sup> Key: BSHA, Boonton Reservoir sediment humic acid; PPHA, Pakim Pond humic acid; BFA, Boonton Reservoir aqueous fulvic acid; PPW, Pakim Pond water; ND, not determined.

results of the dialysis experiments were valid. To interpret the results, it was necessary to run two experiments to confirm that the dialysis system had reached equilibrium. First, every experiment contains at least one control bottle. A control bottle has a dialysis bag filled with buffered water immersed in a buffered solution of DDT. If the length of the experiment is sufficient to allow the DDT to diffuse through the bag, then the concentration of DDT should be the same on both sides of the bag at the end of the experiment. It was found that 1 day was not a sufficient length of time for DDT, but 3 days was sufficient. All of the experiments reported here were run 4-7 days.

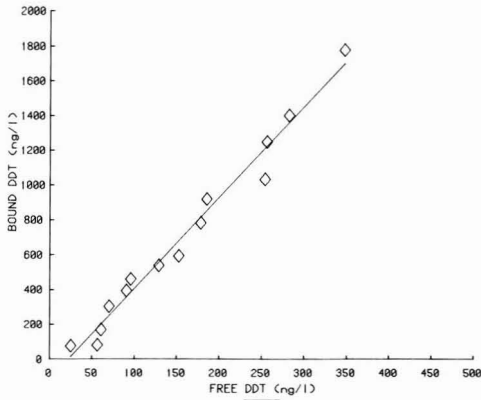
The second experiment reproduced some of the points in the dialysis experiments except that the DDT and the humic acid both started on the inside of the dialysis bag. In this experiment the equilibrium point was approached from two opposing sides, one with the DDT starting outside the bag and the other starting inside. For the points where this was done, the results were the same within experimental error. This confirms that the dialysis system was at equilibrium at the end of the experiment.

In the design of the experiment it is only possible to underestimate the amount of bound DDT. That is, if the experiment is not run long enough to allow the DDT to diffuse completely throughout the solution, the measured bound concentration (inside the bag) will be artificially low. The dialysis procedure does not allow for artificially high results. It should be noted that sorption onto glassware and dialysis materials does not affect the results. If the system is at equilibrium, both the free and the bound concentration are in equilibrium with the DDT sorbed onto the glassware and the dialysis bag, and they are therefore at equilibrium with each other.

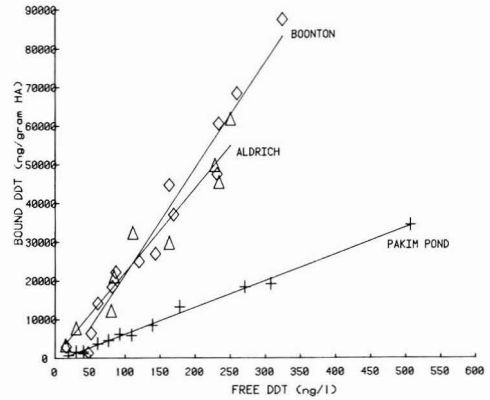
#### Dialysis Results

Figure 1 presents the results from a typical dialysis experiment. In this graph the concentration of bound DDT in ng/L is plotted vs. the free concentration in ng/L. At any point on the graph, the concentration of DDT inside the dialysis bag (the total concentration) is the sum of the free and bound concentrations. Inspection of Figure 1 shows that under these experimental conditions, greater than 75% of the total DDT is in the bound form. The experiment was run with Boonton sediment humic acid at an ash-free concentration of 16.2 or 8.8 mg/L as TOC. The pH was 8.3, and the ionic strength was equal to 0.01. Thus, under fairly realistic environmental conditions a substantial portion of the DDT that would normally be analyzed as dissolved is, in fact, bound to dissolved humic materials.

The results can be expressed in a fashion analogous to an adsorption isotherm. That is, the bound DDT can be expressed in ng/g of humic acid and this can be plotted vs. the free concentration in ng/L. This type of data analysis eliminates any straightforward dependence on the



**Figure 1.** Typical dialysis results: [Boonton humic acid] = 16.2 mg/L; pH 8.3; *I* 0.01.



**Figure 2.** Association curves for DDT with different humic acids: [Pakim Pond humic acid] = 18.0 mg/L; [Boonton humic acid] = 16.2 mg/L; [Aldrich humic acid] = 15.4 mg/L; pH 8.3; *I* 0.01.

concentration of humic acid. These plots will be referred to as "association curves".

The term "association curve" is used because it is not clear whether the humic acid-hydrophobic pollutant interaction is surface sorption or dissolution in the colloidal humic phase. Chiou et al. (12) have suggested that the association between organic compounds and sediments is better described by a liquid-liquid partitioning model than by a surface sorption model. In their discussion the organic matter present in sediment is treated as an immobilized liquid phase into which the hydrophobic compounds can partition. Other authors (13, 14) have treated these phenomena as adsorption. For the association between dissolved humic acid and hydrophobic pollutants, neither of these models seems appropriate. Most measurements of the molecular weight of dissolved humic materials give a value of 1000-5000 daltons for fulvic acids (15, 16) and 2000-20 000 daltons for humic acids (17). Both liquid partitioning and surface sorption require the presence of a second bulk phase where the DDT will either accumulate at the interface or dissolve in the nonaqueous phase. In the case of dissolved humic materials there is no second bulk phase. Furthermore, the DDT and the humic acid have sizes within the same order of magnitude. This brings up the question of which is the cart and which is the horse. Once could just as well speculate about the "adsorption" or "partitioning" of humic materials to DDT and investigate whether or not this association affected the aqueous behavior of the humic material. So that these ambiguities could be avoided, the terms "association" and "binding" have been chosen to describe the phenomena.

It is likely that the forces involved in these associations are similar to those involved in both the partitioning and adsorption of hydrophobic compounds from water. The free energy of association is probably a function of dispersion forces between the DDT and the humic polymer and changes in the self association forces of liquid water in the presence of DDT (18, 19). These are the forces that cause the so-called hydrophobic bond. The association of DDT with dissolved humic material may be analogous, therefore, to the sorption of DDT to sediment.

Figure 2 presents a series of association curves using different humic acids. The curves appear to be linear, even at DDT concentrations as high as 500 ng/L. Least-squares linear regression analyses were performed on the data. The mathematical model in this linear association curve is

$$\text{bound DDT} = M(\text{free DDT}) + B \quad (1)$$

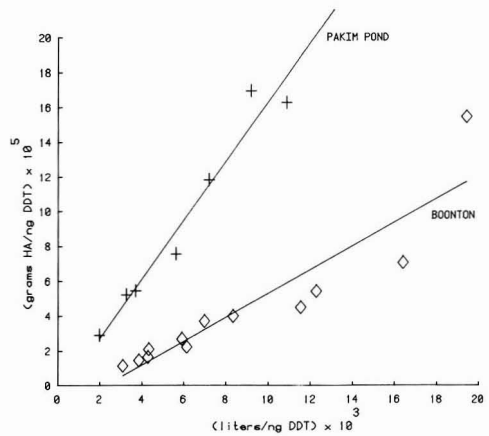


**Figure 3.** Linearized Langmuir isotherm plot of the results of two dialysis experiments: [Pakim Pond humic acid] = 18.0 mg/L; [Boonton humic acid] = 16.2 mg/L; pH 8.3; *I* 0.01.

The value for the correlation coefficient for each line was greater than 0.965.

The slopes of all the curves are statistically different at the 95% confidence level ( $p = 0.05$ ). The results show that Boonton sediment humic acid has the highest slope (274), followed by Aldrich humic acid (215), and finally Pakim Pond humic acid (70). These slopes are expressed on an ash-free basis, as are all of the slopes presented here. If the slopes of the lines are multiplied by 1000 they become analogous to weight/weight partition coefficients. The units of the slope are then (ng DDT/g of humic material)/(ng DDT/g of water). In order to convert the values of the slopes back to some environmentally useful units such as percent bound, it is necessary to know the concentration of humic acid. This is presented in all of the figures shown here. As a reference point, if an association curve has a slope of 100 and it passes through the origin, at 10 mg/L of humic acid there will be 50% bound.

An attempt was made to determine whether or not the data were better described by a double reciprocal plot, analogous to a Langmuir isotherm. Figure 3 shows the data for Boonton reservoir and Pakim Pond humic acid plotted in a linearized Langmuir form (20). In both cases the correlation coefficients were lower than for the linear

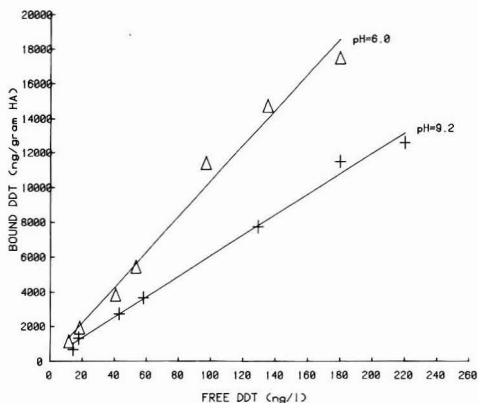


**Figure 4.** Effect of pH on the association curve for DDT: [Pakim Pond humic acid] = 18.8 mg/L;  $I$  0.01.

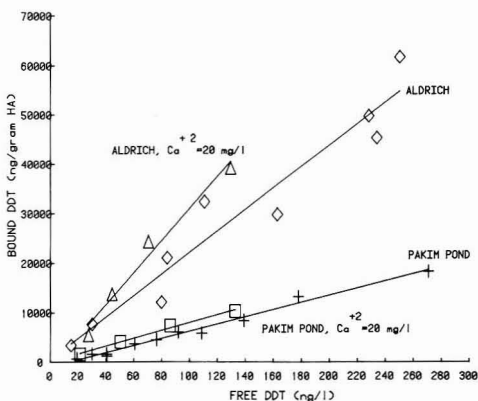


**Figure 5.** Effect of calcium on the association curve for DDT: [Pakim Pond fuming acid] = 18.0 mg/L, pH 8.3,  $I$  0.01,  $[Ca^{2+}]$  = 0 mg/L; [Pakim Pond fuming acid] = 18.1 mg/L, pH 8.3,  $I$  0.01,  $[Ca^{2+}]$  = 20 mg/L; [Aldrich fuming acid] = 15.4 mg/L, pH 8.3,  $I$  0.001,  $[Ca^{2+}]$  = 0 mg/L; [Aldrich fuming acid] = 13.0 mg/L, pH 8.3,  $I$  0.001,  $[Ca^{2+}]$  = 20 mg/L.

association curves shown in Figure 2. This was true for Boonton humic acid even when the worst two points were eliminated from the Langmuir plot. It appears that there is nothing gained by plotting the data in this fashion. The curves plotted in Figure 2 showed no apparent curvature at concentrations of 0.9 mg of DDT/g of BSHA and 0.03 mg of DDT/g of PPHA. This suggests that there is no shortage of association sites at these concentrations and that the linear model is adequate over the concentration range tested.

Figure 4 shows the effect of pH on the association curve using Pakim Pond humic acid. At pH 6 the slope of the line is 102, while at pH 9.2 the slope is 59. These slopes are different at the 0.5% level. At pH 8.3 the slope is 70, but this is not significantly different from the value at pH 9.2. The data show that there is more bound DDT at lower pH levels.

Figure 5 shows the effect of calcium on the association curve. The curves for Pakim Pond and Aldrich humic acid are plotted in the presence and absence of  $Ca^{2+}$ . In both cases the addition of calcium appeared to increase the amount of DDT bound. The observed differences, however, are not significant at the 5% level.

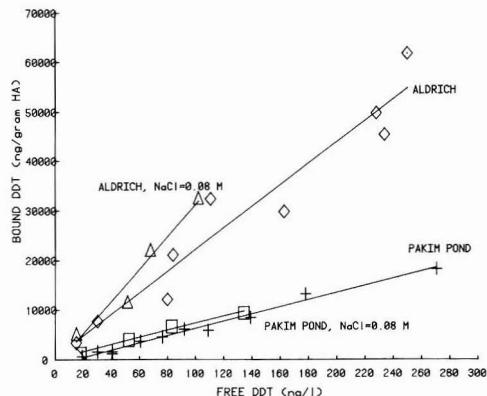


**Figure 6.** Effect of ionic strength on the association curve for DDT: [Pakim Pond fuming acid] = 18.0 mg/L, pH 8.3,  $I$  = 0.01; [Pakim Pond fuming acid] = 18.1 mg/L, pH 8.3,  $I$  0.08; [Aldrich fuming acid] = 15.4 mg/L, pH 8.3,  $I$  0.001; [Aldrich fuming acid] = 13.0 mg/L, pH 8.3,  $I$  0.08.

Figure 6 shows the effect of increased ionic strength on the association curve. In this graph the curves for Pakim Pond and Aldrich humic acid were repeated at an ionic strength of 0.08 (NaCl). At higher ionic strength more DDT appears to be in the bound form, but the increase is not significant at the 5% level.

For the association curves generated to date (over 30, some of which are not presented here) all but one have y-intercepts that are indistinguishable from zero ( $p = 0.05$ ). This is very close to the expected number of deviations. It seems reasonable, therefore, to assume that all of the association curves pass through the origin. The curves also appear linear, and all have correlation coefficients greater than 0.955. This suggests that the curves can be described by one parameter, analogous to a partition coefficient, which we will be referred to as the "association constant". The mathematical model for this interaction is

$$\text{bound DDT} = K(\text{free DDT}) \quad (2)$$

From this one parameter model, every point on the association curve represents an independent measurement of the association constant. This makes the appropriate statistical tests more powerful. If the data are analyzed by using this one parameter model, the effects of increased calcium and ionic strength are statistically significant for both Pakim Pond and Aldrich humic acid. Both the presence of calcium and increased ionic strength cause an increase in the association constant ( $p = 0.05$ ). The one-parameter model also indicates that there is no significant difference in the extent of binding between Boonton Reservoir humic acid and Aldrich humic acid (Figure 2).

Table II shows the association constants for the data in Figures 2-8. This table presents the association constants in terms of both humic acid organic matter and humic acid organic carbon.

Figure 7 presents three association curves, using Pakim Pond humic acid at three different humic acid concentrations. The association constants are presented in Table II. The results suggest that the association constant is dependent on the concentration of humic acid. If the association constant was independent of the concentration of humic acid, all the association curves should have the same slope, and the association constants should be identical. The constants at 40 and 20 mg/L are indistinguishable. The constant at 10 mg/L, however, is significantly higher than the other two ( $p = 0.05$ , one tailed test).

Table II. Preliminary Results: Association Constants of DDT under Various Aqueous Conditions

humic material	concn <sup>a</sup> mg/L	pH	I	[Ca], mg/L	log K	log K <sub>c</sub>	n	95% limits <sup>c</sup>
PPHA	8.3	8.3	0.01	0	4.73	5.09	13	18 100
PPHA	4.1	8.3	0.01	0	4.85	5.19	9	32 800
PPHA	16.6	8.3	0.01	0	4.73	5.07	10	12 300
PPHA	8.3	6.0	0.01	0	5.09	5.35	7	16 400
PPHA	8.3	9.2	0.01	0	4.77	5.13	7	16 500
PPHA	8.3	8.3	0.01	20	4.86	5.20	8	19 400
PPHA	8.3	8.3	0.08	0	4.86	5.20	4	23 200
Aldrich	8.5	8.3	0.01	0	5.35	5.61	9	32 300
Aldrich	7.1	8.3	0.001	20	5.46	5.72	4	183 000
Aldrich	7.1	8.3	0.08	0	5.48	5.74	4	147 000
BSHA	8.8	8.3	0.01	0	5.35	5.61	13	25 200
Pakim Pond water	4.3	8.3	0.001	0		4.84	4	11 000
Boonton water	3.0	8.3	0.001	ND <sup>d</sup>		4.83	4	28 000

<sup>a</sup> Concentration as DOC. <sup>b</sup> K<sub>c</sub>: association constant in terms of organic carbon. <sup>c</sup> Refers to K<sub>c</sub>. <sup>d</sup> ND: not determined.

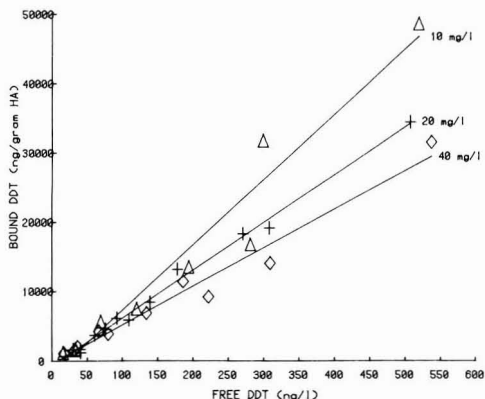


Figure 7. Effect of humic acid concentration on the association curve for DDT: pH = 8.3; I 0.01; concentrations include ash.

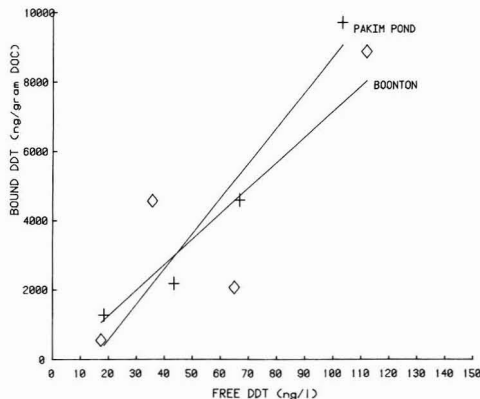


Figure 8. Association curves for DDT in natural waters: [Pakim Pond DOC] = 4.3 mg/L; [Boonton Reservoir DOC] = 3.0 mg/L; pH 8.3; I 0.001.

This indicates that the association constant increases as the humic acid concentration decreases.

Figure 8 presents two association curves using filtered (0.22 μm) natural water samples. The sample from Pakim Pond was collected shortly after the humic acid precipitated out of the water column in September 1981, so the DOC of 4.3 was unusually low for this body of water. The DOC of 3.0 for Boonton Reservoir was typical. For both samples the experiments showed that binding of DDT to dissolved organic carbon was occurring. The data are somewhat noisy due to the low DOC values and the small number of data points, especially for Boonton Reservoir. The association constants presented in Table II for Pakim Pond and Boonton water correspond to 23% and 17% bound, respectively. This experiment shows that the DOC in real water samples can bind a substantial fraction of the total DDT.

Discussion

The association constants presented here cover a quite wide range of values. The lowest is for the binding between DDT and Boonton Reservoir DOC (K<sub>c</sub> = 67 800, log K<sub>c</sub> = 4.83), while the highest is for the binding between DDT and Aldrich humic acid in the presence of 0.8 M NaCl (K<sub>c</sub> = 544 000, log K<sub>c</sub> = 5.74). The extent of binding for the three samples isolated from natural waters (PPHA and the two water samples) is less than the extent of binding for the two humic acids isolated from soil and sediment (BSHA and Aldrich HA). Kenaga et al. (21) have measured the sorption constant of DDT to particulate sedi-

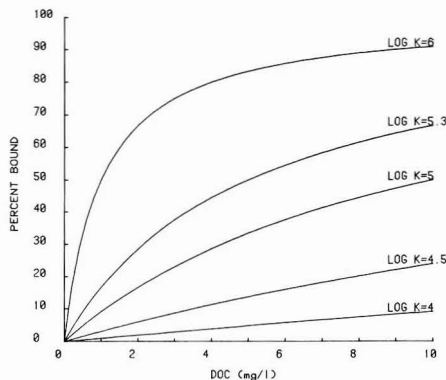


Figure 9. Plots of percentage of [bound pollutant] vs. [DOC] for different values of the association constant.

mentary organic carbon. The value they find is 238 000, which is comparable to the values shown in Table II for dissolved humic materials. From the values for K<sub>c</sub> and the DOC of an aqueous solution, the percentage of bound pollutant can be calculated using eq 3, which is plotted in

$$\% \text{ bound} = \frac{10^{-6}K_c[\text{DOC}]}{10^{-6}K_c[\text{DOC}] + 1} \times 100 \quad (3)$$

Figure 9 for a variety of values of log K<sub>c</sub>.

The effects of pH, calcium, and ionic strength are consistent with the known effects of solution parameters on the aqueous behavior of humic materials. As the hydrogen ion and metal ion concentrations increase, the molecular size of the humic polymer will increase (22-24). The humic polymer may coil as the pH is reduced or as the ionic strength is increased (25). It will be more prone to sorption on a variety of surfaces as the hydrogen ion and metal ion concentration increase (26-31). The charge on the polymer will decrease as the pH is lowered or as the metal ion concentration is increased (17, 32, 33). The changes indicate that the humic polymer becomes less hydrophilic as its charge is neutralized or as the ionic strength is increased. It seems reasonable that the less hydrophilic form of the polymer would bind hydrophobic compounds more effectively. The hydrophobic organic compounds will be more likely to associate with uncharged portions of the polymer. The effects of pH and calcium are therefore probably due to neutralization of the charge on the humic polymer. The effect of increased ionic strength could also be due to salting out of the hydrophobic organic compound. That is, the chemical potential of a dissolved nonionic compound in water will increase with increased ionic strength.

The apparent dependence of the association constant on the humic acid concentration is puzzling. This is similar, however, to the phenomena reported by O'Connor and Connally (33) concerning the adsorption of organic compounds to sediments. These authors found that the sorption coefficient for organic compounds to sediments decreased as the amount of sediment used in an experiment increased. In a sediment sorption experiment it is possible that as more sediment is added, more DOC is also added. That is, some of the organic carbon in the sediment may dissolve in the aqueous phase. If this newly introduced DOC could bind the pollutant of interest, the sorption coefficient would decrease with increased sediment concentration. An analogous possibility exists for the dialysis experiments reported here. If a portion of the humic acid can leak through the dialysis bag and if this portion can bind the DDT, the association constant would decrease with increased humic acid concentration. However, as mentioned in the Experimental Section, we detected no leakage of UV absorbing materials.

#### Literature Cited

- (1) Hassett, J. P.; Anderson, M. A. *Environ. Sci. Technol.* **1979**, *13*, 1526-1529.
- (2) Wershaw, R. L.; Burcar, P. J.; Goldberg, M. C. *Environ. Sci. Technol.* **1969**, *3*, 271-273.
- (3) Porrier, M. A.; Bordelon, B. R.; Laseter, J. L. *Environ. Sci. Technol.* **1972**, *6*, 1033-1035.
- (4) Boehm, P. D.; Quinn, J. G. *Geochim. Cosmochim. Acta* **1973**, *37*, 2459-2477.
- (5) Matsuda, K.; Schnitzer, M. *Bull. Environ. Contam. Toxicol.* **1973**, *6*, 200-204.

- (6) Zepp, R. G.; Baughman, G. L.; Schlotzhauer, P. F. *Chemosphere* **1981**, *10*, 109-117.
- (7) Griffin, R. A.; Chian, E. S. K. EPA Publication, EPA-600/2-80-027, 1980.
- (8) Hassett, J. P., State University of New York, Syracuse, personal communication, 1982.
- (9) Perdue, E. M. Symposium on Terrestrial and Aquatic Humic Materials, University of North Carolina, Chapel Hill, NC, November, 1981.
- (10) Levesee, G. J. Symposium on Terrestrial and Aquatic Humic Materials, University of North Carolina, Chapel Hill, NC, November, 1981.
- (11) Chrostowski, P. C. Ph.D. Thesis, Drexel University, Philadelphia, PA, 1981.
- (12) Chiou, C. T.; Peters, L. J.; Freed, V. H. *Science (Washington, D.C.)* **1979**, *206*, 831-832.
- (13) Karickhoff, S. W.; Brown, D. S.; Scott, T. A. *Water Res.* **1979**, *13*, 241-248.
- (14) Means, J. C.; Wood, S. G.; Hassett, J. J.; Banwart, W. L. *Environ. Sci. Technol.* **1980**, *14*, 1524-1528.
- (15) Buffle, J.; Deladoey, P.; Haerdi, W. *Anal. Chim. Acta* **1978**, *101*, 339-357.
- (16) Underdown, A. W.; Langford, C. H.; Gamble, D. S. *Anal. Chem.* **1981**, *53*, 2139-2140.
- (17) Schnitzer, M.; Khan, S. U. "Humic Substances in the Environment"; Marcel Dekker: New York, 1972.
- (18) Horne, R. A. In "Water and Water Pollution Handbook"; Ciaccio, L. L., Ed.; Marcel Dekker: New York, 1972.
- (19) Hildebrand, J. H. *Proc. Natl. Acad. Sci. U.S.A.* **1979**, *76*, 194.
- (20) Weber, W. J. "Physicochemical Processes for Water Quality Control"; Wiley-Interscience: New York, 1972.
- (21) Kenaga, E. E.; Goring, C. A. I. In "Aquatic Toxicology"; Eaton, J. G.; Parrish, P. R., Hendricks, A. C., Eds.; American Society for Testing and Materials: Philadelphia, PA, 1980.
- (22) Wershaw, R. L.; Pinckney, D. J. *J. Res. U.S. Geol. Surv.* **1973**, *1*, 701-707.
- (23) Lee, M. C.; Snoeyink, V. L.; Crittenden, J. C. *J. Am. Water Works Assoc.* **1981**, *73*, 440-446.
- (24) Ghosh, K.; Schnitzer, M. *Soil Sci.* **1980**, *129*, 266-276.
- (25) Thurman, E. M.; Malcolm, R. L. *Environ. Sci. Technol.* **1981**, *15*, 463-466.
- (26) Mantoura, F. C.; Riley, J. P. *Anal. Chim. Acta* **1975**, *76*, 97-106.
- (27) McCreary, J. J.; Snoeyink, V. L. *Water Res.* **1980**, *14*, 151-160.
- (28) Davis, J. A.; Gloor, R. *Environ. Sci. Technol.* **1981**, *15*, 1223-1229.
- (29) Randtke, S. J.; Jepsen, C. P. *J. Am. Water Works Assoc.* **1982**, *74*, 84-93.
- (30) Weber, W. J.; Pirbazari, M.; Long, J. B.; Barton, D. A. In "Activated Carbon Adsorption of Organics from the Aqueous Phase"; Suffet, I. H., McGuire, M. J., Eds.; Ann Arbor Science: Ann Arbor, MI, 1980; Vol. 1.
- (31) Hunter, K. A. *Limnol. Oceanogr.* **1980**, *25*, 807-822.
- (32) Dempsey, B. A.; O'Melia, C. R. Symposium on Terrestrial and Aquatic Humic Materials. University of North Carolina, Chapel Hill, NC, November, 1981.
- (33) O'Connor, D. J.; Connally, J. P. *Water Res.* **1980**, *14*, 1517-1523.

Received for review January 20, 1982. Accepted June 21, 1982.



# Organic Carbon Removal by Advanced Waste Water Treatment Processes

Foppe B. DeWalle\*

Department of Environmental Health, University of Washington, Seattle, Washington 98195

William G. Light

Research and Development Division, Abcor, Inc., Wilmington, Massachusetts 01887

Edward S. K. Chlan

Department of Civil Engineering, Georgia Institute of Technology, Atlanta, Georgia 30332

■ Fourteen physical-chemical processes singularly or in combination were evaluated for their ability to remove dissolved organic carbon in the effluent of a waste water reclamation facility treating secondary effluent. The largest organic carbon removals were obtained with reverse osmosis (RO) at an 85% product water recovery. As RO removals before and after activated carbon treatment were similar, RO may be employed directly following coagulation.

## Introduction

Physical-chemical treatment processes such as coagulation/filtration and activated carbon have been used in conventional drinking water treatment to reduce volatile and other trace organic contaminants to levels that are acceptable by the Interim Primary Drinking Water Regulations (1). Highly treated effluents from advanced waste water treatment (AWT) plants that generally consist of coagulation, filtration, and activated carbon following the biological treatment, however, often contain levels of trace organics comparable to levels present in conventional water supplies before physical-chemical treatment. If reuse of municipal waste waters for potable purposes is to be a viable alternative, additional treatment may be required to reduce the concentrations of trace organics in AWT effluent to even lower levels. The objective of the present study was to identify and evaluate cost effective treatment processes that can reduce by an order of magnitude the levels of total organic carbon (TOC) in effluents from well-operated AWT plants. The most promising treatment processes identified in a literature review were evaluated with respect to TOC removal in laboratory and pilot-scale tests using an actual AWT effluent.

Fifty potential treatment processes, identified in 500 literature citations, were rated based on their anticipated efficacy and costs for removing trace organics from AWT effluents. The processes were rated according to the predicted capability for removing organics within the four chemical groups that typically comprise nearly all of the effluent TOC: low molecular weight polar organics (about 50% of the TOC (2)), humic and fulvic substances (about 45% of the TOC (3)), and halogenated organics (about 1% of the TOC (4)). With this approach, four processes were concluded to be most cost effective for achieving a 90% removal of chemicals within the four prevalent categories of organics in AWT effluent. These include two oxidants (ozonation in combination with ultraviolet (UV) irradiation and hydrogen peroxide in combination with UV irradiation), a membrane process (reverse osmosis), and a series of complementary adsorbents (ion exchange/polymeric resins). In addition to the four most highly rated processes, four oxidation processes were identified.

Removal efficiencies for TOC of >90% have been reported for ozone (5) and hydrogen peroxide (6) when UV

is also employed to enhance oxidation. Although at high dosages (7) or for certain organic fractions (8) ozone alone can achieve >70% organic removal, removal efficiencies are generally well below this value as are those for hydrogen peroxide alone (9). Reverse osmosis (RO) has also been shown to remove >90% of the organics in AWT effluent (10). For high rejecting polyamide RO membranes, nearly complete removal of high molecular weight organics (fulvic and humic substances) and between 50% and 75% removal for low molecular weight polar organics (11, 12) would be expected. The fourth highly rated approach for achieving >90% TOC removal is to use several complementary adsorbent resins in series. Hydrophilic organics such as low molecular weight organic acids and humic/fulvic acids can be effectively removed by using weak base anion-exchange resins (13-15) or polymeric resins (16). Carbonaceous polymeric resins have been developed specifically to remove chlorinated organics.

Other processes were evaluated and concluded to be incapable of accomplishing the performance goal of >90% TOC removal. Precipitants, for example, were not selected for laboratory and pilot-scale tests because of the suspected very low removal efficiency for low molecular weight polar organics (17), even though alum plus filtration (18), high molecular weight polymers (19, 20), or polymers plus filtration (21) can give >95% removal of humic acids.

## Materials and Methods

The AWT effluent used in the screening evaluation was obtained from the 0.55 m<sup>3</sup>/s (15 mgd) Water Factory 21 advanced waste water reclamation facility in Fountain Valley, Orange County, CA. In this full-scale plant, activated sludge effluent is treated by using chemical clarification for solids removal, air-stripping for ammonia and volatiles removal, recarbonation for pH adjustment, mixed media filtration for additional solids removal, and activated carbon adsorption for soluble organics removal as shown in Table I (10).

To allow for relating process performance results to AWT plants in general, every effort was made to ensure that the organic carbon for the AWT effluent as measured by TOC was not much greater than 5 mg/L. Adequate shipping and preservation techniques were employed to ensure that the characteristics of the AWT effluents were not significantly altered between the sampling, processing, and analysis.

Fourteen processes or combinations of processes were selected for screening studies at laboratory scale. These included the following:

- (i) the four most highly rated processes
  - (1) reverse osmosis
  - (2) ozonation/ultraviolet irradiation
  - (3) hydrogen peroxide/ultraviolet irradiation
  - (4) ion exchange/polymeric resin

**Table I. Design Parameters for Reclamation Plant<sup>a</sup>**  
(Flow: 0.66 m<sup>3</sup>/s (15 mgd))

chemical clarification (23.9¢/1000 gal) <sup>b</sup>	rapid mix (1.2 min, pH 11, 350-400 mg/L CaO and 0.1 mg/L polymer addition), flocculation ( $G = 100 \text{ s}^{-1}$ for 10 min, $G = 25 \text{ s}^{-1}$ for 10 min, $G = 20 \text{ s}^{-1}$ for 10 min), clarification with settling tubes (2.7 m <sup>3</sup> /(m <sup>2</sup> h), $D = 40$ min)
airstripping (9.8¢/1000 gal)	draft towers (3000 m <sup>3</sup> of air/m <sup>3</sup> of water or natl vent.), down flow (26.4 m <sup>3</sup> /(m <sup>2</sup> h))
recarbonation (5.6¢/1000 gal)	pH decrease to 7.5 by carbon dioxide from lime recalcining furnace, chlorination at 8 mg/L, clarification (5 m <sup>3</sup> /(m <sup>2</sup> h))
mixed media filtration (3.9¢/1000 gal)	coal, sand, garnet with 0.76 m depth (12 m <sup>3</sup> /(m <sup>2</sup> h))
carbon adsorption <sup>c</sup> (16.7¢/1000 gal)	granular activated carbon (Filtrosorb 300), down flow (12 m <sup>3</sup> /(m <sup>2</sup> h), 34 min empty bed determination time)
reverse osmosis (62¢/1000 gal)	(a) sodium hexametaphosphate ppt inhibitor (2 mg/L), chlorination (0.5 mg/L); (b) polypropylene cartridge filters (25 µm presize); (c) sulfuric acid addition (pH 5.5 for scale prevention); (d) spiral-wound cellulose acetate membranes (1260 modules in 24-12-6 configuration, 538 psi); (e) 85% permeate recovery (31.7 m <sup>3</sup> /(m <sup>2</sup> h)); (f) packed tower de-carbonators (22 m <sup>3</sup> of air/m <sup>3</sup> of water)
chlorination (6.6¢/1000 gal)	dosage 20 mg/L ( $D = 30$ min)
deep well injection (8¢/1000 gal)	

<sup>a</sup> Reference 10. <sup>b</sup> Clarification effluent for reverse osmosis testing. <sup>c</sup> AC effluent used for testing of 14 process combinations.

(ii) modifications of two of the highly rated oxidant processes

- (5) ozonation
- (6) ozonation/UV plus activated carbon
- (7) hydrogen peroxide
- (8) hydrogen peroxide/iron catalyst
- (9) hydrogen peroxide/UV plus activated carbon
- (10) ultraviolet irradiation

(iii) and four other oxidants

- (11) ferrate
- (12) persulfate
- (13) perborate
- (14) permanganate

Four resins were screened in adsorption tests: S-37, a very weak base macroporous anion-exchange resin having secondary and tertiary amine and phenol hydroxyl functional groups and a phenol formaldehyde matrix (Diamond Shamrock, Redwood City, CA); IRA-504, a strong base macroporous anion-exchange resin with quarternary amine functional groups and polystyrene matrix having a capacity

of 2.0 mequiv/g; IRA-4500, a strong base anion-exchange resin with quarternary amine functional groups and an acrylic matrix having a capacity of 4.4 mequiv/g; XAD-7, a macroporous adsorbent with an acrylic matrix (Rohm and Haas, Philadelphia, PA). The resins were packed in a 50-cm glass column prerinse with base, acid, and distilled water and operated on the site with a 3-min detention time.

The ozonation tests were conducted with 750 mL of AWT effluent placed in an enclosed 1000-mL baffled and stirred ozonation vessel. The ozone was supplied at a rate of 102 mg/min and a flow rate of 3.3 L/min, representing 15% of the GL-1 ozonation capacity using pure oxygen (PCI Ozone Corp., West Caldwell, NJ). The reactor off-gas was collected in scrubbers filled with 20 000 mg/L KI, which was back-titrated with 0.025 N phenylarsine oxide. The UV/ozone experiments were conducted in the same vessel with a quartz tube containing the UV source protruding downward from the top of the enclosed vessel. The UV source was a 5.5-W quartz lamp with low-pressure gaseous mercury discharge providing a monochromatic light source at 254 nm and an intensity of 875 µW/cm<sup>2</sup> at 2.5-cm distance (Penray lamp, Ultraviolet Products, Inc., San Gabriel, CA). The light source is powered through a 14-W transformer providing 800 V to start the lamp and 270 V during operation.

The 110-L batch reverse osmosis tests were conducted with a 500 L/day unit containing eight external tubular membrane core assemblies with a total surface area of 0.37 m<sup>2</sup> and a 2238 W (3 hp) diaphragm pump (SC-4, Western Dynetics, Newburg Park, CA). The cellulose acetate type CA 190 was rated at a minimum flux of 0.73 m<sup>3</sup>/(m<sup>2</sup> day) (18 gal/(ft<sup>2</sup> day)) at 25 °C and 35 kg/cm<sup>2</sup> (500 psig) and a rejection of 90% using a 5000 mg/L NaCl solution. The 5-h tests with acidified (pH 5.5) activated carbon effluent showed a flux of 1.3 m<sup>3</sup>/(m<sup>2</sup> day) and a salt rejection of 95.5%. Tests were also conducted with the same pumping assembly using a B-10 permeator (DuPont, Wilmington, DE), containing polyamide hollow fibers with a surface area of 140 m<sup>2</sup>, which is rated at 5677 L/day (1500 gal/day) and a flux rate of 0.04 m<sup>3</sup>/(m<sup>2</sup> day).

The tests with reverse osmosis and resins were conducted at the reclamation plant between March 29 and April 4, 1980, while the ozonation test was conducted at the University of Washington. A second activated carbon effluent sample was collected on October 3, 1980, for additional oxidant testing. The influent and effluent samples were collected with an all glass/Teflon-lined sampler by using glass syringes to displace the liquid. The samples were analyzed with an ultralow-level total organic carbon analyzer (Model DC-54, Dohrman, Santa Clara, CA), consisting of a sample input module (PR-1) and totalizer/reaction module (DC-52). The unit measures both purgable and nonpurgable TOC. A 10-mL sample containing acidified persulfate was helium sparged for removal of volatile organics followed by UV oxidation of the organics and a second sparging step. The oxidized carbon was measured as methane with a flame ionization detector following reduction by a hydrogen-enriched nickel catalyst. The lower limit of the limit is 50 µg/L while it realized a 5% precision on repeated analysis of the same sample. An aliquot of the composite sample had a pH of 6.8, a conductivity of 1450 mmho, 887 mg/L total dissolved solids, and 21 mg/L inorganic carbon.

Additional experiments were conducted with five promising oxidants that are sometimes used in water treatment of industrial treatment processes with AWT effluent collected on October 3, 1980. Four of the oxidants,

Table II. Levels of COD and TOC in Reclamation Plant Effluents<sup>a</sup> and TOC Values Noted in the Present Study

	chemical oxygen demand, mg/L	total organic carbon, mg/L	TOC (this study), mg/L
activated sludge effluent	46.6 (25-76)	12.8 (11.1-14.2)	
clarification effluent	25.8 (17-49)	9.2 (6.5-12)	5.4
activated carbon effluent	13.4 (3.9-29)	5.0 (1.9-7.7)	5.5/3.5/5.7
cellulose-acetate reverse osmosis effluent	1.3 (1-7)	0.7 (0.4-1.6)	0.86

<sup>a</sup> Reference 10.

i.e., persulfate, perborate, permanganate, and ferrate, were available as solids, while hydrogen peroxide was the only liquid oxidant evaluated. Persulfate is a triple salt of 2 mol of potassium monopersulfate (KHSO<sub>5</sub>), 1 mol of potassium hydrogen sulfate (KHSO<sub>4</sub>), and 1 mol of potassium sulfate (K<sub>2</sub>SO<sub>4</sub>), and commercially available as oxone (DuPont, Wilmington, DE). It has a water solubility of 256 g/L at 20 °C while a 10 g/L solution results in a pH of 2.3. The oxidant has been used to oxidize phenols, olefins, and amines and is often added to laundry bleach, denture cleaners, and toilet bowl cleaners.

Perborate (NaBO<sub>3</sub>·4H<sub>2</sub>O) is an alkaline white powder that is a stable dry form of hydrogen peroxide (NaBO<sub>2</sub>·H<sub>2</sub>O<sub>2</sub>·3H<sub>2</sub>O). It is manufactured from borax, sodium hydroxide, and hydrogen peroxide. It has a solubility of 20 g/L to result in a pH of 10.4.

Potassium permanganate (KMnO<sub>4</sub>) is a purple crystal and attains a maximum solubility of 65 g/L at 20 °C (Carus Chemical Corp., La Salle, IL). It has been commonly used in drinking water treatment to oxidize organics such as phenol (above pH 7), odors, and mercaptans and inorganics such as ferrous iron and cyanides. After formation of the insoluble MnO<sub>2</sub> the residue can be removed by coagulation.

Ferrate (K<sub>2</sub>FeO<sub>4</sub>) is a reddish-black powder that is stable at temperatures up to 198 °C. It oxidizes compounds evolving oxygen and carbon dioxide and precipitates as ferric hydroxide. It is not commercially available and has to be manufactured according to the procedures of Schreyer et al. (22) using chlorination of ferric nitrate. It is a very effective bactericide at concentrations of a few milligrams per liter (23). Organic conversions by ferrate range from 33% for benzene to 93% for allylbenzene and almost complete conversion for phenol (24).

Hydrogen peroxide (H<sub>2</sub>O<sub>2</sub>) is a clear, waterlike liquid, and a 50% concentration has 23% active oxygen content and contains 600 g of H<sub>2</sub>O<sub>2</sub>/L (FMC, Philadelphia, PA). The liquid is a strong oxidizer and liberates oxygen upon decomposition. With a 3:1 mole ratio, it is able to convert 99% of most chlorophenols and nitrophenols (25). Using hydrogen peroxide/UV at 1% by volume resulted in greater than 95% TOC removal (26).

### Results and Discussion

The TOC in the carbon effluent during the initial part of the testing was 5.5 mg/L but decreased to 3.5 mg/L during the latter part of the testing period following a short plant shutdown. It was 5.7 mg/L during the second testing period. These values are comparable to the median concentrations observed at the plant (10) (Table II).

The ion-exchange resins showed low organic carbon removal efficiencies using the activated carbon effluent

Table III. Total Organic Carbon in Effluent after Treatment of AWT Effluent with Most Effective Processes

	influent TOC, mg/L	effluent TOC, mg/L
S-37 resin adsorption after activated carbon	5.5	3.8
polyamide reverse osmosis after activated carbon	3.5	0.66
polyamide reverse osmosis after coagulation	5.4	0.48
cellulose acetate reverse osmosis after activated carbon	3.5	0.86
cellulose acetate reverse osmosis after coagulation	5.4	1.6
ozonation after activated carbon	3.5	1.2
ozonation/UV after activated carbon	3.5	0.79
hydrogen peroxide	5.7	0.32

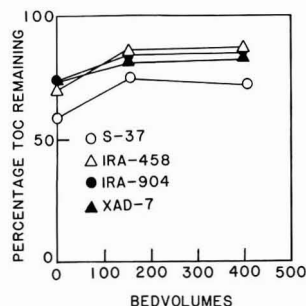


Figure 1. Permeation of organics through resin columns using activated carbon column effluent.

(Table III). After 400 bed volumes, the removal with the S-37 resin was 28% while the other resins had removals of as low as 14% (Figure 1). This would indicate that a stronger basic character of the amine group does not enhance the organic removal. The phenol-formaldehyde matrix apparently provided better removal than the polystyrene or acrylic matrix.

Among the systems tested, the membrane reverse osmosis produced the lowest effluent organic carbon concentration treating activated carbon effluent. The highest removals were obtained with the polyamide hollow-fiber membranes as compared to the cellulose acetate membranes (Figure 2). During the batch concentration, both retentate and permeate showed increasingly higher organic concentrations. As the increase of the retentate concentration was greater than the increase of the permeate concentration, the instantaneous removal percentage increased during the batch run. This increase is due primarily to low molecular weight organics that permeate the membrane during the initial volume reduction. As their relative mass in the retentate decreases, the percentage rejection increases. This rejection improvement was most noticeable for the cellulose acetate as compared to the polyamide, as the latter retains lower molecular weight organics to a greater extent as shown by its higher rejection. The average permeate concentration at an 85% product recovery is 0.86 mg/L for the CA-RO and 0.66 mg/L for the PA-RO. Similar removal efficiencies can be expected from a continuous flow operation, while lower effluent concentrations can be realized by using a product recovery of 70% instead of 85%.

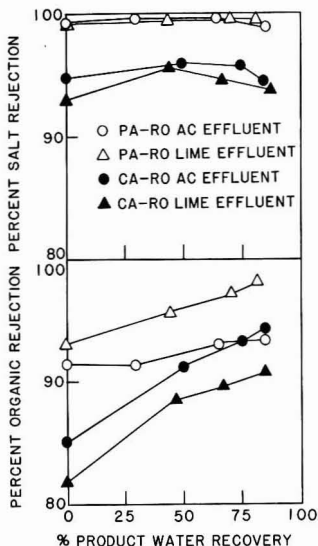


Figure 2. Organics removed during reverse osmosis of activated carbon column effluent and lime effluent.

As the reverse osmosis system is more costly than lime coagulation, filtration, and activated carbon together, selection of RO greatly increases the cost of advanced waste treatment. It is therefore important to determine what unit processes can be omitted from the sequence prior to RO. The present study therefore evaluated both membrane types by using lime-clarified effluent, thereby omitting the sand filtration and activated carbon step. The results in Figure 2 show that removal percentages similar to those with activated carbon effluent can be realized. As activated carbon removes both adsorbable and low molecular weight biodegradable organics (3), one would expect a higher rejection with activated carbon effluent, which was indeed noted for the CA membrane. The higher rejection of the PA membrane before activated carbon treatment does not follow this pattern.

Substantial organic carbon removals were observed with ozone and ozone/UV using activated carbon effluent (Figure 3). The former reached a 65% removal while the latter was able to remove 77%. A noticeable break in the removal curve was observed after 30 min in the ozone system and after 40 min in the ozone/UV system, indicating that the UV extended the range of compounds that can be oxidized by ozone but did not increase the rate of oxidation. Similar breakpoints were noted by Chian et al. (8) for ozonation of UF retentates after 100 min and for the lower molecular RO retentate after 60 min. The UV alone did not result in any organic removals. It should be realized that the ozone dosages in the batch test are substantially higher than in a flow-through system with approximately 95% leaving the reactor in the off-gas. During the test run a total of 6180 mg was applied to 4.3 mg of organic carbon, a 700-fold excess. In flow-through systems the ratio generally ranges from 1 to 10. Lower removals are therefore expected in continuous flow-through systems.

The evaluation of additional oxidants was conducted by using activated carbon effluent collected from Water Factory 21 on October 3, 1980. The effluent had a TOC of 5.7 mg/L, which is slightly higher than the values noted before, and a pH of 6.7. The solid oxidants were made as a 1% stock solution, and increasing amounts were added under mixing to different aliquots of the effluent. After

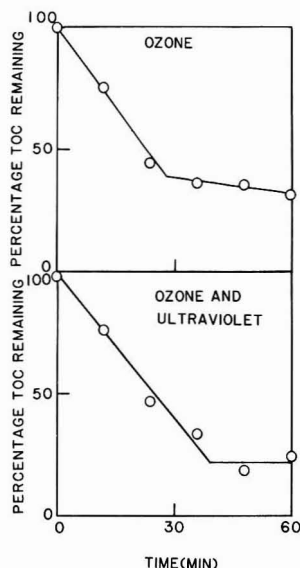


Figure 3. Decrease of organics during ozonation of activated carbon column effluent.

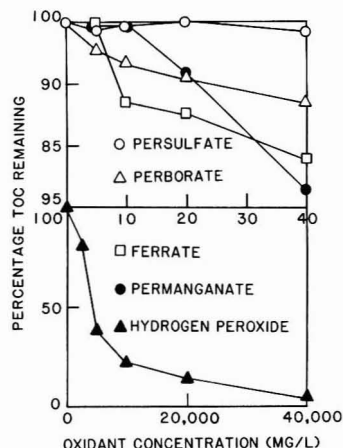


Figure 4. Decrease of organics during oxidation of activated carbon effluent.

20 min, the liquid was tested for its residual TOC by using the low-level TOC analyzer. The results shown in Figure 4 indicate that permanganate is the most effective solid oxidant as it removes 13.7% of the TOC of the activated carbon effluent at a dosage of 40 mg/L. The liquid oxidant  $H_2O_2$  was especially effective as it removes 94% of the TOC at the highest dosage evaluated. However, at a concentration comparable to the solid oxidants, i.e., 40 mg/L, it only removed a calculated 0.3% of the TOC. The results of the TOC oxidation by hydrogen peroxide at a dosage of 2% by volume showed that most of the oxidation was completed in less than 4 min. No differences were noted between  $H_2O_2$ /UV and use of  $H_2O_2$  with a 10 mg/L iron catalyst as recommended by Keating et al. (25).

Treatment of the effluent from the oxidation step resulted in further TOC reduction. Activated carbon treatment after 15 min of ozone/UV exposure resulted in a TOC reduction to 0.85 mg/L TOC, which is slightly

higher than the residual TOC observed after 30-min ozonation. Activated carbon treatment of the H<sub>2</sub>O<sub>2</sub>/UV treated effluent showed a violent liberation of O<sub>2</sub> and CO<sub>2</sub> and resulted in an effluent TOC of 1.28 mg/L.

Analysis of the full-scale CA-RO process showed a 90.3% COD removal and 96.7% salt rejection, which gradually decreased to 86.5% after 500 days (10). Pilot tests were also conducted with lime-clarified effluent by using the cellulose acetate spiral-wound membranes (8150 HR, UOP, San Diego) and the polyamide spiral-wound membrane (4600, UOP, San Diego). The CA membranes at 350 psi and 85% product water recovery showed a 94.4% salt rejection, a 92.6% COD reduction, and a -0.027 slope of the flux decline curve, while the polyamide membranes at 400 psi and 85% permeate recovery showed a 98.8% salt rejection, a greater than 95% COD retention, and a -0.013 initial slope of the flux decline curve (10). These rejection results are essentially in agreement with the data from the current study indicating that filtration and activated carbon adsorption can be omitted prior to RO without greatly affecting the organic concentration in the RO permeate and still produce a permeate with a TOC below 1 mg/L. Pilot-scale continuous flow-through ozonation experiments were conducted at the reclamation plant following multimedia filtration and prior to activated carbon adsorption. A dosage of 5 and 10 mg/L ozone and a 30-min contact time was found to decrease the COD by 15% and 29%, respectively (10). The cost of supplying the highest dosage, i.e., 36¢/1000 gallons, was not offset by the cost saving of 12¢/1000 gallons resulting from the increased activated carbon life.

An economic evaluation was made of the two processes that showed substantial organic carbon removals in AWT effluent by obtaining quotations from vendors. To simplify the analysis of a 100 gal/min (6.3 L/s) system, we estimated the operating costs from the amortization costs (10% interest) and electrical energy costs (RO pumping, ozone generation, UV amperage). Labor and waste disposal costs were considered to be similar for all processes and were therefore not further evaluated. The reverse osmosis costs included B-10 modules (5-year life, 20-year plant life) and an 85% product recovery. The ozone/UV system was designed at a 25 kg of ozone/kg of TOC and 25 kW h/kg TOC together with sufficient refrigeration. The ozone/UV system was estimated to cost \$200,000 with a \$66,000 annual operating cost, while the RO system was estimated at \$300,000 with a \$75,000 annual operating cost. Thus at comparable annual operating costs, lower effluent TOC values are realized with the RO system. As membrane fouling and deterioration are the main problems associated with RO, long-term testing is required to further substantiate this conclusion. For the full-scale plant (0.66 m<sup>3</sup>/s) it was estimated that direct filtration followed by reverse osmosis is expected to cost 75¢/1000 gallons, which is only slightly more than the sequence using coagulation, filtration, and carbon adsorption, while producing a better effluent TOC quality.

### Conclusions

The comprehensive data generated by the present study indicate that low organic carbon removals in AWT effluent are achieved by ion-exchange/adsorption processes possibly because preceedings activated carbon has removed most of the adsorbable fulvic-like materials. Among the six oxidants evaluated, only ozone and hydrogen peroxide resulted in substantial removals. The largest organic carbon removals were observed with reverse osmosis at an 85% permeate recovery, indicating sufficient diffusional restriction of the organics by the membrane. As the or-

ganic carbon retention by PA-RO before and after activated carbon is comparable, activated carbon is apparently not effective in removing low molecular weight carboxylated organics that pass RO membranes. At the reclamation plant this is reflected by a decrease of the COD/TOC ratio from 2.68 in the activated carbon effluent to 1.86 in the RO effluent (10). Similarly, the calculated proportion of the COD represented by low molecular weight purgeable organics increases from 0.047 in the influent to 0.54% in the RO permeate (10). An economic analysis indicated that annual RO operating costs were comparable to ozone/UV while producing a better effluent quality. Direct filtration of activated sludge effluent followed by RO represents the most effective combination. Long-term testing is required to further substantiate this conclusion.

### Acknowledgments

We acknowledge the assistance provided by David Argo, Chief Engineer of the Water Reclamation Plant, in the execution of the sampling and process testing. Sidney Hannah was the project officer of EPA study 68-03-2850.

### Literature Cited

- (1) U.S. Environmental Protection Agency, *Fed. Regist.* **1978**, *43*, 28, 5756.
- (2) Van Lier, W. C.; Van der Berg, E.; Lettinga, G. *Prog. Water Technol.* **1978**, *10*, 517-536.
- (3) DeWalle, F. B.; Chian, E. S. K. *J. Environ. Eng. Div. (Am. Soc. Civ. Eng.)* **1974**, *100*, 1039.
- (4) McCarty, P. L. Technical Report No. 236, Grant No. EIA S-803873, U. S. Environmental Protection Agency, Cincinnati, OH, 1980 p 149.
- (5) Mank, C. E.; Prengle, H. W. *Pollut. Eng.* **1976**, *8*, 12, 42.
- (6) Berglund, L.; Gjessing, E.; Johansen, E. S. "Removal of Organic Matter from Water by UV and Hydrogen Peroxide"; FMC Corp., Princeton, NJ, 1979.
- (7) Roan, S. G. U.S. Environmental Protection Agency Report EPA-67012-73-075, 1973.
- (8) Chian, E. S. K.; Smith, J. W.; DeWalle, F. B. "Proceedings, Second International Symposium on Ozone"; International Ozone Institute: Syracuse, NY, p 566.
- (9) Leitis, E. Westgate Research Corp., Annual Report, January 31, 1979.
- (10) Argo, D. G. "Evaluation of Membrane Processes and Their Role in Waste Water Reclamation"; U.S. Department of Interior, Office of Water Research and Technology, Washington, D.C., November 30, 1979; Vol. I.
- (11) Chian, E. S. K.; Cheng, S. S.; DeWalle, F. B.; Kuo, P. P. *Prog. Water Technol.* **1977**, *9*, 761.
- (12) Light, W. G. In "Chemistry in Water Reuse"; Cooper W. J., Ed.; Ann Arbor Science: Ann Arbor, MI, 1981; pp 341-353.
- (13) Evans, S.; Maalman, T. F. *J. Environ. Sci. Technol.* **1979**, *13*, 741-743.
- (14) Rowe, M. C. *Effluent Water Treat. J.* **1975**, *15*, 519.
- (15) Baird, R. B.; Gute, J. P.; Jacks, C. A.; Jenkins, R. L.; Neisses, L.; Scheybeler, B. Paper presented at Symposium on Chemistry of Water Reuse, 157th National Meeting, Houston, TX, 1980; American Chemical Society: Washington, D. C., 1980.
- (16) Thurman, E. M.; Malcolm, R. L.; Aiken, G. R. *Anal. Chem.* **1978**, *50*, 775.
- (17) Chian, E. S. K.; DeWalle, F. B. *J. Environ. Eng. Div. (Am. Soc. Civ. Eng.)* **1976**, *102*, 411.
- (18) Mangravite, F. J. *J. Am. Water Works Assoc.* **1975**, *67*, 88.
- (19) Edzwald, J. K. *J. Environ. Eng. Div. (Am. Soc. Civ. Eng.)* **1977**, *103*, 989.
- (20) Narkis, N.; Rebhun, M. *J. Am. Water Works Assoc.* **1975**, *67*, 101.
- (21) Glazer, H. T.; Edzwald, J. K. *Environ. Sci. Technol.* **1979**, *13*, 299.
- (22) Schreyer, J. M.; Thompson, G. W.; Ockerman, L. T. *Inorg. Synth.* **1953**, *4*, 164.

- (23) Waite, T. D. *Jour. Environ. Eng. Div. (Am. Soc. Civ. Eng.)* 1979, 105, 1023.
- (24) Waite, T. D.; Gilbert, M. J. *Water Pollut. Control Fed.* 1978, 50, 543.
- (25) Keating, E. J.; Brown, R. A.; Greenberg, E. S. *Ind. Water Eng.* 1978, 15, 6.
- (26) Malaiyandi, M.; Sadar, M.; Lee, P.; O'Grady, R. *Water Res.* 1980, 14.

Received for review July 20, 1980. Revised manuscript received June 10, 1981. Accepted July 13, 1982.

## Sludge Disposal in Southern California Basins

George A. Jackson\*

Environmental Quality Laboratory, California Institute of Technology, Pasadena, California 91125

■ Disposal of digested sewage sludge in coastal marine waters off Southern California is technically feasible, although it is not permissible under present policies of the state and federal governments. A one-dimensional model of physical and chemical processes in the San Pedro-Santa Monica Basin was developed to project environmental responses to different disposal strategies. The model suggests that deep disposal (800 m) would have crucial impacts on oxygen concentrations but shallower disposal (400 m) would not. Trace metal and sulfide buildup should not be significant problems. Organic particle buildup poses unknown problems for deep-living fauna.

The need to dispose of municipal sewage sludge with environmental impact minimized by health, environmental, and aesthetic criteria has caused a continued search for new options. Southern California has traditionally disposed of sewage effluent and some digested sludge in the coastal ocean. Sludge disposal in the deeper waters of nearby marine basins would be an extension of present practices to reduce environmental impacts.

Disposal in the marine basins off Southern California would seem to offer a number of advantages compared to disposal on the shelf (less than 100 m depth). It would put sludge in an area with a less productive biological community; it would increase the isolation of undesirable sludge constituents; it might immobilize sludge in areas that are the ultimate sinks of coastal sediments. However, the poorer circulation and lower oxygen concentrations in deeper waters could amplify environmental effects of sludge disposal to levels that could prove politically unacceptable. This paper and the one by Koh (1) are the result of a project to make predictions on environmental effects of deep ocean sludge disposal off the metropolitan Los Angeles/Orange County area (2).

Although present oceanic disposal of organic wastes in shallow waters has had effects on marine ecosystems, their magnitude, their mechanistic causes, and their significance are either unknown or controversial. Prediction of ecological effects in deep basins is made more difficult than prediction of effects in shallow water by our ignorance of such basic factors as their currents, ecosystem dynamics, and organismic biology (3). We chose to predict the effect of sludge disposal on chemical factors that are of known importance to marine organisms: degradation of sludge can change the concentrations of such biologically important constituents of seawater as dissolved oxygen, sulfide, and trace metals; sedimentation of particulates onto the bottom can change biological suitability of the

sediments. We looked at these two types of impacts separately because there is not enough information on currents and mixing within the offshore basins to justify the more complete model that would link the two.

Exchange of seawater from the Southern California Bight with open oceanic waters is limited by vertical water-density structure and by bathymetry. The extent to which water at a given location is isolated from the open ocean varies considerably. Surface waters can move through the Bight with flow interrupted only by the mainland or the offshore islands. Barriers to water movements increase with depth, cutting off communication between Santa Barbara and Santa Monica Basins around 250 m depth and between Santa Cruz Basin and the open ocean at 350 m (Figure 1). Valley waters at these intermediate depths are trapped in dead-end canyons, exchanging horizontally with waters outside through slow advective and turbulent processes. Deeper, in what have been called basins, surrounding valley walls cut off waters from all horizontal communication with the open ocean.

Surface currents in the Southern California Bight are complex, involving the California Current, the Southern California Countercurrent, and surface wind stresses (4). Residence time for surface water in the Bight is about 3 months. The rapid turnover and high oxygen concentrations of these surface waters protect them from major changes induced by sludge disposal.

Bottom water exchange in these basins is controlled by water at the depth of the lowest gap in the surrounding valley wall (5). Over this gap, called the sill, flows a variable amount of denser water that sinks to the bottom, bringing more oxygen (6). This flow can come in a torrent, displacing all the old basin water, or it can come in a relatively continuous trickle, causing a continuous upward flow of more than 0.2 m day<sup>-1</sup>. There is also a continuous vertical eddy diffusion exchange that allows basin waters to mix with overlying waters. These two processes of vertical advection and eddy diffusion keep basin waters from total isolation.

Intermediate waters exchange with basin waters below and surface waters above through vertical advection and eddy diffusion. They also exchange laterally down the canyons and through the openings by way of horizontal dispersive and advective processes. Sverdrup and Fleming (7) showed that intermediate water in Santa Monica Basin flows south, from Santa Cruz Basin. These intermediate waters will be called upper basin waters to emphasize their isolation from rapid horizontal exchange processes characteristic of the surface layer; bottom basin waters will be called lower basin waters to distinguish them from the upper basins.

Oxygen in deeper waters is consumed by the oxidation of organic matter. Higher oxygen consumption rates in

\* Address correspondence to Institute of Marine Resources, University of California, San Diego, La Jolla, CA 92093.

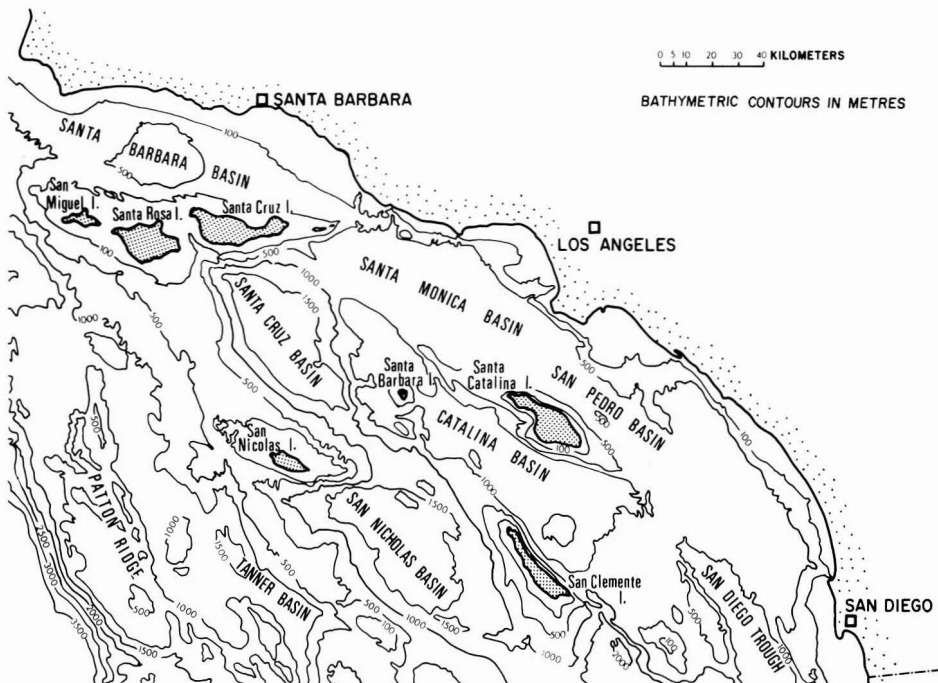


Figure 1. Marine basins of the Southern California Bight.

coastal waters lead to depletion of oxygen in valley waters relative to open oceanic waters.

Santa Monica and San Pedro Basins are the basins nearest Los Angeles (Figure 1). Properties of basin waters are controlled in part by communication with open ocean waters at the San Pedro Basin sill depth of 737 m. The interconnected basins have an area of 2460 km<sup>2</sup> at sill depth and a volume of 290 km<sup>3</sup> below that sill depth. Oxygen concentrations in the basins are about 0.2 mL/L or 9 μM (surface concentrations are about 7 mL/L or 0.3 mM). Low oxygen concentrations in the basins result from the presence of the oxygen minimum in the oceanic water at the sill depth as well as organic matter decay in the basins. Benthic surveys have shown the lower basins to be depauperate but not dead (3).

Vertical profiles have been taken over a wide area in Santa Barbara Basin (8) and in Santa Monica and San Pedro Basins (9). Vertical distributions within a basin vary but show no apparent horizontal gradients. Because horizontal gradients are much smaller than vertical gradients, it has been assumed that waters within a basin are horizontally well mixed, that Santa Monica and San Pedro Basin are really one, that rate-limiting processes cause only vertical variations, and therefore, that concentration of a substance depends only on the depth. These approximations are the basis for the one-dimensional model developed in this paper.

The model was developed for discharge from a submarine outfall only for digested sewage sludge (i.e., not for effluent). Once discharged from the end of a pipe on the bottom, the fresh water-suspended solids mixture of sludge would rise due to its buoyancy and entrain ambient seawater until it reaches a level of neutral buoyancy, which is expected to be about 50 m above the discharge pipe (1). The depth at which the plume stops rising is considered the injection depth in basin-wide chemical modeling. This sludge-seawater mixture will spread horizontally, its

particles will start to rain out on the sediments below, bacteria will begin to consume it and ambient oxygen, and its trace-metal-containing particles will start to dissolve. Even though the discharge point is on the bottom, the buoyancy of the sludge prevents it from being laid down on the bottom en masse; instead it must be considered as an injection into the water column.

#### Methods

The model uses a one-dimensional (vertical) eddy-diffusion description of the physics to relate the concentrations of reactive particulate sludge, dissolved oxygen, nitrate, and trace metals. This model yields vertical concentrations as a function of sludge injection depth; horizontally the system is assumed to be well mixed. Any lateral exchange of basin waters with external waters caused by currents flowing through the basin or waters mixing across the openings is expressed as a source or sink term at that depth. All processes are assumed to be at steady state. Mathematically the model is a set of four coupled differential equations. These are solved numerically, by using a finite difference scheme incorporating Newton's method to handle the nonlinear interactions. The program package to do this, PASVA3, was developed and described by Pereyra (10, 11).

Changes in concentration (*C*) of a substance at a given depth will be affected by vertical advection, vertical mixing, horizontal exchange, particle settling, and any sources or sinks:

$$\frac{\partial C}{\partial t} = \text{vertical advection} + \text{particle settling} + \text{horizontal exchange} + \text{vertical eddy diffusion} + \text{sources, sinks} \quad (1)$$

Each of these terms can be mathematically described. Concentration change for an advection process must

Table I. Standard Oxidation Reaction Rates Used in the Model<sup>a</sup>

	no nitrate use	nitrate use by sediments	nitrate use by sediments and sludge
sludge degradation rates, day <sup>-1</sup>			
for oxygen, <i>r</i>	$r_{\max} \frac{\beta}{1 + \beta}$	$r_{\max} \frac{\beta}{1 + \beta}$	$r_{\max} \frac{\beta}{1 + \alpha + \beta}$
for nitrate, <i>r'</i>	0	0	$r_{\max} \frac{\alpha}{1 + \alpha + \beta}$
sediment uptake rates, mol of O <sub>2</sub> equiv m <sup>-3</sup> day <sup>-1</sup>			
for oxygen, <i>l</i>	$l_m \frac{\beta}{1 + \beta}$	$l_n \frac{\beta}{1 + \alpha + \beta}$	$l_n \frac{\beta}{1 + \alpha + \beta}$
for nitrate, <i>l'</i>	0	$l_n \frac{\alpha}{1 + \alpha + \beta}$	$l_n \frac{\alpha}{1 + \alpha + \beta}$

<sup>a</sup>  $\alpha = N/N_{cr}$ ,  $\beta = O/O_{cr}$ ,  $N_{cr}$  = half-saturation concn of nitrate = 39 mmol m<sup>-3</sup> = 39 μM,  $O_{cr}$  = half-saturation concn of oxygen = 6.7 mmol m<sup>-3</sup> = 6.7 μM,  $l_m$  = max sediment oxidant uptake without nitrate uptake = 10.7 mmol m<sup>-2</sup> day<sup>-1</sup> ( $Z \leq 740$  M) = 3.8 mmol m<sup>-2</sup> day<sup>-1</sup> ( $Z > 740$  M),  $l_n$  = max sediment oxidant uptake with nitrate and oxygen uptake = 14.2 mmol m<sup>-2</sup> day<sup>-1</sup> ( $Z \leq 740$  M) = 5.8 mmol m<sup>-2</sup> day<sup>-1</sup> ( $Z > 740$  M),  $r_{\max}$  = max rate of sludge particle degradation = 0.01 day<sup>-1</sup>.

account for vertical movement and for replacement water coming from the sides. If  $v_z$  (m day<sup>-1</sup>) is the downward flow velocity, then the rate of concentration change caused by vertical advection is

$$-v_z \frac{\partial C}{\partial z} + f_u \Delta C$$

where  $C$  = concentration of substances being considered.

$$f_u \text{ (day}^{-1}\text{)} = \text{upwelling input rate} = \frac{dv_z}{dz} + v_z \frac{1}{A} \frac{dA}{dz} \quad (2)$$

$A$  (m<sup>2</sup>) = basin cross sectional area at depth  $z$

$$\Delta C = C_{\text{ext}} - C \quad \text{if } f_u \geq 0 \\ = 0 \quad \text{if } f_u < 0$$

$C_{\text{ext}}$  = concentration outside basin

Water flowing into the basin is assumed to flow into a depth where the temperatures,  $T$ , are the same. Thus  $\Delta T = 0$ .

Changes caused by particle settling, for constant particle settling velocity,  $v_s$  (m day<sup>-1</sup>), is given by  $-v_s \partial C / \partial z$ . Sludge particles exhibit a broad distribution of settling velocities (12). An intermediate value of 0.78 m day<sup>-1</sup> has been used.

Vertical mixing [when the vertical eddy diffusion coefficient is  $\epsilon_z$  (m<sup>2</sup> day<sup>-1</sup>)] is given by

$$\frac{1}{A} \frac{\partial}{\partial z} \left( \epsilon_z A \frac{\partial C}{\partial z} \right) = \epsilon_z \left[ \frac{\partial^2 C}{\partial z^2} + \frac{\partial C}{\partial z} \left( \frac{1}{A} \frac{dA}{dz} + \frac{1}{\epsilon_z} \frac{d\epsilon_z}{dz} \right) \right] \quad (3)$$

Diffusive horizontal exchange of this layer, which will depend on the concentration gradient at the openings and the width of the openings, is  $\sim [W(z)/A(z)]K\Delta C$ , where  $W(z)$  is the width of the basin openings at  $z(m)$ ,  $\Delta C$  = concentration outside minus concentration inside basin near the opening, and  $K$  is an exchange coefficient. Horizontal advection moves the same amount of water in as it does out. Net concentration changes will be  $(W/A)v_{ha}\Delta C$ , where  $v_{ha}$  (m day<sup>-1</sup>) is the horizontal advective velocity. The two processes can be described together simply as horizontal exchange:  $f_h \Delta C$ , where  $f_h$  (day<sup>-1</sup>) =  $WK/A + Wv_{ha}/A$  = horizontal exchange rate.

Sludge input,  $g$ , is assumed to be triangular, centered in the middle of a 10-m band. If  $B$  is the sludge input rate,

moles of oxygen equiv day<sup>-1</sup>, and  $z_{in}$  is the nominal input depth, then

$$g = 0 \quad \text{if } z = z_{in} \\ = B(z - z_{in})/5 \quad \text{if } z_{in} \leq z \leq z_{in} + 5 \\ = B(10 - (z - z_{in}))/5 \quad \text{if } z_{in} + 5 \leq z \leq z_{in} + 10 \\ = 0 \quad \text{if } z_{in} + 10 \leq z \quad (4)$$

Changes in concentration are given as  $g/A$ .

Oxygen in the basins can be consumed by pelagic and benthic respiration as well as sludge oxidation. Comparison of oxygen uptake rates for pelagic and benthic processes suggests that benthic processes are more important for these basins. Pelagic respiration of naturally occurring organic matter is not included in the model. The mathematical relationships used to describe oxygen demand by the sediments and sludge particulates must express reduced demand for oxygen and increased demand for nitrate when oxygen concentrations are low. A modified hyperbolic relationship from enzyme kinetics studies has been used in this study (Table I) (13).

The exact rate at which sediments presently consume oxygen in Santa Monica-San Pedro Basin is unknown. A mass balance on oxygen entering and leaving the lower basin yields an oxygen consumption rate of 1.7 mmol of O<sub>2</sub> m<sup>-2</sup> day<sup>-1</sup> (38 mL of O<sub>2</sub> m<sup>-2</sup> day<sup>-1</sup>). This might be equivalent to a rate of 3.8 mmol m<sup>-2</sup> day<sup>-1</sup> (85 mL of O<sub>2</sub> m<sup>-2</sup> day<sup>-1</sup>) if the lower basin had a higher oxygen concentration. Oxygen uptake rate in the upper basin should be between this (3.8 mmol m<sup>-2</sup> day<sup>-1</sup>) and 45 mmol m<sup>-2</sup> day<sup>-1</sup> measured at 20 m depth (Figure 2). Smith (14) calculated from a relation suggested by Hargrave (15) that respiration in the sediments of southern California should be 240 mL of O<sub>2</sub> m<sup>-2</sup> day<sup>-1</sup> (10.7 mmol m<sup>-2</sup> day<sup>-1</sup>). This oxygen consumption rate has been used for the upper Santa Monica-San Pedro Basin. These sedimentary respiration rates have been used for the case of no nitrate inhibition (Table I).

Nitrate taken up by the sediments is being reduced to N<sub>2</sub> (Goldberg, personal communication). As a result, nitrate reduction involves the transfer of five electrons, as opposed to the four electrons involved in O<sub>2</sub> reduction. If O<sub>2</sub> and NO<sub>3</sub><sup>-</sup> are to be considered as competitors in supplying oxidants, nitrate supply rates should be expressed as oxygen equivalents by multiplying by a factor of 1.25.

Nitrate reduction rates in the lower Santa Monica-San Pedro Basin are as large or larger than oxygen reduction rates. A mass balance calculation of nitrate entering and



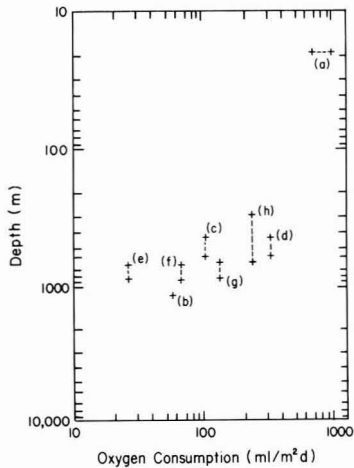


**Figure 2.** Sediment oxygen consumption rates: (a) Scripps pier, 1974 (Smith, personal communication); (b) San Diego Trough (14); (c) Santa Barbara Basin (6); (d) Santa Barbara Basin,  $I_{\max}$  as calculated from c as in Appendix 2 (2); (e) lower Santa Monica-San Pedro Basin, actual rate; (f) lower Santa Monica-San Pedro Basin,  $I_{\max}$  calculated for oxygen uptake independent of nitrate uptake; (g) lower Santa Monica-San Pedro Basin,  $I_{\max}$  calculated for oxygen + nitrate uptake; (h) upper Santa Monica-San Pedro Basin, assumed  $I_{\max}$ .

leaving the lower basin gives a nitrate reduction of 1.5 mmol of  $\text{NO}_3 \text{ m}^{-2} \text{ day}^{-1}$ , equivalent to 1.9 mmol of  $\text{O}_2 \text{ m}^{-2} \text{ day}^{-1}$  for nitrate being reduced to  $\text{N}_2$ .

The values for the various sediment and water column respiration parameters can be inferred from the literature or from mass balance calculations on the Santa Monica-San Pedro Basin. Respiration measurements on midwater organisms suggests a half-saturation constant for oxygen,  $Q_{10}$ , of  $6.7 \mu\text{M}$  (16). Values for the half-saturation concentration for nitrate,  $N_{1/2}$ , and maximum sediment respiration in the lower basin were determined from mass balance arguments by using nitrate and oxygen concentrations in the lower basin and in source waters (2). The rates of concentration change caused by sediment respiration are  $-l(1/A)(dA/dz)$  for oxygen and  $-0.8l(1/A)(dA/dz)$  for nitrate (0.8 is the conversion factor from oxygen equivalent to nitrate equivalent).

Sludge degradation depends on reactive particulate concentration, on a maximum rate of degradation, and on oxidant concentration. Maximum degradation rate at basin temperatures,  $r_{\max}$ , should be  $0.01 \text{ day}^{-1}$  (17). Effect of oxygen and nitrate concentrations on particle degradation used was the same as for sediment respiration (Table I).

If  $P$  is the reactive sludge particulate concentration, then the rates are  $-(r + r^{\wedge})P$  for particulate sludge,  $-rP$  for oxygen,  $-0.8r^{\wedge}P$  for nitrate, and  $+(r + r^{\wedge})P$  for oxidized organic matter.

The amounts of trace metals and oxygen-consuming organics that can be expected if sludge were to be discharged into the basin are shown in Table II. These numbers are the estimates of suspended solids to be discharged in 1985.

The relationship between density gradient and vertical eddy diffusivity (18),  $\epsilon_z$ , has been used to calculate vertical eddy diffusivities for San Pedro-Santa Monica Basin:

$$\epsilon_z (\text{cm}^2 \text{ s}^{-1}) = 4 \times 10^{-6} / \left[ \frac{g}{\rho} \frac{\partial \rho}{\partial z} \right] \quad (5)$$

where all units are cgs.

**Table II.** Projected Sludge Discharges, 1985:<sup>a</sup> Full Secondary Treatment

	hyper-ion <sup>c</sup>	JWPCP <sup>c</sup>	OCSDC <sup>c</sup>	total
sludge quantity, <sup>b</sup> dry tons day <sup>-1</sup>	370	475	300	1145
BOD of sludge, <sup>b</sup> 10 <sup>6</sup> mol of O <sub>2</sub> day <sup>-1</sup>	8.1	10.5	6.6	25.2
trace metals, kg day <sup>-1</sup>				
As	7			>7
Hg	4	2		>6
Ag	36	18	7	61
Cd	41	34	34	109
Ni	94	155	46	295
Pb	59	328	138	525
Cr	506	777	189	1472
Cu	486	460	392	1338
Zn	545	1407	474	2426
trace organics, kg day <sup>-1</sup>				
DDT's	0.10	2.45	0.04	2.59
PCB's	0.64	2.73	1.25	4.62
TICH	0.73	5.45	1.30	7.48
chlorinated benzene	21.36	30.45	14.55	66.36

<sup>a</sup> Values provided by LA/OMA (2). <sup>b</sup> BOD calculated by using the relationship 1 dry ton sludge =  $2.2 \times 10^4$  mol of O<sub>2</sub>. <sup>c</sup> Hyperion, Treatment Plant, City of Los Angeles; JWPCP, Joint Water Pollution Control Plant, Los Angeles County Sanitation District; OCSDC, Orange County Sanitation Districts.

**Table III.** Standard Values of Parameters Expressed as Functions of Depth,  $z$  (m)

$$\begin{aligned}
 A &= \text{basin area, m}^2 \\
 &= 10^6 \times (37.8957 - 1.51256 \times 10^{-2}z - 1.11949 \times 10^{-4}z^2 + 0.126566 \times 10^{-6}z^3 - 3.93305 \times 10^{-11}z^4) / (1 - 1.07884 \times 10^{-3}z) \\
 N_{\text{ext}} &= \text{entering nitrate concn, mol m}^{-3} \\
 &= 1.050184 \times 10^{-2} + 8.870298 \times 10^{-5}z - 7.899890 \times 10^{-8}z^2 + 1.853268 \times 10^{-11}z^3 \\
 O_{\text{ext}} &= \text{entering oxygen concn, moles m}^{-3} \\
 &= 5.800599 - 2.180700 \times 10^{-2}z + 2.832816 \times 10^{-5}z^2 - 1.219102 \times 10^{-8}z^3 \\
 \epsilon_z &= \text{vert eddy diffusivity, m}^2 \text{ day}^{-1} \\
 &= 6.308810 - 5.426779 \times 10^{-3}z - 4.257471 \times 10^{-5}z^2 + 7.383693 \times 10^{-8}z^3 \\
 v_z &= \text{vert advective velocity, m day}^{-1} \\
 &= 1.531712 - 9.940010 \times 10^{-3}z + 1.897540 \times 10^{-5}z^2 - 1.069165 \times 10^{-8}z^3 \quad \text{if } z \leq 740 \text{ m} \\
 &= -0.24 \quad \text{if } z > 740 \text{ m} \\
 f_h &= \text{horiz exchange rate, day}^{-1} \\
 &= -1.898462 \times 10^{-1} + 1.723385 \times 10^{-3}z - 5.383155 \times 10^{-6}z^2 + 7.103985 \times 10^{-9}z^3 - 3.387205 \times 10^{-12}z^4 \quad \text{if } z \leq 740 \text{ m} \\
 &= 0 \quad \text{if } z > 740 \text{ m}
 \end{aligned}$$

Data taken in the San Pedro Basin and in the Santa Monica Basin during a cruise were treated together. Polynomials in  $z$  were fitted to temperature, density, and dissolved oxygen concentration as functions of depth (Table III) for the region between 300 and 750 m and for the region between 750 and 900 m. These power fits were used in place of the actual data in subsequent calculations. Thus, the density derivative needed to calculate  $\epsilon_z$  came from differentiating the cubic expression fit to the density vs. depth profile. The resulting vertical eddy diffusivity was also fit to a rational function of depth (Table III). As a result, temperature, dissolved oxygen, area,  $\epsilon_z$ , and their derivatives were known as functions of depth through the water column.

Rates of physical processes were estimated by fitting the differential equations for temperature and oxygen to observed changes in the vertical distributions in these parameters.

The equation describing temperature changes in the basin is

$$\frac{\partial T}{\partial t} = \epsilon_z \left[ \frac{\partial^2 T}{\partial z^2} + \frac{\partial T}{\partial z} \left( \frac{1}{A} \frac{dA}{dz} + \frac{1}{\epsilon_z} \frac{d\epsilon_z}{dz} \right) \right] - v_z \frac{\partial T}{\partial z} \quad (6)$$

Solved for  $v_z$ , this becomes

$$v_z = \left[ \epsilon_z \left( \frac{\partial^2 T}{\partial z^2} + \frac{\partial T}{\partial z} \left( \frac{1}{A} \frac{dA}{dz} + \frac{1}{\epsilon_z} \frac{d\epsilon_z}{dz} \right) \right) - \frac{\partial T}{\partial t} \right] / \frac{\partial T}{\partial z} \quad (7)$$

The various derivatives can be approximated for two sets of hydrographic data taken period  $\Delta t$  apart. The term  $\partial T/\partial t$  was approximated as  $\Delta T/\Delta t$ , where  $\Delta T$  is the temperature difference at a given depth for the two different sampling times. Similarly, other terms in equation 3 can be approximated by averaging the values given by the power fits for the two different sample sets and  $v_z$  calculated. Vertical velocities were fit to a power series (Table III). Velocities for the periods examined ranged from 0.6 m day<sup>-1</sup> upward to 1.3 m day<sup>-1</sup> downward.

This technique for calculating upwelling velocities does not work well in the lower basin because errors in the functions used to fit temperature, area, and vertical eddy diffusivity are greater there. Such errors are magnified with the use of derivatives. A cruder technique less sensitive to parameter errors is to balance heat flow at 700 and at 800 m:

$$Q_{700}(T_{700} - T_{740}) - \epsilon_{z,700} A_{700} \nabla T_{700} = Q_{800}(T_{800} - T_{740}) - \epsilon_{z,800} A_{800} \nabla T_{800} \quad (8)$$

where the numerical subscripts denote the depth at which the variable is evaluated and  $Q$  is the vertical volume flow. The resulting vertical velocity calculated from data of July–November 1970 is  $-0.24$  m day<sup>-1</sup> (the negative sign indicates that flow is upward). It has been assumed that this velocity is constant with depth in the lower basin.

The equation describing basin oxygen concentration,  $O$ , is similar to that for temperature but includes terms describing oxygen added by water coming from the sides and terms describing consumption within the basin:

$$\frac{\partial O}{\partial t} = \epsilon_z \left[ \frac{\partial^2 O}{\partial z^2} + \frac{\partial O}{\partial z} \left( \frac{1}{A} \frac{dA}{dz} + \frac{1}{\epsilon_z} \frac{d\epsilon_z}{dz} \right) \right] - v_z \frac{\partial O}{\partial z} + f_u \Delta O + f_h \Delta O - l \frac{dA}{dz} \quad (9)$$

With oxygen concentration described by power series fits to the hydrographic data and with  $v_z$  and  $f_u$  calculated from the temperature data, the unknowns remaining are the horizontal exchange rate,  $f_h$ , external oxygen concentration,  $O_{ext}$ , and oxygen consumption. Benthic oxygen consumption was assumed to have the same form as the upper basin no nitrate utilization case in Table I. Incoming water was assumed to have the oxygen as a function of temperature characteristics of Santa Cruz Basin water sampled on July 1970 and to mix with water of the same temperature. This basin is the source for intermediate SM-SP Basin water (7). This relationship was described with a cubic power fit (Table III).

Horizontal exchange rates can thus be calculated:

$$f_h = \frac{1}{\Delta O} \left\{ l \frac{dA}{dz} + v_z \frac{\partial O}{\partial z} - f_u \Delta O + \frac{\partial O}{\partial t} \right\} - \frac{\epsilon_z \left[ \frac{\partial^2 O}{\partial z^2} + \frac{\partial O}{\partial z} \left( \frac{1}{A} \frac{dA}{dz} + \frac{1}{\epsilon_z} \frac{d\epsilon_z}{dz} \right) \right]}{\Delta O} \quad (10)$$

Horizontal exchange rates are about  $7 \times 10^{-3}$  day<sup>-1</sup> at 300

m and a third as much near the sill depth (Table III).

There is, of course, no horizontal exchange in the lower basin. The oxygen consumption rate there can be determined from previously determined terms (Table I).

### Mathematical Formulation

This model to study effects of sludge disposal in Santa Monica–San Pedro Basin calculates concentrations and fates of (a) particulate sludge containing reducing organic matter and selected trace metals, (b) oceanic dissolved oxygen and nitrate, and (c) dissolved trace metals with both dissolved and oceanic sources. We consider the various substances to be at steady state.

The nonlinear, coupled differential equations used to describe concentrations of oxygen ( $O$ ), nitrate ( $N$ ), particulate organic matter ( $P$ ), and oxidized organic matter ( $D$ ) are given in eq 11–14, where  $f_u$ ,  $f_h$ ,  $\epsilon_z$ ,  $v_z$ ,  $A$ , and  $g$  have

$$0 = -v_z \frac{\partial O}{\partial z} + \epsilon_z \left[ \frac{\partial^2 O}{\partial z^2} + \frac{\partial O}{\partial z} \left( \frac{1}{A} \frac{dA}{dz} + \frac{1}{\epsilon_z} \frac{d\epsilon_z}{dz} \right) \right] + (f_u + f_h) \Delta O - l \frac{dA}{dz} - rP \quad (11)$$

$$0 = -v_z \frac{\partial N}{\partial z} + \epsilon_z \left[ \frac{\partial^2 N}{\partial z^2} + \frac{\partial N}{\partial z} \left( \frac{1}{A} \frac{dA}{dz} + \frac{1}{\epsilon_z} \frac{d\epsilon_z}{dz} \right) \right] + (f_u + f_h) \Delta N - 0.8l \frac{dA}{dz} - 0.8r'P \quad (12)$$

$$0 = -v_z \frac{\partial P}{\partial z} + \epsilon_z \left[ \frac{\partial^2 P}{\partial z^2} + \frac{\partial P}{\partial z} \left( \frac{1}{A} \frac{dA}{dz} + \frac{1}{\epsilon_z} \frac{d\epsilon_z}{dz} \right) \right] + (f_u + f_h) \Delta P - v_s \frac{\partial P}{\partial z} - (r + r')P + \frac{g}{A} \quad (13)$$

$$0 = -v_z \frac{\partial D}{\partial z} + \epsilon_z \left[ \frac{\partial^2 D}{\partial z^2} + \frac{\partial D}{\partial z} \left( \frac{1}{A} \frac{dA}{dz} + \frac{1}{\epsilon_z} \frac{d\epsilon_z}{dz} \right) \right] + (f_u + f_h) \Delta D + (r + r')P \quad (14)$$

been defined and  $l$  = oxygen demand of sediments (mol m<sup>-2</sup> day<sup>-1</sup>),  $l'$  = nitrate demand of sediments (mol m<sup>-2</sup> day<sup>-1</sup>),  $r$  = oxygen consumption rate of suspended sludge particles (day<sup>-1</sup>),  $r'$  = nitrate consumption rate of suspended sludge particles (day<sup>-1</sup>),  $\Delta N = N - N_{ext}$ ,  $N_{ext}$  = nitrate concentration of water entering basins at depth  $z$ ,  $\Delta D = D - D_{ext}$ ,  $D_{ext}$  = concentration of dissolved organic matter entering basin at depth  $z$ .

Values for  $f_u$ ,  $f_h$ ,  $\epsilon_z$ ,  $v_z$ , and  $A$  are functions only of depth. Value at any depth were calculated by using the power series fits (Table III).

The forms and values of  $r$ ,  $r'$ ,  $l$ , and  $l'$  depend on which oxidation mechanisms are being considered. The three alternatives considered here involve oxygen utilization by sediments and sludge particles with no nitrate utilization, with nitrate utilization only by the sediments, or with nitrate utilization by sludge particles and sediments. The standard practice will be nitrate uptake by the sediments only.

The upper boundary was 300 m, the lower boundary 900 m. Boundary conditions at 300 m were determined by assuming that surface water circulation sets the various concentration values (Table IV). The more complex situation at the bottom boundary layer was handled differently for oxygen and nitrate than for the particulate and oxidized organics. Because water entering Santa Monica–San Pedro Basin from surrounding basins was assumed to have neither particulate nor oxidized organic matter, their concentrations were set to zero at 900 m. Sediment utilization of oxygen and nitrate is a function of their

Table IV. Standard Input Values for Basin Model

substance	sludge input, mol day <sup>-1</sup>	external basin concn, mol m <sup>-3</sup>	ref
BOD	2.0 × 10 <sup>7</sup>	0	
Cd	9.75 × 10 <sup>2</sup>	9 × 10 <sup>-6</sup>	31
Cr	2.82 × 10 <sup>4</sup>	9.6 × 10 <sup>-7</sup>	32
Cu	2.10 × 10 <sup>4</sup>	2.0 × 10 <sup>-6</sup>	33
Pb	2.5 × 10 <sup>3</sup>	1.3 × 10 <sup>-7</sup>	32
Ni	5.0 × 10 <sup>3</sup>	3.4 × 10 <sup>-5</sup>	34
Ag	5.6 × 10 <sup>2</sup>	3.7 × 10 <sup>-7</sup>	32
Zn	3.7 × 10 <sup>4</sup>	5 × 10 <sup>-6</sup>	35

P<sup>a</sup> = particulate organic concn at 300 m (upper boundary) = 0

N<sup>a</sup> = nitrate concn at 300 m = 30 mmol m<sup>-3</sup> = 30 μM

O<sup>a</sup> = dissolved oxygen concn at 300 m = 62 mmol m<sup>-3</sup> = 62 μM

D<sup>a</sup> = oxidized organic matter concn at 300 m = 0

v<sub>s</sub> = settling velocity of particulate organic = 0.78 m day<sup>-1</sup>

<sup>a</sup> 300 m.

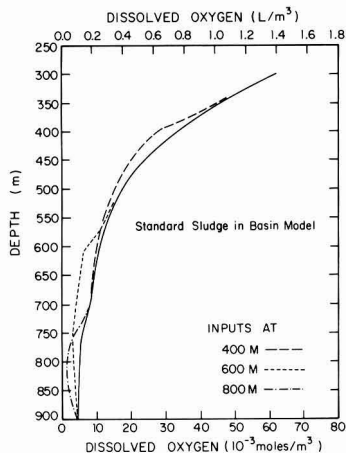


Figure 3. Dissolved oxygen concentration in Santa Monica-San Pedro Basin for standard conditions, only oxygen reaction with sludge particles. Sludge inputs are to 400, 600, and 800 m. The solid line represents present no discharge condition.

concentrations and has to be included in the bottom boundary condition formulations. If the flux away from the bottom equals the flux from water flowing over the sill into the basin minus the flux to the sediments, then the bottom condition for oxygen is

$$\epsilon_z(900 \text{ m}) \frac{\partial O}{\partial z}(900 \text{ m}) - v_z(900 \text{ m})O(900 \text{ m}) = -v_z(900 \text{ m})O_{\text{ext}}(900 \text{ m}) - l(O(900 \text{ m})) \quad (15)$$

and for nitrate is

$$\epsilon_z(900 \text{ m}) \frac{\partial N}{\partial z}(900 \text{ m}) - v_z(900 \text{ m})N(900 \text{ m}) = -v_z(900 \text{ m})N_{\text{ext}}(900 \text{ m}) - l'(N(900 \text{ m})) \quad (16)$$

where *l* and *l'* are defined in Table I.

Trace metals are predominantly in particulates in treated sewage effluents (both primary and secondary) discharged to the ocean (19, 20), and in digested sludge (12). Theoretical calculations show that under the reducing conditions of sewage, most trace metals form sulfide or oxide precipitates (12, 20). Trace-metal release rates

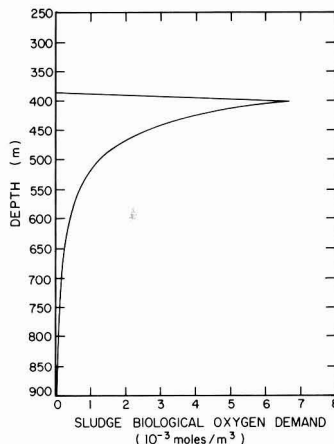


Figure 4. Concentration of particulate sludge (oxygen-demanding fraction) in Santa Monica-San Pedro for discharge at 400 m under standard conditions.

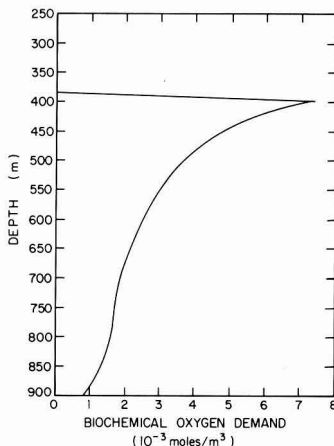


Figure 5. Concentration of particulate sludge in Santa Monica-San Pedro Basin for discharge at 400 m with no decomposition.

from sludge particulates are similar to the rate of particulate oxidation (17, 21). Therefore, particulate trace-metal concentrations were assumed to be proportional to particulate sludge concentrations, and dissolved metal concentration increases were assumed to be proportional to oxidized organic concentrations. Proportionality factors were the same as those of pre-discharge sludge.

## Results

Sludge discharge at 400 m without nitrate sludge oxidation results in a small decrease in oxygen concentration between 400 and 500 m (Figure 3). Oxidizable particulate sludge is predominantly within 100 m of the discharge depth (Figure 4). Importance of oxidation in confining the sludge to such a narrow depth range is shown by comparison with a sludge profile for the case of no oxidation (Figure 5). Concentration decreases in the latter case are by horizontal exchange with other basins. Figure 5 is the same as for that of nonoxidizable sludge particulate matter to within a constant factor. This inert sludge will be ignored in the rest of this report because of its noninteracting nature.

**Table V. Effect of Sludge Discharge at 800 m under Standard Assumptions**

	A no discharge	B discharge	B:A
total particle content, $10^9$ mol of BOD		2.2	
residence time, days <sup>a</sup>		110	
oxygen consumption, $10^7$ mol day <sup>-1</sup>			
sediments	1.59	1.42	0.9
particles		0.46	
lowest oxygen concn, $\mu$ M	4.6	1.3	0.28
depth region with oxygen less than $4 \mu$ M, m		745-900	
nitrate consumption, sediments $10^7$ mol day <sup>-1</sup>	0.88	0.94	1.1
lowest nitrate concn, $\mu$ M	33	33	1.0
max soluble trace-metal concn, mol m <sup>-3</sup>			
Cd	$9 \times 10^{-6}$	$9.2 \times 10^{-6}$	1.02
Cr	$9.6 \times 10^{-7}$	$7.3 \times 10^{-6}$	7.6
Cu	$2 \times 10^{-6}$	$6.7 \times 10^{-6}$	3.4
Pb	$1.3 \times 10^{-7}$	$6.9 \times 10^{-7}$	5.3
Ni	$3.4 \times 10^{-5}$	$3.5 \times 10^{-5}$	1.03
Ag	$3.7 \times 10^{-7}$	$4.95 \times 10^{-7}$	1.34
Zn	$5 \times 10^{-6}$	$1.33 \times 10^{-5}$	2.7
particle fates, fraction			
settle to bottom		0.76	
oxidized		0.21	
flow out of basin		0.03	

<sup>a</sup> Residence time is defined as total sludge particle content of Santa Monica-San Pedro Basin divided by input rate. Residence time of nondegraded particles is 135 days.

Sludge input also increases trace-metal concentrations. Particulate trace-metal distributions are the same as those of the particulate organic matter (Figure 4), although absolute concentrations are different. Dissolved trace-metal concentrations are not as sharp as particulates (Figure 6). Maximum concentration of the dissolved trace-metal copper would be 3.8 times the background concentration for the case considered.

**Discharge at 800 m.** Sludge disposal into lower Santa Monica-San Pedro Basin would deplete oxygen throughout the lower basin to a concentration of less than  $4 \mu$ M ( $4 \text{ mmol m}^{-3}$ ) (Table V, Figure 3). The minimum oxygen concentration predicted for standard assumptions is  $1.3 \mu$ M, 28% of the present minimum concentration. Sludge would consume oxygen at one-third of the rate at which

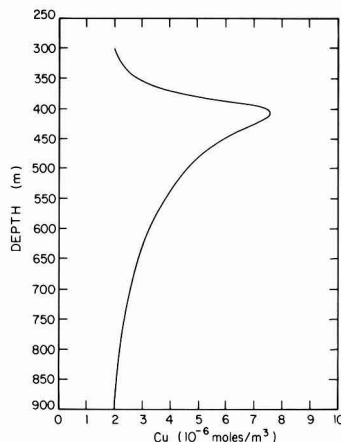


**Figure 6.** Dissolved copper concentration for sludge discharge at 400 m under standard conditions.

sediments presently consume oxygen in the whole basin (400-900 m depth).

Sludge discharge would increase dissolved metal concentrations. Increased concentrations would range from 8 times background for chromium to 1.02 times background for cadmium. Copper, to which phytoplankton growth is very sensitive, would become 3.4 times more concentrated.

Oxidizable sludge particles would have a resident time in the basin of 110 days; nonoxidizable particles would have a residence time of 135 days. Approximately 76% of oxidizable sludge would settle out before being oxidized; 21% would be oxidized in the water column. Thus, for discharge at 800 m, sedimentation on the bottom is the fate for most particles.

These predictions were made with "standard" or baseline assumptions. How dependent on the assumptions are they? Variations of several important parameters such as total sludge BOD (biochemical oxygen demand) and particle fall velocities give similar results. The pattern of oxygen depletion is similar in all cases, varying only in degree. Halving the oxygen demand would increase the minimum oxygen concentration, from 1.3 to  $2.5 \mu$ M, but the lower basin would still be heavily depleted in oxygen (Table VI, Figure 3). Particle settling velocities of  $6 \text{ m day}^{-1}$  (as opposed to the standard  $0.78 \text{ m day}^{-1}$ ) would

**Table VI. Effect of Sludge Discharge at 800 m for Variations on Standard Assumptions<sup>a</sup>**

	std assumptions <sup>a</sup>	2 x std BOD	1/2 x std BOD	fast settling ( $v_s = 6$ $\text{m day}^{-1}$ )	slow settling ( $v_s = 0.08$ $\text{m day}^{-1}$ )
total basin particle content, $10^9$ mol of BOD	2.2	4.7	1.04	0.26	49
particle residence time, days	110	113	104	26	243
oxygen consumption, $10^7$ mol day <sup>-1</sup>					
sediments	1.4	1.3	1.4	1.5	1.3
particles	0.5	0.6	0.3	0.1	0.8
lowest oxygen concn, $\mu$ M	1.3	0.5	2.5	4.0	0.5
region with oxygen $< 4 \mu$ M, m	745-900	745-900	755-895		730-900
max Cu, $10^{-6}$ mol m <sup>-3</sup>					
soluble	6.7	4.8	8.7	3.1	8.0
particulate	14	14.5	13.3	1.8	27
particle fates, fraction					
fall to bottom	0.76	0.84	0.70	0.96	0.09
oxidized	0.21	0.13	0.28	0.04	0.35
go out of basin	0.03	0.03	0.02	0	0.56

<sup>a</sup> Standard assumptions: BOD input =  $2 \times 10^7 \text{ mol day}^{-1}$ ;  $v_s = 0.78 \text{ m day}^{-1} = 0.9 \times 10^{-3} \text{ cm/s}$ .

Table VII. Effect of Sludge Discharge at 600 m for Variations on Standard Assumptions<sup>a</sup>

	std assumptions <sup>a</sup>	BOD input		particle velocity $v_s$ , m day <sup>-1</sup>		particle reactivity $r_{max}$		horiz exchange $f_h$	
		2 × std	1/2 × std	6	0.08	2 × std	1/2 × std	2 × std	1/2 × std
total basin particle content, 10 <sup>9</sup> mol of BOD	2.29	5.1	1.1	0.63	3.5	1.8	2.7	1.8	2.6
particle residence time, days	115	128	107	32	174	88	137	91	132
oxygen consumption, 10 <sup>7</sup> mol day <sup>-1</sup>									
sediments	1.3	1.2	1.4	1.5	1.3	1.3	1.4	1.4	1.2
particles	1.0	1.5	0.5	0.3	1.2	1.3	0.6	0.9	0.9
lowest oxygen concn, μM	3.2	1.6	4.2	4.2	2.7	2.7	3.8	4.1	2.3
region with oxygen < 4 μM, m	715-855	610-890			590-750	620-860	755-840		630-870
max Cu concn, 10 <sup>-6</sup> mol m <sup>-3</sup>									
soluble	7.8	6.4	8.5	3.6	12	10	5.6	6.1	9.1
particulate	7.2	7.3	7.2	1.2	18	6.9	7.5	7.1	7.4
particle fates, fraction									
fall to bottom	0.22	0.28	0.20	0.79	0.02	0.14	0.31	0.17	0.27
oxidized	0.47	0.37	0.52	0.13	0.60	0.62	0.31	0.45	0.46
go out of basin	0.31	0.35	0.28	0.08	0.38	0.24	0.38	0.38	0.27

<sup>a</sup> Standard assumptions: BOD input = 2 × 10<sup>7</sup> mol day<sup>-1</sup>;  $v_s$  = 0.78 m day<sup>-1</sup>;  $r_{max}$  = 0.01 day<sup>-1</sup>.

Table VIII. Effect of Sludge Discharge at 400 m for Variations on Standard Assumptions<sup>a</sup>

	std assumptions <sup>a</sup>	BOD input		particle velocity $v_s$ , m day <sup>-1</sup>		particle reactivity $r_{max}$		horiz exchange $f_h$	
		2 × std	1/2 × std	6	0.08	2 × std	1/2 × std	2 × std	1/2 × std
total basin particle content, 10 <sup>9</sup> mol of BOD	1.6	3.3	0.8	0.9	1.4	1.0	2.4	1.1	2.0
particle residence time, days	81	83	80	44	70	49	121	57	104
oxygen consumption, 10 <sup>7</sup> mol day <sup>-1</sup>									
sediments	1.5	1.4	1.5	1.5	1.5	1.5	1.5	1.5	1.4
particles	1.2	2.4	0.6	0.6	1.1	1.5	0.9	0.9	1.4
lowest oxygen concn, μM	4.6	4.6	4.6	4.5	4.6	4.6	4.6	4.6	4.6
region with oxygen < 4 μM									
max Cu concn, 10 <sup>-6</sup> mol m <sup>-3</sup>									
soluble	7.5	7.4	7.7	3.6	9.6	10.6	5.4	4.7	12
particulate	7.0	7.0	6.9	0.1	11	6.3	7.4	6.4	7.3
particle fates, fraction									
fall to bottom	0.06	0.06	0.06	0.61	0	0.03	0.11	0.04	0.08
oxidized	0.59	0.58	0.60	0.25	0.56	0.73	0.43	0.45	0.70
go out of basin	0.35	0.36	0.34	0.14	0.44	0.24	0.46	0.52	0.22

<sup>a</sup> Standard assumptions: BOD input = 2 × 10<sup>7</sup> mol day<sup>-1</sup>;  $v_s$  = 0.78 m day<sup>-1</sup>;  $r_{max}$  = 0.01 day<sup>-1</sup>.

increase predicted minimum oxygen concentration to 4 μM. However, increased sediment oxygen demand caused by increased organic matter input would decrease oxygen concentration in a way not included in this model.

The conclusion is that a major sludge discharge at 800 m into the lower basin would significantly deplete the supply of dissolved oxygen there.

**Discharge at 600 m.** Sludge disposal into lower parts of upper Santa Monica-San Pedro Basin, at 600 m depth, would put the sludge into a region of greater exchange with other basins and of high oxygen concentrations. These factors increase the fraction of sludge leaving the basin to 31% and the fraction being oxidized to 47% and decrease the fraction settling to the bottom to 22% (Table VII). The minimum oxygen concentration becomes 3.2 μM, greater than the 1.3 μM minimum when sludge is discharged at 800 m. However, this shallower discharge depth increases the distance particles can fall before reaching the basin bottom. The result is that the upper depth of the region with oxygen less than 4 μM rises to 715 m. The effect of discharge at 600 m is to decrease the oxygen depletion intensity but to increase the depth range over

which it occurs. Moving from 800 to 600 m depth of discharge also causes the maximum soluble copper concentration to increase slightly, from 3.4 to 3.9 times the background value.

Variation of model assumptions shows that conclusions about disposal at 600 m are more tentative than those for disposal at 800 m; half-standard oxygen demand would minimize oxygen depletion but would increase peak trace-metal concentrations; fast-settling velocities would again minimize oxygen depletion, and increased horizontal exchange rates, twice standard values, would keep minimum oxygen concentration above 4 μM. There is, however, insufficient evidence to state that disposal at 600 m would have minimal effects.

**Discharge at 400 m.** Sludge disposal into the upper part of upper Santa Monica-San Pedro Basin, at a depth of 400 m, would subject sludge to greatest oxidation and fastest dilution with extrabasin waters. Particle residence time is shorter than for disposal at 600 m, 81 days as opposed to 115 days (Table VIII). The majority of sludge, 59%, is oxidized within the basin, 35% leaves the basin, and only 6% falls to the bottom. Disposal at 400 m has

minimal effect on the oxygen content of the lower basin. Highest soluble copper concentration is, however, 3.8 times the background concentration.

Results for other conditions are similar. Effects on lower basin waters are minimal. With the exception of the high fall-velocity case, 6% of the particles or less reach the sediments. Thus, large-scale chemical effects of sludge disposal are the least at 400 m.

### Discussion

Sludge disposal in marine basins will have local effects more intense than those predicted on a basin-wide scale, such as the sedimentation around an outfall (1). However, the size of sludge inputs, comparable to those of natural processes, has made it important to examine basin-scale results. Sludge disposal could deplete basin oxygen and possibly nitrate and could increase trace metal and, perhaps, sulfide concentrations. The exact size of these effects depends on mechanisms and rates of sludge degradation, sludge settling, and water mixing and transport. Should oxygen be depleted too greatly, the basins will become inhospitable to animals now present, nitrate regeneration will be retarded, and sulfide concentrations could increase. This model has been used to predict basin-wide effects of sludge discharge under a range of strategies and assumptions.

The central assumption in this model is that any horizontal layer within the Santa Monica-San Pedro Basin is well mixed (i.e., concentrations are uniform within a layer). Concentrations within a given depth layer are determined by vertical mixing, by upward (or downward) water movement, by chemical reactions, by particles falling into the next layer, and by exchange with waters outside the basin. A major impact of sludge disposal at these depths that is incorporated in the present model is the increase in oxygen and nitrate consumption rates over naturally occurring rates. Not all sludge will oxidize: sludge consists of a fraction (about 70%) that is not oxidized and would settle on the bottom or be carried out of the basin. This inert phase was considered only briefly because it did not seem as chemobiologically important as the oxidizable phase. The model developed here coupled oxygen, nitrate, and sludge chemical interactions with physical processes.

Basin responses are different in the slowly circulating lower basin than in the horizontally exchanging upper basin; within the upper basin, water in contact with high oxygen surface waters acts differently from those with lower oxygen content. Results show that sludge disposal at 800 m would have a large relative effect, at 600 m might have a large effect, and at 400 m would not greatly change chemical parameters.

This model does not compensate for increased sediment respiration caused by increased organic matter sedimentation. A comparison with suspended respiration shows that this is reasonable. The maximum sedimentation rate is the maximum particle concentration,  $7 \times 10^{-3}$  mol of BOD  $m^{-3}$  (Figure 4), times the settling velocity,  $0.7 \text{ m day}^{-1}$ , a value of  $5 \times 10^{-3}$  mol of BOD  $m^{-2} \text{ day}^{-1}$ . Were this all to be oxidized in the sediments, it would increase the background sediment oxygen demand of  $10 \times 10^{-3}$  mol of  $O_2 \text{ m}^{-2} \text{ day}^{-1}$  by at most 50%. Incomplete oxidation of this organic matter would decrease this value. Furthermore, the rapid decrease in particulate concentration with depth would limit even this change in sediment oxygen demand to a small area. The omission of increased sediment oxygen demand is thus a reasonable approximation for a basin model. However, in local areas around an outfall this might not be true (1).

Table IX. Comparison of Lower Santa Monica-San Pedro Basin Sedimentation with Projected Sludge Discharge

substance	lower SM-SP Basin flux <sup>a</sup> (A)	projected sludge discharge: full secondary treatment (B)	B:A
organic C, BOD $10^9$ mol of $O_2$ /year	2.6 <sup>b</sup>	9.2	3.5
heavy metals, tons/year			
Cd	c	40	
Cr	130	537	4
Cu	56	488	9
Pb	36	192	5
Hg	c	> 2.2	
Ni	37	108	3
Ag	3	22	7
Zn	123	886	7

<sup>a</sup> Total present fluxes including anthropogenic (22, 36).  
<sup>b</sup> Assuming complete oxidation of all C. <sup>c</sup> No estimate available.

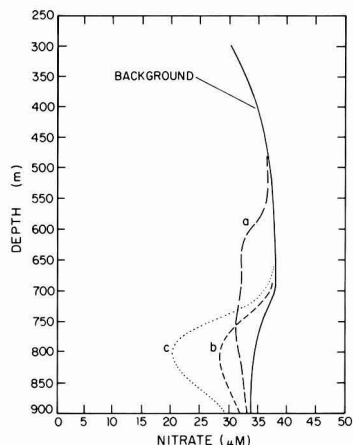


Figure 7. Nitrate concentration in Santa Monica-San Pedro Basin with sludge input when nitrate and oxygen oxidize particles: (a) twice the standard BOD input at 600 m; (b) standard BOD input at 800 m; (c) twice the standard BOD input at 800 m.

Heavy-metal sedimentation rates have already increased greatly as a result of anthropogenic processes, either waste discharge (22) or atmospheric fallout (23). A comparison of projected sludge outputs of metals with the present sedimentary accumulation rates in the lower Santa Monica-San Pedro Basin shows ratios ranging from 3 to 9 times as great (Table IX).

**Nitrate Reduction.** Estimates of sludge-caused perturbations were made with assumption that the sediments are the only nitrate reducers. Nitrate reduction in the water column was omitted because oceanographic evidence suggests that nitrate reduction in the water column does not occur for oxygen concentrations greater than  $4.5 \mu\text{M}$  (24, 25). The expression for nitrate reduction used here considers oxygen inhibition of nitrate reactions at high oxygen concentrations but does not eliminate them. This model allows no nitrate reaction in the water column at high oxygen concentrations.

This assumption of no nitrate reaction with sludge particles will not be valid when massive loadings cause oxygen to decrease below  $4 \mu\text{M}$ . The importance of nitrate reduction under those circumstances where there would be heavy oxygen depletion in the lower basin can be

checked (Figure 7). Calculations that included nitrate as well as oxygen reaction with sludge particles in the otherwise standard model showed that minimum nitrate concentration in the lower basin would decrease to 28  $\mu\text{M}$  from the present 33  $\mu\text{M}$ . Total nitrate reduction in the basin would increase by 56% over the present value. Disposal of sludge with twice the oxygen demand would decrease the minimum lower basin nitrate concentration to 20  $\mu\text{M}$  and increase total nitrate reduction to almost twice the present rate.

**Sulfide Production.** The continued presence of fairly large concentrations of nitrate (at least 20  $\mu\text{M}$ ) in basin waters even after oxygen is virtually eliminated indicates that sludge organic matter should not reduce sulfate to sulfide in the water column. However, sulfides could be produced in the sediments and released into the water column, where they would be oxidized back to sulfate, or they could be released directly from the sludge.

Effects of sludge disposal on sedimentary sulfate reduction and sulfide release are too complex to model at present (26). Sulfate reduction could be increased by organic sedimentation, but whether it would or not depends on other factors as well. For example, Sholkovitz (27) found strong sulfate reduction in sediments of lower Santa Barbara Basin where oxygen concentration was between 2 and 4  $\mu\text{M}$  but little sulfate reduction on basin slopes, where sedimentation appeared to be the same, but water oxygen concentrations were about 18  $\mu\text{M}$ . The rate at which sulfide species leave the sediments depends on the presence of iron available for formation of pyrites and the presence of sufficient oxygen at the water-sediment interface to oxidize sulfides to sulfates. Further study of basin sediments would have to be made to determine rates of sulfide release to the water column.

The sulfide concentration from sludge release will depend on a balance between water column sulfide oxidation rate and sulfide release rate. The sulfide oxidation rate in seawater can be described by (28)

$$-d\Sigma[S^{2-}]/dt = k[O_2]\Sigma[S^{2-}] \quad (17)$$

where  $k = 3.6 \times 10^{-2} \text{ } \mu\text{M}^{-1} \text{ day}^{-1}$ . Sulfides in sludge are mostly metal sulfide precipitates with the greatest amount present in FeS(s) (12). Maximum particulate iron and, therefore, particulate sulfide concentrations for 400-m discharge would be  $6.7 \times 10^{-8} \text{ M}$ , and oxygen concentration would be 30  $\mu\text{M}$ . This particulate concentration, dissolving at the maximum 0.01  $\text{day}^{-1}$  rate, would add  $6.7 \times 10^{-10} \text{ M}$  sulfide/day to solution. At steady state, sulfide oxidation would equal sulfide dissolution. The steady-state sulfide concentration would be  $6.5 \times 10^{-10} \text{ M}$ . If sulfide oxidation is part of the dissolution process, the concentration would be less than this. Thus, the maximum sulfide concentration for disposal at 400 m from sludge dissolution should be less than  $10^{-9} \text{ M}$ .

**Biological Impacts.** The lower Santa Monica-San Pedro Basin is not dead (3). However, inadequate information on the ecology and physiology of animals there limits the predictions that can be made. Population sizes that will be affected by different disposal strategies can be estimated very crudely.

One approach is to argue that animals cannot survive in water with less than a given oxygen concentration. If a certain area/volume would have its oxygen concentration lowered below that value, then all of the animals within that area would be affected. If it were known which would be affected, then their biomass within that area could be calculated. Oxygen concentrations lower than required might not actually eliminate a species but might only shift its range to higher oxygen-containing waters. The calcu-

Table X. Biomass in Different Depth Ranges of Santa Monica-San Pedro Basin<sup>a</sup>

	lower basin	lower upper basin
depth range, m	740-900	600-740
volume, m <sup>3</sup>	$2.9 \times 10^{11}$	$3.6 \times 10^{11}$
benthic area, m <sup>2</sup>	$2.5 \times 10^9$	$0.6 \times 10^9$
midwater fauna		
number density, no./10 <sup>4</sup> m <sup>3</sup>	32	32
total number in volume	$9 \times 10^8$	$1 \times 10^9$
biomass density, g/10 <sup>4</sup> m <sup>3</sup>	<i>b</i>	10
total biomass in volume, g	<i>b</i>	$4 \times 10^8$
epibenthic fauna		
biomass density, kg/haul	0.86 (fish only)	32
total biomass in area, g	$2 \times 10^8$	$2 \times 10^9$
benthic fauna		
biomass density, g/m <sup>2</sup>	4	15
total biomass in area, g	$10 \times 10^9$	$9 \times 10^9$
total biomass in range, g	$10 \times 10^9$	$11 \times 10^9$

<sup>a</sup> Animal densities were taken from SCCWRP's report (3) with epibenthic densities calculated by assuming that the otter trawl sampled 10<sup>4</sup> m<sup>2</sup>/haul (calculated for a net 7.6 m wide, towed for 20 min at 2 knots). <sup>b</sup> No data, but assumed small compared to benthic fauna.

lation of animal biomass that would be displaced/eliminated is based on the assumption that all the biomass used in these estimates (Table X) would be affected.

The use of an oxygen concentration of 4  $\mu\text{M}$  as that critical oxygen concentration below which no animals live seems reasonable. Several observations, physiological and environmental, support this. The critical concentration at which animal respiration began to decrease with decreasing oxygen concentrations is as low as 4.5  $\mu\text{M}$  in midwater crustaceans and fishes (16). This concentration represents the lower limit at which the animals could function aerobically. Judkins (personal communication) observed that 90% of the zooplankton avoided a layer of water with oxygen concentrations of 4.5  $\mu\text{M}$  (0.1 mL/L) off the Peru coast. Data for lower Santa Monica-San Pedro Basin, which has oxygen concentrations as low as 4.5  $\mu\text{M}$ , suggest that oxygen concentrations there are barely large enough to sustain some animals. The value of 4  $\mu\text{M}$  as the critical concentration for animal survival is similar to the critical concentration suggested by these studies but less than the present concentration in lower Santa Monica-San Pedro Basin.

Sludge discharge at 600 and 800 m would decrease oxygen concentrations below 4  $\mu\text{M}$  for large depth ranges: discharge at 800 m would, thus, depopulate the lower Santa Monica-San Pedro Basin, a volume of  $2.9 \times 10^{11} \text{ m}^3$  and an area of  $2.5 \times 10^9 \text{ m}^2$ . Crude estimates for biomass of midwater, epibenthic, and benthic fauna yield an estimate of 10<sup>7</sup> kg in the lower basin (Table X). The value for epibenthic biomass does not include invertebrates and was judged to be based on insufficient data (3), but it could only be comparable to that for infauna if it were 50 times larger.

If sludge discharge at 600 m were to reduce oxygen concentrations to less than 4  $\mu\text{M}$  from 600 m to bottom, it would affect an additional volume of  $3.6 \times 10^{11} \text{ m}^3$  and a benthic area of  $0.59 \times 10^9 \text{ m}^2$ . This would affect 10<sup>7</sup> kg more organisms than discharge at 800 m. The biomass affected between 600 and 740 m and that between 740 and 900 m are approximately the same despite the greater animal density shallower because of the greater benthic area in the lower region. Sludge discharge at 400 m would not lower oxygen content below 4  $\mu\text{M}$  but would impact benthic fauna by locally increasing the sedimentation rate.

Table XI. Comparison of Predicted Soluble Trace-Metal Concentrations with Those from the 1978 Water Quality Control Plan for Ocean Waters of California<sup>a</sup>

element	max allowable ambient concn, M <sup>b</sup>	predicted max soluble concn for discharge, M		
		400 m	600 m	800 m
cadmium		$2.7 \times 10^{-8}$	$9.3 \times 10^{-9}$	$9.3 \times 10^{-9}$
chromium	$3.9 \times 10^{-8}$	$8.5 \times 10^{-9}$	$8.6 \times 10^{-9}$	$7.1 \times 10^{-9}$
copper	$7.8 \times 10^{-8}$	$7.6 \times 10^{-9}$	$7.7 \times 10^{-9}$	$6.6 \times 10^{-9}$
lead	$3.9 \times 10^{-8}$	$8.0 \times 10^{-10}$	$8.1 \times 10^{-10}$	$6.8 \times 10^{-10}$
nickel	$3.4 \times 10^{-7}$	$3.5 \times 10^{-8}$	$3.5 \times 10^{-8}$	$3.5 \times 10^{-8}$
silver	$4.1 \times 10^{-9}$	$5.2 \times 10^{-10}$	$5.2 \times 10^{-10}$	$4.9 \times 10^{-10}$
zinc	$3.1 \times 10^{-7}$	$1.5 \times 10^{-8}$	$1.5 \times 10^{-8}$	$1.3 \times 10^{-8}$

<sup>a</sup> Reference 37. <sup>b</sup> 6-month median.

The area over which the sedimentation of organics would double is 120 km<sup>2</sup>. The sedimentation model (1), which does not consider particle oxidation, predicts that on the order of one-third of the sludge lands within this area for standard settling velocity.

Midwater fauna live by filtering particulate matter out of the water, scavenging, or predation. Sludge disposal might affect these animals by poisoning them with higher trace-metal concentrations, by mixing with their normal food to form a deleterious diet, or by interfering with the chemical cues that they need to find their food.

A comparison of predicted trace-metal concentrations with regulatory limits can indicate their significance. The California State Water Resources Control Board has used toxicological data for marine organisms to set its receiving water standards (Table XI). The model developed in Appendix 2 (2) predicts that discharge at 400, 600, or 800 m will not exceed the established standards for the trace metals studied. To the extent that these standards do encompass toxic effects of midwater organisms, the increased trace-metal concentrations associated with sludge discharge will not harm the midwater populations.

One way to assess the impact of sludge organic matter is to compare predicted concentrations with those naturally occurring. The maximum particulate sludge concentration for discharge under standard conditions was  $6.7 \times 10^{-3}$  mol of BOD m<sup>-3</sup> for discharge at 400 m,  $6.9 \times 10^{-3}$  mol of BOD m<sup>-3</sup> for discharge at 600 m, and  $13.3 \times 10^{-3}$  mol of BOD m<sup>-3</sup> for discharge at 800 m. These are equivalent to organic carbon concentrations of 80, 83, and 160 μg L<sup>-1</sup>, respectively, if 1 mol of BOD is equivalent to 1 mol of carbon. The particulate organic carbon concentration in the San Diego Trough below 300 m is between 5 and 15 μg L<sup>-1</sup> (29) and in Santa Catalina Basin is about 50 μg L<sup>-1</sup> (30). Thus, sludge discharge could increase the particulate organic carbon concentrations by as much as 1 order of magnitude over background concentrations. If these high organic concentrations act as a food source or interfere with animal feeding activity, sludge discharge could impact the zooplankton community. The actual effects these high organic concentrations would have on zooplankton are presently unknown.

**Halogenated Hydrocarbons.** Major sludge components not examined in this study known to affect organisms are the various hydrocarbons and their halogenated derivatives. The magnitude of their concentrations can be calculated if all hydrocarbons stay on particulates and if peak hydrocarbon concentrations are associated with peak particulate concentrations at the same particulate copper:hydrocarbon ratio as in the initially discharged sludge. Then, peak chlorinated benzene concentrations for discharge at 400 m would be about 20 μg/m<sup>3</sup>, about 20

parts per trillion. Predicted DDT inputs at 1/25 of this, implying maximum DDT concentrations of about 1 part per trillion in the water, two parts per million in the particulate phase. This is based on the horizontally well-mixed model.

### Conclusion

A model was developed to study the large-scale environmental consequences of disposing of sewage sludge in deeper waters off Southern California. Disposal at 600 m or deeper would have serious consequences on oxygen concentrations; sludge disposal at 400 m would avoid the serious oxygen depletion associated with deeper disposal. It would increase trace-metal particulate organic carbon and dissolved organic concentrations. Trace-metal concentrations would still be within a range believed to be nondeleterious; particulate carbon would be much greater than present background with possible, but unexplored, consequences on planktonic filter feeders; how dissolved organics affect scavenging or other traits of midwater organisms is a question that can only be posed, but not yet answered.

This analysis has not attempted to predict effects of sludge disposal on species distribution, community structure, diversity, faunal indices, or any of the other measures of an ecological assemblage because the basins are areas for which none of these are presently known. Prediction of ecological changes would involve an understanding of the mechanisms by which organisms interact with sludge. An attempt has been made to calculate the behavior of major sludge components known or suspected to be important in those mechanisms and to guess the magnitude of the effects. Hopefully, this work helps to define the scale of biological and ecological observations that need to be made before all environmental changes can be properly assessed. The controversy that still rages over the impact of present sludge disposal practices, in areas that have been intensively studied for over a decade, reminds us of the difficulty of doing more.

### Acknowledgments

I thank J. J. Morgan, R. C. Y. Koh, and N. H. Brooks for helpful discussions and D. Kent and T. Fall for their assistance.

### Literature Cited

- (1) Koh, R. C. Y. *Environ. Sci. Technol.*, following article in this issue.
- (2) Jackson, G. A.; Koh, R. C. Y.; Brooks, N. H.; Morgan, J. J. Environmental Quality Laboratory Report No. 14, California Institute of Technology: Pasadena, CA, 1979.
- (3) Mearns, A. J.; Ward, J. Q.; Moore, M. D. "Biological Conditions in Santa Monica and San Pedro Basins"; Southern California Coastal Water Research Project: El Segundo, CA, 1978.
- (4) Jones, J. H. Technical Report 101, Southern California Coastal Water Research Project: El Segundo, CA, 1971.
- (5) Emery, K. O. "The Sea off Southern California"; Wiley: New York, 1960.
- (6) Sholkovitz, E. R.; Gieskes, J. M. *Limnol. Oceanogr.* 1974, 16, 479-489.
- (7) Sverdrup, H. U.; Fleming, R. H. *Bull. Scripps Inst. Oceanogr.* 1941, 4, 261-378.
- (8) Sholkovitz, E. R. Ph.D. Thesis, University of California, San Diego, CA, 1972.
- (9) Minard, D. R. "Water Quality in Submarine Basins off Southern California"; Federal Water Pollution Control Administration, Pacific Southwest Region, U.S. Department of the Interior, 1968.
- (10) Pereyra, V. *Rev. Union Mat. Argen. Assoc. Fis. Argent.* 1965, 22, 184-201.



- (11) Lentini, M.; Pereyra, V. *SIAM J. Numer. Anal.* 1977, 14, 91.
- (12) Faisst, W. K. Report 13, Environmental Quality Laboratory, California Institute of Technology: Pasadena, CA, 1976.
- (13) Neame, K. D.; Richards, T. G. "Elementary Kinetics of Membrane Carrier Transport"; Blackwell Scientific: London, 1971.
- (14) Smith, K. *Limnol. Oceanogr.* 1974, 19, 939-944.
- (15) Hargrave, B. T. *J. Fish. Res. Board Can.* 1973, 30, 1317-1326.
- (16) Childress, J. J. *Comp. Biochem. Physiol. A* 1975, 50A, 787-799.
- (17) Muellenhoff, W. P. Ph.D. Thesis, Oregon State University, Corvallis, OR, 1977.
- (18) Sarmiento, J. L.; Feely, H. W.; Moore, W. S.; Bainbridge, A. E.; Broecker, W. S. *Earth Planet. Sci. Lett.* 1976, 32, 357-370.
- (19) Chen, K. V.; Jan, T. K.; Rohatgi, N. *J. Water Pollut. Cont. Fed.* 1974, 46, 2663-2675.
- (20) Morel, F. M. M.; Westall, J. C.; O'Melia, C. R.; Morgan, J. *J. Environ. Sci. Technol.* 1975, 9, 756-761.
- (21) Rohatgi, N.; Chen, K. Y. *J. Water Pollut. Cont. Fed.* 1975, 47, 2298-2316.
- (22) Bruland, K. W.; Bertine, K.; Koide, M.; Goldberg, E. D. *Environ. Sci. Technol.* 1974, 8, 425-432.
- (23) Bertine, K. K.; Goldberg, E. D. *Environ. Sci. Technol.* 1977, 11, 297-299.
- (24) Fiadeiro, M.; Strickland, J. D. H. *J. Mar. Res.* 1968, 26, 187-201.
- (25) Goering, J. J.; Cline, J. D. *Limnol. Oceanogr.* 1970, 15, 306-309.
- (26) Berner, R. A. In "The Sea"; Goldberg, E. D. Ed.; Wiley: New York, 1974; Vol. V, Chapter 13.
- (27) Sholkovitz, E. *Geochim. Cosmochim. Acta* 1973, 37, 2043-2073.
- (28) Cline, J. D.; Richard, F. A. *Environ. Sci. Technol.* 1969, 3, 838-843.
- (29) Holm-Hansen, O. *Mem. Inst. Ital. Idrobiol.* 1972, 29 Suppl., 37-51.
- (30) Holm-Hansen, O.; Strickland, J. D. H.; Williams, P. M. *Limnol. Oceanogr.* 1966, 11, 548-561.
- (31) Boyle, E. A.; Sclater, F.; Edmond, J. M. *Nature (London)* 1976, 263, 42-44.
- (32) Morgan, J. J.; Sibley, T. H. *Proc. Civil Eng. Oceans III* 1975, 2, 1332-1352.
- (33) Boyle, E. A.; Sclater, F.; Edmond, J. M. *Earth Planet. Sci. Lett.* 1977, 37, 38-54.
- (34) Sclater, F. R.; Boyle, E.; Edmond, J. M. *Earth Planet. Sci. Lett.* 1976, 31, 119-128.
- (35) Bruland, K. W.; Knauer, G. A.; Martin, J. H. *Nature (London)* 1978, 271, 741-743.
- (36) Hulsemann, J.; Emery, K. O. *J. Geol.* 1961, 69, 279-290.
- (37) California State, The Resources Agency, State Water Resources Control Board, Resolution No. 78-12, 1978.

Received for review October 9, 1981. Revised manuscript received July 13, 1982. Accepted July 19, 1982. This paper reports on part of the ongoing research by Caltech's Environmental Quality Laboratory on alternative practices for disposal of digested sewage sludge in the ocean. Support has been provided by the Ford Foundation (Grant No. 740-0469), the Rockefeller Foundation (Grant No. CA NES 7706), and a consortium of the County Sanitation Districts of Los Angeles County, the City of Los Angeles, and the County Sanitation Districts of Orange County since August 1977.

## Initial Sedimentation of Waste Particulates Discharged from Ocean Outfalls

Robert C. Y. Koh

Environmental Quality Laboratory, California Institute of Technology, Pasadena, California 91125

■ A model is developed to evaluate the initial deposition of particles due to discharge of sewage sludge in the ocean. The three-dimensional sedimentation modeling shows that the sludge particles would be widely dispersed. The bottom initial fallout distribution is expected to be much elongated along the bottom contours due to nonisotropy of the ocean current. This is useful in assessing the environmental consequences of alternative strategies for ocean sludge disposal in southern California where offshore deep basins (depths to 900 m) are within short distances from shore (on order of 10-20 km).

### Introduction

Disposal of human wastes, whether on land, in the ocean, or in the atmosphere, always involves an impact on the environment. Availability of deep water relatively close to shore has stimulated ocean discharge of sewage effluent and sludge in southern California. These discharge systems have adequately met the classical design criteria of maintaining aquatic oxygen concentrations and satisfying bathing water standards but have had documented effects on marine benthic ecosystems. While the significance of these ecological changes is not understood, federal policy is to stress land disposal and eliminate ocean disposal of sludge—generally a much costlier alternative which also

shifts direct environmental impact from the ocean to the land and the atmosphere.

The treatment of the sewage produced by the 10 million people in the Los Angeles and Orange Counties area is predicted to produce (at full secondary treatment as presently mandated by law) 1145 dry tons of sludge per day. The Sanitation Districts of Los Angeles and Orange Counties and the City of Los Angeles organized an investigation known as LA/OMA (Los Angeles/Orange County Metropolitan Area Regional Wastewater Solids Management Program) to determine the optimal alternatives for sludge handling and disposal. Even though ocean discharge is not permitted, the Districts as well as the City felt it wise to include ocean discharge as an alternative to be studied.

This paper describes one aspect of the study related to the ocean-discharge alternative. In particular it discusses the physical aspects of the fate of the particulates in sludge if it is discharged into the relatively deep ocean basins off southern California such as the Santa Monica-San Pedro Basin. For definiteness, it will be assumed that a pipeline is terminated at approximately 400 m depth, although the analysis is similar for other depths as well as other modes of discharge. The 400 m depth appears more favorable than deeper depths according to the biological modeling results given in Jackson and co-workers (1, 2).

When sludge first exists from a pipeline (whether or not equipped with a diffuser), it will undergo a phase of motion that is influenced by its momentum and buoyancy as well as the ambient current and density stratification. This phase typically lasts only a matter of minutes and results in a certain initial dilution and equilibrium height of rise. During this phase, the ambient conditions can be considered steady (since the time scale of changes in ambient conditions is on the order of hours), and the particulates can be assumed to be part of the discharged fluid (since fall velocities are very small). The phenomenon of flocculation may take effect during this time. However, no method is available to estimate its importance.

Following this initial phase, the diluted mixture is advected and dispersed by the currents and turbulence in the ocean while the particulates slowly fall down (or float up, as the case may be).

We shall not be concerned with the details of how the dispersion occurs on any given day but rather will attempt to estimate the longer term fallout pattern of the particulates when the effects are integrated over a long time (such as months and years).

It is clear that in order to do this, we must have the following information: (i) the fall velocities of the particulates; (ii) The ocean currents and density stratification near the site; (iii) the flow rate and other characteristics of the discharge. Unfortunately, we have little information on either the fall velocities or the currents. It is thus impossible to make reliable estimates. The best that can be achieved would be a parametric estimation of orders of magnitude. However, the method is demonstrated and shows how more input data would be used.

### Formulation

Consider a single particle of sludge with fall velocity  $w$  situated at position  $x_0, y_0, z_0$  at time  $t = 0$  in an infinite quiescent ocean. We seek the probability density  $p(x, y, z, t; x_0, y_0, z_0)$  such that  $p \, dx \, dy \, dz$  is the probability of finding that particle in the interval  $x$  to  $x + dx, y$  to  $y + dy, z$  to  $z + dz$  at time  $t$ . We assume stationarity and postulate that  $p$  is Gaussian of the form

$$p = \left( \frac{1}{(2\pi)^{3/2} \sigma_x \sigma_y \sigma_z} \right) \exp \left\{ - \frac{(x - x_0)^2}{2\sigma_x^2} - \frac{(y - y_0)^2}{2\sigma_y^2} - \frac{(z - (z_0 - wt))^2}{2\sigma_z^2} \right\} \quad (1)$$

where  $\sigma_x$  and  $\sigma_y$  are functions of  $t$  only,  $\sigma_z = (2\epsilon_z t)^{1/2}$ ,  $\epsilon_z =$  vertical diffusion coefficient, and it has implicitly been assumed that  $x, y, z$  are along principal axes of the stochastic velocity field.

In the present case, there is an ocean bottom given by  $z = z_b(x, y)$ . We now make the intuitive assumption that the relative rate of particle fallout on  $z = z_b(x, y)$  is given by

$$E = wp|_{z=z_b} + \epsilon z \frac{\partial p}{\partial z} \Big|_{z=z_b} \quad (2)$$

Thus assumption is admittedly simplistic and is used only as a rough approximation. Physically it means that the probability  $p$  is unaffected by the bottom (i.e., the bottom is transparent to the particles) and that the fallout is given by the net downward vertical transport implied by  $p$  evaluated at  $z = z_b$ . Substitution of eq 1 into eq 2 yields

$$E = \frac{1}{4\pi\sigma_x\sigma_y(\pi\epsilon_z t)^{1/2}} \left( \frac{z_0 - z_b + wt}{2t} \right) \exp \left\{ \frac{(x - x_0)^2}{2\sigma_x^2} - \frac{(y - y_0)^2}{2\sigma_y^2} - \frac{[z_0 - z_b - wt]^2}{4\epsilon_z t} \right\} \quad (3)$$

which relates to the probability that a particle with fall velocity  $w$  which was originally at  $x_0, y_0, z_0$  at time  $t = 0$  will get to the bottom at position  $x, y$  in time  $t$ . If, in addition, we know the distribution of heights  $g(z_0)$  and fall velocities  $f(w)$ , then the initial fallout distribution on the bottom is

$$B = \int_0^\infty dt \int_0^\infty dw \int_0^H dz_0 E(x, y, t; x_0, y_0, z_0, w) f(w) g(z_0) \quad (4)$$

where  $z_0 = H$  is at the water surface.

**Distribution of Initial Height  $g(z_0)$ .** To obtain an estimate of the distribution of initial height  $g(z_0)$ , we appeal to the body of literature on buoyant jets and plumes in a stratified fluid. We assume that the discharge is buoyancy dominated and use the results of Wright (3) to estimate the equilibrium rise height  $z_e$ :

$$z_e/l_b = C_{12}(l_a/l_b)^{2/3} \quad (5)$$

where

$$l_b = gQ_0((\Delta\rho)_0/\rho)/u^3$$

$$l_a = u/[(g/\rho)|d\rho/dz|]^{1/2}$$

Here  $u =$  current speed,  $\rho =$  receiving water density,  $(\Delta\rho)_0 =$  difference in density between receiving water and effluent,  $Q_0 =$  discharge rate, and  $g =$  gravitational acceleration. From Wright,  $C_{12}$  can be approximated by 1.8 for all his data regardless of whether the experiment was buoyancy dominated near or far field.

In addition, if there were no ambient current, we use the result based on buoyant plume theory (see, e.g., Fischer et al. (4))

$$z_e = \alpha(3.98) \left( Q_0 \frac{g(\Delta\rho)_0}{\rho} \right)^{1/4} \left[ \frac{g|d\rho}{\rho|dz} \right]^{-3/8} \quad (6)$$

where  $\alpha$  is a numerical factor to account for the difference between equilibrium height and maximum height of rise.

For application to the present problem, we use the following typical data (same as in Faisst (5), pp 119-120):

$$Q_0 = 5 \text{ mgd}$$

$$\frac{1}{\rho} \left| \frac{d\rho}{dz} \right| = 1.5 \times 10^{-6} \text{ m}^{-1}$$

$$(\Delta\rho)_0 = 24.5 \times 10^{-3} \text{ g/cm}^3$$

and take  $\alpha = 0.8$  for definiteness (mgd = million gallons/day). Equations 5 and 6 then reduce to

$$z_e = 46Q_0^{1/3}(1/u)^{1/3} \quad z_e = 145Q_0^{1/4} \quad (7)$$

The value of  $z_0$  that applies should be the smaller of the two.

The value of  $Q_0$  in eq 5 and 6 is subject to some control through design. For example, if ten (noninterfering) plumes result from a diffuser, the  $Q_0$  would only be 0.5 mgd for each.

By use of eq 5 and 6 and the current data measured in Santa Monica-San Pedro Basin, the distributions shown

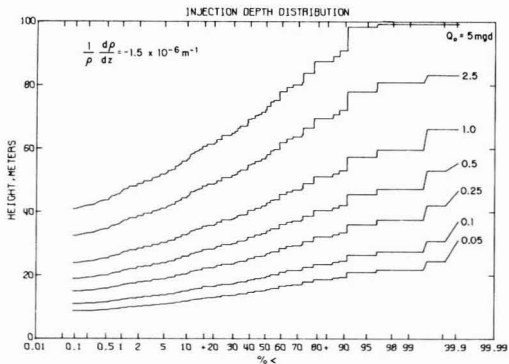


Figure 1. Distribution of height of rise of discharged plumes for various port flows, derived from an ambient current distribution. Stratification is fixed at a typical value.

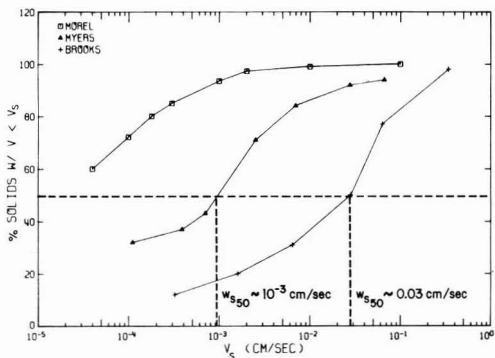


Figure 2. Summary of sedimentation data: distribution of all velocity of wastewater solids (digested sludge; Myers (6) and Brooks (7); sewage effluent solids, Morel (8)).

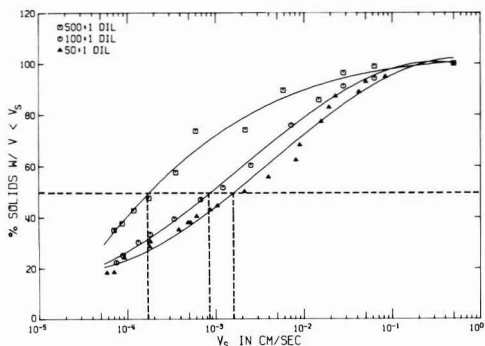


Figure 3. Distribution of fall velocity of sludge particles at various dilutions (from Faisst (4)).

in Figure 1 are obtained. (The current data will be further discussed in a later section.) It is seen that the rise height decreases as  $Q_0$  decreases but can range over several tens of meters. The overall range is about 10–100 m.

**Distribution of Fall Velocities  $f(w)$ .** Figures 2 and 3 show distributions of fall velocities of sludge particles as determined in the laboratory by several investigators. The range is very wide, and there is some indication that flocculation is at play. More definitive determination of fall velocities is required. For our present purposes, we

can only parameterize and bracket the range as less than a few tenths centimeters per second with the bulk in the range  $10^{-4}$ – $10^{-2}$  cm/s. It is interesting to note that with  $w = 10^{-3}$  cm/s and  $z_0 = 50$  m, the time  $z_0/w$  is about 58 days.

**Estimation of Horizontal Diffusion from Ocean Current Measurements.** Since the expected time of residence of sludge particles in the water column is quite long (due to the small fall velocities), it is of interest to examine the horizontal diffusion of the particulates.

An effort was made to measure the currents in selected locations in Santa Monica Basin. The current data in Figure 4 were taken in water of 470 m depth with the current meter about 40 m above the bottom. There is seen to be a great disparity between the component toward N 100° E (parallel to the local bottom contour) and the component toward N 190° E. With the exception of a spectral peak at the semidiurnal frequency, the latter component has effectively a level power spectrum. The parallel component, on the other hand, shows spectral peaks at both the diurnal and semidiurnal periodicities. It can also be seen from Figure 4 that the character of this current component exhibited the occurrence of some "event" during the period May 8 to May 21, 1978. It is not known what caused this marked difference in character.

For the present purpose, the current meter records are high-pass filtered to remove long-term variations for which the data cannot be expected to be representative. We chose a filter with the half-power cutoff at 0.09 cycles/day.

In an attempt to deduce the dispersive characteristics, we appeal to Taylor's theorem and apply it to the two components of the velocity separately since they are effectively uncorrelated. Taylor's theorem states that for a stationary process, the mean-square dispersion  $\sigma^2$  along a given axis  $x$  is given by

$$\sigma^2 = 2 \int_0^t (t - \tau) C(\tau) d\tau$$

where  $C(\tau)$  is the Lagrangian autocovariance of the velocity at lag  $\tau$ . We assume that the Lagrangian autocovariance function can be estimated by the autocovariance functions of the two Eulerian velocity components. The data for the parallel component were divided into two parts containing the first 12 days (the "event") and the remainder of the data samples. Autocovariance estimates were made for the two parts separately as well as for the entire amount of data. Taylor's theorem was then applied to yield estimates of the variances  $\sigma_x^2$  as functions of time. Figure 5 shows  $\sigma_x^2(t)$  for the  $u$  (parallel) component of the current. It can be seen that the variance grows at a rate somewhat higher than linear in time. At 1 day,  $\sigma_x^2 \approx 5 \text{ km}^2$ , and at 3 days,  $\sigma_x^2 \approx 15 \text{ km}^2$ . If an overall Fickian diffusion coefficient were to account for this, it would be on the order of  $2.5 \text{ km}^2/\text{day}$ .

The  $v$  (perpendicular) component of the current was analyzed in the same way, and the variance was found to grow effectively linearly with time with a Fickian diffusion coefficient of  $0.1 \text{ km}^2/\text{day}$ . There is thus a 25:1 ratio in the horizontal dispersive coefficients in the two directions. This alone would result in a 5:1 ratio of the lengths of the zone of significant fallout of particulate matter.

**Horizontal Distribution of Fallout Pattern.** We return now to eq 3 and permit  $z_b$  to be a function of the horizontal coordinates  $x$  and  $y$ . We further assume  $\sigma_x = (2\epsilon_x t)^{1/2}$  and  $\sigma_y = (2\epsilon_y t)^{1/2}$ , i.e., that the horizontal diffusion is Fickian in nature. It is believed that these are probably justified since we can have at best only an order of magnitude estimate of  $\epsilon_x$  and  $\epsilon_y$ .

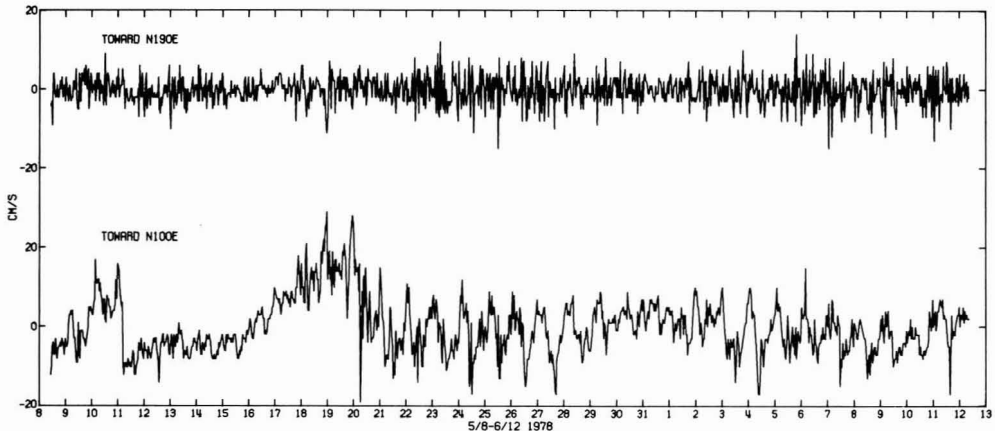


Figure 4. Ocean currents measured in Santa Monica Basin slope in water of 470 m depth (meter depth = 430 m).

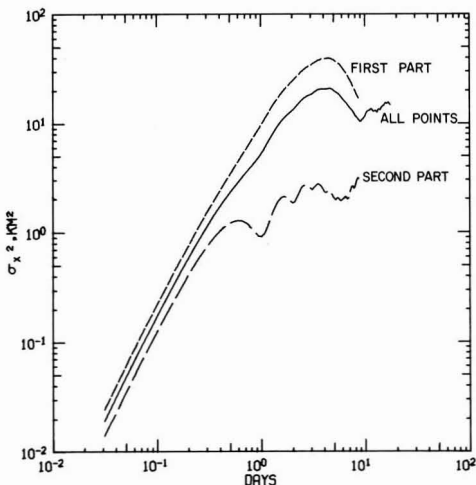


Figure 5. Growth of variance (by Taylor theorem) of current component toward N 100° E.

Since  $E$  is the rate of settling to the bottom (eq 2), the quantity

$$F = \int_0^t E dt$$

is the amount that has reached the bottom at  $(x,y)$  by time  $t$ . Letting the upper limit tend to  $\infty$  then gives  $F_\infty$  as the amount that would ultimately settle out as a function of the horizontal coordinates. By integration, it can be deduced that

$$F_\infty = \frac{2(\pi)^{1/2}}{A} \exp \left\{ \frac{w(z_0 - z_b)}{2\epsilon_x} - \frac{w}{2} (\phi/\epsilon)^{1/2} \right\} \times \left[ \frac{w(z_0 - z_b)}{\phi(\epsilon_x)^{1/2}} \left( 1 + \frac{2}{w} (\epsilon_x/\phi)^{1/2} \right) + \frac{w}{\phi^{1/2}} \right] \quad (8)$$

where

$$\phi = \frac{(x_0 - x)^2}{\epsilon_x} + \frac{(y - y_0)^2}{\epsilon_y} + \frac{(z_0 - z_b)^2}{\epsilon_z}$$

$$A = 16\pi^{3/2} / (\epsilon_x \epsilon_y \epsilon_z)^{1/2}$$

The physical interpretation of  $F_\infty(x,y; z_0, w, \epsilon_x, \epsilon_y, \epsilon_z)$  is simply the fraction of particulates that would fall per unit area at  $x,y$  as a result of injection height  $z_0$ , fall velocity  $w$ , and diffusion coefficients  $\epsilon_x, \epsilon_y$ , and  $\epsilon_z$ . The expression for  $F_\infty$  in eq 8 is obtained based on various assumptions and must be regarded as providing no more than a rough estimate. However, inasmuch as the basic variables such as  $w, z_0, \epsilon_x, \epsilon_y$ , and  $\epsilon_z$  are only known to a rough approximation, it is believed that the assumptions leading to eq 8 are justified since it provides at least a rational method of estimation of the fallout distribution. Moreover, the evaluation of  $F_\infty$  given the parameters  $z_0, w, \epsilon_x, \epsilon_y, \epsilon_z$ , and  $z_b(x,y)$  can be made very rapidly and simply without any iterations so that eq 8 provides a very convenient (though rough) starting point in the investigation of the problem.

**Horizontally Isotropic Diffusion in Ocean of Constant Depth.** We first apply the method to investigate the simpler case of horizontally isotropic diffusion in an ocean of constant depth. We shall find  $F_\infty$  for various values of the parameters  $z_0, \epsilon_x, \epsilon_y, \epsilon_z$ , and  $w$ . Since there are substantial uncertainties associated with each of these parameters, it is highly desirable to select a "basic" set of values about which each of the parameters will be varied in turn but one at a time. Based on the discussion in previous sections of this paper, the following set of basic values will be selected:  $z_0, 50$  m,  $w, 10^{-3}$  cm/s;  $\epsilon_x, 2.5$  km<sup>2</sup>/day =  $2.9 \times 10^5$  cm<sup>2</sup>/s;  $\epsilon_y, 2.5$  km<sup>2</sup>/day =  $2.9 \times 10^5$  cm<sup>2</sup>/s;  $\epsilon_z, 1$  cm<sup>2</sup>/s. Note that even though measurements of ocean current at candidate site of sludge discharge shows that  $\epsilon_x$  and  $\epsilon_y$  might bear a ratio of 25 to each other, we cannot justify them to be different in the present parametric case of a horizontal ocean bottom. The case of nonisotropic horizontal diffusion in a nonhorizontal ocean bottom will be discussed in a later section.

Figure 6 shows the function  $F_\infty(r)$  (where  $r = (x^2 + y^2)^{1/2}$ ) for various values of the parameters. Six graphs are presented in the figure, each one corresponding to a set of values of the parameters. Within each graph, four curves are shown, one for each of the four fall velocities  $10^{-1}, 10^{-2}, 10^{-3}$ , and  $10^{-4}$  cm/s. The graph at the upper left corresponds to the basic set of values for the parameters. By comparison of these graphs, the effect of each of the parameters can be appreciated. Note that the ordinate is  $F_\infty$ , which is the fraction of particles falling per km<sup>2</sup> at the various distances away from the discharge. Thus if  $Q$  is the rate of particulates being imparted into the ocean (say in tons/year), then  $QF_\infty$  is the equilibrium rate of sedimentation in tons/(km<sup>2</sup> year). It can be seen that in

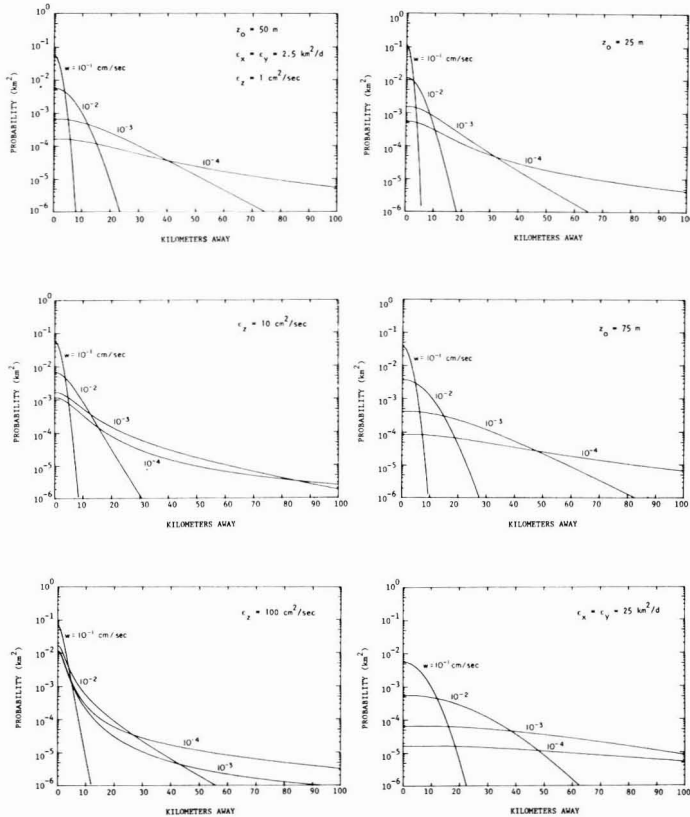


Figure 6. Effects of parameters on distribution function  $F_\infty$  = ratio of sedimentation (per  $\text{km}^2$ ) to source input vs. distance from source. Parameters are varied from the basic set of the upper left graph as indicated.

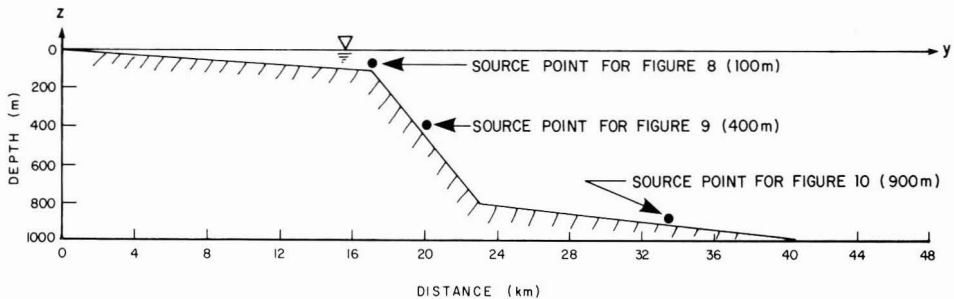


Figure 7. Idealized profile of Santa Monica shelf used in sedimentation modeling (assumed uniform along the coast).

the basic case ( $10^{-3}$  cm/s in upper left graph),  $F_\infty(0)$  is  $6.5 \times 10^{-4}$   $\text{km}^{-2}$  and it decreases by a factor of 10 at about 40 km away. Increasing  $\epsilon_z$  increases  $F_\infty(0)$  because more particles would reach bottom by vertical diffusion. Increasing  $z_0$  or  $\epsilon_x$  decreases  $F_\infty(0)$  as expected.

**Horizontally Nonisotropic Diffusion in Ocean of Variable Depth.** The methodology developed can also be applied to the case when the diffusion characteristics are nonisotropic and when the bottom of the ocean is not horizontal such as in the case of interest off southern California (see Jackson (2)).

Examination of the bathymetry off southern California with consideration of the distance from shore to reach each depth, it was found that to reach a depth on the order of 400–500 m, the pipeline would most likely be located such

that the terminus is on the slope of the basin rather than near the Santa Monica submarine canyon. The local bottom topography can be approximated by a two-dimensional succession of planes as shown in Figure 7. The approximate method developed in this paper on the estimation of bottom fallout rates was applied to this case, and the results are shown in Figures 8–10. In each of these figures, two contour maps of bottom fallout rates are shown for the fall velocities of  $10^{-3}$  and  $10^{-2}$  cm/s. The contour values represent fractions/ $\text{km}^2$ . Because of symmetry about the  $y$  axis, only half of each deposition pattern is shown. Figure 8 shows the case when the discharge is made at a depth of about 100 m, Figure 9 at a depth of about 400 m, and Figure 10 at a depth of about 900 m. The nonisotropic nature of the pattern can be clearly seen. Also

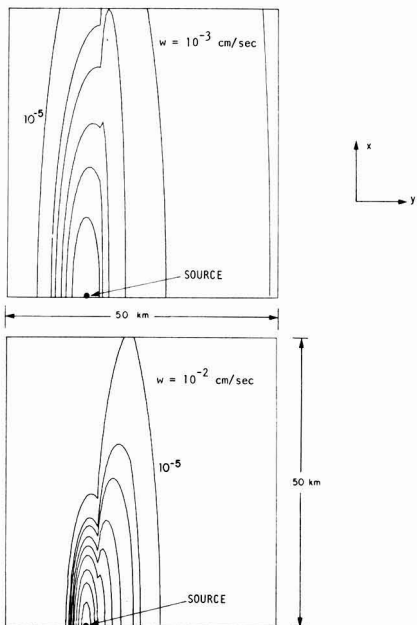


**Figure 8.** Particle fallout probability distribution (in  $\text{km}^{-2}$ ): contour values at  $10^{-5}$ ,  $10^{-4}$ ,  $5 \times 10^{-4}$ ,  $10^{-3}$ ,  $2 \times 10^{-3}$ ,  $5 \times 10^{-3}$ ,  $10^{-2}$ ,  $2 \times 10^{-2}$ ; parameters  $\epsilon_x = 2.5 \text{ km}^2/\text{day}$ ,  $\epsilon_y = 0.1 \text{ km}^2/\text{day}$ ,  $\epsilon_z = 1 \text{ cm}^2/\text{s}$ ,  $z_0 = 50 \text{ m}$ ; depth of discharge point = 100 m.

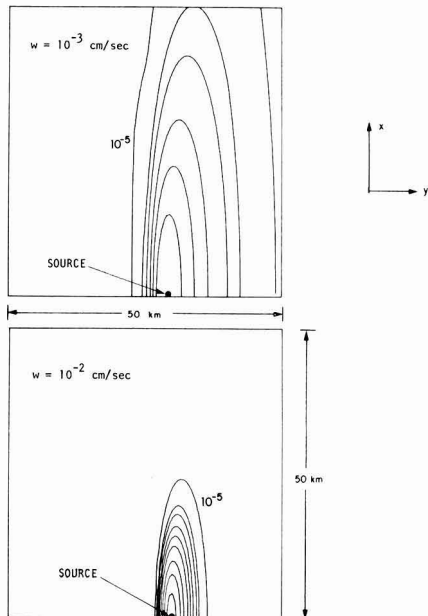


**Figure 10.** Particle fallout probability distribution (in  $\text{km}^{-2}$ ): contour values at  $10^{-5}$ ,  $10^{-4}$ ,  $2 \times 10^{-4}$ ,  $5 \times 10^{-4}$ ,  $10^{-3}$ ,  $2 \times 10^{-3}$ ,  $5 \times 10^{-3}$ ,  $10^{-2}$ ,  $2 \times 10^{-2}$ ; parameters  $\epsilon_x = 2.5 \text{ km}^2/\text{day}$ ,  $\epsilon_y = 0.1 \text{ km}^2/\text{day}$ ,  $\epsilon_z = 1 \text{ cm}^2/\text{s}$ ,  $z_0 = 50 \text{ m}$ ; depth of discharge point = 900 m.

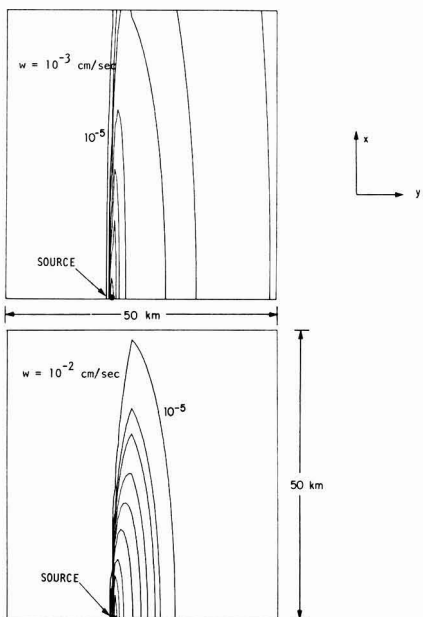


**Figure 9.** Particle fallout probability distribution (in  $\text{km}^{-2}$ ): contour values at  $10^{-5}$ ,  $10^{-4}$ ,  $2 \times 10^{-4}$ ,  $5 \times 10^{-4}$ ,  $10^{-3}$ ,  $2 \times 10^{-3}$ ,  $5 \times 10^{-3}$ ,  $10^{-2}$ ,  $2 \times 10^{-2}$ ,  $2 \times 10^{-2}$ ; parameters  $\epsilon_x = 2.5 \text{ km}^2/\text{day}$ ,  $\epsilon_y = 0.1 \text{ km}^2/\text{day}$ ,  $\epsilon_z = 1 \text{ cm}^2/\text{s}$ ,  $z_0 = 50 \text{ m}$ ; depth of discharge point = 400 m.

it can be noticed that more material settles in deeper depths than the discharge depth as would be expected due to the sinking of the particulates.

### Discussion

These results show that ocean disposal of sludge to the Santa Monica-San Pedro Basin via submarine outfall will result in the deposition of the particulates in a fairly extensive area on the bottom. A few percent of the particulates would settle out near the outfall terminus (within a kilometer) while the bulk would not. The area over which half the particulates would settle out might be on the order of  $100 \text{ km}^2$ .

All calculations of deposition presented thus far pertain to a relative fraction per unit area. To use the results to estimate actual deposition rate, it is necessary to multiply by the source rate. If the total organic input from sludge outfall is  $2 \times 10^7 \text{ mol of } \text{O}_2/\text{day}$  and if the background oxidation rate of the benthos is  $10^4 \text{ mol}/(\text{day km}^2)$ , then the value of the relative deposition  $F_\infty$  for the sludge deposition to equal natural oxidation is  $5 \times 10^{-4} \text{ km}^{-2}$ . Examination of Figure 9 reveals that the oblong area enclosed by the  $5 \times 10^{-4}$  contour (for  $w = 10^{-3} \text{ cm/s}$ ) is on the order of  $120 \text{ km}^2$ .

Alternatively, the total amount of sludge discharged might be estimated as  $3 \times 10^5 \text{ metric tons/year}$ . The natural sedimentation rate has been estimated as on the order of  $30 \text{ mg}/(\text{cm}^2 \text{ year}) = 300 \text{ tons}/(\text{km}^2 \text{ year})$ . Thus the value of  $F_\infty$  that renders them equal is  $300/(3 \times 10^5) = 10^{-3} \text{ km}^{-2}$ . This is a higher value, and the corresponding area in Figure 9 is smaller than that for  $5 \times 10^{-4} \text{ km}^{-2}$ .

### Summary

In this paper, the local initial deposition rates of hypothetical sludge discharged into the ocean are examined. In summary, the following points are noted:

(1) Available information on the fall velocity distribution of sludge particulates indicates that it is quite variable and may be influenced significantly by flocculation. At present

only an order of magnitude of the fall velocity is known.

(2) The density stratification and currents at possible discharge sites in Santa Monica Basin are such that the discharged sludge would rise to a distance on the order of 50 m above the bottom due to buoyancy.

(3) Two mechanisms participate in the downward migration and sedimentation of the particulates, (i) falling and (ii) downward diffusion. The second mechanism is significant for particulates with small fall velocities (e.g.,  $10^{-3}$  cm/s).

(4) Approximate estimation of horizontal diffusion using current meter data measured along the slope in the Santa Monica Basin indicates that the phenomenon is anisotropic with diffusion along the bottom contour substantially more energetic than in the perpendicular direction.

(5) Based on available data, an approximate determination was made of the initial bottom fallout pattern for several choices of discharge site. Results indicate that for fall velocity of  $10^{-3}$  cm/s the areal extent of the zone where the sedimentation rate is equal to the background oxidation rate is on the order of 120 km. This area has an oblong shape with the long axis oriented effectively along the contour.

(6) The general conclusion that can be reached is that a few percent of the particulate would settle within a kilometer of the discharge. The bulk would be quite dispersed over an oblong shaped region oriented along the bottom contour.

*Acknowledgments*

I thank N. H. Brooks, J. J. Morgan, and G. A. Jackson

for stimulating discussions and T. Fall and M. Gray for assistance in preparation of the manuscript.

*Literature Cited*

- (1) Jackson, George A.; Koh, Robert C. Y.; Brooks, Norman H.; Morgan, James J. EQL Report No. 14, Environmental Quality Laboratory, California Institute of Technology, Pasadena, CA, 1979.
- (2) Jackson, George A. *Environ. Sci. Technol.*, preceding paper in this issue.
- (3) Wright, S. J. Report No. KH-R-36, W. M. Keck Laboratory of Hydraulics and Water Resources, California Institute of Technology, Pasadena, CA, 1977.
- (4) Fischer, Hugo B.; List, E. John; Koh, Robert C. Y.; Imberger, Jörg; Brooks, Norman H. "Mixing in Inland and Coastal Waters"; Academic Press: New York, 1979.
- (5) Faist, W. K. EQL Report No. 13, Environmental Quality Laboratory, California Institute of Technology, Pasadena, CA, 1976.
- (6) Myers, E. P. Ph.D. Thesis, California Institute of Technology, Pasadena, CA, 1974.
- (7) Brooks, N. H., "Settling Analyses of Sewage Effluents"; memorandum to Hyperion engineers, July 5, 1956.
- (8) Morel, F. M. M.; Westall, J. C.; O'Melia, C. R.; Morgan, J. J. *Environ. Sci. Technol.* 1975, 9, 756-761.

*Received for review October 9, 1981. Revised manuscript received July 13, 1982. Accepted July 19, 1982. Acknowledgment is made to the Sanitation Districts of Los Angeles and Orange Counties, the City of Los Angeles, and the Ford and Rockefeller Foundations for financial support.*

## Characterization of Fluorocarbon-Film Bags as Smog Chambers

Nelson A. Kelly

Environmental Science Department, General Motors Research Laboratories, Warren, Michigan 48090

■ Experiments were conducted to characterize fluorinated ethylene-propylene copolymer (FEP Teflon) plastic bags as reactors for the photolysis of hydrocarbon/nitrogen oxides mixtures (smog chambers). The results of several tests show that such bags are suitable for the sunlight irradiation of urban air without extensive conditioning but unsuitable for rural air even after conditioning. At typical urban levels of hydrocarbons and nitrogen oxides, ozone production was reproducible in both differently conditioned and sized bags. Also, the dark ozone half-life in the bags was comparable to that in other larger smog chambers, and the surface reaction between ozone and Teflon produced negligible amounts of gas-phase products. However, large amounts of carbon monoxide were released by new Teflon film and caused large ozone production at low  $\text{NO}_x$  levels in the bags. Even conditioned bags, with negligible CO release, exhibited some excess reactivity and were therefore unsuitable for simulating rural photochemistry.

*Introduction*

Recently, smog chambers made of inert, transparent, fluorocarbon film have been widely used to investigate photochemical reactions in both synthetic and ambient air samples (1-8). For example, we conducted captive-air irradiations of ambient Houston air to evaluate the capacity of morning samples of air to generate ozone (5, 9). Samples of the morning air were diluted with zero air

and/or spiked with nitrogen oxides ( $\text{NO}_x$ ) or hydrocarbons (HC) to assess the effects of different control strategies and future emission scenarios. Also, trends in the maximum ozone produced in the bags were compared with the EPA Empirical Kinetics Modeling Approach (EKMA) (9).

Many researchers are hesitant, however, to apply smog chamber results to the atmosphere because there is disagreement in the scientific community regarding the effects of spectral distribution, walls, and contamination on the results (10-14). This is due to the wide variety of irradiation sources, wall materials, and chamber cleanup or conditioning procedures employed in different smog chambers. For experiments conducted outdoors in FEP Teflon (registered trademark of E. I. Du Pont de Nemours and Co, Wilmington, DE) bags, which are transparent to the full solar spectrum, spectral distribution effects, which cause major differences in indoor chambers, should not be a problem. However, the effects of wall conditioning and contamination are potentially very important for Teflon chambers. For example, Lonneman et al. (15) reported that some bags made of new FEP Teflon film released large amounts of volatile residues from the film manufacturing process. Others have reported that used Teflon bags exhibited far greater reactivity than new bags (16); they attributed this to excess OH radicals produced by the release of products left over from previous experiments (17). In addition, the general permeability of many plastic films, including Teflon, to a wide variety of compounds such as HC and  $\text{NO}_x$  has been documented by groups who

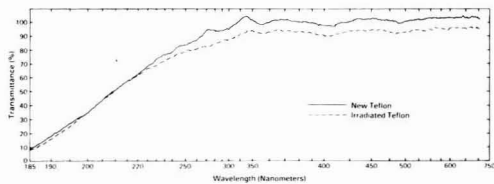


**Figure 1.** Ultraviolet-visible transmission spectra of new and used Teflon film.

hoped to use such bags for storing mixtures (18–20). This report summarizes the progress we have made and the problems we have observed in our attempts to optimize the bag irradiation procedure as applied to studying the photochemistry of ozone production. Included are (1) chamber characterizations including studies of contamination due to the nature of Teflon film, (2) measurements of the dark ozone half-life in bags as well as the consequences of the ozone/Teflon reaction, and (3) studies of the reproducibility and validity of bag irradiations.

#### Experimental Section

The reactors tested in this study were made from 0.05-mm (0.002 in.) FEP Teflon, type A (hereafter referred to as Teflon). Two square sheets of film, 137 cm on an edge were heat-sealed together around the edges. When inflated, a bag was pillow-shaped and had a volume of approximately 450 L, giving a surface-to-volume ratio of 0.083  $\text{cm}^{-1}$ . Two bulkhead fittings were located in the middle of the bag. One was a 3.75-mm fitting and was used to sample the contents of the reactor; the other was a 6.35-mm fitting and was used to fill or pump out the bag. Both fittings were also made of Teflon.

Bags made of thin Teflon film are fragile but have excellent light transmission. For example, samples of the 0.05-mm film held over an Eppley ultraviolet radiometer transmitted >95% of the solar radiation. Spectra of both new and used bags in Figure 1 show the excellent transmission of the full solar spectrum (wavelengths >300 nm). There was only a small reduction in the transmission of used film, which was probably caused by wrinkling of the film when the bags were inflated and deflated. Attempts to make the bags sturdier by using 0.13-mm (0.005 in.) film for the bottom panel that contained the two fittings, as well as making the whole bag from 0.13-mm film, did little to improve the durability. Furthermore, the results of Lonneman et al. (15) suggest that 0.13-mm film is more contaminated by organic compounds than 0.05-mm film, although this may just be a function of the specific rolls of film involved. Therefore, we have settled on bags made of 0.05-mm Teflon as preferable for photochemical reactors.

Irradiation experiments were conducted outdoors with the bags suspended on nylon nets. Bags were filled through the 0.635-mm fitting either with ambient air in ~10 min by using a metal bellows pump or with cylinder air in ~5 min. When desired, additions of HC or  $\text{NO}_x$  were made during filling, by using syringes and a septum in the filling line. For  $\text{NO}$  additions, this typically resulted in ~10% conversion to  $\text{NO}_2$  by thermal oxidation. After a bag was filled with either ambient air or a synthetic mixture, the ozone produced in the bag was measured for 10 min of each hour during the experiment with a Monitor Labs 8110 chemiluminescent ozone analyzer. This instrument was calibrated about every 3 days against a Dasibi 1003-AH ultraviolet photometer.

Occasionally, on windy days, new bags would begin leaking after being used only 1 day and therefore had to be discarded. Failure usually occurred at the heat-sealed

edges. When bags survived past the first day, they were pumped out in the evening and filled with zero air overnight. The following morning they were again pumped out and reused. The purpose of this procedure was to minimize contaminants desorbing from the walls.

While ozone was the only variable routinely measured during the irradiation experiments,  $\text{NO}_x$  and HC measurements were occasionally made in the bags. Hydrocarbons were measured with a Perkin-Elmer Model 900 gas chromatograph (GC), which used two columns with independent sampling systems, detectors, and electrometers for each column (7). The two columns separated hydrocarbons into light hydrocarbons ( $\text{C}_2\text{--C}_5$ ) and heavy hydrocarbons ( $\text{C}_5\text{--C}_{12}$ ). The nitrogen oxides were measured with a Teco Model 14B analyzer using a 450 °C molybdenum converter with an efficiency for  $\text{NO}_2$  >95% as determined by gas-phase titration. Differences less than 5 ppb  $\text{NO}_x$  could be measured in dry air, although humidity, which caused a positive interference, reduced the detection limit for ambient air analysis. A Beckman 6800 GC was used to measure CO by catalytically converting the CO to methane, which was then measured by a flame ionization detector. The detection limit was 0.2 ppm CO. The Beckman analyzer was also used to measure total hydrocarbons. Also, for some experiments, nonmethane hydrocarbons (NMHC) and CO were measured with a Bryon 401 GC. The Byron analyzer measures NMHC by separating them from methane chromatographically, converting them to  $\text{CO}_2$  using a cupric oxide catalyst heated to 700 °C, and then catalytically converting  $\text{CO}_2$  to methane to give a ppm carbon (ppmC) response for every carbon atom initially present in an organic compound. Methane, CO, and  $\text{CO}_2$  were also measured as separate peaks by the analyzer during each NMHC analysis.

Finally, to determine the ozone half-life in the dark, bags were filled with ozone generated from zero air by a MacMillan MEC-1000 generator, and the ozone was sampled for 10 min of each hour for approximately a 10-h period.

#### Results and Discussion

**Smog chamber characterization.** We sought to determine the "background reactivity" of the bags (the amount of ozone formed in new or used bags in the absence of added reactants or when only HC or only  $\text{NO}_x$  were added) as well as the amount formed from a reactive mixture. Therefore, four types of irradiation experiments were performed: (1) experiments with zero air only; (2) experiments with zero air plus hydrocarbons; (3) experiments with zero air plus  $\text{NO}_x$ ; (4) experiments with zero air plus hydrocarbons plus  $\text{NO}_x$ . The results of these tests are shown in Table I and are referred to as series 1–4, respectively. Several different experiments comprise series 1. First, several new bags filled with zero air and irradiated for a day produced less than 5 ppb ozone. Second, a bag that had been used the day before to irradiate ambient Houston air was flushed out, filled with zero air overnight, refilled with zero air the next morning and irradiated; only 14 ppb ozone was produced. We have observed up to 35 ppb  $\text{O}_3$  produced by the irradiation of clean air in used bags that were not allowed to degas overnight before subsequent use, so further reference to used bags indicates they have undergone overnight cleaning. Third, other used bags that had previously been used to irradiate ethylene/ $\text{NO}_x$  mixtures produced 5–10 ppb ozone when they were filled with zero air and irradiated for a day. Also, in series 2, both new and used bags containing zero air plus butane, ethylene, or propylene produced negligible ozone. Thus, both new and used bags produced low amounts of ozone when zero air or zero air plus hydrocarbons were irradiated. In contrast, some large outdoor chambers, which are harder



Table I. Ozone Production by Irradiated Bags Filled with Zero Air or Zero Air and Additions

additions	bag condition	O <sub>3</sub> (max), ppb	comments
		Series 1	
none	new	<5	bags had been used to irradiate reactive mixtures the day before
		Series 2	
1.0 ppm butane	new	<5	
0.05 ppm ethylene	new	<5	
0.02 ppm propylene	used	<5	contained 10 ppb NO <sub>x</sub> in zero air the day before
		Series 3	
0.22 ppm NO <sub>x</sub>	new	15-36	three different bags
0.22 ppm NO <sub>x</sub>	used	11	
0.09 ppm NO <sub>x</sub>	new	86	
0.09 ppm NO <sub>x</sub>	new	45	conditioned with 1000 ppb ozone for 1 day prior to experiment
see above	used	180	above mixture irradiated for a second day
0.05 ppm NO <sub>x</sub> <sup>a</sup>	new	30	
0.04 ppm NO <sub>x</sub> <sup>a</sup>	new	45	
0.04 ppm NO <sub>x</sub> <sup>a</sup>	used	11	
0.02 ppm NO <sub>x</sub> <sup>a</sup>	used	24	conditioned by a 1-day irradiation of zero air
see above	used	36	above mixture irradiated for a second day
0.01 ppm NO <sub>x</sub> <sup>a</sup>	new	103-110	two different bags
		Series 4	
1.1 ppm ethylene plus 0.22 ppm NO <sub>x</sub>	new	495	O <sub>3</sub> (max) at 1400
0.6 ppm ethylene or 1.1 ppm butane plus 0.005-0.010 ppm NO <sub>x</sub> <sup>a</sup>	new	64-110	six different bags; O <sub>3</sub> (max) depended linearly on added NO <sub>x</sub>

<sup>a</sup> These NO<sub>x</sub> concentrations were measured with an NO<sub>x</sub> analyzer after the addition was made. The others are estimates based on the amount of pure NO added with a syringe.

to flush out in between runs, produced 150-160 ppb ozone when clean air was irradiated (3).

The results, i.e., low ozone production in new and used bags spiked with hydrocarbons, indicate that significant amounts of NO<sub>x</sub> were not released by new or used bags. Indeed, specific measurements of NO<sub>x</sub> in both new and used bags containing zero air and stored outdoors indicated that increases were <0.5 ppb NO<sub>x</sub> over the period of a day, as measured with a high-sensitivity NO<sub>x</sub> analyzer described elsewhere (21). Several of the used bags had been used to irradiate mixtures containing 50-100 ppb NO<sub>x</sub> prior to these tests.

In series 3, bags of clean air plus NO<sub>x</sub> were irradiated. At all added NO<sub>x</sub> levels, new bags formed substantially more O<sub>3</sub> than bags that had been previously used for a photolysis experiment. This was especially true at low NO<sub>x</sub>. If the bags were free of contaminants, maximum ozone would be 0-7 ppb as predicted by the simple photostationary equilibrium (5, 22) for NO<sub>x</sub> levels from 0.01 to 0.22 ppm, respectively, and with ~10% of the

initial NO<sub>x</sub> as NO<sub>2</sub>. Clearly this is not the case as much higher ozone levels were observed, and in general, maximum ozone increased as the initial NO<sub>x</sub> decreased (an outlier to this generalization is the experiment at 0.09 ppm NO<sub>x</sub> that produced 86 ppb O<sub>3</sub>). Later we will show that new bags release large amounts of CO when they are irradiated, and this accounts for the ozone production by added NO<sub>x</sub>. The relatively low ozone production at high NO<sub>x</sub>, which is probably caused by the slow NO to NO<sub>2</sub> conversion process, disappeared when bags were irradiated for a sufficiently long time. For example, in an ozone-conditioned bag containing 0.09 ppm NO<sub>x</sub>, maximum ozone was 45 ppb the first day (vs. 86 ppb in an unconditioned bag) but increased to 180 ppb on the second day. The comparison between conditioned and unconditioned bags suggests that ozone conditioning was beneficial in reducing the effects of contamination but certainly did not eliminate them. In marked contrast, in an ozone-conditioned bag containing 0.09 ppm NO<sub>x</sub>, maximum ozone was 45 ppb the first day (vs. 86 ppb in an unconditioned bag) but increased to 180 ppb on the second day. The comparison between conditioned and unconditioned bags suggests that ozone conditioning was beneficial in reducing the effects of contamination but certainly did not eliminate them. In marked contrast, in a bag conditioned by irradiation (referred to as a used bag) at an NO<sub>x</sub> level of 0.02 ppm show that this bag was relatively contamination free. Here, only 24 ppb ozone was produced on the first day and 36 ppb on the second—a drastic improvement over the results in new bags at 0.01 ppm NO<sub>x</sub> where over 100 ppb O<sub>3</sub> was produced the first day. However, there was still excess ozone above the simple photostationary amount, indicating that a 1-day irradiation was not sufficient to condition bags for use at low NO<sub>x</sub>. We want to emphasize three major points based on the results in series 3: (1) the tests at low NO<sub>x</sub> were the most sensitive tests for hydrocarbon or CO contaminants since at higher concentrations NO initially inhibited ozone formation; (2) new bags exhibited far greater reactivity than used bags; (3) used bags formed relatively small amounts of ozone (11-24 ppb) at urban levels of NO<sub>x</sub> (0.02-0.2 ppm).

In the fourth series of irradiation experiments, synthetic hydrocarbon/NO<sub>x</sub> mixtures were irradiated in new bags. When 1.1 ppm ethylene was added to 0.22 ppm NO<sub>x</sub>, 495 ppb O<sub>3</sub> was produced in 5 h. This can be compared to 15-36 ppb O<sub>3</sub> when just 0.22 ppm NO<sub>x</sub> was irradiated (series 3). The difference shows that the contaminants released by the new bags cannot compete with the reactive hydrocarbon at high NO<sub>x</sub>. In contrast, at low NO<sub>x</sub> levels of 0.005-0.010 ppm, ozone formation was independent of added hydrocarbons and was linearly dependent on NO<sub>x</sub>, increasing 8-10 ppb for each ppb of added NO<sub>x</sub>. If O<sub>3</sub> formation is thought of as a competition between OH radicals to react either with NO<sub>2</sub>, which terminates the formation, or with hydrocarbons and CO, which propagates it, then at low NO<sub>x</sub> the process is so dominated by the CO contamination released by the bags that hydrocarbon addition has no effect. For example, at CO and NO<sub>2</sub> concentrations of 2 ppm and 5 ppb, respectively, the ratio of the rates OH + CO to OH + NO<sub>2</sub> is ~10, so 90% of the OH reacts with CO. The point to be made here is that contamination by CO in new bags did not dominate the effects of added hydrocarbons at high NO<sub>x</sub>, but did at low NO<sub>x</sub>. Therefore, even new bags will be able to differentiate between two urban mixtures with the same NO<sub>x</sub> but different hydrocarbon reactivities while they will not do the same for two low NO<sub>x</sub> (rural-type) mixtures with different hydrocarbon reactivities.

For conditions where there is a strong competition between the free-radical termination and propagation steps, as is the case in new bags at high NO<sub>x</sub>, it is interesting to further estimate when CO will be as important in the propagation reactions as hydrocarbons. This will occur when the CO concentration is 10-30 times that of the

**Table II. Carbon Monoxide Measurements in Bags of Zero Air**

bag and condition	sunlight exposure	$\Delta \text{CO},^a$ ppm	$\Delta t,^b$ h
1, new	yes	4.1	5
2, new	no	$\sim 0.2$	15
2, new	yes	5.5	8.5
3, used	yes	$\sim 0.2$	7
4, used	yes	$\sim 0.2$	5
5, new	yes	6.5	7
6, new <sup>c</sup>	yes	4.0	2.5
7, new <sup>c</sup>	yes	8.7	5.0

<sup>a</sup> Initial CO minus final CO. <sup>b</sup> This is the time interval between initial and final CO measurements. <sup>c</sup> Carbonyl compounds were measured in these bags.

hydrocarbon, as estimated by using the OH + HC rate coefficients of butane and ethylene, respectively (23).

**Specific Tests for Contamination by Hydrocarbons or CO.** As stated previously, the NO/NO<sub>2</sub>/air photolysis experiments showed that hydrocarbonlike species were influencing the results. Therefore, specific measurements of HC and CO were made in bags of zero air stored for various periods of time. Two different types of experiments were performed: (1) experiments in which bags of clean air were stored indoors in a laboratory or in a heated chamber for several days; (2) experiments in which bags of clean air were stored outdoors. The first series of experiments was more relevant to the use of bags as storage containers and is therefore described elsewhere (24). However, several observations were made during indoor storage that are potentially important to the use of bags for smog chambers. Basically, those tests showed that Teflon bags are permeable to a large number of organic compounds as well as NO and NO<sub>2</sub>. As a compound permeates through the film, it actually dissolves into the interstices of the film and has a lifetime there depending on its solubility and diffusion coefficient (24). Therefore, if bags are exposed to high levels of some contaminants, they can hold them and then release them at a later time. Apparently, the film may come from the manufacturer contaminated with fluorocarbons as reported by Lonnenman et al. (15). Thus, our results concerning hydrocarbon contamination must be generalized with caution since different rolls of film may have different histories and thus different types and rates of contaminant release.

The second series of experiments tested for the presence of contaminants in the bags under actual field conditions, i.e., storage outdoors. Gas chromatographic measurements using a Perkin-Elmer 900 GC on a new bag filled with zero air that initially contained  $\sim 0.03$  ppmC NMHC showed an increase to 0.08 ppmC overnight. The increase appeared as a number of small peaks with retention times  $>C_5$  hydrocarbons. Also, several new bags filled in the morning with zero air and irradiated showed increases in NMHC of  $<0.05$  ppmC (below the detection limit of the analyzer) by evening. For the latter measurements a Byron Model 401 analyzer was used that measures total non-methane organic compounds including oxygenated and halogenated organics. Thus, we did not observe that large amounts of hydrocarbons were released by new bags when they were stored outdoors for a day under either dark or sunlight conditions. Similar tests for hydrocarbon release by used bags also showed increases  $<0.05$  ppmC. This is consistent with the observation that used bags did not produce substantial ozone when small amounts of NO<sub>x</sub> are added, i.e., they were shown to be relatively hydrocarbon-free by using the simple photochemical tests described earlier (Table I, series 3).

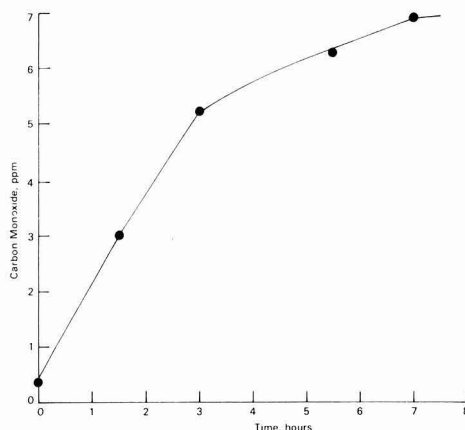


**Figure 2.** [CO] vs. time for bag 5 (Table II).

On the other hand, tests for CO release in new bags showed that large amounts of CO are somehow released when the bags are irradiated. As shown in Table II, new bags exposed to sunlight released 4.1–8.7 ppm CO in 5–7 h. Although CO for all the tests in Table II was measured chromatographically, simultaneous measurements using a nondispersive infrared analyzer in one experiment confirmed that the contaminant was indeed CO. A new bag held in the dark released a negligible amount of CO (near our detection limit of 0.2 ppm). Furthermore, used bags (defined for Table II as bags that have been exposed to sunlight for at least 5 h) produced a factor of 20–40 less CO than new bags. Results are shown in Figure 2 for bag 5, in which several measurements of CO were made (rather than just initial and final measurements). The rate of CO increase diminished after  $\sim 4$  h; this is consistent with our observation that after a 1-day exposure ( $\sim 10$  h) further CO release is minimal. Incidentally, hydrocarbon and NO<sub>x</sub> increases for the bags in Table II were  $<0.1$  ppmC and  $<2$  ppb, respectively. Therefore, the CO cannot come from gas-phase hydrocarbon oxidation. Two pieces of evidence also rule out permeation into the bags as the source of the CO. First, storage of 3.7 ppm CO in a bag for 16 h resulted in minimal losses ( $<5\%$ ). Second, the CO concentration outside the bags was  $<0.2$  ppm at the remote site where bags 1–5 were tested.

To further investigate potential sources of CO, we obtained attenuated total reflectance spectra of new Teflon film samples using a Fourier transform infrared spectrometer to detect possible CO precursors in or on the film. The spectra did not exhibit any strongly absorbing bands that could be attributed to either adsorbed CO ( $2000\text{--}2300\text{ cm}^{-1}$ ) or carbonyl compounds ( $1700\text{--}1800\text{ cm}^{-1}$ ). Difference spectra of irradiated vs. unirradiated film were also run and exhibited no measurable differences. For a gas-phase CO concentration of 5 ppm, we calculate that  $10^2\text{--}10^3$  molecules of carbonyl precursor in the film per molecule of CO produced are required for detection of the precursor by this infrared technique (assuming an average extinction coefficient for carbonyl of  $10^2\text{ L mole}^{-1}\text{ cm}^{-1}$ ). Therefore, this technique would only reveal gross contamination in the film.

Since carbonyl compounds are potential photochemical precursors of CO, a final series of experiments was conducted to test for their presence. Two bags (bags 6 and 7 in Table II) were filled with zero air and irradiated for a day using sunlight. Hydrocarbon and CO measurements

were made in the bags several times during the day, and after a 5-h period ~100 L of air from each bag was bubbled through a midjet impinger containing an acetonitrile solution of 2,4-dinitrophenylhydrazine (DNPH) acidified with perchloric acid. The products of the DNPH-carbonyl reaction were analyzed by high-performance liquid chromatography as described elsewhere (25). Total hydrocarbon concentrations increased by less than 0.1 ppmC, and only three carbonyl compounds were observed, formaldehyde, acetaldehyde and acetone, at concentrations of 2, 11–12, 5–6 ppb, respectively. Meanwhile, the CO increased by 4.0 ppm in 2.5 h and 8.7 ppm in 5.0 h (see Table II, bags 6 and 7). Although the blank corrections and sensitivity limits of the DNPH technique reduced the accuracy of the results by about a factor of 2 at such low levels, clearly the carbonyl concentrations were insufficient to account for the observed CO levels. Thus, although the mechanism for CO production by Teflon bags remains unidentified, the probable source is photodecomposition of substances in the film, rather than those in the gas-phase.

Using the photochemical model developed by Graedel (26), we can account for nearly all of the ozone production at low NO<sub>x</sub> as being due to the ppm quantities of CO entering the gas phase. The model predicts ~8 ppb ozone will be produced for each ppb NO<sub>x</sub> at NO<sub>x</sub> levels <0.01 ppm and CO levels of 1–3 ppm, while we observe ~8–10 ppb ozone/ppb NO<sub>x</sub> in Table I. The model also predicts that ozone production will decrease with increasing NO<sub>x</sub> for NO<sub>x</sub> > 0.02 ppm and a CO concentration of 1–3 ppm, which is the general trend in Table I, series 3. Later we will show that at urban levels of pollutants, CO release by new bags does not cause a large effect on ozone production in bags, and new and used (clean) bags give similar and reproducible results.

One way to reduce the effects of contaminant release is by reducing the surface-to-volume ratio by increasing the chamber size. However, this is a relatively inefficient way to do this, compared to just cleaning up the small bags. For example, the 13 × 10<sup>4</sup> L chamber of Jeffries and co-workers (4) has a surface-to-volume ratio ~6 times less than our bags, so equivalent rates of offgassing from the walls of both chambers will result in 6 times lower contamination in the larger chamber. However, the cost of such a large chamber is easily 100 times that of a bag, and it is not feasible to run several at one time. Also, while such size is necessary in chambers used for aerosol formation studies, such is not the case for photochemical ozone formation. This will be discussed further later.

**Ozone Half-Life in Bags.** In order for smog chambers to simulate the ambient atmosphere, ozone removal by the bag walls should be small. Therefore, several tests of ozone half-life were made in the dark at two different temperatures. The results shown in Table III indicate that the dark half-life under ambient summertime conditions ranged from 18–34 h, with an average of 27 h. This is only slightly lower than the half-lives in very large chambers with volumes of 3–13 × 10<sup>4</sup> L, which vary from 28–38 h (3, 4) and is larger than those of most indoor chambers, which vary from 8–25 h (10). There was no significant difference between new and used bags. Under lower temperature conditions in the wintertime, the half-life increased to 73–83 h for two tests. The results indicate that the wall loss rate is low and temperature dependent.

Although the wall loss rate is low, the discovery by Daubendiek and Calvert (27) that ozone and Teflon react with each other introduces the possibility that reactive gas-phase products are formed that may further participate

Table III. Ozone Half-Life in the Dark at Two Different Temperatures<sup>a</sup>

temp, °C	bag condition	no. of tests	half-life, h	
			range	av ± 1σ
18 ± 4	new	5	19.0–34.1	25.2 ± 5.7
	used	13	17.4–47.5	27.5 ± 8.6
-8 ± 4	new	2	73.7–83.5	78.6 ± 6.9

<sup>a</sup> Initial ozone levels were 100–200 ppb. Half-lives were obtained by plotting ln [O<sub>3</sub>] vs. time to determine the removal rate coefficients *k<sub>r</sub>*, with O<sub>3</sub> half-life = 0.693/*k<sub>r</sub>*. The plots were linear with correlation coefficients of 0.99–1.00.

in ozone-forming reactions. By use of kinetic theory (28) along with the surface-to-volume ratio of the bags to obtain the collision frequency between ozone and the bag walls, the effective collision yield for ozone removal can be calculated. For summertime conditions, where the half-life is ~27 h, the collision yield is 9 × 10<sup>-9</sup>, i.e., 9 collisions per billion between ozone and Teflon remove an ozone molecule. From the data of Daubendiek and Calvert (27), the rate coefficient for chemical reaction between ozone and olefinic sites on Teflon film was *k* = 5 × 10<sup>-2</sup> cm<sup>3</sup> s<sup>-1</sup> site<sup>-1</sup>. Their estimate of the number of olefinic sites on a 0.18-m<sup>2</sup> piece of 0.13-mm thick film was 9 × 10<sup>20</sup> active sites. If we assume our bags have a surface structure similar to the film of Daubendiek and Calvert, then each bag has about 1.9 × 10<sup>22</sup> active sites. The first-order rate coefficient for reaction between ozone and Teflon to produce CF<sub>2</sub>O is then 7.6 × 10<sup>-5</sup> h<sup>-1</sup>. Since the first-order rate coefficient corresponding to an ozone half-life of 27 h is 2.5 × 10<sup>-2</sup> h<sup>-1</sup>, the ratio of the rate coefficient for CF<sub>2</sub>O formation to the total O<sub>3</sub> removal rate coefficient is 3 × 10<sup>-3</sup>. Thus, if the initial ozone concentration is 100 ppb, wall removal will reduce this to 97 ppb in 1 h and will produce about 9 × 10<sup>-3</sup> ppb CF<sub>2</sub>O. Even if CF<sub>2</sub>O is as photochemically reactive as formaldehyde (CH<sub>2</sub>O), such levels would have an insignificant effect on either urban or rural captive-air irradiation experiments.

Finally, if OH reacts with olefinic Teflon sites ~3 × 10<sup>6</sup> times faster than O<sub>3</sub>, which is the average reactivity ratio for OH and O<sub>3</sub> reactions with ethylene or propylene (23), then ~3% of the OH radicals that reach the walls will be removed to form chemical products as an upper limit. As discussed later, however, a very small percentage of the OH radicals will reach the walls at NO<sub>x</sub> levels >0.04 ppm.

**Reproducibility and Validity of Bag Irradiation Experiments.** It is apparent from the zero-air/NO<sub>x</sub> experiments shown in Table I that at low levels of NO<sub>x</sub> the experiments were not meaningful. New unconditioned bags are clearly unsuitable for studying the photochemistry at low NO<sub>x</sub>, i.e., typical rural mixtures, due to the release of CO. Even for used bags, with their vastly reduced CO release, the technique remains in doubt at low NO<sub>x</sub> since there is still residual ozone production by the cleanest air available. Ozone production from these chamber effects is comparable in magnitude to the amounts expected from local photochemistry in rural areas (21).

The question we wish to answer, then, is are bag irradiations a valid way to estimate the ozone production of ambient urban air, which is more reactive than rural air, or will chamber effects still be apparent? Will differently conditioned and sized bags give similar results when run side-by-side with the same ambient urban-level mixture? To address these questions, we performed replicate experiments using ambient Houston, Denver, or Detroit air. The results for O<sub>3</sub>(max) are shown in Table IV with several

Table IV. Replicate Captive-Air Experiments

day	bag	condition <sup>a</sup>	[NMHC], <sup>b</sup> ppm C	[NO <sub>x</sub> ], <sup>b</sup> ppm	O <sub>3</sub> (max), ppb
Houston, Summer of 1977					
229	1	used	0.2	0.015	133
	2	used			128
230	3	used	0.5	0.045	95
	4	new			90
250	5	new	2.7	0.234	415
	6	new			410
251	7	new	0.7	0.065	145
	8	new			145
254	9	new			145
	10	new <sup>c</sup>	1.4	0.041	173
	11	new			156
Denver, Winter of 1978					
348	1	used	2.2	0.40	105
	2	used			94
	3	new			94
	4 <sup>d</sup>	used	0.5	0.19	133
	5 <sup>d</sup>	new			127
Detroit, Summer of 1981					
211	1	new	0.3	0.059	242
	2	new			241
225	3	new	0.6	0.088	206
	4	used			219

<sup>a</sup> New indicates the bag had never been used for HC-NO<sub>x</sub> irradiations; used indicates it had been used for such an experiment. <sup>b</sup> These are initial values, estimated from continuous measurements made on ambient air while the bags were filling. <sup>c</sup> This bag was conditioned for 1 day with 1000 ppb ozone prior to use. <sup>d</sup> These bags were filled with ambient air plus 0.11 ppm C<sub>3</sub>H<sub>8</sub> and 0.11 ppm SO<sub>2</sub>.

ozone profiles shown in Figure 3 (for a complete discussion of our captive-air experiments at the Houston and Denver sites, see ref 5, 6, 8, and 9). With ambient Houston air, the differences in maximum ozone between replicates were less than 6%. The ozone profiles were also very similar. Furthermore, new and used bags, which should have drastically different CO release rates, compared favorably. Also, the effect of conditioning a bag with 1000 ppb ozone prior to use can be seen by comparing bags 10 and 11 on day 254 (Table IV). There was a 10% increase in maximum ozone in the ozone-treated bag. This was probably the result of an increased half-life due to lower wall losses of ozone in this bag, rather than an increase in the ozone production rate. Regardless of the reason, the effect was small.

Similarly, for the wintertime Denver irradiations conducted at lower temperatures, the agreement in maximum ozone and the ozone profiles in new and used bags was good with differences of only 4-10%. Incidentally, the NO<sub>x</sub> loss rate was measured in all five bags on day 348, and it, too, was reproducible (8). For the three replicate bags 1-3, the NO<sub>x</sub> loss rate was  $4.1 \pm 0.2\% \text{ h}^{-1}$ , while for the two replicate bags 4 and 5 it was  $6.0 \pm 0.3\% \text{ h}^{-1}$ .

Repeatability was equally as good for experiments conducted in Detroit with another set of bags. In addition to the replicates using ambient air, two sets of experiments were conducted by using synthetic mixtures, one to evaluate the reproducibility of NO<sub>x</sub> or hydrocarbon loss as well as ozone production and another to compare the ozone formation in our standard bags to a larger chamber. First, two new bags were filled with zero air spiked with 0.025 ppm NO<sub>x</sub> and 0.22 ppm ethylene. Irradiation produced 180-190 ppb O<sub>3</sub> in 4 h (from 1300 to 1700) in both bags with nearly identical profiles. Meanwhile, both the

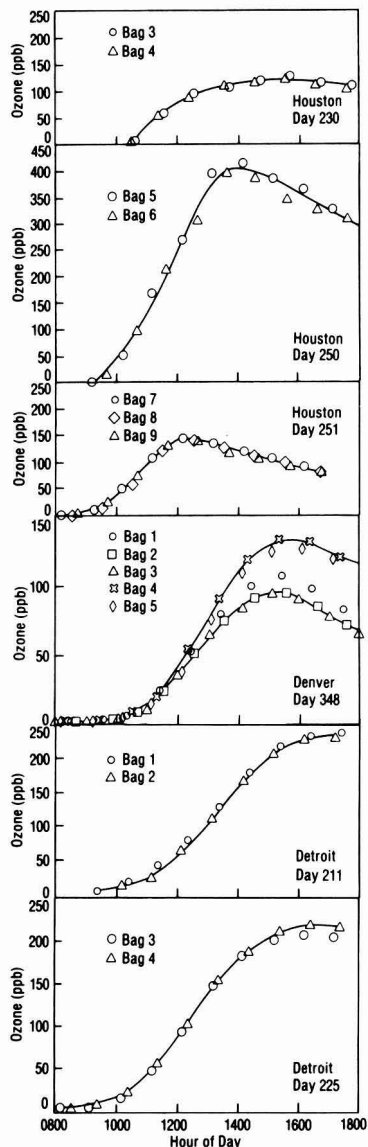


Figure 3. Ozone profiles for replicate captive-air irradiations.

NO<sub>x</sub> and ethylene losses over the 4-h period from 1300 to 1700 were used to estimate the average OH during that period, by using previously described methods (5, 8), yielding  $1.6 \times 10^{-7}$  and  $1.1 \times 10^{-7}$  ppm, respectively, with exact agreement in the two bags for the estimated OH based on the loss of each species. The higher average OH concentration estimated by NO<sub>x</sub> loss is somewhat puzzling and may indicate some heterogeneous loss of NO<sub>x</sub> which was unexpected under dry conditions. Further work on the NO<sub>x</sub> loss in smog chambers is needed. Finally, O<sub>3</sub> formation in a bag was compared to a larger Teflon chamber with a volume of ~2000 L. The large chamber was cylindrical with both a height and diameter of 137 cm, yielding a surface-to-volume ratio of 0.044 or about half that of the smaller bag. After conditioning the bag and large chamber by irradiating zero air for a day, we irra-

diated a mixture of 0.9 ppm propylene and 0.1 ppm NO<sub>x</sub> in zero air for a day. The ozone production was virtually identical in the two reactors, resulting in a maximum ozone of 232 ppb in the chamber and 237 ppb in the bag. Further tests were planned, but leaks in the large chamber developed and it was not possible to keep it inflated to a volume larger than the small chamber for more than 2–3 h. Under these conditions, i.e., comparing a leaky large chamber to a leak-free bag, the ozone profiles were initially identical until the large chamber leaked down, and then the ozone production rate was vastly reduced in the “large” chamber, presumably due to the reduced sunlight and increased surface-to-volume ratio in the crumpled chamber.

Others have also observed little effect from different chamber sizes and surface-to-volume ratios on the resulting smog chemistry. Jaffe et al. (12) tested several wall materials, including Teflon, at two surface-to-volume ratios that were similar to those of our 450-L bag and 2000-L chamber. For the reactive propylene/NO<sub>x</sub> system, with an O<sub>3</sub>(max) ~1000 ppb, no significant differences in any of the reaction variables were noted for a Teflon chamber. In fact, the major effect on the photochemistry was observed for different irradiation spectra which will not be a problem for outdoor Teflon chambers as discussed earlier. Sickles et al. (29) obtained high correlation between O<sub>3</sub>(max) in 250-L bags and 27 000-L chambers for relatively unreactive hydrocarbons and concluded that the bags are suitable for studying smog photochemistry.

Chamber size probably has little effect on ozone production for reactive systems since ozone is produced by a free-radical chain reaction, with short lifetimes for the major radicals. For example, the OH radical, which is the chain carrier in photochemical smog production, has a diffusion lifetime in our bags, estimated by using the method of Hecklen (30), of ~60 s. On the other hand, the gas-phase chemical lifetime will be ~0.1 s for an NO<sub>2</sub> concentration of 0.04 ppm. (Actually, it will be even shorter since OH reacts with other species besides NO<sub>2</sub>.) The chemical lifetime of HO<sub>2</sub> is equally small since its rate coefficient for reaction with either NO or NO<sub>2</sub> is similar to that for OH + NO<sub>2</sub> (31). Thus, loss of either OH or HO<sub>2</sub> to the chamber walls is insignificant for urban-level NO<sub>2</sub> concentrations. However, at low NO<sub>x</sub>, a significant fraction of the OH radicals can reach the walls where they may form chemical products ~3% of the time as estimated earlier. This may account for the excess reactivity even in conditioned bags at low NO<sub>x</sub> in Table I, series 3.

There is other evidence that captive-air experiments in Teflon bags provide a good simulation of ambient urban-air photochemistry. For example, by measuring the ethylene loss during one experiment in Houston, the average OH level was estimated to be  $1.3 \times 10^{-7}$  ppm (5). In Denver, by measuring NO<sub>x</sub> loss, the average OH was estimated to be  $4.3 \times 10^{-8}$  ppm (8). These levels are comparable to estimated ambient levels under summer (32) and winter (33) conditions. Also, comparisons have been made between the maximum ozone produced in the Houston captive-air irradiations (including the experiments in Table IV) and that predicted by EPA's Empirical Kinetics Modeling Approach (9). The correlation between the observed and predicted ozone was high ( $r^2 = 0.82$ ). These results suggest that contamination and wall effects do not materially affect the trends in ozone production in the bags containing urban air.

#### Conclusions and Recommendations

Although we observed that substantial amounts of CO were released when new bags were first irradiated, this

artifact did not affect the ozone production or NO<sub>x</sub> loss when captured urban air was photolyzed, as shown by the reproducibility of such experiments in new vs. used bags (that did not release CO). Also, both new and used bags released negligible amounts of HC and NO<sub>x</sub> into the gas phase in comparison to the initial levels of these substances in urban air. Finally, the small bags gave ozone profiles identical with larger chambers and were far cheaper and less prone to leaks. All of the results suggest that bag irradiations are a valid way to assess the potential of ambient urban air to produce ozone.

In marked contrast, when the NO<sub>x</sub> concentrations approach those in rural areas, ozone production depended strongly on bag condition, i.e., whether the bags were new or used. The CO release by new bags overwhelmed the effects of hydrocarbons. Even when the bags were used, and thus conditioned, excess ozone production was observed. We suggest that at low NO<sub>x</sub>, the longer lifetimes of the reactive free radicals, especially OH, allow them to react with olefinic sites on the Teflon walls to produce products that stimulate ozone formation.

Although we did not observe significant effects by contamination in our urban air photolyses, different batches of Teflon film may have greater amounts of initial contaminants than we observed. Therefore, we recommend that new bags be conditioned for photolysis experiments by filling with zero air or zero air plus ozone and irradiating for 1 day. The sunlight and mild heating will remove any HC, NO<sub>x</sub>, and CO from the Teflon film. Bags used for hydrocarbon/NO<sub>x</sub> irradiations should also be conditioned overnight by filling them with zero air. The bags can then be pumped out and reused the following morning for further urban irradiations. Finally, in order to assure the quality of the data, many of the standard smog chamber reactivity tests recommended by Dimitrades at a conference on smog chambers (11) should be part of any captive-air irradiation program. For ozone formation, these tests include (1) the formation of ozone from clean air, (2) the formation of ozone and oxidation of NO in hydrocarbon-free air, (3) the formation of ozone and loss of HC in NO<sub>x</sub>-free air, (4) the loss of HC, NO<sub>x</sub>, and O<sub>3</sub> in the dark, and (5) replicate experiments. For test 2 we recommend NO<sub>2</sub> levels <0.05 ppm to measure ozone production and NO levels <0.05 ppm to measure NO oxidation.

#### Acknowledgments

Help in performing the irradiation and storage tests was provided by William Scruggs and Jerome Zemla. David McEwen and Robert Kohn of the Analytical Chemistry Department ran FTIR and ultraviolet/visible spectra, respectively, of the Teflon film. Helpful discussions were provided by Michael Whitebeck, Martin Ferman, and George Wolff of General Motors Research, William Lonneman and Joseph Bufalini of EPA, Alan Knight of Dupont, and Joseph Sickles of Research Triangle Institute. I gratefully acknowledge the assistance of these people.

#### Literature Cited

- (1) Altshuler, A. P.; Kocczynski, S. L.; Lonneman W. A.; Sutterfield, F. D. *Environ. Sci. Technol.* 1970, 4, 503–506.
- (2) Sickles, J. E. Ph.D. Thesis, University of North Carolina, Chapel Hill, NC, 1976.
- (3) Ripperton, L. A.; Sickles, J. E.; Eaton, W. C. “Oxidant-Precursor Relationships During Pollutant Transport Conditions: An Outdoor Smog Chamber Study”; U.S. Environmental Protection Agency, Research Triangle Park, NC, EPA-600/3-76-107, 1976.
- (4) Jeffries, H.; Fox, D.; Kamens, R. “Outdoor Smog Chamber Studies: Effect of Hydrocarbon Reduction on Nitrogen

- Dioxide"; U.S. Environmental Protection Agency, Research Triangle Park, NC, EPA-650/3-75-001, 1975.
- (5) Kelly, N. A., preprints of the 1980 Annual Meeting of the Air Pollution Control Association, Montreal, Quebec, June 1980, paper no. 50.6; also available as Publication GMR-3300, General Motors Research Laboratories, Warren, MI.
  - (6) Ferman, M. A.; Wolff, G. T.; Kelly, N. A. *J. Environ. Sci. Health, Part A* 1981, *A16*, 315-339.
  - (7) Monson, P. R.; Ferman, M. A.; Kelly, N. A., preprints of the 1978 Annual Meeting of the Air Pollution Control Association, Houston, TX, June 1978, paper no. 50.4; also available as Publication GMR-2736, General Motors Research Laboratories, Warren, MI.
  - (8) Kelly, N. A., preprints of the 1981 Annual Meeting of the Air Pollution Control Association, Philadelphia, PA, June 1981, paper no. 21.4; also available as Publication GMR-3605, General Motors Research Laboratories, Warren, MI.
  - (9) Kelly, N. A. *J. Air Pollut. Control Assoc.* 1981, *31*, 565-567.
  - (10) Calvert, J. G.; Jeffries, H. E. (independent authors) "International Conference on Oxidants, 1976—Analysis of Evidence and Viewpoints, Part II. The Issue of Reactivity"; U.S. Environmental Protection Agency, Research Triangle Park, NC, EPA-600/3-77-114, 1977.
  - (11) "Smog Chamber Conference Proceedings"; U.S. Environmental Protection Agency, Research Triangle Park, NC, EPA-600/3-76-029, 1976.
  - (12) Jaffe, R. J.; Smith, F. C.; Last, K. W. "Study of the Factors Affecting Reactions in Environmental Chambers, Phase III"; U.S. Environmental Protection Agency, Research Triangle Park, NC, EPA-650/3-74-004b, 1974.
  - (13) Bufalini, J. J.; Koczcynski, S. L.; Dodge, M. C. *Environ. Lett.* 1972, *3*, 101-109.
  - (14) Bufalini, J. J.; Walter, T. A.; Bufalini, M. M. *Environ. Sci. Technol.* 1977, *11*, 1181-1185.
  - (15) Lonneman, W. A.; Bufalini, J. J.; Kuntz, R. L.; Meeks, S. A. *Environ. Sci. Technol.* 1981, *15*, 99-103.
  - (16) Carter, W. P. L. "Proceedings of a Workshop on Chemical Kinetic Data Needs for Modeling the Lower Troposphere"; NBS Special Publication 557: Washington, D.C., 1979; p 78.
  - (17) Carter, W. P. L.; Lloyd, A. C.; Spring, J. L.; Pitts, J. N., Jr. *Int. J. Chem. Kinet.* 1979, *11*, 45-101.
  - (18) Seeger, G. W.; Hern, D. Rockwell International, Creve Coeur, MO, Report AMC0710.T0103FR, 1976.
  - (19) Polasek, J. C.; Bullin, J. A. *Environ. Sci. Technol.* 1978, *12*, 708-712.
  - (20) Thrum, K. E.; Harris, J. C.; Beltis, K. "Gas Sample Storage"; U.S. Environmental Protection Agency, Research Triangle Park, NC, EPA-600/7-79-095, 1979.
  - (21) Kelly, N. A.; Wolff, G. T.; Ferman, M. A. *Atmos. Environ.* 1982, *16*, 1077-1088.
  - (22) Leighton, P. A. "Photochemistry of Air Pollution"; Academic Press: New York, 1961; p 155.
  - (23) Atkinson, R.; Darnall, K. R.; Lloyd, A. C.; Winer, A. M.; Pitts, J. N., Jr. *Adv. Photochem.* 1979, *11*, 375-488.
  - (24) Kelly, N. A., preprints of the 1982 Annual Meeting of the Air Pollution Control Association, New Orleans, LA, June 1982, paper no. 33.4; also available as Publication GMR-3989, General Motors Research Laboratories, Warren, MI.
  - (25) Lipari, F. L.; Swarin, S. J. publication GMR-3617, General Motors Research Laboratories, Warren, MI, April 16, 1981.
  - (26) Graedel, T. E. *J. Geophys. Res.* 1979, *84*, 273-286.
  - (27) Daubendick, R. L.; Calvert, J. G. *Environ. Lett.* 1974, *6*, 253-272.
  - (28) Daniels, F.; Alberty, R. A. "Physical Chemistry", 3rd ed.; Wiley: New York, 1961; p 310.
  - (29) Sickles, J. E. Wright, R. S.; Sutcliffe, C. R.; Blackard, A. L.; Dayton, D. D., preprints of the 1980 Annual Meeting of the Air Pollution Control Association, Montreal, Quebec, June 1980, Paper 50.1.
  - (30) Heicklen, J. "Colloid Formation and Growth: A Chemical Kinetics Approach"; Academic Press: New York, 1976; p 8.
  - (31) Hampson, R. F. "Chemical Kinetic and Photochemical Data Sheets for Atmospheric Reactions"; Federal Aviation Administration, Report No. FAA-EE-80-17, U.S. Department of Transportation, Washington, D.C., April 1980.
  - (32) Calvert, J. G. *Environ. Sci. Technol.* 1976, *10*, 256-262.
  - (33) Perner, D.; Ehhalt, D. H.; Patz, H. W.; Plotts, V.; Roth, E. P.; Volz, A. *Geophys. Res. Lett.* 1976, *3*, 466-468.

Received for review July 22, 1981. Revised manuscript received April 26, 1982. Accepted July 15, 1982.

## Acid Precipitation and Lake Susceptibility in the Central Washington Cascades

Richard M. Logan, John C. Derby, and L. Clint Duncan\*

Chemistry Department, Central Washington University, Ellensburg, Washington 98926

■ Bulk precipitation was monitored at five sampling sites across the Cascade mountains east and windward of the urban Puget Sound area January 1981 through July 1981. The volume weighted average pH over the collection period at the Cascade Crest (Snoqualmie Pass) was 4.71. Sulfate was the dominant anion. The average strong acid composition in terms of sulfate and nitrate over the five collector sites ranged from 57 to 62 equiv % sulfuric acid. The sulfate deposition for 1981 at the Cascade Crest is estimated to be 16.0 kg ha<sup>-1</sup> year<sup>-1</sup> of SO<sub>4</sub> (sea salt corrected). The strong acid content of the samples was observed to increase in the summer months. Twenty-nine watershed source lakes lying along the Cascade Crest 3-20 miles north of the precipitation collectors were sampled during the summer of 1981. All of the source lakes were found to be susceptible but not acid, with alkalinities ranging from 4 to 190  $\mu$ equiv/L. (Median alkalinity was 57  $\mu$ equiv/L.) The composition of the waters in terms of alkalinity and calcium concentration was similar to that of nonacidified waters of northwestern Norway and northwestern Ontario.

### Introduction

The occurrence of acid precipitation in Europe, Canada, and the United States has been extensively documented in recent years (1-3). Most reports concerning the United States have described observations in the eastern portion of the country. There are now an increasing number of observations of the phenomenon along the west coast (4). Lake acidification has been reported in regions where the precipitation is acidic and the strata consists of thin topsoil and resistant rock (5, 6).

The composition of bulk deposition falling at sites across the central Cascade mountains in Washington was studied from January 1981 through July 1981 to learn of the magnitude and nature of acid deposition in the Cascades.

Bulk collectors (for rain, snow, dry fallout, etc.) were established at five sites lying in an appropriate SE line across the Cascade mountain range from midwinter 1981 through late summer 1981 (see Figure 1). The precipitation collection sites lie at locations along the Interstate-90 route across Snoqualmie Pass. The locations are ESE of the urban Seattle-Tacoma area and NW of Mt. St. Helens. The country between North Bend and Cle Elum is sparsely populated and is characterized by rugged mountains with timbered rocky slopes.

The Cascade range in Washington State runs north-south, roughly paralleling the Pacific coastline. The Crest line is approximately 150 miles east of the ocean. The population density from the ocean east to the Cascade crest varies with (i) a low density along the coast (19.5 people/mile<sup>2</sup> in Gray's Harbor and Jefferson counties), (ii) a relatively higher density in the urban Puget Sound area (354 people/mile<sup>2</sup> in Pierce, King, and Snohomish counties), and (iii) a very low density within a 10-mile wide path on either side of the crest. Counties to the east of the crest again have a relatively low population density (25.5 people/mile<sup>2</sup> in Yakima, Kittitas, and Chelan counties).

Moist Pacific marine air sweeps generally westerly over the coastal and urban Puget Sound area, then over the

Cascades. There is heavy precipitation in the mountains between fall and spring and usually a substantial snowpack (as much as 400 in.) in the winter (4000-ft level). Normally, more than  $\approx 65\%$  of the precipitation will accumulate as snowpack at elevations higher than 4000 ft. Precipitation quantities generally increase with elevation up to the Cascade crest from the west side and then decrease proportionately with elevation on the east side. For example, average yearly precipitation quantities are as follows: Seattle = 36 in.; North Bend = 61 in.; Cascade Crest (Stampede Pass) = 91 in.; Cle Elum = 22 in.; and Ellensburg = 7 in.

There are two major anthropogenic sulfur and nitrogen oxide point sources to the WSW of the 1981 collector sites. They are the Centralia Power Plant in Centralia, WA ( $\approx$  average 59 000 tons of SO<sub>2</sub>/year,  $\approx$  average 37 000 tons of NO<sub>x</sub>/year) and the ASARCO Smelter in Tacoma, WA ( $\approx$  average 80 000 tons of SO<sub>2</sub>/year). There is one natural point source, which is Mt. St. Helens. The volcano's SO<sub>2</sub> emissions from January 1981 to August 1981 were approximately steady with a rate comparable to 111 918  $\pm$  80 tons of SO<sub>2</sub>/year (7). The total anthropogenic SO<sub>2</sub>/NO<sub>x</sub> emissions for the urban areas WSW of the collectors in 1979 were estimated by the Southwest and Puget Sound air pollution control authorities (8) to be 196 145 tons of SO<sub>2</sub>/year and 129 913 tons of NO<sub>x</sub>/year.

There have been some reports of acid deposition in the Northwest. Larson et al. (9) sampled precipitation during a single event in the fall of 1973 at 40 locations in the Seattle-Tacoma area and found pHs in the range 3.6-4.5. Deither (10) collected and analyzed precipitation in the north-central Cascades during 1974 and 1975, and reported a mean pH of 4.85 over that study period. Logan (11) sampled precipitation from May through October 1978 at Stampede Pass on the Cascade crest and found the precipitation to be acidic with a volume weighted average pH of 4.66.

Much of the region north of Snoqualmie Pass and south of Stevens Pass (Figure 2) lies in the Alpine Lakes Wilderness Area and is administered by the Snoqualmie and Wenatchee National Forests. That area is dotted with over 700 lakes. The geology of the Cascades varies with different reactivities of bedrock exposed at different locations (12). The area studied shows examples of granodiorite, andesite, and basalt.

There are little quantitative data (13) concerning the quality of the Cascade high mountain lakes with respect to acidification. Twenty-nine watershed source lakes and two reservoirs were sampled during the summer of 1981 to learn of their status. The remote lakes lie within a corridor approximately 10 miles wide and 20 miles long along the Cascade crest, between Snoqualmie Pass to the south and Stevens Pass to the north.

### Experimental Section

**Deposition Sampling.** Study sites were established at the locations indicated in Figure 1 by early January, 1981. The sites were at least 300 ft from highways and/or apparent point sources. Bulk collectors of two designs were used. Winter samples were obtained in open 640 cm<sup>2</sup>

Table I. Summary of Precipitation Data at Five Sites across the Cascades January 18, 1981, to July 30, 1981

collector location	ppt collected, cm	est annu ppt, cm	pH <sup>b</sup>	vol av concn, $\mu\text{equiv/L}$							
				NH <sub>4</sub> <sup>+</sup>	Na <sup>+</sup>	Ca <sup>2+</sup>	Mg <sup>2+</sup>	K <sup>+</sup>	SO <sub>4</sub> <sup>2-</sup>	NO <sub>3</sub> <sup>-</sup>	Cl <sup>-</sup>
North Bend	79.4	155	4.68	17.04	15.11	5.56	5.06	3.45	25.08	19.7	16.6
Bandara Airfield <sup>a</sup>	92.6		4.67	4.65	15.96	4.39	1.32	1.91	15.2	10.87	18.27
Snoqualmie Summit	95.9	231	4.71	3.25	5.02	3.04	0.61	1.59	14.8	8.55	4.80
Lake Kachess <sup>a</sup>	57.8		4.72	3.15	8.96	4.82	1.87	2.27	18.04	10.78	9.81
Cle Elum	20.5	56	4.84	6.67	12.62	9.02	1.69	2.35	20.00	12.53	15.70

<sup>a</sup> Missed two sampling periods. <sup>b</sup> pH =  $-\log(\sum_i V_i 10^{-\text{pH}_i} / \sum_i V_i)$ ; average concentration =  $\sum_i V_i C_i / \sum_i V_i$ .

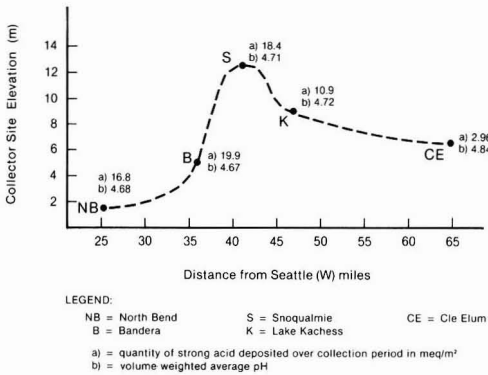


Figure 1. Location of collector sites in Washington Cascades.

collector area polyethylene buckets supported at least 2 m above the snow or ground. Spring and summer samples were obtained by using a 730 cm<sup>2</sup> collector area funnel which drained to storage containers through a looped Tygon tube.

**Lake Sampling.** Lake samples were collected at lake outlets in 0.5-L polyethylene bottles held approximately 50 cm below the surface on filling.

**Collection.** On collection, sample containers were capped, transported to the laboratory as soon as possible, and thawed if necessary. The precipitation samples were weighed. All samples were held at approximately 4 °C until analysis.

**Analytical.** A tabulation showing quality control data (precision and recovery) on the methods used is included in the supplementary material.

**pH.** An Orion Model 801 pH meter equipped with a Beckman Futura electrode or an Orion Model 221 pH meter equipped with an Orion 91-06 combination electrode was used for all pH measurements. The pH system was calibrated at pH 7.00 and slope calibrated at pH 4.00 before use. Sample readings were taken until the observed value was constant for 2–3 min.

**Acidity.** Acidity was determined by potentiometric titration of 100.0-mL sample aliquots with 0.01000 N NaOH using a microburet. Samples were swept with prepurified nitrogen prior to and during titration. Strong and total acid end points were obtained by using the Gran method (14).

**Alkalinity.** Samples (100.0 mL) were titrated with 0.02000 N HCl with use of a microburet. End points were detected by using the Gran method (14).

**Conductivity.** A YSI Model 31 conductivity bridge was used to obtain specific conductance values at 25 °C. Cell constants were determined with 1.000 × 10<sup>-4</sup> M KCl.

**Ammonium Ion.** Ammonium ion concentrations were obtained by using the Phenate method (15). All sample

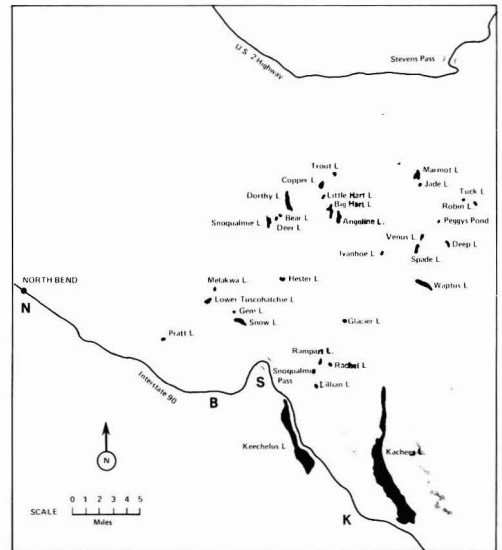


Figure 2. Lakes surveyed in the summer of 1981.

absorbances were determined with a Bausch & Lomb Spectronic 20.

**Metals.** Calcium, magnesium, sodium, and potassium ion concentrations were determined by using flame atomic absorption techniques (16). An Instrumentation Laboratory Model 251 spectrophotometer with a single slot burner was used.

**Sulfate.** Sulfate ion concentrations were determined turbidimetrically (17) by using a HACH-2100A turbidometer.

**Nitrate.** Nitrate ion concentrations were determined by using the Brucine method (15).

**Chloride.** Chloride ion concentrations were obtained by using a modification of the automated colorimetric thiocyanate procedure (16) adapted for manual operation.

The average charge balance, anion:cation concentration ratio for 74 precipitation samples was  $-/+ = 0.94$  with  $s = 0.14$ , while that for 31 lake samples was  $-/+ = 0.94$  with  $s = 0.18$ . The measured sample conductivities were compared with those calculated by using the analytical ion concentrations and limiting equivalent ionic conductances. The results expressed as measured conductance:calculated conductance were 0.87 with  $s = 0.18$  for 70 precipitation samples and 0.90 with  $s = 0.18$  for 31 lake samples.

**Results and Discussion**

**Precipitation Studies.** The information shown in Table I serves as a summary of the data obtained from January 18, 1981, to July 30, 1981, at the five sites across



the Cascades. Winter 1981 was an unusual year in that a majority of the precipitation that fell was wet.

The volume weighted (see Table I for algorithm) average pHs for the total collection period ranged from 4.68 for the most westerly collection sites to 4.84 for the most easterly collection site.

The weighted average pH for all waters collected was 4.70, substantially below the pH 5.6 expected for waters containing only equilibrium concentrations of dissolved carbon dioxide (18). pH values calculated (19) by using sample strong acid content as determined by titration correlated well with the measured pH values. The relationship for 71 samples was

$$pH_{\text{calcd}} = 0.86 pH_{\text{measd}} + 0.63 \quad (\text{corr coeff} = 0.93) \quad (1)$$

where

$$pH_{\text{calcd}} = -\log ([\text{HAcY}] + [\text{HCO}_3^-] + 2[\text{CO}_3^{2-}] + [\text{OH}^-] + [\text{NH}_3]) \quad (2)$$

where [HAcY] = titratable strong acid concentration;  $[\text{HCO}_3^-]$ ,  $[\text{CO}_3^{2-}]$  = calculated bicarbonate and carbonate concentrations, respectively, at  $P_{\text{CO}_2} = 330 \text{ ppm}$ ,  $t = 25^\circ \text{C}$ , and the calculated  $[\text{H}^+]$ ;  $[\text{NH}_3]$  = concentration of  $\text{NH}_3$  at the analytical  $[\text{NH}_4^+]$ .

There was no significant difference in the average pH and/or average strong acid content of samples collected at the four westerly sites across the Cascades. The higher pH observed at the more arid easterly site can be rationalized in terms of increased dust neutralization (20) at that location as evidenced by the higher  $\text{Ca}^{2+}$  concentration at that site.

There was a general seasonal winter-to-summer decrease in sample pH at sites other than the most easterly Cle Elum site. For example, the least-squares regression of the observed trends of pH with day ( $d$ ) yielded equations 3-5. The correlation of pH in the day was significant at the 5% level at all sites but Cle Elum.

$$\text{NB (westerly site)} \quad pH = -0.0049(d) + 5.18 \quad (3)$$

$$r = -0.77$$

$$\text{S (summit)} \quad pH = -0.0027(d) + 5.04 \quad (4)$$

$$r = -0.52$$

$$\text{CE (easterly site)} \quad pH = -0.0014(d) + 5.13 \quad (5)$$

$$r = -0.23$$

The deposition of strong acid at the 4000-ft level was estimated by using the weighted average strong acid content ( $20 \mu\text{equiv/L}$ ) observed at the Snoqualmie Summit collector and the average yearly precipitation quantity ( $91 \text{ in/yr}$ ) reported for the 4000-ft level at the Stampede Pass NOAA weather station about 15 miles away. The estimated strong acid deposition quantity of  $46.2 \text{ mequiv of } \text{H}^+ \text{ m}^{-2} \text{ year}^{-1}$  is significant in view of the observation that normally greater than  $\approx 65\%$  of the Cascade precipitation at the 4000-ft level is retained as snow. Snow melt in these areas then will release substantial quantities of acid over a short period of time with resulting shock on aquatic life in receiving waters.

Sulfate was the dominant anion in all precipitation samples even after correction for sea salt input. With the assumption that sulfuric acid, sea salt sulfate, and nitric acid are the only sources of sulfate and nitrate, the proportionate equivalent ratios of the two acids deposited at each site were estimated after correction for sea salt sulfate. The corrected average  $\text{SO}_4^{2-}/\text{NO}_3^-$  equivalent ratio ranged from 1.3-1.4 at the two most westerly collection sites to 1.7-1.6 at the remaining three sites on and east of the Crest.

From the 1979 regional emission totals of  $\text{SO}_x$  (196 145 tons) and  $\text{NO}_x$  (129 913 tons) for five counties in the Puget Sound area and southwestern Washington (8) (Lewis, King, Kitsap, Pierce, and Snohomish) and with assumption of complete or equal oxide conversion, the equivalent ratio of sulfuric acid to nitric acid would be 1.8.

The average nitrate concentration at the westerly North Bend site was significantly higher than that observed at the other locations. The observation of  $\text{NO}_3^-$  washout with increasing elevation is in accord with a greater rate of  $\text{NO}_x$  conversion to dissolved  $\text{NO}_3^-$  than the corresponding transformation of  $\text{SO}_2$  to solution  $\text{SO}_4^{2-}$ .

The  $\text{SO}_4^{2-}$  concentrations increased as the sample strong acid content increased from winter to spring to summer. Least-squares linear regression analysis showed that there was significant correlation (at the 5% level) of  $\text{SO}_4^{2-}$  concentration with day yet indicated no significant change of  $\text{NO}_3^-$  concentration with time. The observed trend may result from the coupling of two factors during spring and summer: (a) the more complete conversion of  $\text{SO}_2$  during the longer and warmer days; (b) the more effective washout of acid aerosols in spring and summer rains (22).

It is assumed that the plume of St. Helens emissions bypassed the collector sites as the average acid content observed in this study is similar to that observed in a "pre St. Helens activity" precipitation study conducted at Stampede Pass in summer 1978. The sulfate deposition at the 4000-ft level in a typical year is estimated to be  $16.3 \text{ kg ha}^{-1} \text{ year}^{-1}$  of  $\text{SO}_4^{2-}$  by using the average  $\text{SO}_4$  concentration observed in this study and the yearly average precipitation rate at the Stampede Pass ( $\approx 4000 \text{ ft}$ ) weather station.

The weighted average ammonium concentration was significantly higher at the westerly North Bend site than the other sites, demonstrating that urban  $\text{NH}_3$  partial pressures were higher than the levels in remote locations.

**Lake Studies.** The lakes of the Alpine Lakes Wilderness Area are remote. All of the waters sampled with the exception of the two storage impoundments (Lake Keechelus and Lake Kachess) were at least 5 miles from road access. The lakes are contained in glacial-carved basins and are, for the most part, surrounded with little or no topsoil. The area is proximate and generally NNW of the precipitation collection sites (Figure 2). The data in Table II describe lake location, elevation, surface area, sampling date, pH,  $[\text{Ca}^{2+}]$ , and alkalinity data on those waters. Lake "ice out" varies with season, elevation, and location ranging from mid-June to early/mid-August. The lakes were open when sampled, except for Lake Gem.

All of the lakes showed moderate to low pHs, alkalinities, and conductances. The median values were respectively pH 6.86,  $57 \mu\text{equiv/L}$ , and  $5.8 \mu\text{S/cm}$ .

Figure 3 shows the relationship between pH and alkalinity for the 29 high lakes and two reservoirs sampled. The alkalinity in an open system equilibrated with  $\text{CO}_2$ , with only carbonate buffering, is given by the relationship of eq 6 and 7 (19). When the pH and alkalinities deter-

$$[\text{alk}]_{\text{net}} = [\text{OH}^-] + [\text{HCO}_3^-] + 2[\text{CO}_3^{2-}] - [\text{H}^+] \quad (6)$$

$$[\text{alk}]_{\text{net}} = \frac{K_w}{[\text{H}^+]} + \frac{P_{\text{CO}_2} K_H K_1}{[\text{H}^+]} + \frac{2P_{\text{CO}_2} K_H K_1 K_2}{[\text{H}^+]^2} - [\text{H}^+] \quad (7)$$

mined in this study were utilized with eq 7 to estimate  $P_{\text{CO}_2}$  ( $25^\circ \text{C}$ ) for each sample, the resulting average was  $P_{\text{CO}_2} = (472 \pm 182) \times 10^{-6} \text{ atm}$ , which compared to the atmospheric concentration  $P_{\text{CO}_2} = 330 \times 10^{-6} \text{ atm}$  indicated that the solutions behaved as if they were supersaturated in  $\text{CO}_2$

Table II. Central Cascade Lakes Surveyed 1981

no. and name	location	elevation, m	size, ha	sample date	pH	alkalinity, $\mu\text{equiv/L}$	Ca	spec conductance, $\mu\text{S/cm}$
1 Pratt	47°26' 121°25'	3385	17.6	6/26	6.97	83.2	103.0	10.5
2 Tuscohatchie	47°26' 121°26'	3420	12.9	6/26	6.88	98.8	112.0	13.2
3 Melakwa	47°29' 121°25'	4490	3.2	6/26	6.49	25.0	36.0	5.8
4 Snow	47°29' 121°24'	4016	64.5	6/30	6.57	37.0	47.0	6.2
5 Gem	47°28' 121°24'	4857	6.0	6/30	5.62	4.0	14.0	3.9
6 Lillian	47°24' 121°18'	4800	6.9	7/1	7.08	80.0	83.0	9.2
7 Rachel	47°26' 121°17'	4660	11.0	7/2	7.14	90.0	97.0	10.0
8 Rampart	47°26' 121°18'	5100	1.8	7/3	6.94	69.4	79.0	7.6
9 Angeline	47°34' 121°16'	5100	80.3	7/9	6.31	16.7	16.0	4.2
10 Big Hart	47°35' 121°17'	5100	77.2	7/9	6.47	22.2	12.0	4.5
11 Little Hart	47°35' 121°17'	4250	11.6	7/9	7.06	64.0	62.0	8.9
12 Copper	47°36' 121°18'	4000	59.8	7/9	7.12	82.8	75.0	8.8
13 Trout	47°37' 121°17'	2012	7.0	7/9	7.06	73.6	66.0	9.7
14 Glacier	47°27' 121°15'	4750	8.6	7/15	6.65	20.6	36.2	4.8
15 Spade	47°32' 121°9'	5050	49.5	7/21	6.88	60.4	55.0	7.75
16 Venus	47°33' 121°9'	5600	22.9	7/21	7.09	84.0	75.0	10.0
17 Ivanhoe	47°32' 121°12'	4700	8.3	7/22	6.30	9.2	20.0	3.4
18 Peggy's Pond	47°34' 121°7'	5600	2.0	7/23	6.99	73.2	61.0	8.4
19 Deep	47°33' 121°7'	4450	21.4	7/23	7.26	132.0	92.0	14.4
20 Waptus	47°30' 121°8'	2980	90.8	7/24	7.24	90.8	76.0	14.6
21 Hester	47°30' 121°20'	4050	27.0	7/28	6.52	22.6	36.6	6.1
22 Keechelus	47°19' 121°20'	2517	1036	8/28	7.62	246.0	263.0	39.5
23 Kachess	47°16' 121°9'	2254	1837	8/28	7.83	346.0	309.0	38.5
24 Snoqualmie	47°35' 121°22'	3225	51.2	8/3	6.64	32.3	17.1	7.95
25 Deer	47°35' 121°21'	3630	18.5	8/3	6.26	15.3	29.2	6.25
26 Bear	47°35' 121°22'	3670	19.8	8/3	6.45	23.6	35.7	7.25
27 Dorothy	47°35' 121°20'	3052	117.4	8/3	6.99	55.1	60.7	8.95
28 Marmot	47°37' 121°9'	4900	54.6	8/11	7.46	190.2	182.0	19.5
29 Jade	47°36' 121°10'	5400	11.3	8/11	6.86	50.4	47.5	5.55
30 Tuck	47°35' 121°6'	5250	6.6	8/12	6.74	38.9	40.3	5.6
31 Robin	47°35' 121°5'	6450	4.3	8/12	6.64	31.5	32.0	4.29

and/or contained additional weak acid buffering. Carbon dioxide supersaturation may well have occurred as a result of the procedures used. The samples were collected cold (3–15 °C), were contained in filled, capped bottles on transport, and then were held at 4 °C in the same containers until analysis. Upon analysis, 100-mL aliquots were allowed to warm to room temperature with gentle stirring over a period of 1–2 h before pHs were recorded.

It is estimated, from Henry's Law constants  $pK_H(25\text{ °C}) = 1.47$  and  $pK_H(15\text{ °C}) = 1.32$ , that a solution saturated in  $\text{CO}_2$  ( $P_{\text{CO}_2} = 330 \times 10^{-6}$  atm) at 15 °C would behave as if  $P_{\text{CO}_2} = 467 \times 10^{-6}$  atm if warmed to 25 °C without loss of  $\text{CO}_2$ . The rate of  $\text{CO}_2$  loss from such a supersaturated solution at room temperature would be slow (19).

Figure 3 shows the pH vs. alkalinity trend for such a supersaturated solution ( $P_{\text{CO}_2} = 467 \times 10^{-6}$  atm) along with the data points for the lakes sampled. The proximity of the curves supports the assumption that buffering is due to bicarbonate alkalinity.

None of the lakes sampled were acid. All had low alkalinities, suggesting high sensitivity to potential acidification. Henriksen (23) proposed that the "degree of acidification" of lakes can be estimated by examining the Ca and  $\text{HCO}_3$  composition of those waters. The suggestion is that Ca and  $\text{HCO}_3$  will be introduced into oligotrophic waters in fixed proportions due to  $\text{CO}_2$  weathering reactions. Addition of mineral acid, however, will result in a proportionate increase of Ca relative to  $\text{HCO}_3$ . Then, "acidification" equals "preacidification alkalinity" minus present-day alkalinity. The problem is identification of "preacidification alkalinity". It is suggested that preacidification alkalinities can be estimated from alkalinity/calcium ion relationships obtained from nonacidified waters.

The least-squares linear regression relating alkalinity to Ca for the 31 lakes of this study is shown as eq 8, while

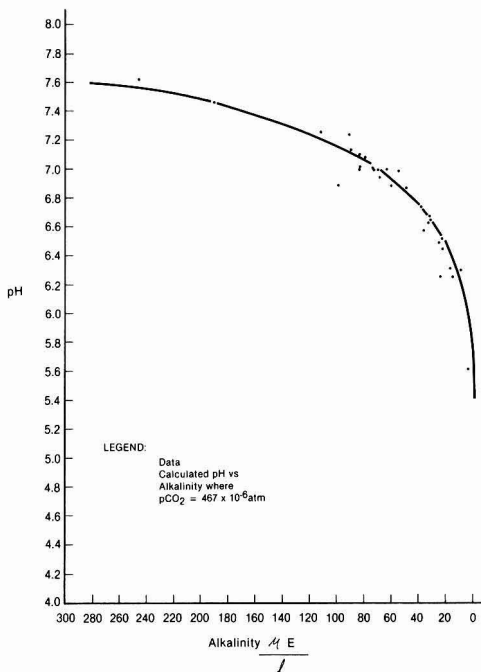


Figure 3. pH vs. alkalinity from 30 central Washington Cascade Lakes, summer 1981.

the  $\text{HCO}_3/\text{Ca}$  relationships for nonacidified lakes in northern and northwestern Norway (23) and central Canada (23) are shown in eq 9 and 10.

this study,  $N = 31$  lakes:

$$[\text{HCO}_3] (\mu\text{equiv/L}) = 1.07[\text{Ca}] (\mu\text{equiv/L}) - 5.77$$
$$r = 0.98 \quad s = 13.93 \quad (8)$$

Norway,  $N = 59$  (23):

$$\text{HCO}_3 (\mu\text{equiv/L}) = 1.32 \text{ Ca} (\mu\text{equiv/L}) - 29$$
$$r = 0.92 \quad (9)$$

Canada,  $N = 98$  (23):

$$\text{HCO}_3 (\mu\text{equiv/L}) = 1.42 \text{ Ca} (\mu\text{equiv/L}) - 32$$
$$r = 0.87 \quad (10)$$

North Cascades,  $N = 22$  (25):

$$\text{HCO}_3 (\mu\text{equiv/L}) = 0.995 \text{ Ca} (\mu\text{equiv/L}) + 2.67$$
$$r = 0.99 \quad s = 13.67 \quad (11)$$

Reynolds and Johnson (25), as part of a 1970 investigation of weathering in the North Cascades in Washington, reported  $\text{HCO}_3$  and Ca concentrations of glacial, lake, and stream waters from the South Cascade Glacier region. The waters analyzed had contacted quartz diorite, migmatite, and metadiorite-strata similar to that surrounding the lakes sampled in this study. The least-squares regression of the North Cascades data is described by eq 11.

The similarity of the  $\text{HCO}_3/\text{Ca}$  correspondence of this study (eq 8) and that of the 1970 North Cascades Glacier study (eq 11) is striking. By assumption of similar strata, the regressions indicate either no "acidification" or similar magnitudes of acidification. Equations 9 and 10, describing nonacidified waters in other locales, predict alkalinities less than those observed in this study up to  $[\text{Ca}] = 92$  or  $74 \mu\text{equiv/L}$ , respectively. If those relationships are used to predict historical alkalinity levels, then the Cascade waters show no evidence of "acidification". The median lake, assuming similar strata, of this study (alkalinity =  $57 \mu\text{equiv/L}$ ) is slightly more alkaline than the lake  $50 \mu\text{equiv/L}$  with Ca cited by Henriksen (24) as an example in his application of the nomograph used for predicting the extent of lake acidification with changes in precipitation acidity. He suggests that such a lake, resulting from pH 4.7 precipitation would enter a "transition zone" (lake pH 5.3–4.7) when the precipitation pH falls to about 4.4 and would turn acid (lake pH <4.7) when precipitation pH falls to  $\approx 4.3$ . In the Cascades, the titration analogy is further complicated by the varying contributions of snowpack and runoff.

#### Acknowledgments

We thank Craig Wilbur of the Washington State Department of Highways and to Ken White and Gran Rhodus of the U.S. Forest Service for their help in siting the collectors and for providing information. We are grateful to Don Ringe, Central Washington University, for his discussions concerning the geology of the area.

#### Supplementary Material Available

A summary of analytical quality control (1 page) will appear following these pages in the microfilm edition of this volume of

the journal. Photocopies of the supplementary material from this paper or microfiche ( $105 \times 148$  mm,  $24\times$  reduction, negatives) may be obtained from Distribution Office, Books and Journals Division, American Chemical Society, 1155 16th St., N.W., Washington, D.C. 20036. Full bibliographic citation (journal, title of article, author) and prepayment, check or money order for \$1.00 for photocopy (\$2.50 foreign) or \$4.00 for microfiche (\$5.00 foreign), are required.

#### Literature Cited

- (1) Likens, G. E.; Wright, R. F.; Galloway, T. J. *Sci. Am.* **1979**, *241*, 43.
- (2) Gibson, J. H., Program Coordinator. "NADP Data Report—Precipitation Chemistry", Colorado State University: Fort Collins, CO, 1980; Vol. III, No. 11.
- (3) Shaw, R. W. *Environ. Sci. Technol.* **1979**, *13*, 407.
- (4) Powers, C. F.; Rambo, D. L. *Environ. Monit. Assess.* **1981**, *1*, 93.
- (5) Schofield, C. L. *Ambio* **1976**, *5*, 5.
- (6) Glass, N. R.; Glass, G. E.; Rennie, P. J. *Environ. Sci. Technol.* **1979**, *13*, 1350.
- (7) Casadevall, T., written communication, U. S. Geological Survey, Vancouver, WA, 1982.
- (8) Report, Puget Sound Air Pollution Control Agency, Engineering Division, Seattle, WA, 1980.
- (9) Larson, T. V.; Charlson, R. J.; Christian, G. D.; Knudson, E. J.; Harrison, H. *Water, Air, Soil Pollut.* **1975**, *4*, 319.
- (10) Dethier, D. P. *Water Resour. Res.* **1979**, *15*, 757.
- (11) Logan, R. M. M. S. Thesis, Central Washington University, Ellensburg, WA, 1980.
- (12) McKee, B. "Cascadia"; McGraw-Hill: New York, 1972; Chapters 7, 12.
- (13) Welch, E. B.; Chamberlain, W. H. "Initial Detection of Acid Lakes in Washington State"; Civil Engineering Department: University of Washington, 1981.
- (14) Rosotti, F. J. C.; Rosotti, H. J. *Chem. Educ.* **1965**, *42*, 375.
- (15) "Standard Methods for the Examination of Water and Wastewater", 14th ed.; American Public Health Association: Washington, D.C., 1976.
- (16) Gibson, J. H., Program Coordinator, "NADP Quality Assurance Report, Central Analytical Laboratory, 1979", Colorado State University: Fort Collins, CO, 1980.
- (17) Tabatabai, M. A. *Sulfur Inst. J.* **1974**, *102*, 11.
- (18) Manahan, S. E. "Environmental Chemistry"; Willard Grant Press: Boston, MA, 1981.
- (19) Stumm, W.; Morgan, J. J. "Aquatic Chemistry"; Wiley-Interscience: New York, 1970; Chapter 4.
- (20) Granat, L. *Tellus* **1972**, *24*, 550.
- (21) "Climatological Data Annual Summary: Washington"; National Climatic Center: Asheville, NC, 1979.
- (22) Glass, G. E., Ed. "EPA Research Report"; Ecological Series, EPA: 600/3-80-044, 1980.
- (23) Henriksen, A. *Nature (London)* **1979**, *278*, 542.
- (24) Henriksen, A. "Proceedings, International Conference on the Ecological Impact of Acid Precipitation"; Sandefjord, March 11–14, 1980, SNSF project; p 68.
- (25) Reynolds, R. C.; Johnson, N. M. *Geochim. Cosmochim. Acta* **1972**, *36*, 537.

Received for review October 5, 1981. Revised manuscript received May 27, 1982. Accepted July 1, 1982. The work upon which this publication is based was supported in part by funds provided by the Office of Water Research and Technology (Project No. F80-48), U.S. Department of the Interior, Washington, DC, through the Washington Water Research Center as authorized by the Water Research and Development Act of 1978.

# Mineral Matter and Trace-Element Vaporization in a Laboratory-Pulverized Coal Combustion System

Richard J. Quann, Matthew Neville, Morteza Janghorbani,<sup>†</sup> Charles A. Mims,<sup>‡</sup> and Adel F. Sarofim\*

Chemical Engineering Department, Massachusetts Institute of Technology, Cambridge, Massachusetts 02139

■ The composition and size distribution of fly ash produced by burning of a Montana lignite at two temperatures, 2050 and 2450 K, were determined. The ash showed a bimodal size distribution with a submicron fraction that was significantly enriched in the volatile trace species. The amount of submicron aerosol increased markedly with combustion temperature, from 4% of the ASTM ash value of the coal at 2050 K to 20% at 2450 K, supporting the hypothesis that the enrichment in more volatile species of the smaller ash particles is due to a process of vaporization and recondensation of mineral constituents.

Numerous field investigations on the characteristics of pulverized coal-fired power plant fly-ash emissions have revealed that the concentrations of certain trace metals, notably the toxic elements, As, Sb, Zn, Se, Pb, and Cr, are systematically enriched in the finer sized fly-ash particulates and, in some cases, in the surface layers of particulates (1-7). Although the focus of these early studies has been on particulates of sizes greater than about 0.5  $\mu\text{m}$  it has been shown recently that submicron particles are also enriched in these elements (6).

One proposed explanation for the observed enrichment trends is that elements that are relatively volatile under conventional boiler conditions vaporize in the high-temperature combustion zone and later condense on the surfaces of preexisting ash particles as the combustion gases are cooled (1). Enrichment of the finer fly-ash particles in the more volatile elements would then be a consequence of their greater surface to volume ratios. Homogeneous condensation of the inorganic vapor to form submicron particles can occur in competition with the heterogeneous condensation processes (8, 9). Homogeneous nucleation of submicron particles would occur in the gas phase became critically supersaturated with respect to certain inorganic vapors. The importance of this fine particle formation process has been demonstrated in recent field studies of utility effluents that have shown that the size distribution of fly ash is distinctly bimodal, with the additional mode occurring in the submicron size range (10).

The factors governing the volatilization of mineral matter and the subsequent processes of heterogeneous and homogeneous condensation are complex and likely to depend at least upon the composition of the coal, the conditions of combustion, and the thermochemical properties of the ash. It is difficult to evaluate systematically the processes of ash vaporization and condensation in full-scale boilers because of the variations in coal composition and operating conditions and the difficulty of closing material balances. Largely for these reasons, we have developed a laboratory-pulverized coal combustion system capable of obtaining fundamental information on the vaporization and condensation of the inorganic constituents of coal. In this paper, we describe the system—a laminar flow drop tube furnace with particulate sampling equipment—and its application to the study of ash vaporization during coal

combustion under well-controlled conditions.

## Combustion System

The central features of the laboratory-scale combustion system are a laminar flow drop tube furnace, into which pulverized coal is continuously injected, and a water-cooled collection probe followed by an Anderson impactor for the continuous recovery, quenching, and on-line size classification of particulate combustion products. The advantages of conducting combustion experiments on such an apparatus are as follows: (1) The combustion conditions can be precisely defined, controlled, and monitored to permit detailed investigations of a number of parameters affecting ash particle formation. (2) Small, homogeneous samples of well-characterized coal are employed for the experiments. (3) All particulate products leaving the furnace can be completely collected and size classified for subsequent analysis, thus eliminating questions inevitably present in field studies on the extent to which collected samples are representative. (4) The laboratory system can simulate environments encountered in both conventional pulverized-coal-fired boilers and extreme conditions such as those proposed for advanced energy conversion systems such as MHD.

In this section, the combustion furnace, continuous coal feeding system, collection system, monitoring capabilities, and operating parameters are described in detail. In subsequent sections, the procedures for sample analysis are described. Results are then presented on the distribution of different elements between size fractions, and these are compared with data from field studies.

**1. Combustion Furnace.** A schematic diagram of the laminar flow drop tube furnace is presented in Figure 1. The furnace has electrically heated graphite elements, the temperature of which can be regulated with an automatic current controller. A central combustion zone is maintained within the core of the furnace by an alumina muffle tube of 50 mm i.d. The maximum operating temperature of the furnace muffle tube is about 1800 K. The main gas, a premixed oxygen-inert mixture, enters through the top of the furnace, where it flows through an alumina honeycomb before entering the furnace combustion zone. The honeycomb serves as both a preheater and flow straightener to deliver the main gas at the specified furnace temperature with a uniform laminar velocity. The composition of the main gas is regulated by dual mass flow controllers. Coal particles entrained in  $10^{-7}$   $\text{m}^3/\text{s}$  of gas are injected axially into the furnace combustion zone via a water-cooled feeder probe. Coal is fed at rates that could be varied between 0.15 and 1.5 mg/s. The main gas flow rate is maintained at  $10^{-4}$   $\text{m}^3/\text{s}$ . On entering the furnace combustion zone, the particles are rapidly heated and ignited.

**2. Coal Feeding System.** A schematic diagram of the coal feeding system is presented in Figure 2. The coal particles are entrained by the carrier gas, which flows over the surface of an agitated coal bed and into a stationary fine gauge tube. The gas velocity in the fine gauge tube is sufficient to keep the particles in suspension. The rate of entrainment is established by the rate at which the coal

\*Massachusetts Institute of Technology Nuclear Reactor Laboratory.

<sup>†</sup>Presently with Exxon Research and Engineering, Linden, NJ.

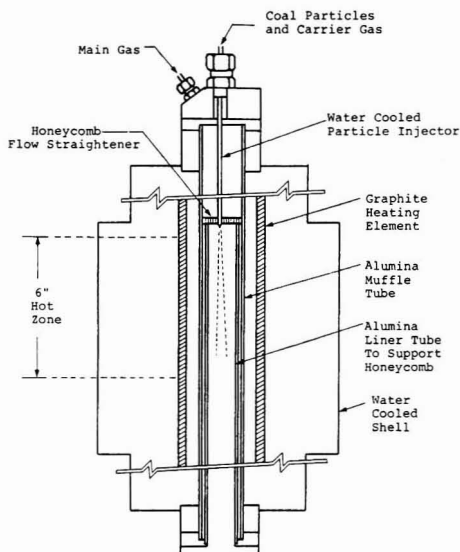


Figure 1. Laminar flow combustion furnace.

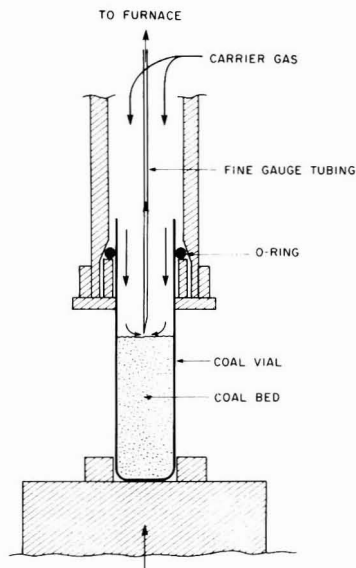


Figure 2. Coal feeding system.

feed vial is driven toward the fine gauge tubing. After an initial transient, a fixed clearance is established between the top of the coal bed and the fine gauge tube. A range of feeding rates is obtainable by changing the speed of the syringe pump used to drive the coal vial toward the stationary tubing; 1–5 g of coal are fed per experiment.

**3. Collection System.** All gas and particulate combustion products are withdrawn from the combustion zone of the furnace by a water-cooled collection probe which is inserted along the axis through the bottom of the furnace. The position of the probe is adjustable to allow time-resolved combustion measurements.

A schematic of the probe is presented in Figure 3. The inner core of the water-cooled probe is fitted with a stainless steel porous tubing through which gas is trans-

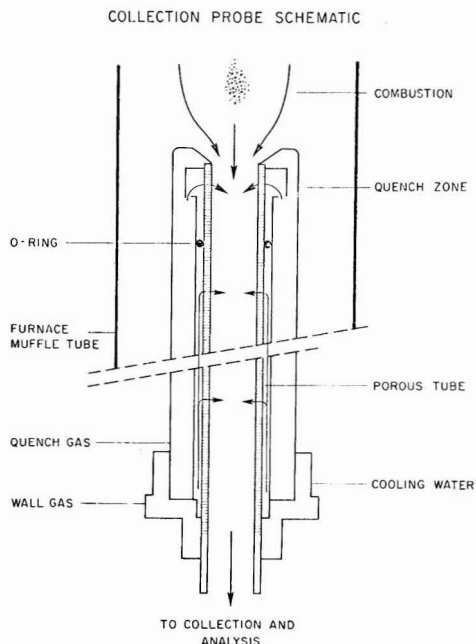


Figure 3. Collection probe.

pired radially during the course of an experiment. In the first 25 mm of the top section of the probe, gaseous and particulate products are quenched to below 470 K by  $3 \times 10^{-4} \text{ m}^3/\text{s}$  of  $\text{N}_2$  gas. A minimal inward radial gas flow at  $6 \times 10^{-6} \text{ m}^3/\text{s}$  is maintained throughout the lower section of the probe to prevent deposition and loss of particulates within the probe. From the collection probe, the gases and particulates enter directly into an Anderson cascade impactor for on-line aerodynamic size classification of the particulates. The impactor contains eight stages with theoretical effective cutoff diameters of 12.4, 7.9, 5.4, 3.7, 2.4, 1.2, 0.77, and  $0.54 \mu\text{m}$ . The smaller submicron particulates pass through the impactor and are collected on a backup membrane filter.

It is known that the performance of the Anderson impactor is limited by problems associated with wall loss, particle bounce, and reentrainment (12, 13). In the present study, we minimize reentrainment and particle bounce by employing greased substrates on the impaction plates. In order to minimize deposition on the entrance wall of the impactor, we constructed a conical head with a porous carbon inner wall through which gas is transpired at a nominal rate to prevent deposition.

**4. Combustion Monitoring.** A two-color optical pyrometer is used to determine the burning-temperature history of ignited coal particles in the furnace combustion zone. For these measurements, a slightly modified feeding system is employed. The coal particle stream in the fine gauge tubing is passed through a dilution stage to reduce particle number densities before entering the water-cooled feeder probe in the furnace. This allows the measurement of the temperature of single coal particles from ignition to burnout (11).

#### Analysis

Raw pulverized coal and size classified particulate combustion products are analyzed for bulk elemental content by using instrumental neutral activation analysis (INAA).

Table I. Montana Lignite Composition

element	concn, ppm (av of six samples $\pm$ 1 sd)	expected precision from INAA count. stat, %
Al	7500.0 $\pm$ 200.0	1
As	4.0 $\pm$ 0.2	10
Ba	377.0 $\pm$ 50.0	30
Ca	15740.0 $\pm$ 75.0	5
Ce	8.5 $\pm$ 2.0	20
Cl	39.5 $\pm$ 1.0	10
Co	0.93 $\pm$ 0.05	10
Cr	7.1 $\pm$ 1.6	10
Eu	0.10 $\pm$ 0.01	10
Fe	2720.0 $\pm$ 150.0	5
Hf	0.63 $\pm$ 0.02	10
K	365.0 $\pm$ 34.0	10
La	5.7 $\pm$ 0.1	5
Mg	7930.0 $\pm$ 230.0	10
Mn	78.0 $\pm$ 2.0	4
Na	212.0 $\pm$ 20.0	10
P	310.0	
Sb	0.73 $\pm$ 0.09	20
Sc	0.93 $\pm$ 0.04	2
Si	9800.0	
Sm	0.49 $\pm$ 0.01	1
Th	1.5 $\pm$ 0.1	10
Ti	235.0 $\pm$ 15.0	14
V	7.3 $\pm$ 0.4	6
W	0.86 $\pm$ 0.11	15
Yb	0.31 $\pm$ 0.06	20
Zn	11.0 $\pm$ 3.0	10

INAA is the method of choice for major, minor, and trace elements because of its high sensitivity for small samples, minimum sample handling and contamination, and freedom from the tedium of wet chemical techniques. The INAA method for coal and fly ash have been developed and previously shown to produce accurate results (14, 15). Samples are irradiated in the MIT Research Reactor and  $\gamma$ -ray counts measured with a high-resolution Ge (Li) detector. Calibration for absolute determination of metal quantities is achieved by the use of an NBS coal standard. NBS opal glass standard 91 was also used for verification of the INAA method.

Bulk analysis for Si and P in the submicron particles on the final backup filter is obtained by fully calibrated electron microprobe analysis (EMA). This technique proved to be highly reproducible and consistent with the INAA results for elements obtained by both methods (e.g., Na, Mg, K, Ca, and Fe). Atomic absorption spectroscopy is used to determine the Si content of the coal. Analysis for phosphorus in the coal was obtained by the Galbraith Laboratories, Knoxville, TN.

With an automatic image analyzer, the size distribution of particulates in the submicron range was obtained from TEM micrographs.

### Results

**Experimental Conditions.** In order to assess the affect of combustions on the vaporization of mineral constituents, we burned coal under conditions that would yield combustion temperatures representative to those encountered in conventional boilers (1500–2100 K) and also a significantly higher temperature. The coal selected for study was a Montana lignite of 7.0% ASTM ash content, size-classified to 75–90  $\mu\text{m}$ . The elemental analysis of the coal, reported as the average of six samples analyzed, is shown in Table I. The coal was burned to completion in oxygen/helium mixtures preheated to a furnace temperature of 1750 K. Oxygen concentrations of 20%, to yield an

Table II. Effects of Combustion Condition on Ash Particulate Distribution Furnace Gas Temperature at 1750 K

impactor stage <sup>a</sup>	O <sub>2</sub> part. press., atm	
	0.20	0.50
	particle temp, K	
	2050	2450
0	0.0388	0.0320
1	0.0079	0.0018
2	0.0043	0.0044
3	0.0033	0.0038
4	0.0024	0.0038
5	0.0013	0.0013
6	0.0006	0.0002
7	0.0004	0.0007
final filter	0.0028	0.0140

<sup>a</sup> g of ash collected/g of coal burned.

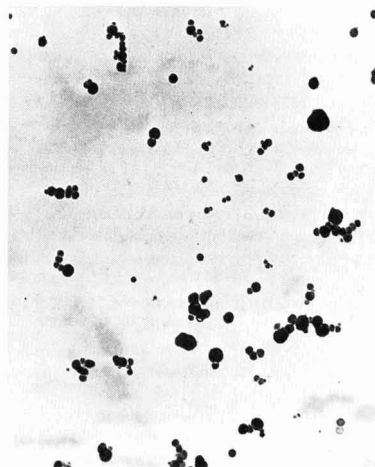


Figure 4. TEM micrograph of submicron ash particles at 1750 K in 20% oxygen.

average combustion of 2050 K, and 50%, for a combustion temperature of 2450 K, were selected. The particle temperatures during combustion were determined by optical pyrometry, as previously mentioned.

**Size Distribution of Ash Product.** Postcombustion particulates were collected on high-purity Fluoropore filters, used as the substrates of the cascade impactor stages and as the final backup filter on which the submicron fraction was collected. The absolute elemental content of the collected material and coal feed samples was obtained by the INAA method. The electrostatic precipitator was employed in place of the final filter to collect samples of the submicron fume on a TEM grid for size analysis.

The amount of ash collected on the stages of the cascade impactor and the final filter is reported in Table II.

The TEM micrograph of Figure 4 illustrates the nature of primary submicron particles and their agglomerate morphology in the fume. The size distribution of the fume's primary particles, obtain by an automated image analyzer, and the impactor sizing of the larger residual particulates are presented together in Figure 5. The bimodal size characteristic of fly ash that is prevalent in utility effluents (8) is also clearly present in the laboratory generated particulates.

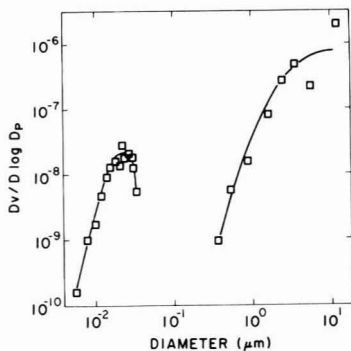


Figure 5. Size distribution of combustion particulates generated in laminar flow furnace at 1750 K in 20% oxygen.

The formation of the larger residual particles involves the coalescence on contact of the molten, micron-sized mineral constituents (primarily  $\text{SiO}_2$ ,  $\text{Al}_2\text{O}_3$ ,  $\text{CaO}$ ,  $\text{MgO}$ , and  $\text{FeO}$ ) in a parent coal particle as its organic mass is gasified during combustion. As discussed by others, variations in residual ash particle size is attributed to fragmentation of coal particles during combustion and cenosphere formation and to variations in the ash content and size of the original coal particles (14, 15). Inhomogeneities in the distribution of mineral matter in the raw pulverized coal may also be an important factor. The isolated data point above  $10 \mu\text{m}$  in Figure 5 corresponds to the material collected on the impactors preseparator stage, indicating that the majority of the mass of the residual ash particles consists of larger particles produced by the coalescence of the fused mineral constituents in coal during combustion.

The increase in amount of submicron particulate with increasing combustion temperature and the narrowness of the primary particulate size distribution in the submicron mode and its separation from the residual mode support the hypothesis that inorganic vapors precipitate in the combustion gases. Once nuclei have formed from the critical supersaturation of inorganic vapors, they will grow by collision and coagulation and by further heterogeneous condensation of inorganic vapors as combustion gases are cooled. From consideration of the high surface area of the submicron particles relative to the surface area of the residual fly ash particles, subsequent condensation should take place on the submicron particles. The fact that field studies have shown enrichment trends of volatile trace elements in particulates with sizes greater than about  $0.4 \mu\text{m}$  indicates that there is a finite, albeit small, surface availability in this regime. Scavenging of highly trace-element-enriched submicron particles by the larger residual particulates may also be a contributing factor to the enrichment trends observed in field studies (16).

**Elemental Composition of Ash Constituents.** Major interest is in the composition of the submicron aerosol, which has the potential of preferential release into the atmosphere by utility boilers. The efficiency of collection of the aerosol in the present study was tested by performing a material balance on selected elements in the coal at the high-temperature condition.

The percentage of selected elements in the coal feed ultimately recovered after combustion in all particulate products is presented in the second column in Table III. Generally, more than 90% of an element in the coal feed was recovered in the particulate product, indicating no significant loss of particulate or inorganic vapor material within the furnace, collection probe, or modified impactor

Table III. Elemental Material Balance on Furnace<sup>a</sup>

element	% recovered with all particulates	% recovered in submicron fume
Al	77.3	2.1
As	99.6	76.9
Ca	96.0	19.4
Cr	100.5	25.0
Fe	91.7	20.7
K	85.0	15.4
La	100.4	6.0
Mg	80.7	50.0
Mn	90.0	13.3
Na	89.0	38.6
Sb	100.0	77.0
Sc	103.4	5.3
Sm	91.3	10.0
Ti	94.0	12.1
Th	103.5	14.5
V	71.3	14.0
W	108.0	24.0

<sup>a</sup> Gas temperature 1750 K, oxygen partial pressure 0.50 atm.

head. The fraction of the different elements recovered in the submicron fume is presented in the third column of Table III. Regardless of the extent to which an element appeared in the fume, i.e., the extent of vaporization during combustion, good material closure was obtained.

The mineral matter that vaporizes can either condense on the larger ash particles or condense homogeneously as a submicron fume. For the conditions of the results presented in Table III, the greater fraction of the ash vaporized is found in the submicron fume. The major elements in the fume for the Montana lignite are the alkaline earth metals. The refractory oxides of these elements condense to form aerosols in the high-temperature zone of the furnace (17). The submicron aerosol provides a much higher surface area than the bulk ash for the subsequent condensation of the more volatile vapors of, for example, Na, As, and Sb or their respective compounds. The direct determination of the elements in the fume is therefore a sensitive measure of the extent of vaporization during combustion. Possible loss of material due to condensation on the larger particulates would appear to be small—for example, close to 80% of the As and Sb in the coal feed was found in the submicron fume at this combustion condition. Furthermore, the percentages of As and Sb collected with the fume on the backup filter, in comparison with low values of, for example, Al, Sc, and La, clearly demonstrate an effective aerodynamic separation of the fume from the larger ash particulates by the impactor.

INAA and EMA were also used to determine the composition of the fume and the fraction of an element in the coal feed that ultimately appeared in the fume at 2050 K combustion. The metal oxide composition of the submicron fume and the trace-element concentrations are presented in Table IV for combustion at both 2050 and 2450 K. As seen, the mass of the fume is dominated by  $\text{MgO}$ , followed by  $\text{CaO}$ ,  $\text{P}_2\text{O}_5$ ,  $\text{FeO}$ , and  $\text{SiO}_2$ . This result is somewhat surprising in comparison with the field studied that have shown silica to dominate the composition of submicron particles. It stresses the need for careful consideration of the characteristics of different coals and the thermochemical properties of the ash. Lignites, in contrast to high rank coals, contain high concentrations of alkali and alkaline earth metals, most of which is ion-exchanged with the combustible carbonaceous matter of coal. Its high volatility indicates that Mg probably vaporized as the

**Table IV. Chemical Characteristics of the Submicron Fume**

condition	20% O <sub>2</sub> (2050 K)		50% O <sub>2</sub> (2450 K)	
	composition	enrichment factor	composition	enrichment factor
MgO	66.23%	3.53	44.13%	2.35
CaO	8.21%	0.26	30.57%	0.97
P <sub>2</sub> O <sub>5</sub>	6.82%	6.7	2.34%	2.30
FeO	5.86%	1.17	5.18%	1.03
SiO <sub>2</sub>	5.11%	0.17	13.53%	0.45
K <sub>2</sub> O	2.50%	4.00	0.50%	0.80
Na <sub>2</sub> O	2.26%	5.54	0.79%	1.94
BaO	1.21%	2.02	0.63%	1.05
Al <sub>2</sub> O <sub>3</sub>	0.97%	0.049	2.13%	0.11
MnO	0.37%	2.57	0.10%	0.69
Cl	2269.0 ppm	3.97	392.0 ppm	0.69
Zn	928.0 ppm	5.90	193.0 ppm	1.24
Cr	683.0 ppm	6.73	127.0 ppm	1.25
As	355.0 ppm	6.21	220.0 ppm	3.85
V	245.0 ppm	2.35	72.9 ppm	0.70
Co	53.3 ppm	4.01	21.4 ppm	1.61
Sb	51.3 ppm	4.92	40.0 ppm	3.84
W	8.5 ppm	0.69	15.0 ppm	1.22
Th	1.5 ppm	0.072	15.0 ppm	0.75
Sm	0.73 ppm	0.10	3.5 ppm	0.48
Sc	0.71 ppm	0.054	3.4 ppm	0.26

metal (bp 1378 K) in the local reducing conditions of the coal particle and later converted to the oxide (bp 3533 K) in the gas phase. Oxidation of the metal in the gas phase would result in the critical supersaturation and homogeneous condensation of the metal oxide, without necessarily requiring sharp temperature drops (17).

Absolute enrichment factors, also reported in Table IV, were calculated for the major and trace species in the fume. The absolute enrichment factor used here is equivalent to the ratio of the designated element's concentration in the fume to its concentration in the ash as a whole. Those elements that are highly enriched in the fume generated at the lower combustion temperature include P, Mg, Na, K, Cl, Zn, Cr, As, Co, and Sb, and those highly depleted include Al, Th, and Sc. Other elements, which include Ce, Eu, Hf, La, and Yb, were not in sufficient concentration in the fume to be detected by the INAA method. In general, these results are consistent with field observations of enrichment or expectations based on thermochemical considerations. Field investigators have frequently calculated enrichment factors by the ratio of the concentration of specific elements to another element e.g., Al or Sc, that consistently shows no dependence of concentration on particle size in the regime of greater than about 0.5 μm. For the fume, however, such a calculation is deceptive, as the concentration of elements that show no dependence on particle size for larger particles may be substantially depleted in the fume. Aluminum, present in the ash and coal mineral matter as the refractory oxide Al<sub>2</sub>O<sub>3</sub>, does not volatilize appreciably even at extreme combustion temperatures (Table III). Hence its bulk concentration as a function of particle size for particles of the larger mode of the fly-ash size distribution is expected to be relatively invariant. These larger particles evolve from decomposition, fusion, and agglomeration of minerals within coal particles during combustion. The use of aluminum or other refractories to determine elemental enrichment factors is suitable in this particle size range. The calculation of enrichment factors by the absolute and relative methods yields the same result for particles in the large size range. The invariance in composition of refractory oxides with respect to particle size does not, however,

**Table V. Comparison of Laboratory Data on Vaporization with Field Data on Enrichment Trends (Ref 1, 3, 4) or Surface Enrichment (Ref 5)<sup>a, b</sup>**

element	% in submicron fume	ref			
		1	3	4	5
Al	0.20	I	NE	NE	NE
Sc	0.23		NE	NE	
Th	0.30		NE	NE	
Sm	0.44		NE	NE	E
Si	0.72	I	NE		NE
Ca	1.10	NE	NE	NE	E
W	2.92		E	I	
Fe	4.97	I	NE	NE	NE
Ba	8.60		I	NE	
V	9.93	I	I	I	E
Mn	10.87	I	NE	I	E
Mg	14.95	I	NE	NE	NE
K	16.82	NE	NE	I	E
Co	16.98	NE	E	NE	
Sb	20.83	E	I	E	
Na	23.45		NE	I	E
Zn	25.00	E	E	E	
As	26.32	E	E	E	
Cr	28.50	E	I	NE	E
P	28.50				E
combustor type	laboratory	pulverized	pulverized	stoker	pulverized

<sup>a</sup> Laboratory conditions at 1750 K gas temperature and 20% oxygen. <sup>b</sup> NE refers to no enrichment, E to enrichment, I to intermediate.

translate from the larger particles (>0.5 μm) down into the submicron range. This is demonstrated by the calculations shown in Table IV, where it is seen that metals (e.g., Mg, Ca, Th, Al, Sm, Sc) whose oxides are refractory have different absolute enrichment factors in the submicron fume. The submicron particles are formed by a distinctly different mechanism—that of ash vaporization followed by homogeneous condensation—than that giving rise to the larger particles. The composition of the submicron ash particles reflects the relative degree of volatilization of specific ash components and will be different than that of the larger particles due to the fact that different metals have different volatilization rates.

On the final filter, about 77% of the mass of the material is accounted for by the metal oxides and trace elements of Table IV. The rest of the mass is presumably due to moisture, or possibly sulfuric acid (the total sulfur content of the coal in the present study was 0.5%). The total amount of metal oxide and trace elements appearing as submicron material collected on the final filter corresponds to approximately 4.0% of the ASTM ash at 2050 K and 20.0% at 2450 K.

The fraction of different elements in the coal feed that appeared in the fume for a combustion temperature of 2050 K was also calculated. In table V, the percent that appeared in the fume, which provides a rough measure of the percent vaporized, is compared to four field studies on enrichment behavior attributed to heterogeneous condensation of vapors on the large particulates. Overall, the elements that show a high volatility in our simulated study are those that show enrichment trends in field studies. The lack of consistency among field studies for certain elements is undoubtedly due to differences in boiler conditions and/or coal type. A comparison of our data on elemental vaporization at 2050 K (Table V) with that at 2540 K (Table III) shows, in general, sharp increases in the extent of vaporization with increased combustion temperature.



Concluding Comments

Studies of the distribution of mineral constituents between the different size fractions of ash produced when coal is burned under well-controlled laboratory conditions have shown that ash vaporization and condensation is important in contributing both to the enrichment of the surface layers of the residual ash particles and to the formation of a submicron aerosol. The submicron aerosol is related to the amount of ash vaporized and increases with increasing combustion temperature.

Literature Cited

- (1) Davison, R. L.; Natusch, D. F. S.; Wallace, J. R.; Evans, C. A., Jr. *Environ. Sci. Technol.* 1974, 8, 1107.
- (2) Kaakinen, J. W.; Jorden, R. M.; Lawasani, M. H.; West, R. E. *Environ. Sci. Technol.* 1975, 9, 826.
- (3) Coles, D. G.; Ragaini, R. C.; Ondov, J. M.; Fisher, G. L.; Silberman, D. *Environ. Sci. Technol.* 1979, 13, 455.
- (4) Block, C.; Dams, R. *Environ. Sci. Technol.* 1976, 10, 1011.
- (5) Keyser, T. R.; Natusch, D. F. S.; Evans C. A., Jr.; Linton, R. W. *Environ. Sci. Technol.* 1978, 12, 769.
- (6) Smith, R. D.; Campbell, J. A. Nielson, K. K., *Atmos. Environ.*, 1979, 13, 558.
- (7) Ondov, J. M.; Ragaini, R. C. Bierman, A. H. *Environ. Sci. Technol.* 1979, 13, 558.
- (8) Desrosiers, R. E.; Riehl, J. W.; Ulrich, G. D.; Chiv, A. S. Seventeenth Symposium (International) on Combustion,

the Combustion Institute, 1979; p 1395.

- (9) Flagan, R. C. Seventeenth Symposium (International) on Combustion, the Combustion Institute, 1979; p 97.
- (10) Markowski, G. R.; Ensor, D. S.; Hooper, R. G.; Carr, R. C. *Environ. Sci. Technol.* 1980, 14, 1400.
- (11) Altricher, D. M. S.M. Thesis, Massachusetts Institute of Technology, Cambridge, MA, 1980.
- (12) Dzubay, T. G.; Hines, E. E.; Stevens, R. K. *Atmos. Environ.* 1976, 10, 229.
- (13) Gordon, G. E.; Gladney, E. S.; Ondov, J. M.; Conry, T. J.; Zoller, W. H. "Intercomparison of Several Types of Cascade Impactors"; presented before the American Chemical Society, Division of Environmental Chemistry, Los Angeles, CA, March 1974.
- (14) Ondov, J. M.; Zoller, W. H.; Olmer, I.; Aras, N. K.; Gordon, G. E.; Rancifelli, L. A.; Abel, K. H.; Filby, R. H.; Shah, K. R.; Ragaini, R. C. *Anal. Chem.* 1975, 47, 1102.
- (15) Racitelli, L. A.; Cooper, J. A.; Perkins, R. W. "Environmental Quality and Safety"; Academic Press: New York, 1976; Vol. 5.
- (16) Neville, M.; Quann, R. J.; Haynes, N. S.; Sarofim, A. F. *J. Colloid Interface Sci.*, in press.
- (17) Neville, M.; Quann, R. J.; Haynes, B. S.; Sarofim, A. F. Eighteenth Symposium (International) on Combustion, the Combustion Institute, 1981; p 1267-74.

Received for review April 6, 1981. Accepted March 11, 1982. This work was supported by the Electric Power Research Institute.

## Analysis for Organic Vapor Emissions near Industrial and Chemical Waste Disposal Sites

Edo D. Pellizzari

Analytical Sciences Division, Chemistry and Life Sciences Group, Research Triangle Institute, Research Triangle Park, North Carolina 27709

■ Vapor-phase organics in ambient air near industrial complexes and chemical waste disposal sites were characterized by capillary gas chromatography/mass spectrometry/computer, (GC)<sup>2</sup>/MS/COMP. Chemicals representing aldehydes, esters, alcohols, ethers, ketones, aromatics, and halogenated hydrocarbons and aromatics were identified and their levels estimated. The multipollutant capability of the sorbent cartridge (GC)<sup>2</sup>/MS/COMP based method was demonstrated.

Introduction

Although the characterization of a few individual substances of the environment has, upon occasion, been given primary emphasis [e.g., dimethylnitrosamine (1, 2), pesticides (3, 4), polynuclear aromatic hydrocarbons (5-7)] a comprehensive identification of all pollutants present in environmental matrices (air, water, food) would be desirable in understanding man's exposure to toxic chemicals. This approach presents a formidable task, because these media are very complex chemical mixtures, with many constituents present at trace levels.

Since the composition of air may differ considerably with geographical area, sampling for organic vapors and the ability to perform a complete characterization become essential. Sources and types of air pollution and problems associated with collection, fractionation, and chemical analysis have been recently reviewed (8).

The existence of mutagenic and carcinogenic vapors among the vapor-phase component of ambient air has been postulated in several instances (1, 8-14) and established

in a number of studies (1, 8, 12-14). As a group, however, the volatile organic constituents of air have largely been neglected by analysts. It is of paramount importance to characterize all the volatile organics in the atmosphere if we are to understand their impact, both singly and as a group, upon human health.

Our goal has been to develop a multipollutant sampling and analysis method for organics in air. The elements of this development have recently been reported (15) along with the strengths and shortcomings.

This report presents research results obtained during the application of the Tenax GC sorbent collection and high-resolution gas chromatographic/mass spectrometric/computer [(GC)<sup>2</sup>/MS/COMP] analysis method. This is an important step in our method development, whereby once the "window of comprehensive analysis" has been defined, then extensive validation studies can be conducted. As such, the selection of study sites was guided by the potential diversity of chemicals present in air which could challenge the analytical method. This criterion was satisfied by sampling at a few industrialized and chemical waste disposal sites.

Experimental Section

**Apparatus.** Ambient air samples were collected by using a Nutech Model 221-A AC/DC sampler (Nutech Corp., Durham, NC) equipped with Tenax GC sorbent cartridges (15). For long term sampling (8-24 h) DuPont Model P-125 personal samplers (E. I. DuPont de Nemours, Wilmington, DE) were employed. The preparation of Tenax GC cartridges and ancillary devices for sampling

and analysis has been previously reported (15).

A Varian MAT CH-7 GC/MS and an LKB 2091 GC/MS equipped with 620L and PDP-11/04 computers, respectively, were employed for qualitative and quantitative analyses of ambient air. Thermal desorption units used for recovering adsorbed vapors on sorbent cartridges have been previously described (15). The operating parameters and capillary columns employed in this study also have been reported (15).

**Sampling.** The geographical areas studied were (1) Iberville, LA Parish, and Baton Rouge, LA and vicinity (January 31 through February 2, 1977), (2) Kin-Buc (Edison, NJ, June 29 and July 1, 1976) and Old Love Canal (Niagara Falls, NY, February 7 and 8, 1978) chemical waste dumps, (3) Niagara Falls, NY (July 11 and 12, 1978), and (4) Curtis Bay, MD (October and November 1975). The detailed sampling conditions and locations have been previously reported (16-20). For short-term (1-2 h) and long-term (8-24 h) sampling periods, sampling rates of 1 L/min and 20-40 mL/min, respectively, were used.

**Quality Control Samples.** Field controls (sampling cartridges spiked with halogenated aliphatic and aromatic compounds) and field blanks were employed for determining recovery and cartridge backgrounds, respectively, for stored samples. Recoveries were greater than 75% for all chemicals examined.

**Analysis.** Instrumental conditions for the analysis of samples were as previously reported (15).

Identification of resolved components was achieved by comparison of the mass spectra of the unknowns to an eight major peak index of mass spectra (21) and to the Wiley library collection (22). Identities of the halogenated and other compounds were confirmed by obtaining authentic compounds corresponding to various isomers for the compounds tentatively reported, chromatographing the authentic material under conditions identical with those employed in the analysis of the air samples, and comparing retention times and fragmentation patterns. Particular note was taken from the relationship between the boiling point of the identified compound and the order of elution of homologous series since a non-polar-phase coated capillary column separates primarily on the basis of boiling point.

Quantification employed one of two methods. The first employed the use of relative molar response (RMR) factors (16). Known quantities of each authentic chemical were delivered to sorbent cartridges by using a permeation system to generate air/vapor mixtures (15, 17). The RMR for each compound was subsequently calculated from the response of the MS to the known amount.

The second method involved the calibration of the GC/MS/COMP system over a concentration range. Air/halogenated hydrocarbon vapor mixtures were prepared, calculated quantities were trapped on Tenax GC cartridges, and the cartridges were thermally desorbed into the (GC)<sup>2</sup>/MS system. Peak areas from the single ion (*m/z*) current were obtained. After preparing the standard curve (Figure 1), cartridges containing unknown concentrations of each halogenated hydrocarbon from the field sites were analyzed. The quantity cartridge was determined from the standard curve. On the basis of the volume of air sampled (15, 18), the concentration ( $\mu\text{g}/\text{m}^3$ ) of the halogenated hydrocarbon was calculated.

## Results and Discussion

**Characterization of Ambient Air Pollutants in Industrialized Areas.** In the Iberville and Baton Rouge Parishes, LA, reside many organic chemical and petroleum producer, user, and storage facilities that are located along

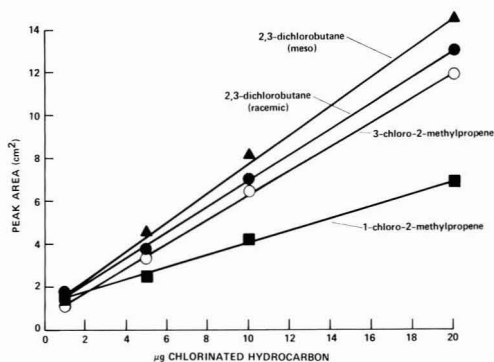


Figure 1. Linear regressions for MS response vs. chlorinated hydrocarbons.

the Mississippi River. This area includes clusters of chemical producers just north of Baton Rouge, the downtown complex, and the industrial sites near Plaquemine and Geismar, LA, which are downriver from Baton Rouge. Because of the potential levels and wide array of ambient air pollutants, this area served as an excellent opportunity for applying and evaluating the GC/MS based method for identifying the quantifying organic chemicals. Also, the availability of emissions data provided a potential target list of sought-for compounds (16).

The estimated levels of vapor-phase organics for sampling conducted in the Iberville Parish is given in Table I. A total of 22 halogenated hydrocarbons (16) were measured at 11 locations; a partial listing is given. Benzene was highest at D3/L8, reaching  $16 \mu\text{g}/\text{m}^3$ . In contrast, the levels in the upwind samples were lower and were represented by D2/L3 and D3/L11. The variability of sampling and analysis is given by the replicate samples from each location.

Inspection of the emissions inventory (16) indicated that the industrial activity was associated with production, usage, or storage of halogenated hydrocarbons. In addition, an incineration facility was located near Baton Rouge. The principal function of this facility was destruction of aliphatic and aromatic hydrocarbons, alcohols, viscous oils, polyglycols, tars, chlorinated aliphatics and aromatics, waxes, and rubber. Table II lists some organics identified and quantified (16) in ambient air near Baton Rouge.

The use of high-resolution gas chromatography in combination with mass spectrometry is necessary for the analysis of complex mixtures such as those found in ambient air. In another monitoring effort isomeric forms of chloromethylpropenes and 2,3-dichlorobutanes (meso and racemic) was resolved and quantified. Ambient air levels of these chemicals near Curtis Bay, MD, are given in Table III. Quantities as high as  $670 \mu\text{g}/\text{m}^3$  of 1-chloro-2-methylpropene and  $156 \mu\text{g}/\text{m}^3$  of 2,3-dichlorobutane (meso) were found. Only one of the two racemic pairs of 2,3-dichlorobutane was detected. Correlations between concentrations and sampling times indicated a simultaneous increase and decrease in the levels of all four compounds, suggesting that the same point source of emission was responsible for the occurrence of all four compounds.

**Characterization of Volatile Organics near Waste Disposal Sites.** In addition to industrialized areas, another environmental situation that may yield an air pollution problem is a waste disposal site. Two were investigated in this study, the Kin-Buc site near Edison, NJ, and the Old Love Canal in Niagara Falls, NY.

Table I. Estimated Levels ( $\mu\text{g}/\text{m}^3$ ) of Vapor-Phase Organics in Ambient Air in Iberville Parish, LA

chemical	D1/L1	D1/L2	D2/L3	D2/L4	D2/L5	D2/L6	D2/L7	D3/L8	D3/L9	D3/L10	D3/L11
1,1,1-trichloroethane	1.1 ± 0.02 <sup>a</sup>	1.8 ± 0.10	T <sup>b</sup>	1.5 ± 0.02	0.4 ± 0.05	2.7 ± 0	8.8 ± 1.2	1.6 ± 0	0.5 ± 0.06	0.4 ± 0.03	0.1 ± 0.06
1,2-dichloroethane	1.7 ± 0.34	1.2 ± 0	T	1.6 ± 0.04	0.3 ± 0.03	3.7 ± 1.1	4.7 ± 0.2	0.4 ± 0	0.3 ± 0.04	0.1 ± 0.02	0.09 ± 0.03
carbon tetrachloride	0.8 ± 0.80	c	T	T	T	T	4.6 ± 1.1	0.3 ± 0.25	0.7 ± 0.20	0.3 ± 0.02	
dichlorobutane isomer	0.2 ± 0.07	2.7 ± 2.0	T	T	7.3 ± 1.6	7.3 ± 1.6	1.4 ± 0.20		0.05 ± 0.02		
tetrachloroethylene	T	1.0 ± 0.90	T	T	0.5 ± 0.05	0.5 ± 0.05	1.2 ± 0.20	0.2 ± 0.02	T	T	T
1,1,2,2-tetrachloroethane	T	0.3 ± 0.02	T	T	T	2.4 ± 0.10	1.6 ± 0.24		0.1 ± 0.09	1.4 ± 0.16	1.1 ± 0.27
chloroform	2.0 ± 0.12	0.4 ± 0	1.0 ± 0.62	0.6 ± 0.01	0.9 ± 0.01	1.4 ± 0.03	5.9 ± 0.69	1.1 ± 0.47			
1,2-dichloropropane	0.9 ± 0.27	0.7 ± 0.04	T	0.2 ± 0	0.2 ± 0	0.1 ± 0	2.2 ± 0.14	T			
dichloropropene isomer	0.6 ± 0.06	0.1 ± 0.07	T	T	T	0.3 ± 0.02	0.3 ± 0.09				
1,1,2-trichloroethane	T	T	T	T	T	T	1.8 ± 0.44				
tetrachlorobutadiene isomer	1.8 ± 0.16	1.7	2.0 ± 0.44	0.6 ± 0.02	1.4 ± 0.04	1.9 ± 0.09	1.9 ± 0.09	16 ± 3.7	6.2 ± 2.5	1.7 ± 0.25	0.4 ± 0.07
benzene											

<sup>a</sup> Average of duplicate samples. <sup>b</sup> Trace. <sup>c</sup> Not detected.

Table II. Volatile Organics Identified in Ambient Air in Baton Rouge, LA, and Vicinity

chemical	chemical
chloroform	dichlorobutane isomer
carbon tetrachloride	chloroprene dimer
1,1-dichloroethane	1,1,2,2-tetrachloroethane
1,2-dichloroethane	hexachloro-1,3-butadiene
1,1,1-trichloroethane	chlorobenzene
1,1,2-trichloroethane	dichlorobenzene isomers
tetrachloroethylene	$\beta$ -chlorostyrene
1,2-dichloropropane	benzene

Table III. Estimated Levels ( $\mu\text{g}/\text{m}^3$ ) of Halogenated Hydrocarbons in Ambient Air near Curtis Bay in Maryland

chemical	P1/L1	P2/L1	P3/L2	P4/L1	P5/L1
1-chloro-2-methylpropene	200	670	a	100	90
3-chloro-2-methylpropene	280	400		110	175
2,3-dichlorobutane (meso)	50	156		26	22
2,3-dichlorobutane (racemic) <sup>b</sup>	75	115		32	47

<sup>a</sup> Not detected. <sup>b</sup> One of the two isomers observed.

Table IV. Estimated Levels ( $\mu\text{g}/\text{m}^3$ ) of Vapor-Phase Organics Surrounding Kin-Buc Waste Disposal Site

chemical	P1/L1	P1/L2	P1/L3	P1/L4
allyl acetate	a	31		
benzene	20	94	9.7	13
benzyl methyl ether		1.0		
n-butyl acetate			0.1	4.8
chloroform	6.4		T <sup>b</sup>	T
chlorotoluene		2.6		
cyanobenzene			T	1.2
methyl ethyl alcohol		0.9		T
methyl ethyl ketone	T		1.5	T
4-methyl-2-pentanone			2.1	6.0
3-methyl-2-pentanone			T	1.1
tetrachloroethylene	0.3	1.6	T	T
trichloroethylene	T	0.2	1.3	10
vinyl acetate				0.5

<sup>a</sup> Not detected. <sup>b</sup> Trace.

Table V. Estimated Levels ( $\mu\text{g}/\text{m}^3$ ) of Organics in Ambient Air Surrounding Kin-Buc Waste Disposal Site

chemical	P6/L1	P6/L2	P6/L3	P6/L4
benzene	10	6.8	190	27
bromoxylene isomer	a			1.5
n-butyl butyrate		T <sup>b</sup>	50	
chloroform	0.9	2.5	27	28
1,2-dichloroethane	T		28	0.3
ethyl acetate	T		230	4.1
n-hexanal	T	1.2	T	2.3
isopropyl acetate				6.5
methyl ethyl ketone	T	0.5	33	0.4
n-pentanal		T	38	15
tetrachloroethylene	0.7	1.2	390	12
1,1,1-trichloroethane	T	0.4	120	75
trichloroethylene	T	T	T	11
1,1-dichloroethane			23	
methyl isobutyl ketone			440	
1,1,2,2-tetrachloroethane			15	1.4

<sup>a</sup> Not detected. <sup>b</sup> Trace.

The air sampling strategy was designed to obtain information as to whether the Kin-Buc site might be contributing to an organic vapor burden. Air samples were collected upwind, crosswind, and downwind with respect to the dump site (19). Also, air samples were taken in the

Table VI. Estimated Levels ( $\mu\text{g}/\text{m}^3$ ) of Organic Vapors in Ambient Air of Household Basements in Niagara Falls, NY

chemical	D2/L1	D1/L2	D1/L3	D1/L4	D3/L5	D3/L6
chlorobenzene	1.9	4.2	1.0	3.7	2.8	<sup>a</sup>
dichlorobenzene isomers (3) <sup>b</sup>	2.3	9.1	0.65	8.7	17	190
trichlorobenzene isomers (3)	0.70	11	0.07	2.4	4.0	33
tetrachlorobenzene isomers (2)	0.03	11	0.06	0.64	0.62	20
pentachlorobenzene		0.49	T <sup>c</sup>	0.02	0.03	0.25
chlorotoluene isomers (2)	6.4	15	1.7	4.6	3.0	490
dichlorotoluene isomers (3)	13	28	0.13	11	9.7	370
trichlorotoluene isomers (4)	4.0	6.6	0.11	2.5	7.2	120
tetrachlorotoluene isomer	0.15	0.17			0.06	
chlorobenzaldehyde isomer		0.18		0.75	0.03	4.1
bromotoluene isomer	0.02	T		0.13	0.07	4.4
chloronaphthalene isomer	0.08	0.08				3.4
1,2-dichloropropane	1.4					
pentachlorobutadiene isomer					T	
1,3-hexachlorobutadiene		0.11		0.03	0.10	0.41
benzene	14	74	4.2	6.3	T	520

<sup>a</sup> Not detected. <sup>b</sup> Values are the sum of the individual isomers detected. <sup>c</sup> Trace.

Table VII. Estimated Levels ( $\mu/\text{m}^3$ ) of Halogenated Hydrocarbons in Ambient Air of Niagara Falls, NY

chemical	D1/L6	D2/L1	D2/L2	D2/L3	D2/L4	D2/L5
chlorobenzotrifluoride isomer	<sup>a</sup>		0.41	0.52	20	
chlorotoluene isomer		0.43	2.3	0.53	12	
dichlorobenzotrifluoride isomer					0.19	
dichlorotoluene isomer		0.04	0.11		0.45	
trichlorobenzene isomer		0.04	5.3	0.04	0.32	
1,3-hexachlorobutadiene		0.05	T <sup>b</sup>		0.39	
trichlorotoluene isomer					0.57	
tetrachlorobenzene isomer			0.23		0.45	
pentachlorobenzene					0.02	

<sup>a</sup> Not detected. <sup>b</sup> Trace.

middle of the dump in an effort to ascertain which organic chemicals were emanating from the landfill itself.

The identity and quantity of some representative compounds for two of the six sampling periods are given in Table IV (19). Chemicals representing aldehydes, esters, alcohols, ethers, ketones, aromatics, and halogenated hydrocarbons and aromatics were detected. Compounds were selected for quantification based upon their occurrence only in samples taken at the downwind location, or because of their apparent high levels. As expected, high levels of many chemicals were found on the site itself (Table V, P6/L3).

In another study, the ambient air in basements of 11 homes and 2 elementary schools near the Old Love Canal dump site was sampled and analyzed by (GC)<sup>2</sup>/MS/COMP. Over 200 chemicals (42 halogenated) were detected, many unique and not found in our other monitoring studies (17). Because authentic standards were not available for all identified substances, their measurement was not possible. Nevertheless, the levels for several halogenated aliphatic and aromatic compounds and benzene were determined and they are given in Table VI. The concentration of chlorinated toluenes was as high as 490  $\mu\text{g}/\text{m}^3$  in one basement (D3/L6). However, none of the chlorinated benzenes and toluenes were detected in air samples from rooms in the 93rd and 99th street schools.

The total burden for halocarbons in air was highest for D3/L6, reaching an estimated level of 1236  $\mu\text{g}/\text{m}^3$  while at the elementary schools it was  $\sim 7.6 \mu\text{g}/\text{m}^3$ .

Several analogues of chlorofluorotoluene, e.g., chlorobenzotrifluoride, dichlorobenzotrifluoride, etc., were identified in the basement air (17). These compounds and others were also identified in ambient air samples taken 6 months later in residential areas of Niagara Falls and 3 miles from Old Love Canal (20). The same chloro-

fluorotoluene compounds were found in air samples downwind from the industrial area; none of these substances were detected in the upwind samples (Table VII, D2/L5 and D1/L6).

At the time when these chemical waste disposal sites were investigated, little information was available as to the buried chemicals, a not uncommon circumstance. However, the power of the (GC)<sup>2</sup>/MS/COMP based sampling and analysis method was clearly demonstrated by the ability to resolve, identify, and quantify a multitude of chemicals.

This research program was initiated to develop and evaluate the utility of a multipollutant sampling and analysis method for toxic organics in the atmosphere. The broad-based capability of the (GC)<sup>2</sup>/MS/COMP method is revealed by the many different chemical classes observed in the samples from industrial and chemical waste dump sites. Furthermore, quantification can be performed by this method. The substantial information content that can be gleaned from a single sample by this method surpasses other techniques currently available to the analyst.

#### Acknowledgments

Appreciation is extended for the assistance provided by the many Research Triangle Institute staff members who contributed their efforts to this program during the past 6 years. The adroit and keen suggestions and criticisms of K. Krost and Drs. A. Ellison, B. Dimitriades, and E. Sawicki throughout the course of this research is gratefully acknowledged.

#### Literature Cited

- (1) Pellizzari, E. D.; Bunch, J. E.; Berkley, R. E.; Bursey, J. T. *Biomed. Mass Spectrom.* 1976, 3, 196.

- (2) Pellizzari, E. D.; Bunch, J. E.; Bursley, J. T.; Berkley, R. E.; Sawicki, E.; Krost, K. *Anal. Lett.* 1976, 9, 579.
- (3) Alford, A. *Biomed. Mass Spectrom.* 1975, 2, 229.
- (4) Safe, S.; Hutzinger, O. "Mass Spectrometry of Pesticides and Pollutants"; CRC Press: Cleveland, OH, 1973; p 77.
- (5) Gunther, F. A.; Buzzetti, F. *Residue Rev.* 1965, 9, 90.
- (6) Davis, H. J. *Anal. Chem.* 1968, 40, 1583.
- (7) McCormick, R. A.; Xintaras, C. *J. Appl. Meteorol.* 1962, 1, 237.
- (8) Hughes, T. J.; Pellizzari, E.; Little, L.; Sparacino, C.; Kolber, A. *Mutat. Res.* 1980, 76, 51.
- (9) Matz, J. Z. *Gesamte Hyg. Ihre Grenzgeb.* 1972, 18, 903.
- (10) Norpoth, K.; Manegold, G.; Brüker, R.; Amann, H. P. *Zentralbl. Bakteriol., Parasitenkd., Infektionskr. Hyg., Abt. 1: Orig., Reihe B* 1972, 156, 341.
- (11) Jones, P. W. "Analysis of Nonparticulate Organic Compounds in Ambient Atmospheres"; 67th Air Poll. Cont. Assoc. Mtg., Denver, CO, June 1973.
- (12) Lao, R. C.; Oja, H.; Thomas, R. S.; Monkman, J. L. *Sci. Total Environ.* 1973, 2, 223.
- (13) Shadoff, L. A.; Kallos, G. J.; Woods, J. S. *Anal. Chem.* 1973, 45, 2341.
- (14) Collier, L. *Environ. Sci. Technol.* 1972, 6, 930.
- (15) Krost, K. J.; Pellizzari, E. D.; Walburn, S. G.; Hubbard, S. A. *Anal. Chem.* 1982, 54, 810.
- (16) Pellizzari, E. D. "Analysis of Organic Air Pollutants by Gas Chromatography and Mass Spectrometry"; U. S. Environmental Protection Agency, EPA-600/277-100, June 1977 and EPA-600/2-79-057, March 1979.
- (17) Pellizzari, E. D.; Bunch, J. E. "Ambient Air Carcinogenic Vapors: Improved Sampling and Analysis Techniques and Field Studies"; U. S. Environmental Protection Agency, EPA-600/2-79-081, May 1979.
- (18) Pellizzari, E. D.; Bunch, J. E.; Berkley, R. E.; McRae, J. *Anal. Lett.* 1976, 9, 45.
- (19) Pellizzari, E. D. "Measurement of Carcinogenic Vapors in Ambient Atmospheres"; U. S. Environmental Protection Agency, EPA-600/7-78-062, April 1978.
- (20) Pellizzari, E. D.; Erickson, M. D.; Zweidinger, R. A. "Formulation of a Preliminary Assessment of Halogenated Organic Compounds in Man and Environmental Media"; U. S. Environmental Protection Agency, EPA-560/13-79-006, July 1979.
- (21) "Eight Peak Index of Mass Spectra"; Mass Spectrometry Data Centre, AWRE, Aldermaston, Reading, Great Britain, RG74PR; Vol. I (Tables 1 and 2), Vol. II (Table 3).
- (22) Stenhagen, E., Ed. "Registry of Mass Spectral Data"; Wiley: New York, 1974; Vol. 4.

Received for review March 29, 1982. Accepted June 28, 1982. Although the research described in this article has been funded wholly or in part by the U.S. Environmental Protection Agency through Contract No. 68-02-1228, 68-02-2864, 68-02-2262, and 68-01-4731 to the Research Triangle Institute, it has not been subjected to the Agency's required peer and administrative review and, therefore, does not necessarily reflect the views of the Agency, and no official endorsement should be inferred.

## Factors Affecting the Amperometric Determination of Trace Quantities of Total Residual Chlorine in Seawater

George T. F. Wong

Department of Oceanography, Old Dominion University, Norfolk, Virginia 23508

■ The standard scheme for the determination of total residual chlorine in seawater by amperometric titration is not suitable for many recent studies that require lower and lower detection limits ( $<0.1 \text{ mg L}^{-1}$  or  $<1.4 \text{ } \mu\text{equiv L}^{-1}$ ). The interference of iodate that originated from the reaction between iodide and hypobromite and from naturally occurring iodate in seawater may yield variable blank and/or grossly underestimated results. The pH chosen in the present analytical scheme is at a value where the reaction between iodate and iodide is sluggish and the extent to which iodate is converted to triiodide is most sensitive to small pH changes. A titration at pH 2 will yield the true concentrations of total residual chlorine after the contribution from naturally occurring iodate is corrected for. The interference from nitrite should be considered if a submilligram per liter level of residual chlorine is to be measured and/or if the titration is carried out at a pH below 3. This interference may be removed by the addition of sulfamic acid.

### Introduction

Amperometric titration is one of the standard methods for the determination of total residual chlorine in fresh water and waste water (1). In this method, a stoichiometrically equivalent amount of triiodide is generated by reacting the hypochlorite formed from the added molecular chlorine with excess iodide at pH 3.5-4.5. The triiodide is then titrated amperometrically with a standard phenylarsine oxide solution. This method has also been used extensively for measuring total residual chlorine in seawater in recent years. Moreover, in many studies on the

toxicity of residual chlorine on organisms, lower and lower concentrations were used and lower and lower detection limits (as low as  $0.001 \text{ mg L}^{-1}$ ) were claimed (2). The applicability of an analytical method to a different medium at reduced concentrations is not always straightforward. In the past few years, several investigators (3-7) have suggested that complications may arise when this analytical scheme is applied to seawater. Hypochlorite reacts with bromide in seawater to form hypobromite (8). Hypobromite may be converted to molecular bromine at pH 4, and bromine may be lost to the atmosphere by volatilization (5, 6). Carpenter et al. (3) suggested that hypobromite may oxidize iodide not only to triiodide but also to iodate:



Since iodate does not react directly with phenylarsine oxide and, at pH 4, the reaction between iodate and iodide to form triiodide is sluggish, any iodate that has not been converted to triiodide will be considered a disappearance of the added chlorine. Creelius et al. (4) reported that this problem may be circumvented by premixing the pH 4 buffer and the iodide solution in the titration vessel prior to the addition of the sample and subsequent titration with phenylarsine oxide. Carpenter and Smith (7) and Wong (6) pointed out that iodate is also a natural constituent of seawater. Thus, it may cause a variable positive blank of up to  $0.1 \text{ mg L}^{-1}$  ( $1.4 \text{ } \mu\text{equiv L}^{-1}$ ) residual chlorine. This source of error may be safely neglected only for concentrations above  $2 \text{ mg L}^{-1}$  ( $28 \text{ } \mu\text{equiv L}^{-1}$ ). Carpenter et al. (3) proposed that iodate may be converted completely to

triiodide by using a lower pH or a larger excess of iodide in the titration. However, other side reactions such as the oxidation of iodide by nitrite may interfere with the analysis under these modified conditions. As this presumably standard method is being applied to samples with lower and lower concentrations, interferences and blanks previously considered minor may become significant. In this paper, these problems are examined in greater details.

### Experimental Section

**Rate of the Reaction between Iodate and Iodide.** Artificial seawater was prepared according to the method of Lyman and Fleming (9). The pH of the seawater was 7.75. The pH values of two aliquots of the artificial seawater were adjusted to 2.75 and 3.67 by the addition of various volumes of 0.1 M sulfuric acid. For other aliquots, the pH values were adjusted to 2.04, 3.93, and 5.53 by the addition of a 0.1 M sulfuric acid–1% (w/v) sulfamic acid mixture, an acetic acid–sodium acetate buffer (1), and a 0.57 M  $\text{KH}_2\text{PO}_4$ –0.1 M  $\text{Na}_2\text{HPO}_4$  solution, respectively. For each solution, 40 mL of the artificial seawater was pipetted into a 50-mL volumetric flask. To this, 3 mL of 15  $\mu\text{M}$   $\text{KIO}_3$  and 1 mL of 5% (w/v) KI solution were added. The solution was then diluted to volume. The absorbance of triiodide in the solution was measured at 353 nm after various periods of time from 4 to 65 min.

**Distribution of Iodate in Estuarine Waters.** Samples of surface waters were collected from the James River estuary and the southern Chesapeake Bay. The concentration of iodate in each sample was determined by the method of Wong (10). In this method, sulfamic acid was added to each sample to destroy any nitrite that might be present. Then, excess iodide and sulfuric acid were added. The pH of the solution was about 2. Iodide reacted with iodate to form triiodide, and absorbance at 353 nm was measured. The absolute concentration was determined by standard addition of iodate to the sample. The uncertainty was about  $\pm 0.004 \mu\text{M}$ .

**Oxidation of Iodide to Iodate by Hypobromite. (a) Polarographic Study.** Borax (4.67 g) was dissolved in 1 L of artificial seawater. The pH of the solution was 8. A quantitative amount of a stock sodium hypochlorite solution was added to the artificial seawater to give a residual chlorine concentration of about 5  $\text{mg L}^{-1}$  (70.3  $\mu\text{equiv L}^{-1}$ ). A 20-mL portion of the seawater was transferred to a polarographic cell, and a polarogram of the chlorinated seawater was recorded. Freshly prepared 5% (w/v) potassium iodide (100  $\mu\text{L}$ ) was added to the solution, and the polarogram was recorded periodically with time. After about 4 h, known amounts of a standard iodate solution were added to the solution, and the polarograms were recorded. In each case, oxygen was removed from the solution by bubbling pure nitrogen through it before each polarogram was recorded. The pH of the solution was monitored throughout the experiment, and it varied from 8.25 to 8.37. The polarograms were recorded with a Princeton Applied Research Model 174 polarographic system. The residual chlorine concentration was determined at the beginning and at the end of the experiment by the standard amperometric titration at pH 4 (1) and the iodometric titration at pH 1.4 (8). The uncertainties of the two methods were  $\pm 5\%$  and  $\pm 3\%$ , respectively.

**(b) Titrimetric Study.** A known volume (700–1000 mL) of artificial seawater was transferred to a number of stoppered Erlenmeyer flasks, and the pHs were adjusted to 2.04, 4.02, 6.96, 8.26, and 9.0 by the dropwise addition of 1 M and/or 0.1 M hydrochloric acid or 1 M sodium hydroxide solution. A known amount of a standardized sodium hypochlorite solution was added to each flask to

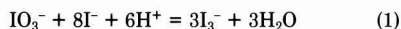
yield an initial total residual chlorine concentration of about 5  $\text{mg L}^{-1}$  (70.3  $\mu\text{equiv L}^{-1}$ ). A 5% (w/v) potassium iodide solution (5 mL) was added to the reaction mixture. After various periods of time, aliquots were removed from the flask, and the concentration of the residual chlorine was determined by an amperometric titration with phenylarsine oxide after the pH of the sample was adjusted to 2, 4, or 7 by the addition of 1:1 (v/v) sulfuric acid, a sodium acetate–acetic acid mixture, and a Michaelis phosphate buffer (11), respectively. The flasks were stoppered at all times except when a reagent was added or aliquots were removed from the reaction mixture in order to minimize the loss of the added chlorine as gaseous bromine or chlorine (6).

**Interference of Nitrite.** Artificial seawater (40 mL) was pipetted into a number of 50-mL stoppered volumetric flasks. The pHs were adjusted to 5.53, 3.93, or 2.66 by the addition of a Michaelis phosphate buffer (11), an acetic acid–sodium acetate buffer, and a 0.1 M sulfuric acid, respectively. A 500  $\mu\text{M}$  sodium nitrite solution (1 mL) and a 5% (w/v) potassium iodide solution (1 mL) were added to each flask, and the solution was diluted to volume. The absorbance of the solution at 353 nm was measured after various periods of time.

In another series of experiments, 40 mL of artificial seawater was again pipetted into each of a number of 50-mL volumetric flasks. Various known amounts of iodate, nitrite, and sulfamic acid were added to each of the flasks. The reaction mixtures were allowed to stand for 1 min so that the reaction between sulfamic acid and nitrite might go to completion. Then 1 mL of 5% (w/v) potassium iodide solution and 1 mL of 0.1 M sulfuric acid were added to each flask, and the solutions were diluted to volume. The final pH of the solution was about 2. The absorbance at 353 nm (due to triiodide) of each solution was measured in a 10-cm cell.

### Results and Discussion

**Interference of Iodate.** The reaction of iodate with excess iodide (reaction 1) is the well-known Dushman re-



action which has been studied extensively in well-defined aqueous solutions by physical and analytical chemists. Dushman (12) proposed the rate law of this reaction to be

$$-d[\text{IO}_3^-]/dt = k[\text{IO}_3^-][\text{I}^-]^2[\text{H}^+]^2 \quad (2)$$

in pure solutions of iodate and iodide buffered with an acetic acid–sodium acetate buffer, where  $t$  is time and brackets denote concentrations. The rate constant  $k$  was reported to be  $2.5 \times 10^{10} \text{ M}^{-4} \text{ min}^{-1}$ .

Equation 2 can be transformed to

$$\beta = e^{-k[\text{I}^-]^2[\text{H}^+]^2 t} \quad (3)$$

where  $\beta = [\text{IO}_3^-]/[\text{IO}_3^-]_0$  and  $[\text{IO}_3^-]$  and  $[\text{IO}_3^-]_0$  are the concentrations of iodate at time  $t$  and time zero, respectively. The term  $\beta$  thus describes the extent to which the Dushman reaction has proceeded under a set of specified conditions. The pH dependence of  $\beta$  is given by  $d\beta/d(\text{pH})$ . The pH at which  $\beta$  is most sensitive to pH changes is given by

$$d^2\beta/d(\text{pH})^2 = 0$$

or

$$\text{pH} = \frac{1}{2} \log (k[\text{I}^-]^2 t) \quad (4)$$

In the standard analytical scheme for the analyses of total

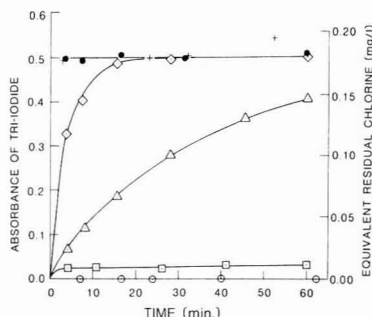


**Figure 1.** Effects of pH on the kinetics of the Dushman reactions, as measured by the absorbance of triiodide at 353 nm: ○ pH 7.75; □ pH 5.53; ▲ pH 3.93; ◇ pH 3.67; ● pH 2.75; + pH 2.04.

residual chlorine in seawater (1), the time available for iodate to react with iodide, that is, the time between the addition of excess iodide and the pH 4 buffer and the initiation and completion of the titration with phenylarsine oxide, is not specified. With use of the rate constant reported by Dushman, an iodide concentration, and a time interval similar to those encountered in the analytical scheme ( $10^{-2}$  M of  $I^-$  and 1–10 min), the pH value can be estimated to be between 3.2 and 3.7. This range of pH covers the value that is used in the analytical scheme. Thus, the extent to which the reaction between iodate and iodide may proceed will be quite sensitive to small variations in pH at the value chosen for the determination of total residual chlorine.

This Dushman reaction was followed in artificial seawater at various pHs in this study by measuring the absorbance ( $A$ ) of triiodide at 353 nm (Figure 1). The concentrations of iodide and iodate used were  $6.02 \times 10^{-3}$  M and  $9 \mu\text{M}$ , respectively. The maximum absorbance that should have been observed if all the iodate were converted to triiodide is 0.508. At pH 7.75, the absorbance never exceeded 0.006, implying that 1% or less of the iodate reacted with iodide in 60 min. At pH 5.53, about 4–6% of the iodate was converted to triiodide. Below pH 3, all the iodate reacted with iodide within 3 min. At pH 2.04, absorbance exceeding the expected maximum was observed when the reaction was allowed to proceed for more than 50 min, and this might be caused by the air oxidation of iodide (13). The fraction of iodate that has been converted to triiodide is most time dependent and pH dependent at pH between 3 and 4.

Since iodide was present in large excess, its concentration may be considered constant in each experiment. If the rate law in pure solutions (eq 2) is also valid in this study, the equation can be transformed to

$$dA/dt = k[I^-]^2[H^+]^2(A_f - A) \quad (5)$$

where  $A_f$  is the absorbance when all iodate is converted to triiodide. Then

$$\ln(A_f - A) = -k[I^-]^2[H^+]^2t + \ln A_f \quad (6)$$

since  $A = 0$  at  $t = 0$ . For the experimental data obtained in artificial seawater,  $\ln(A_f - A)$  was linearly related to  $t$ , suggesting that the rate law (eq 2) may also be valid in artificial seawater. The rate constant was determined from the slope of this line to be  $5 \times 10^{10} \text{ M}^{-4} \text{ min}^{-1}$ , a value that is similar to that reported by Dushman (12). Thus, in the determination of total residual chlorine in seawater, the contribution from iodate will be variable and unpredictable if the pH is not maintained at exactly the same value in all analyses and if the time between the addition of iodide

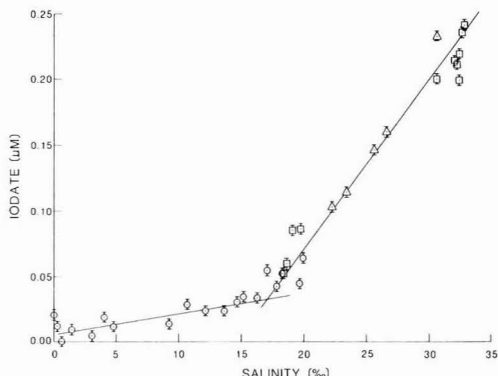


**Figure 2.** Concentration of iodate in the James River estuary and the southern Chesapeake Bay. Samples were collected on Oct. 31, 1979 (○), Jan. 18, 1980 (□), and Mar. 20, 1980 (▲).

and the pH 4 buffer to a sample and the titration with phenylarsine oxide is not identical in all cases.

The interference of iodate can be circumvented by decreasing the pH in the analytical scheme (3) to less than 3. If this modification is used, any iodate formed from the oxidation of iodide by hypobromite will be converted to triiodide. This amount of triiodide will be identical with that generated by reacting hypobromite directly with excess iodide. Thus, this source of error will be eliminated. The concentration of naturally occurring iodate may be determined from the absorbance of triiodide formed via the Dushman reaction in the water prior to chlorination (10, 14, 15). An amount equivalent to 3 times the concentration of iodate must then be subtracted from the apparent total residual chlorine concentration determined at pH 2 to give the real concentration of total residual chlorine.

The magnitude of the positive blank caused by naturally occurring iodate is also dependent on the natural variability of the concentration of iodate in estuarine waters and seawater. The concentrations of iodate in the James River and the southern Chesapeake Bay are shown in Figure 2. The concentration varied from 0 to  $0.24 \mu\text{M}$  for salinities between 0‰ and 33‰. The concentrations at the high salinities were similar to those reported in the surface waters in many parts of the oceans (14, 16–18) and correspond to a blank of  $0.05 \text{ mg L}^{-1}$  ( $0.7 \mu\text{equiv L}^{-1}$ ) in total residual chlorine. The concentration of iodate is not linearly related to salinity. The relationship may be described approximately with two linear lines with an inflection point at about 17‰. This nonlinear relationship may be caused by a nonconservative behavior of iodate. Neal and Truesdale (19) suggested that iodate may be removed from solution by sorption onto particulates. Alternatively, it may be the result of three end member mixing: James River water (0‰), water from northern Chesapeake Bay (17‰), and Atlantic Ocean water (33‰).

Recently, Smith and Butler (20) reported the speciation of iodine in the Yarra River, Australia. This is the only published systematic study on dissolved iodine in rivers. They observed that iodate was linearly related to salinity from 0‰ to 35‰. The maximum iodate concentration observed was  $0.22 \mu\text{M}$ . Thus, in both studies, the iodate concentration approached zero as salinity approached zero. However, since the concentration of iodate in surface seawater is variable (17), the relationship between iodate and salinity may vary from estuary to estuary. Temporal variations of the concentration of iodate during the sam-

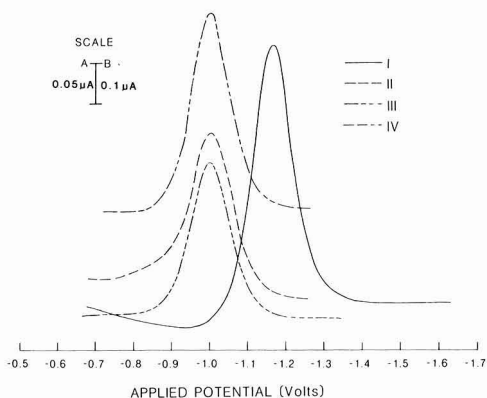


**Figure 3.** Selected polarograms of chlorinated seawater with various treatments: (I) chlorinated seawater; (II) 4 min after the addition of 0.1 mL of 5% (w/v) KI solution to the chlorinated seawater; (III) 237 min after the addition of KI; (IV) addition of 0.7 mL of 50  $\mu\text{M}$  potassium iodate to the solution. Trace I was recorded with a full scale of 0.5  $\mu\text{A}$  (scale A). The other traces were recorded with a full scale of 1  $\mu\text{A}$  (scale B) with various offsets.

**Table I.** Polarogram of Chlorinated Seawater under Various Conditions

sample	applied voltage, <sup>a</sup> V	current, <sup>b</sup> $\mu\text{A}$
A. chlorinated seawater	-1.17	0.34
B. chlorinated seawater with added iodide after various periods of time (min)		
4	-1.00	0.39
9	-1.00	0.36
16.5	-1.00	0.36
34	-1.00	0.40
63	-1.00	0.37
237	-1.00	0.37
C. chlorinated seawater with added iodide and various volumes of 50 $\mu\text{M}$ potassium iodate (mL)		
0.1	-1.00	0.39
0.3	-1.00	0.42
0.5	-1.00	0.45
0.7	-1.00	0.48

<sup>a</sup> Applied voltage at current peak. <sup>b</sup> Current at current peak.

pling period of 5 months may be yet another factor affecting the relationship between salinity and iodate concentrations in this study. Thus, the blank due to iodate cannot be estimated a priori and should be determined for each study.

**Oxidation of Iodide to Iodate with Hypobromite.** The formation of iodate was followed by measuring its polarograms. Data are shown in Figure 3 and Table I. In the absence of iodide, chlorinated seawater exhibited a current peak at -1.17 V (Figure 3, I). This peak was not due to iodate as iodate was absent; however, the position of the peak was very similar to that of iodate in natural seawater (-1.1 V) (21). The addition of iodide to the chlorinated seawater led to a shift of the current maximum to -1.0 V, and the peak height did not change significantly in 4 h. The addition of iodate to the solution caused an increase in peak height at -1.0 V, which was directly proportional to the concentration of added iodate in the solution.

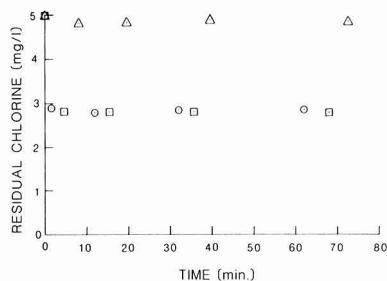


**Figure 4.** Concentration of residual chlorine in artificial seawater buffered at pH 4 and in the presence of iodide after various times of storage. The concentrations were determined by amperometric titrations at pH 2 ( $\Delta$ ), 4 ( $\circ$ ), and 7 ( $\square$ ).

The peak at -1.17 V in chlorinated seawater in the absence of added iodide may be due to hypobromite, which is the most dominant oxidizing species under these conditions. (Molecular oxygen was removed by bubbling nitrogen through the solution.) The species that yielded the current peak at -1.0 V upon the addition of iodide has not yet been identified. There were at least two possibilities. In the presence of iodide, hypobromite might be converted to hypoiodite, leading to a new current peak. Alternatively, hypobromite might oxidize iodide directly to iodate as suggested by Carpenter et al. (3). In the latter case, the current peak would be caused by iodate. The latter possibility was supported by the fact that the addition of iodate increased the peak height at the same applied potential. Since the peak height at -1.0 V did not change with time, the latter explanation implied that the formation of iodate from hypobromite and iodide terminated after the first 4 min, the time that has elapsed when the first polarogram was recorded. The apparent amount of iodate formed could be estimated by the standard addition method to be about 6  $\mu\text{M}$ . If all hypobromite was converted to iodate, the maximum amount of iodate that could have been formed was 26.3  $\mu\text{M}$ .

The initial chlorine concentrations determined by the amperometric and iodometric titrations were 5.75 and 5.45  $\text{mg L}^{-1}$ , respectively. The difference of 0.3  $\text{mg L}^{-1}$  could be explained by the combined uncertainties of  $\pm 8\%$  of these two methods. The concentrations at the end of the experiment were correspondingly 4.39 and 5.04  $\text{mg L}^{-1}$ . The decrease in the residual chlorine concentration was probably due to chlorine demand in artificial seawater as a result of the presence of trace quantities of organic compounds. However, when iodometric titration was used, only 7% of chlorine was consumed, whereas when amperometric titration was used, about 24% of chlorine was lost. The difference in the final concentrations as determined by the two methods was 0.65  $\text{mg L}^{-1}$ . If this difference were due to the formation of iodate, since iodate was included in the iodometric method but was only partially or not included at all in the amperometric method, then the amount of iodate formed would be about 3  $\mu\text{M}$ . This value was consistent with the value of 6  $\mu\text{M}$  estimated from the polarographic studies.

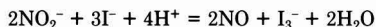
When iodide was allowed to react with the added chlorine in artificial seawater at pH 4 or above, any iodate formed should not have reacted readily with the excess iodide to produce triiodide. Thus, if aliquots of the solutions were adjusted to pH values of 7 and 4 and then titrated with phenylarsine oxide, any iodate formed would lead to a lower residual chlorine concentration. On the other hand, if an aliquot were adjusted to pH 2, a total recovery of residual chlorine would be expected. The re-



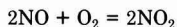
sults of such an experiment at pH 4 are shown in Figure 4. When the sample was titrated at pH 2, the concentration was not significantly different from the control, which was prepared by adding a volume of a stock sodium hypochlorite solution to an identical volume of deionized water. However, when the samples were titrated at pH 4 and 7, a 40% loss in residual chlorine was observed. This loss apparently occurred in the first few minutes of contact of the iodide and the added chlorine, as no further decrease in concentration was observed afterward. Titrations at pH 4 and 7 gave the same concentrations. Similar results were obtained in artificial seawater buffered to pH 7.0, 8.3, and 9.0. When iodide was allowed to react with the added chlorine in seawater buffered at pH 2, titrations at all three pH values yielded identical results, which were not noticeably different from the control. This is expected as triiodide will be the only product at such a low pH. The increased recovery of residual chlorine in chlorinated artificial seawater buffered at a pH of 4 or above by amperometric titration at pH 2 rather than pH 4 or 7 is consistent with the suggestion of Carpenter et al. (3) that hypobromite may oxidize iodide to iodate and that the traditional amperometric titrimetric method for the determination of residual chlorine may lead to gross underestimations.

In my previous study (6), it was observed that when iodide was added to a chlorinated solution of 1 mM sodium borate and 0.84 mM bromide at pH 8.7, the concentration of residual chlorine measured by a titration at pH 4 decreased slowly with time. Titrations at pH 2 did not give higher concentrations, indicating that no iodate was formed. In this study, increased concentrations of residual chlorine were detected in artificial seawater buffered at a similar basic pH if it was titrated at pH 2. A plausible cause of this apparent discrepancy may be the difference in ionic strength of the reaction mixtures although this explanation is by no means definitive. The mechanism and rate of oxidation of iodide to iodate by hypobromite are not well known. Tomicek and Filipovic (22) suggested that iodide is first oxidized to hypoiodite, which may disproportionate to form iodate and iodide (23). However, hypoiodite may also decompose to form iodide and oxygen (24). The relative rates of these two reactions may then determine the products formed. Li and White (25) observed that the rate of the disproportionation reaction increases with increasing ionic strength. Thus, the formation of iodate should be favored in artificial seawater relative to a dilute borate solution.

**Interference of Nitrite.** Nitrite is a well-known interference in iodometric titrations (13). In acidic solutions, nitrite oxidizes the excess iodide to triiodide:



The extent to which this reaction may be driven to the right is obviously pH dependent. The nitrite consumed can be regenerated from the air oxidation of nitric oxide:



Thus, the magnitude of the interference increases with time and can potentially be significant even in the presence of only a small amount of nitrite. In the standard amperometric method (1, 26), nitrite was not considered a significant source of interference, probably because the pH used (pH 3.5–4.5) is only mildly acidic. However, when lower and lower detection limits are sought, the effect of nitrite may become important even if only a small fraction of it has reacted with iodide.

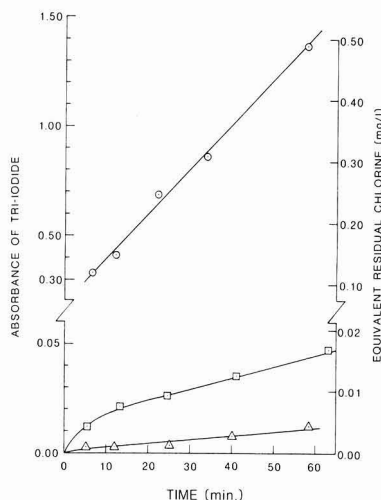


**Figure 5.** Oxidation of iodide to triiodide by nitrite at pH 2.66 (○), 3.93 (□), and 5.53 (△) as measured by the absorbance of triiodide at 353 nm.

The pH dependence of the interference of nitrite is shown in Figure 5 by following the absorbance of the triiodide formed. In all cases, the absorbances increased monotonically with time, indicating that triiodide was formed continuously at pH as high as 5.53. At the pH used in the present analytical scheme (pH 3.93), an amount of triiodide equivalent to that formed by 0.01 mg L<sup>-1</sup> (0.14 μequiv L<sup>-1</sup>) of residual chlorine was observed after 15 min. Although the nitrite concentration used in these experiments (10 μM) was somewhat elevated in comparison to those observed in surface seawaters in the oceans, similar concentrations may be observed in coastal waters, especially in the vicinity of sewage outfalls. Thus, interference from nitrite should be considered if concentrations below 0.1 mg L<sup>-1</sup> (1.4 μequiv L<sup>-1</sup>) are to be measured.

The interference of nitrite does not increase as a simple function of pH. When pH was decreased from 5.53 to 3.93, the absorbance increased only for several hundredths of an absorbance unit at any given time of reaction. However, when the pH was decreased from 3.93 to 2.66, the absorbance increased from several tenths to over one absorbance unit. An interference in excess of 0.1 mg L<sup>-1</sup> (1.4 μequiv L<sup>-1</sup>) of residual chlorine was observed in less than 10 min at pH 2.66. Thus, if a pH below 3 is to be used in the amperometric titration in order to circumvent the interference from iodate, nitrite must be carefully eliminated. The interference of nitrite increases with increasing concentrations of nitrite. In the absence of nitrite, the absorbance of a solution containing iodate was 0.059. In the presence of even 5 μM of nitrite, the absorbance increased about 6-fold after 1 min. At higher concentrations of nitrite, higher absorbance was observed.

Sulfamic acid has been used extensively for destroying nitrite in iodometric titrations (13) and for the spectrophotometric determination of iodate in seawater (10, 15) via the reaction



The effectiveness of sulfamic acid for the removal of the nitrite interference is shown in Figure 6. In this experiment, all the solutions contained 30 μM of nitrite and about 0.5 μM of iodate. The absorbance of the solution at 353 nm decreased with increasing amounts of added

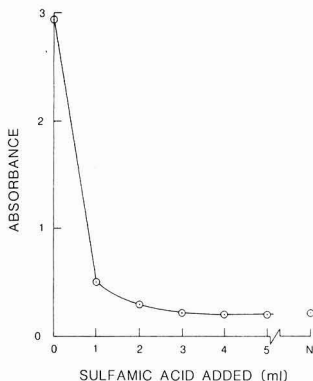


**Figure 6.** Absorbance of triiodide at 353 nm formed from a fixed concentration of iodate in the presence of  $30 \mu\text{M}$  of nitrite upon the addition of various volumes of 1% (w/v) sulfamic acid; N denotes the case where neither nitrite nor sulfamic acid was present in the solution.

sulfamic acid. A constant absorbance was recorded when 3 mL or more of 1% (w/v) sulfamic acid was added to the solution, and this absorbance was identical with that in a sample containing the same amount of iodate and no nitrite. A concentration of nitrite of  $30 \mu\text{M}$  is unlikely to occur in estuarine water and seawater.

#### Acknowledgments

K. Takayanagi and T. Oatts assisted during various parts of the experiments.

#### Literature Cited

- (1) Rand, M. C.; Greenberg, A. E.; Taras, M. J. "Standard Methods for the Examination of Water and Waste Water", 14th ed.; American Public Health Association: Washington, D.C., 1976.
- (2) Block, R. M.; Burton, D. T.; Gullans, S. R.; Richardson, L. B. In "Water Chlorination: Environmental Impact and Health Effects"; Jolley, R. L., Gorchev, H., Hamilton, D. H., Jr., Eds.; Ann Arbor Science: Ann Arbor, MI, 1978; Vol. 2, pp 351-360.
- (3) Carpenter, J. H.; Moore, C. A.; Macalady, D. L. *Environ. Sci. Technol.* **1977**, *11*, 992-994.
- (4) Crecelius, E. A.; Roesijadi, G.; Thatcher, T. O. *Environ. Sci. Technol.* **1978**, *12*, 1088.
- (5) Goldman, J. C.; Quinby, H. L.; Capuzzo, J. M. *Water Res.* **1979**, *13*, 315-323.
- (6) Wong, G. T. F. *Water Res.* **1980**, *14*, 51-60.
- (7) Carpenter, J. H.; Smith, C. A. In "Water Chlorination: Environmental Impact and Health Effects"; Jolley, R. L., Gorchev, H., Hamilton, D. H., Jr., Eds.; Ann Arbor Science: Ann Arbor, MI, 1978; Vol. 2, pp 195-208.
- (8) Wong, G. T. F.; Davidson, J. A. *Water Res.* **1977**, *11*, 971-978.
- (9) Lyman, J.; Fleming, R. H. *J. Mar. Res.* **1940**, *3*, 134-136.
- (10) Wong, G. T. F. *Deep-Sea Res.* **1977**, *24*, 115-125.
- (11) Heyrovsky, J.; Zuman, P. "Practical Polarography"; Academic Press: New York, 1968.
- (12) Dushman, S. *J. Phys. Chem.* **1904**, *8*, 453-481.
- (13) Kolthoff, I. M.; Belcher, R. "Volumetric Analysis III. Titration Methods. Oxidation-Reduction Reactions"; Interscience: New York, 1957.
- (14) Wong, G. T. F.; Brewer, P. G. *J. Mar. Res.* **1974**, *32*, 25-36.
- (15) Truesdale, V. W. *Mar. Chem.* **1978**, *6*, 253-273.
- (16) Wong, G. T. F.; Brewer, P. G. *Geochim., Cosmochim. Acta* **1977**, *41*, 151-159.
- (17) Tsunogai, S.; Hemmi, T. *J. Oceanogr. Soc. Jpn.* **1971**, *27*, 67-72.
- (18) Truesdale, V. W. *Mar. Chem.* **1978**, *6*, 1-13.
- (19) Neal, C.; Truesdale, V. W. *J. Hydrol. (Amsterdam)* **1976**, *31*, 281-291.
- (20) Smith, J. D.; Butler, E. C. V. *Nature (London)* **1979**, *277*, 468-469.
- (21) Herring, J. R.; Liss, P. S. *Deep-Sea Res.* **1974**, *21*, 777-783.
- (22) Tomicek, O.; Filipovic, P. *Coll. Czech. Chem. Commun.* **1938**, *10*, 340-352.
- (23) Morgan, K. J. *Q. Rev.* **1954**, *8*, 123-146.
- (24) King, C. V.; Jette, E. J. *Am. Chem. Soc.* **1930**, *52*, 608-610.
- (25) Li, C. H.; White, C. F. *J. Am. Chem. Soc.* **1943**, *65*, 335-339.
- (26) Environmental Protection Agency, Cincinnati, Ohio, "Methods for Chemical Analysis of Water and Wastes"; Manual EPA-600-4-79-020, 1979.

Received for review November 9, 1981. Revised manuscript received May 20, 1982. Accepted July 19, 1982. This work was supported by the Department of Energy through Contract No. EE-77-S-05-5572.

# Chlorination of Estuarine Water: The Occurrence and Magnitude of Carbon Oxidation and Its Impact on Trace-Metal Transport

James G. Sanders

Academy of Natural Sciences, Benedict Estuarine Research Laboratory, Benedict, Maryland 20612

■ The application of chlorine to estuarine water usually resulted in the oxidation of a finite quantity of organic carbon, averaging 35  $\mu\text{mol/L}$ . The oxidation may be salinity dependent; with one exception, all samples of >5‰ salinity showed a loss of carbon. In every case, the quantity of carbon associated with the smallest molecular weight fraction increased after chlorination, likely because of scission of macromolecules. However, copper distributions within various size fractions of natural organics did not change significantly. The quantity of carbon oxidized is small in comparison to the total complexation capacity of estuarine waters. Therefore, significant shifts in metal speciation should not occur due to loss of organic complexes. Coprecipitation with other metal oxyhydroxides does occur, may be enhanced by chlorination, and can represent a significant transport mechanism.

## Introduction

The addition of chlorine to estuarine systems via sewage effluent or cooling water discharges from power plants affects the quantity and structure of organic compounds present in natural systems. Although the chemistry of chlorine in seawater is still being unraveled, chlorine degradation is accompanied by the formation of volatile halocarbons (1, 2), deamination (3), and oxidation of organic carbon to  $\text{CO}_2$  (4-6). Of these reactions, the latter is by far the most important (5, 6).

Naturally occurring organic compounds are of great importance in determining the chemical speciation of trace metals (7, 8); thus, the oxidation of carbon by chlorination could have significant impact upon the bioavailability and potential toxicity of trace metals to the biota (9-11). For example, chlorination of Biscayne Bay water significantly reduced its copper complexation capacity (12), suggesting that the organic fraction involved in the complexation of Cu may be the same fraction oxidized during chlorine degradation.

Because of this possible impact on trace-metal availability, I have focused on the interactions between chlorination, dissolved organic carbon (DOC), and trace metals in the vicinity of a power plant utilizing estuarine water for cooling purposes. This paper describes the effects of chlorine on the concentration and molecular size of natural organic compounds from this system and its impact upon organic-metal associations.

## Materials and Methods

**Sample Sites and Collection.** The majority of samples were taken from the Patuxent River, a subestuary of the Chesapeake Bay (Figure 1). Samples were collected between Western Branch and the estuary mouth (Solomons) covering a salinity range of 0-20‰. Samples were taken in all four seasons; water temperatures ranged from -1 to 28 °C (Table I). Two additional samples were collected from the Potomac River at Sandy Point (5‰ salinity) and Mathias Point (10‰ salinity) during the spring of 1981.

Samples were collected by hand just below the surface in acid-washed 20-L polyethylene carboys. The carboys were rinsed with river water before sample collection.

On two occasions, samples were collected from the intake and discharge canals of the Chalk Point Power Station (PEPCO) and surrounding areas. Five replicate 200-mL samples were collected at each site.

The samples were brought into the laboratory and stored untreated at 20 °C until used (usually less than 3 days). Before the water was used in an experiment, it was decanted from the carboys and filtered through glass-fiber filters (Gelman GF/C) in acid-washed plasticware. The filtered water was then placed in acid-washed 4-L polypropylene jugs for manipulation.

**Chlorination.** After the samples were placed in the jugs, NaOCl (5% stock solution) was added to various levels (Table II). The actual concentration of the stock solution was analyzed by amperometric titration (13) before each experiment. Secondary standard solutions were prepared according to the actual concentrations measured. A 30-mL sample was removed from each jug before chlorinating for an initial measurement of dissolved organic carbon (DOC) concentration (see below). The experimental solutions were allowed to sit on a lighted laboratory bench for 10-30 days at 20 °C to allow the chlorine to degrade. Degradation times are listed in Table II. On two occasions, experiments were sampled for DOC while underway. In all experiments, 30-mL samples were removed at completion for DOC analysis. Duplicate samples were removed at the same time for analysis of total copper concentrations (see below).

**Ultrafiltration.** After the completion of the experiment, the control sample and the sample that received the highest level of chlorination were fractionated by using Amicon ultrafilters (1000-100000 nominal molecular weight). The ultrafilters were handled and stored according to manufacturer's instructions and cleaned before use as follows: an overnight soak in distilled  $\text{H}_2\text{O}$ , three 1-h soaks in distilled  $\text{H}_2\text{O}$ , 1-h soak in 10%  $\text{HNO}_3$ , four 30-min rinses in distilled  $\text{H}_2\text{O}$ , and a final rinse in "carbon-free" (Baker HPLC-grade)  $\text{H}_2\text{O}$ . The pressure cells were all plastic in construction and were rigorously acid cleaned for each use. The conventional silicone rubber o-rings were replaced with acid-washed viton o-rings.

The samples were fractionated in the following manner. A 400-mL sample was placed into the cell containing the ultrafilter with the *smallest* molecular weight cutoff. Only the filtrate was retained; the concentrate was discarded. The first 20 mL of filtrate was discarded, then triplicate samples for DOC and duplicate samples for Cu analysis were taken. The cells were then dismantled, rinsed with carbon-free water, and reassembled with the next largest filter in place. A new 400-mL sample was placed in the cell and the procedure repeated. This *reverse* fractionation scheme minimizes a number of problems inherent to sequential fractionations and/or analysis of concentrates, most importantly, metal and organic contamination, membrane polarization, and the attraction between organic molecules in concentrated solutions. Each sample was fractionated once.

**DOC Analysis.** The concentration of dissolved organic carbon (DOC) in various samples was analyzed by using a persulfate oxidation technique similar to Menzel and

Table I. Location of Water Samples Used for Experimental Manipulations

sample	river	location	season	salinity, ‰	temp, °C
80-1	Patuxent	Solomons	fall	19	4
80-2	Patuxent	Mill Creek	winter	0	0
81-3	Patuxent	Solomons	winter	20	-1
81-4	Potomac	Sandy Point	spring	5	12
81-5	Potomac	Mathias Point	spring	10	12
81-6	Patuxent	Solomons	summer	18	27
81-7	Patuxent	Broomes Island	summer	16	27
81-8	Patuxent	Benedict	summer	12	28
81-9	Patuxent	Western Branch	fall	0	20
81-10	Patuxent	Nottingham	fall	3	22
81-11	Patuxent	Chalk Point	fall	10	24
81-12	Patuxent	Solomons	fall	20	14
81-CP1	Patuxent	Chalk Pt. intake, discharge	summer	12	28
81-CP2	Patuxent	Chalk Pt. intake, discharge	fall	11	13

Table II. Initial Chlorine Concentrations (in mg/L as Chlorine) and Duration of Experiments

sample	chlorination levels, mg/L	duration, days
80-1	0, 0.5, 1, 5, 10	10
80-2	0, 0.5, 1, 5, 10	14
81-3	0, 1, 5, 10	14
81-4	0, 1, 5, 10	3, 10
81-5	0, 1, 5, 10	1, 2, 3, 5, 10
81-6	0, 10	20
81-7	0, 10	20
81-8	0, 10	20
81-9	0, 10	20
81-10	0, 10	10
81-11	0, 10	10
81-12	0, 10	30

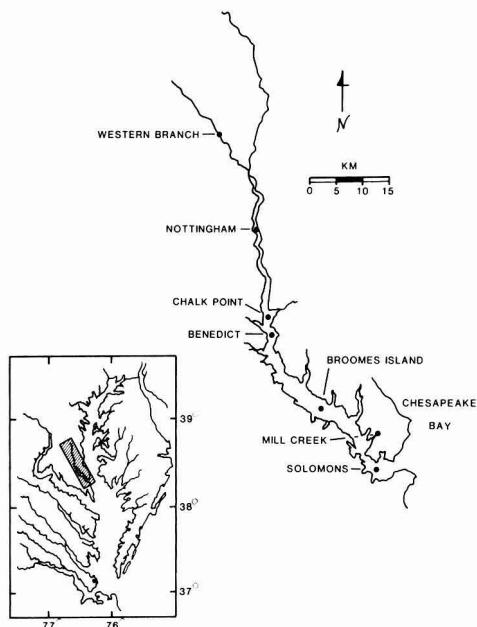


Figure 1. Sampling locations in the Patuxent River. The inset shows the river's location in the Chesapeake Bay area.

Vaccaro (14). The analyses were performed on an Oceanography International 524C carbon analyzer. Usual precision was less than 4%. Each sample was analyzed in triplicate. If the precision for any group was greater

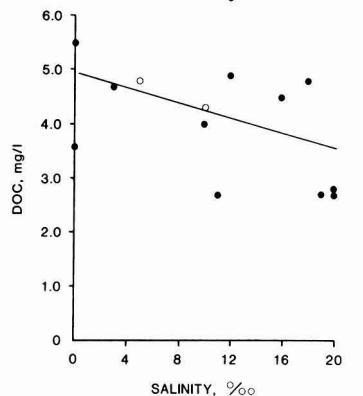


Figure 2. DOC concentrations vs. salinity in the Patuxent (●) and Potomac (○) Rivers, 1980-1981. The equation for the regression is  $Y = -0.069X + 4.93$ ;  $r^2 = 0.18$ .

than 10%, the analyses were repeated. Standard carbon samples (0-50 μg of C) were prepared in large batches from oven-dried potassium biphthalate and were analyzed along with each batch of samples.

**Copper Analysis.** The concentration of total dissolved Cu in the various samples was determined after preconcentration (chelation and solvent extraction (15)). Duplicate samples were collected in rigorously cleaned (16) Teflon bottles, acidified with 0.1% "Ultrex" HNO<sub>3</sub>, concentrated, and analyzed by graphite furnace atomic absorption spectrophotometry. Limits of detection were approximately 0.2 μg/L; precision of the analysis at 1 μg/L was 10%.

Results

**DOC in the Patuxent and Potomac Estuaries.** Dissolved organic carbon concentrations in the Patuxent River ranged from 2.7 to 6.0 mg/L, with an average of 4.1 mg/L (Table III). DOC concentrations decreased with increasing salinity, but the relationship was not significant ( $0.10 > p > 0.05$ ; Figure 2). Significantly higher concentrations occurred during summer and fall when water temperatures were greater than 15 °C (samples 81-6 through 81-11 and 81-CP1).

Only two samples were taken in the Potomac River. Concentrations in these samples were similar (Table III).

**Molecular Weight Distributions.** With the exception of samples 80-1 and 81-12, all samples were fractionated by using ultrafiltration. However, due to equipment

Table III. Initial DOC Concentrations (in mg/L as Carbon) and Molecular Weight Distributions (as % of Total Carbon That Passes Through the Filter of Interest) in Both Control and Chlorinated Water Samples

sample	salinity, ‰	DOC, mg/L	control sample, % DOC				chlorinated sample, % DOC			
			<1000 <sup>a</sup>	<10 000 <sup>a</sup>	<50 000 <sup>a</sup>	<100 000 <sup>a</sup>	<1000 <sup>a</sup>	<10 000 <sup>a</sup>	<50 000 <sup>a</sup>	<100 000 <sup>a</sup>
80-1	19	2.7								
80-2	0	3.6	28.3	26.6	51.7	91.1	29.2	39.6	65.5	93.9
81-3	20	2.8	41.6	45.3	73.4	91.4	44.4	54.2	81.0	89.5
81-4	5	4.8	19.9	34.4	72.5	84.6	23.6	46.1	68.8	86.8
81-5	10	4.3	37.2	82.0		86.9	38.8	84.0		90.2
81-6	18	4.8								
81-7	16	4.5								
81-8	12	4.9								
81-9	0	5.5		92.7		86.3		88.1		98.1
81-10	3	4.7		85.8		87.1		87.8		89.9
81-11	10	4.0		89.5		91.7		96.5		91.9
81-12	20	2.7								
81-CP1	12	6.0								
81-CP2	11	2.7								

<sup>a</sup> Molecular weight.

Table IV. Loss of Organic Carbon in Chlorinated Estuarine Samples

sample	initl DOC, mg/L	C lost <sup>a</sup>		mol of C lost/mol of Cl <sub>2</sub>
		mg/L	μM	
80-1	2.7	0.41	34.0	0.25
80-2	3.6	0	0	
81-3	2.8	0 <sup>b</sup>	0 <sup>b</sup>	
81-4	4.8	0	0	
81-5	4.3	0.29	24.2	0.11
81-6	4.8	0.57	47.5	0.35
81-7	4.5	0	0	
81-8	4.9	0.58	48.3	0.36
81-9	5.5	0	0	
81-10	4.7	0	0	
81-11	4.0	0.38	31.7	0.24
81-12	2.7	0.39	32.5	0.24
81-CP1	6.0	0.33 <sup>c</sup>	27.5 <sup>c</sup>	
81-CP2	2.7	0.14 <sup>c</sup>	11.7 <sup>c</sup>	

<sup>a</sup> C lost in sample chlorinated with 10 mg/L. <sup>b</sup> Control samples lost C; see text. <sup>c</sup> "Apparent" C lost: see text.

failure, samples 81-6 through 81-8 were not separated successfully. In addition, Amicon stopped making the <1000 mol wt filter in 1981; thus, samples 81-9 to 81-11 do not have this fraction.

The results of the fractionation of control samples is listed in Table III. These fractionations were not run immediately; rather, they were done after the chlorination experiment had run its course. Therefore, molecular weight distributions may have changed somewhat during the experiment's duration. Although the data are not extensive, there does not appear to be a relationship dependent upon salinity. As with DOC, samples collected at temperatures above 15 °C (81-6 through 81-11) have a greater percentage of carbon in lower molecular weight fractions (Table III).

**Chlorination of Estuarine Water.** Natural water samples collected and chlorinated varied widely in their reactions to chlorination. The response of the samples was monitored primarily in two ways: (1) loss of organic carbon (as measured by DOC); (2) change in the molecular weight distribution of carbon. Each of these is discussed separately below.

**Loss of Organic Carbon.** Natural waters varied in their loss of carbon due to chlorination, from no measurable carbon loss to nearly 50 μmol of C lost/L, or 0-0.6 mg/L (Table IV). Samples that exhibited oxidation of carbon averaged 34.7 μM (0.42 mg/L) or 0.25 mol of C/mol of Cl<sub>2</sub> at 10 mg/L. The amount of carbon lost was not

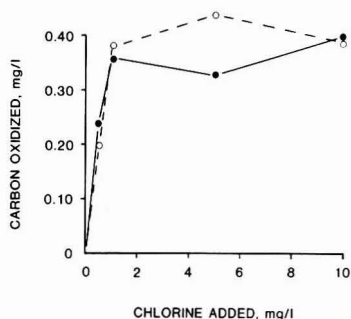


Figure 3. DOC loss vs. concentration of chlorine added in samples 80-1 (—) and 81-12 (---).

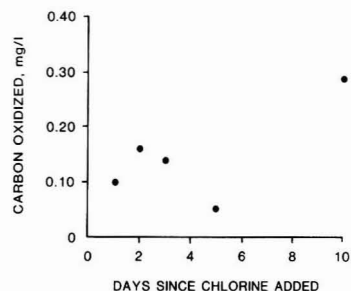


Figure 4. DOC loss with time in sample 81-5, chlorinated to 10 mg/L.

dependent upon the concentration of DOC. The quantity of carbon oxidized also was not dependent upon the level of chlorination. In the two instances when variable levels of chlorination resulted in carbon loss (80-1, 81-12), 1 mg/L was sufficient to cause maximum carbon oxidation (Figure 3). Carbon loss was dependent upon salinity; with one exception, loss occurred in all samples with salinity >5‰ and did not occur in samples of lower salinity (Table IV).

Carbon oxidation appears to increase slowly over time (Figure 4), although the available data are not extensive.

**Molecular Weight Distributions.** With one exception (81-9), chlorinated water samples contained a greater percentage of organics in the <1000 and <10 000 mol wt fractions (Figure 5, Table III). This phenomenon was apparent in all samples, even those that exhibited no overall loss of carbon. The difference between control and chlorinated molecular weight distributions was not large;

**Table V. Total Dissolved Cu Concentration and Its Distribution in Molecular Weight Fractions in Control and Chlorinated Water Samples**

sample	Cu, $\mu\text{g/L}$	control sample, %Cu			chlorinated sample, %Cu		
		<1000 <sup>a</sup>	<10 000 <sup>a</sup>	<100 000 <sup>a</sup>	<1000 <sup>a</sup>	<10 000 <sup>a</sup>	<100 000 <sup>a</sup>
80-1							
80-2							
81-3	2.6	41.5	61.9	86.5	42.9	68.2	98.8
81-4	1.1	21.6	24.3	66.2	14.5	14.5	61.4
81-5	1.6	32.5		90.4	32.6		68.5
81-6	3.8						
81-7	3.4						
81-8	4.1						
81-9	4.0		72.5	72.5		78.6	65.0
81-10	2.0		80.8	83.1		51.5	81.0
81-11	2.0		65.7	86.7		42.4	42.4
81-12							

<sup>a</sup> Molecular weight.

**Table VI. Bacterial Growth in Sample 81-3, Which Exhibited a Reverse Pattern of Carbon Loss**

Cl added, mg/L	C lost, mg/L	bacterial density, cells/mL	
		AODC	plate counts
0	0.35	$2.5 \times 10^7$	$9.2 \times 10^5$
1	0.37	$3.9 \times 10^6$	$1.2 \times 10^5$
5	0	$7.8 \times 10^5$	$5.3 \times 10^4$
10	0	$3.8 \times 10^5$	~0

chlorinated samples contained 2–32% more carbon ( $\bar{x}$  = 14%) in the <10 000 mol wt fraction.

The total dissolved Cu in each experiment and the percentage associated with each molecular weight fraction is listed in Table V. In most instances, approximately 30% of the Cu was associated with the <1000 mol wt fraction and 70% with the <10 000 mol wt fraction. There was no significant difference between the distributions in control and chlorinated samples.

**Heterotrophic Oxidation of Carbon.** The reaction of sample 81-3 to chlorination was quite different than expected and led to a change in the experimental design. In this instance, the control sample lost significant amounts of carbon (0.35 mg/L); similar concentrations of carbon were lost at the lowest level of chlorination. No carbon was lost from samples chlorinated with 5 or 10 mg/L. This reversal suggested that biological activity might be the cause of the carbon loss; therefore, the level of bacterial activity was tested in each sample by using two techniques, acridine orange direct counts (AODC (17)) and dilution plate counts. Both techniques indicated that bacterial levels in the samples were inversely proportional to the concentration of chlorine added (Table VI). Because of these results, all subsequent experiments were autoclaved after filtration and allowed to cool overnight before chlorine was added. Autoclaving did not significantly affect DOC levels; it is not known what effect it may have on molecular weight distributions. Other than this instance, DOC concentrations in unchlorinated samples did not change significantly during the experiments.

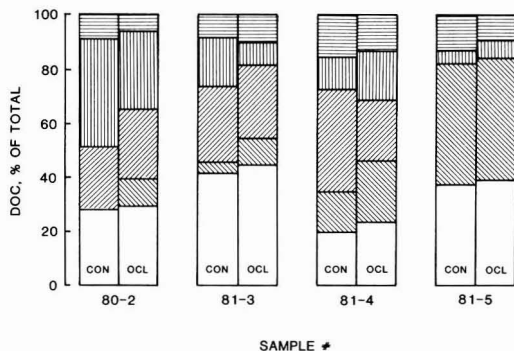


**Figure 5.** Distribution by molecular weight fractions of DOC (as percent of total DOC) in control (CON) and chlorinated (OCL) water samples: □, <1000; \/, 1000–10 000; //, 10 000–50 000; |||, 50 000–100 000; ≡, >100 000 mol wt. Samples 81-9 to 81-11 are not shown but are included in Table III.

**DOC in the Vicinity of the Chalk Point Power Station.** The DOC concentrations in the vicinity of the Chalk Point plant were significantly lower in the discharge canal than in the intake area (Table VII). Samples from the middle of the river above the plant were essentially the same concentration as the intake samples and also significantly higher than the discharge area. The “apparent” loss of DOC between the intake and discharge averaged 0.24 mg/L (20  $\mu\text{M}$ ).

*Discussion*

**DOC in the Patuxent River.** The range of DOC concentration within Patuxent River samples (2.7–6.0 mg/L) is well within the ranges reported for other estuarine areas on the Atlantic coast of the U.S. (18–21). The Patuxent River had been sampled previously (22), and the range of total organic carbon (TOC) concentration was similar (1.9–4.0 mg/L).

The difference between “summer” (>15 °C) and “winter” (<15 °C) DOC concentrations in this study was significant;

**Table VII. DOC Concentrations in the Vicinity of the Chalk Point Power Station and the “Apparent” Loss of Carbon in Cooling Waters<sup>a</sup>**

sample	DOC, mg/L $\pm$ SD			“apparent” DOC loss	
	intake area	discharge canal	above plant	mg/L	$\mu\text{M}$
81-CP1	6.35 $\pm$ 0.25	6.02 $\pm$ 0.20		0.33	27.5
81-CP2	2.74 $\pm$ 0.12	2.60 $\pm$ 0.04	2.72 $\pm$ 0.04	0.14	11.7

<sup>a</sup> In each case, the difference between means is significantly different ( $p < 0.05$ ; Student’s *t* test).

summer concentrations averaged 4.9 mg/L, while winter samples averaged 2.9 mg/L (Table III). Sigleo and Helz (22) also reported higher (but not significantly so) concentrations in summer samples taken from the Patuxent River. The seasonal difference likely is due to increased biological productivity during the warmer months. The standing crop of phytoplankton and zooplankton within the river increase by 1–2 orders of magnitude from winter to summer; therefore, it is not unreasonable to assume that higher organism densities will lead to higher DOC concentrations.

The colloidal material within the river is dominated by inorganic terrestrial material during the winter and by autochthonous organic compounds during the summer (22); it is possible that the carbon component of this material undergoes a similar shift. A shift from terrestrial to autochthonous compounds could explain the larger percentage of carbon in the smallest molecular weight fraction during summer months. However, Sigleo et al. (23) conclude that *in situ* microorganisms are the primary source of colloidal organic material in the Patuxent River at all times.

**Oxidation of Organic Carbon by Chlorination.** The application of chlorine to estuarine waters usually resulted in oxidation of a finite quantity of carbon. The studies described here suggest that this oxidation may be influenced by salinity. With one exception, all samples of salinity >5‰ showed a loss of carbon. Salinity dependence may be due to differing types of organic matter present at varying salinities. Colloidal material from the Patuxent River varies greatly in %C and ash and in its empirical formula when sampled from fresh water to the river mouth (6). It is likely that the percentage of carbon present in compounds resistant to oxidation varies also. An alternative explanation is that bromine substitution for chlorine, which is virtually instantaneous at salinities >5‰, provides a suite of compounds that are stronger oxidants than the chlorine compounds they replace (2).

Similar quantities of carbon were oxidized in Chesapeake Bay waters in an earlier study (6). In that study, samples with salinities ranging from 0.2 to 18‰ had losses of 40–50  $\mu\text{M}$  carbon. Helz et al. (5) also found comparable releases of  $\text{CO}_2$ , approximately 35  $\mu\text{M}$ , from chlorination of Patuxent River water (0.3‰).

At low concentrations of chlorine (0.5–1 mg/L) the quantity of carbon oxidized in the present experiments was dependent upon chlorine concentration, with a ratio of 2.5 mol of C/mol of  $\text{Cl}_2$ . Above 1 mg/L chlorine, the quantity of carbon oxidized does not increase, indicating that only a portion of the DOC is "available" in an oxidizable form.

Another effect of chlorination is the significant increase in carbon associated with lower molecular weight fractions (Table III). In every chlorinated sample, the percentage of carbon in the <1000 mol wt fraction increased an average of 8%, and in all but one sample, there was an average increase of 14% in the <10000 mol wt fraction. Similar increases in the <1000 mol wt fraction were noted after chlorination in Chesapeake Bay and Patuxent River samples (6). They suggest that the increase is due to scission of macromolecules (24); I concur. It is interesting that the increase in smaller molecular weight fractions occurred in every chlorinated sample, not just in samples that exhibited carbon oxidation. Therefore, the breakage of large molecules may be a more common effect of chlorination than carbon oxidation.

**Trace-Metal Distribution in Unchlorinated and Chlorinated Samples.** Copper concentrations in the Patuxent River are quite high (Table V), resulting largely

from Cu inputs from the Chalk Point cooling system (600 Kg of Cu/year (25)) and from greatly reduced river flows during 1980–1981. Chlorination did not affect either the total Cu concentration (with one exception; see below) or its distribution in the various molecular weight fractions, even though the distribution of DOC did shift toward lower molecular weight fractions. The complexation capacity of estuarine and coastal marine waters is in the range of 10–300  $\mu\text{g/L}$  (12, 19, 26); therefore, a much larger quantity of carbon likely would have to be oxidized to substantially reduce the complexation capacity. Carpenter and Smith (12) demonstrated a significant reduction (50–100%) in complexation capacity in Biscayne Bay after chlorination. They were working with water containing only 6–10  $\mu\text{g/L}$  complexation capacity, however. Complexation capacity in the Patuxent likely is much higher.

A number of unusual events occurred during these experiments; of particular note was the formation of a visible precipitate in the chlorinated half of sample 81-8. No precipitate was visible in the unchlorinated control half. The chlorinated and control samples were filtered at the end of the experiment and the filters acid digested. The bulk composition of this particulate was not identified but contained 1130 ng of Cu, equivalent to 750 ng/L, or approximately 20% of the total Cu present in the sample. The control filter contained approximately 75 ng of Cu. Repeat attempts to produce another precipitate in water of similar salinity from the same region failed. Although this only occurred once, it poses an interesting mechanism for Cu transport in the vicinity of power plants.

Chlorination of natural water samples causes oxidation of reduced metals, particularly Mn and Fe species, leading to their precipitation as oxyhydroxides (6). The filter digests in the present study contained large amounts of Mn; the precipitate in the chlorinated sample contained 19.6  $\mu\text{g}$  of Mn, corresponding to 26  $\mu\text{g/L}$  precipitated. The control sample contained much less precipitated Mn—approximately 1.2  $\mu\text{g}$ , or 1.6  $\mu\text{g/L}$ . This precipitation reaction, along with coprecipitation of Cu, could be the mechanism occurring here; indeed, it has been suggested as a major mechanism for Cu removal in the Patuxent (25).

**Potential Impact of Power-Generating Facilities.** Samples collected in the discharge canal of an actively chlorinating power plant contained significantly lower concentrations at DOC, 20  $\mu\text{M}$  on average. These values are similar to those obtained in lab experiments (Tables IV, VI) and suggest that the DOC loss is due to power plant operations. Natural variability in DOC concentrations, the loss of C to surface films in the warmer discharge canal, and the difficulty of obtaining representative water samples in both intake and discharge areas preclude an inference of causality, but the similarity between lab experiments and field observations is striking.

In the Patuxent River, a large portion of the river flow passes through the cooling system of the Chalk Point plant, especially in years of low flow (25). Assuming an average cooling water demand of 20  $\text{m}^3/\text{s}$  by the Chalk Point plant (25) and chlorination 7 months/year (27), an estimated total of  $2.0 \times 10^7$  mol of C/year could be oxidized as a result of passage through the Chalk Point plant alone. With an average river discharge rate of 17  $\text{m}^3/\text{s}$  (25) and an average DOC concentration of 4 mg/L (0.33 mmol/L; Table III), a total of  $1.8 \times 10^8$  mol/year of DOC passes downriver. Therefore, in an average year, about 11% of the DOC entering in the freshwater flow of the Patuxent River could be removed by the Chalk Point plant. In a year of extreme low flow (as was 1981), river discharge averages as low as 5  $\text{m}^3/\text{s}$ , and the amount of DOC re-

moved due to oxidation could approach 40%.

Therefore, chlorine-induced carbon oxidation probably represents a significant pathway for carbon transfer within the Patuxent River system. In rivers where cooling flows are not so important, the potential impact would probably be much less.

The loss of carbon should not have a significant impact upon organically associated metals as the complexation capacities of estuarine systems far exceed the quantity of carbon lost. Oxidation of reduced metals resulting from chlorination, and their subsequent precipitation, can be an important transport mechanism in an estuary as heavily impacted as the Patuxent River.

*Acknowledgments*

I thank C. D. Zamuda, D. A. Wright, and C. F. D'Elia for comments and suggestions and A. C. Sigleo, J. C. Means, and G. R. Helz for criticism of the manuscript.

*Literature Cited*

(1) Rook, J. J. *Water Treat. Exam.* 1974, 23, 234.  
 (2) Helz, G. R.; Hsu, R. Y. *Limnol. Oceanogr.* 1978, 23, 858.  
 (3) Helz, G. R.; Sugam, R.; Hsu, R. Y. In "Water Chlorination: Environmental Impact and Health Effects"; Jolley, R. L., Gorchev, H., Hamilton, D. H., Eds.; Ann Arbor Science: Ann Harbor, MI, 1978; Vol. 2, p 209.  
 (4) Eppley, R. W.; Renger, E. H.; Williams, P. M. *Estuarine Coast. Mar. Sci.* 1976, 4, 147.  
 (5) Helz, G. R.; Dotson, D. A.; Sigleo, A. C. In "Water Chlorination: Environmental Impact and Health Effects"; Jolley, R. L., Cumming, R. B., Mattice, J. S., Eds.; Ann Arbor Science: Ann Arbor, MI; Vol. 4, in press.  
 (6) Sigleo, A. C.; Helz, G. R.; Zoller, W. H. *Environ. Sci. Technol.* 1980, 14, 673.  
 (7) Mantoura, R. F. C.; Dickson, A.; Riley, J. P. *Estuarine Coast. Mar. Sci.* 1978, 6, 387.  
 (8) Zuehlke, R. W.; Kester, D. R. In "Trace Metals in Seawater"; Wong, C. S., Ed.; Proceedings of a NATO Advanced Research Institute, in press.  
 (9) Barber, R. T.; Ryther, J. H. *J. Exp. Mar. Biol. Ecol.* 1969, 3, 191.  
 (10) Barber, R. T.; Dugdale, R. C.; MacIsaac, J. J.; Smith, R. L. *Invest. Pesq.* 1971, 35, 171.

(11) Sunda, W.; Guillard, R. R. L. *J. Mar. Res.* 1976, 34, 511.  
 (12) Carpenter, J. H.; Smith, C. A. In "Water Chlorination—Environmental Impact and Health Effects"; Jolley, R. L., Gorchev, H., Hamilton, D. H., Eds.; Ann Arbor Science: Ann Arbor, MI, 1978; Vol. 2, p 195.  
 (13) Goldman, J. C.; Quinby, H. L.; Capuzzo, J. M. *Water Res.* 1979, 13, 315.  
 (14) Menzel, D. W.; Vaccaro, R. F. *Limnol. Oceanogr.* 1964, 9, 138.  
 (15) Kinrade, J. D.; Van Loon, J. C. *Anal. Chem.* 1974, 46, 1894.  
 (16) Patterson, C. C.; Settle, D. M. *Proc. Mater. Res. Symp. 7th NBS Spec. Publ.* 422, 1976; p 321.  
 (17) Hobbie, J. E.; Daley, R. J.; Jasper, S. *Appl. Environ. Microbiol.* 1977, 33, 1225.  
 (18) Mattson, J. S.; Smith, C. A.; Jones, T. T.; Gerchakov, S. M.; Epstein, B. D. *Limnol. Oceanogr.* 1974, 19, 530.  
 (19) Smith, R. G. *Anal. Chem.* 1976, 48, 75.  
 (20) Wheeler, J. R. *Limnol. Oceanogr.* 1977, 22, 573.  
 (21) Mackinnon, M. D. In "Marine Organic Chemistry"; Durumsa, E. K., Dawson, R., Eds.; Elsevier: Amsterdam, 1981; p 415.  
 (22) Sigleo, A. C., Helz, G. R. *Geochim. Cosmochim. Acta* 1982, 45, 2501.  
 (23) Sigleo, A. C.; Hoering, T. C.; Hare, P. E. *Year Book—Carnegie Inst. Washington* 1980, 79, 394.  
 (24) Glaze, W. H.; Peyton, G. R. In "Water Chlorination: Environmental Impact and Health Effects"; Jolley, R. L., Gorchev, H., Hamilton, D. H., Eds.; Ann Arbor Science: Ann Arbor, MI, 1978; Vol. 2, p 3.  
 (25) Eaton, A.; Chamberlain, C. "Cu Cycling in the Patuxent Estuary"; Final Report No. P42-78-04; Dept. of Natural Resources, Power Plant Siting Program, MD, 1980.  
 (26) Mantoura, R. F. C. In "Marine Organic Chemistry"; Durumsa, E. K., Dawson, R., Eds.; Elsevier: Amsterdam, 1981; p 179.  
 (27) Academy of Natural Sciences. In "Chalk Point 316 Demonstration of Thermal Entrainment and Impingement Impacts on the Patuxent River"; 1981, p 22.

Received for review February 16, 1982. Revised manuscript received May 28, 1982. Accepted July 21, 1982. This research was supported by the Maryland Department of Natural Resources, Power Plant Siting Program (No. P70-80-04) and the Academy of Natural Sciences.

## Synthesis and Analysis of Crystalline Silica

Frank H. Chung

Sherwin-Williams Research Center, Chicago, Illinois 60628

■ Inadequate interlaboratory precision of silica analysis is shown in the round robin studies sponsored by NIOSH and AIHA. The inconsistency in analytical results is caused by loose analytical procedures and lack of primary standards. Primary standards of cristobalite and tridymite were synthesized from high-purity quartz to cope with this situation. A matrix-flushing X-ray diffraction procedure is described for silica analysis. The integrated intensities, flush constants, and detection limits for the three forms of crystalline silica are presented.

*Introduction*

Chronic exposure to crystalline silica may cause silicosis or fibrosis in the pulmonary system. Hence the amount of airborne silica in work places is regulated and monitored by the Occupational Safety and Health Administration

(OSHA). Recent eruptions of the Mt. St. Helens volcano brought up a controversy between the environmentalists and the geologists over the amount of crystalline silica (quartz, cristobalite, and tridymite) in the volcanic ash (1). The environmentalists at the Washington State Department of Labor and Industries, the University of Washington, and the National Institute for Occupational Safety and Health (NIOSH) found typically 5-10% cristobalite, 1-2% quartz, and <1% tridymite, while the geologists at the U.S. Geological Survey, the Washington State University, and the Battelle Pacific Northwest Laboratories found little or no free silica (2), although both sides used X-ray diffraction (XRD) as the analytical tool.

Apparently the controversy has stemmed from three factors: different sampling practice, lack of primary standards, and varied analytical procedures. The first factor should be easy to settle. For health effects, the



Table I. NIOSH/PAT Quartz Study (Four Dust-Generated Samples, 1980)

	$\alpha$ -quartz found, mg/filter															
	overall (61) <sup>a</sup>			colorimetric (21) <sup>a</sup>				infrared (12) <sup>a</sup>				XRD (28) <sup>a</sup>				
	1 <sup>b</sup>	2	3	1	2	3	4	1	2	3	4	1	2	3	4	
arithmetic mean, $\bar{X}$	0.0669	0.0759	0.0936	0.0800	0.0585	0.0680	0.0834	0.0775	0.0744	0.0855	0.1147	0.0801	0.0702	0.0778	0.0921	0.0820
std dev, S	0.0276	0.0282	0.0315	0.0323	0.0277	0.0329	0.0299	0.0341	0.0252	0.0202	0.0323	0.0182	0.0277	0.0265	0.0287	0.0366
S/ $\bar{X}$ , %	41.2	37.2	33.7	40.4	47.4	48.4	35.9	44.0	33.9	23.6	28.2	22.7	39.5	34.1	31.2	44.6

<sup>a</sup> Number of labs participating. <sup>b</sup> Filter numbers.

Table II. AIHA Cristobalite Study

	cristobalite found, %		$\bar{X}$	S	S/ $\bar{X}$ , %
	J-M	other labs			
1st round	50.9	49.5, 51.8, 65.0, 68.5, 77.1, 86.9	64.2	14.4	22.4
2nd round	57.3	49.0, 53.0, 53.9, 56.7, 58.2, 59.0, 59.1, 64.0, 75.0, 83.0, 100	64.0	14.8	23.1

respirable portion (<15- $\mu$ m size) of the airborne dust should be collected; for geological studies, a composite sample might be more representative. The other two factors, however, need some deliberation and collaboration.

#### Round Robin Data

Since 1975, the National Institute for Occupational Safety and Health (NIOSH) has sponsored a Proficiency Analytical Testing (PAT) program to monitor the performance of various analytical laboratories in their ability to analyze for various air pollutants. The data of a NIOSH silica study (3) in 1980 are cited in Table I in order to show the extent of agreement. The samples are quartz dust deposited on PVC membrane filters (0.5- $\mu$ m pore size, 37 mm diameter, MSA) that are deliberately contaminated with silicates. Note that a total of 61 laboratories did the analysis of four different silica samples; among them 28 laboratories used X-ray diffraction, 21 laboratories used a colorimetric (Talvite) method, and 12 laboratories used an infrared method. Details of the methods are found in the NIOSH Manual of Analytical Methods (4), although some laboratories may make minor modifications to these methods.

Only the quartz form of silica was included in the PAT program. Naturally, the analysis of other forms of silica should be explored. The American Industrial Hygiene Association (AIHA) sponsored two round robins for cristobalite analysis, the first round in 1977-1978 and the second round in 1979-1980. A "secondary standard" was sent to participating laboratories for determination of its cristobalite content. Each laboratory was to choose its own analytical procedure and find its own primary standard although there is no known source of certified cristobalite. The "secondary standard" was a homogenized Celite distributed by George Swallow at Johns-Manville. It contains cristobalite as the major component with a very small amount of  $\alpha$ -quartz in an amorphous matrix. Seven laboratories participated in the first round robin (5), and twelve laboratories participated in the second round robin (6). The X-ray diffraction technique was used by all participating laboratories. The results of the two round robins are listed in Table II, where  $\bar{X}$  stands for arithmetic mean and S for standard deviation.

With the X-ray diffraction techniques of analysis, Klug and Alexander (7) reported a precision (S/ $\bar{X}$ ) of  $\pm 5\%$ , and Chung (8) demonstrated a precision of  $\pm 8\%$  or better. Evidently the round robin data indicate that the interlaboratory precision for silica analysis is inadequate whether the sample is quartz on membrane filter (PAT data) or cristobalite in bulk powder (AIHA data).

#### Experimental Section

X-ray diffraction is about the only technique that can differentiate quantitatively among the three forms of crystalline silica. However, it needs validated analytical procedures to attain precision; it requires certified primary standards to achieve accuracy. The wide spread of silica data from different laboratories calls for corrective mea-

Table III. Primary Standards

	quartz	cristo- balite	trid- ymite
Min-U-Sil, PGS calcination of Min-U-Sil 2 h, 1100 °C	~100%	0	0
48 h, 1450 °C	38.2%	61.8%	0
fusion of Min-U-Sil/NaCl 3 h, 1100 °C	0	62.6%	37.4%
72 h, 1100 °C	0	0	~100%
$k_i$ (integrated intensity)	3.80	4.24	0.836
$k_i$ (peak height)	3.80	4.00	0.740
sensitivity, counts/(s %)	254	256	57
detection limit, % <sup>a</sup>	0.1	0.1	0.3

<sup>a</sup> Silica in light matrix without interference.

tures. The results of some efforts toward this cause are reported below.

**Synthesis of Standards.** For quantitative X-ray diffraction analysis, very few certified primary standards are available. Each laboratory has to seek its own primary standards. When the compound sought is not readily available in pure state such as cristobalite and tridymite, problems crop up.

During the course of carrying out the analysis for the AIHA cristobalite round robin, different experiments were tried in this laboratory to synthesize primary standards starting from pure quartz. The primary standards for the three forms of crystalline silica were obtained as follows:

**$\alpha$ -Quartz.** High-purity  $\alpha$ -quartz under the trade name Min-U-Sil in 5-, 10-, 15-, and 30- $\mu$ m size is available from Pennsylvania Glass Sand (PGS) Corp., Pittsburgh, PA 15235. The Chemical Reference Laboratory of NIOSH in Cincinnati, OH, recommended the 5- $\mu$ m Min-U-Sil as primary standard for quartz analysis.

**Cristobalite.** The primary standard for cristobalite was prepared by calcination of straight  $\alpha$ -quartz as follows (9): Put a few grams of 5- $\mu$ m Min-U-Sil in a platinum crucible. Heat the crucible up to 1450 °C in an electric furnace (Deltec 30T Hi Temp oven) and maintain that temperature for 48 h. Turn off the furnace, and let the crucible cool to room temperature.

X-ray diffraction analysis of the product by the matrix-flushing method indicates a clean cristobalite with  $0.38 \pm 0.02\%$   $\alpha$ -quartz. Hence 99.6% conversion was attained. When the calcination was run for 2 h at 1100 °C in a Thermolyne muffle furnace, a binary mixture of 61.8% cristobalite and 38.2% quartz was produced. Consistent results were obtained by using either of these two preparations as primary standards for cristobalite.

**Tridymite.** The primary standard for tridymite was made by fusion of  $\alpha$ -quartz in molten salt, described as follows: Mix 1 part of 5- $\mu$ m Min-U-Sil and 5 parts of sodium chloride (mp 801 °C, bp 1413 °C). Grind the mixture for 30 min in a Fisher auto grinder. Transfer the mixture into a platinum crucible and heat to 1100 °C for 72 h in a muffle furnace. Take out the crucible and let it cool to room temperature. Grind the fused pellet to a powder. Drop the powder into hot water to dissolve the sodium chloride. Repeat the hot-water washing until the water is free from salt. Filter out the silica and dry at 105 °C for an hour.

X-ray diffraction analysis of the product thus obtained indicates a pure tridymite. The role of molten salt is to isolate the silica from the atmosphere and to change the activation energy of phase transition. When the fusion time was shortened to 3 h at 1100 °C, a binary mixture of 62.6% cristobalite and 37.4% tridymite resulted. Either

Table IV. Integrated Intensity

	scanning integra- tion, counts	peak area, cm <sup>2</sup>	peak weight, g	peak height, counts/s
cristobalite (101)	325 130	26.57 × 5	0.1190 × 5	13800
(200)	55 200	23.06	0.1011	1980
corundum (113)	67 065	26.85	0.1198	2960
(104)	58 150	23.52	0.1040	2690
(110)	24 810	10.20	0.0446	1150
$k_i$	4.16	4.24	4.26	4.00

the pure tridymite or the binary mixture can be used as primary standard, and both give consistent results of analysis.

The relevant data of the primary standards are summarized in Table III.

**Analysis by X-ray Diffraction.** Anderson (10) reviewed the analytical methods for free silica, including colorimetric, X-ray diffraction, infrared, thermal, dye adsorption, and microscopic techniques. To date, only X-ray diffraction (XRD) is practical to assay all forms of crystalline silica. The simplest approach for quantitative XRD analysis is the matrix-flushing procedure (11). It involves the determination of a flush constant  $k_i$ ,  $k_i = I_i/I_c$ , which is the intensity ratio for a 50/50 mixture of primary standard (i) and corundum (c). The flush constant  $k_i$  is independent of matrix effect. Once  $k_i$  is known, the weight fraction  $X_i$  of compound  $i$  in any unknown samples can be obtained with the following intensity-concentration equation (12):

$$x_i = (X_c/k_i)(I_i/I_c)$$

where  $X$  is the weight fraction and  $I$  is the XRD intensity of the strongest resolved reflections of component  $i$  and corundum,  $c$ . The routine for collecting intensity data is presented below (8, 13). More details can be found in the cited references.

Add 0.8–1.2 g of  $Al_2O_3$  (Linde A, 1  $\mu$ m) to a primary standard or 0.4–0.6 grams of  $Al_2O_3$  to an unknown sample to make a mixture of about 2 g. Note that the amounts of  $Al_2O_3$  added to standards and unknowns to obtain optimum intensity ratios, are different. A noninterfering compound can be added to reduce the intensities if necessary. Grind the mixture for 20 min to ensure optimum particle size and sample homogeneity. Load the mixture into sample holder by the free-falling method (14) recommended by NBS to avoid preferred orientation and density gradient, if any. Measure the integrated intensity of the strongest resolved reflection of  $Al_2O_3$ , and silica, preferably the quartz peak at  $d = 3.34$  Å, the cristobalite peak at  $d = 4.05$  Å, the tridymite peak at  $d = 4.33$  Å, and the corundum peak at  $d = 2.085$  Å.

The integrated intensities can be measured by scanning integration (or step scanning if possible), peak area, or peak weight. The scanning integration uses the accumulated counts in the scaler while the counter scans through the peak of reflection. The peak area is the area in cm<sup>2</sup> under the peak on a strip chart (scan speed, 0.25°/min; chart speed, 0.5 in./min) measured with a planimeter. The peak weight is the weight in grams of the peak cut from the strip chart. For semiquantitative work, peak height can be used, which is the maximum counting rate in counts/s of the peak. A set of intensity data collected from a mixture of 53.91% cristobalite (99.6% pure) and 46.09%  $Al_2O_3$  is listed in Table IV: The flush constant  $k_i$  calculated from

Table V. Cristobalite in Celite

	I		II	
	Celite (200)	Al <sub>2</sub> O <sub>3</sub> (104)	Celite (200)	Al <sub>2</sub> O <sub>3</sub> (104)
% wt	36.53	63.47	52.15	47.85
peak wt, g	0.0422	0.1502	0.0565	0.1078
% cristobalite in Celite	58.7		57.8	
av, %			58.2	
Johns-Manville, %			57.3	

these different versions of intensity data agree well within experimental errors. The coefficient of variation ( $S/\bar{X}$ ) of the matrix-flushing procedure was statistically evaluated to be 8% or better.

A regular XRD scan of the "secondary standard" from Johns-Manville for the AIHA round robin indicates that the line profile of the natural cristobalite (Celite) is much broader than that of the synthetic cristobalite due to different lattice imperfections. The use of integrated intensities for its analysis can compensate this difference. Peak height data can be used for quartz analysis because there is no noticeable difference in line profiles between quartz samples from various sources.

Statistical considerations show that an intensity ratio is determined with the greatest precision in the shortest time when the numerator and denominator are equal. In practice it is advantageous to make the intensity ratio ( $I_i/I_o$ ) close to unity by adding the proper amount of Al<sub>2</sub>O<sub>3</sub> or choosing the right reflections, although this is not always possible. A set of intensity data for the second round-robin sample from AIHA is presented in Table V. Note that the second strongest peaks of cristobalite (200) and corundum (104) were measured, besides the statistical considerations, because they are better resolved and more convenient. The corresponding flush constant for this pair of reflections is  $k_i = 0.832$ , calculated from the data in Table IV. The amount of cristobalite in celite was found to be 58.2% which was reported to AIHA and checks well with the results from Johns-Manville.

### Conclusions

X-ray diffraction is the only technique feasible for assaying the three forms of crystalline silica. However, in-

adequate interlaboratory precision data created confusion. Therefore, concerted efforts are needed to develop practical analytical procedures and certified primary standards.

Depending on the purpose of analysis, silica samples may come as a bulk powder or as dust-laden filters. For silica on membrane filters, a multiple-exposure XRD method with imbedded standards was reported by Chung (15). For silica in bulk powder, a matrix-flushing (8) approach is presented here. The primary standards of cristobalite and tridymite can be synthesized from high-purity quartz. It is preferable to have these primary standards made in larger quantity and distributed by a reputable source to avoid ambiguity.

### Literature Cited

- (1) *Anal. Chem.* **1980**, *52*, 1136A.
- (2) *Anal. Chem.* **1980**, *52*, 1272A.
- (3) Groff, J. H., memorandum to PAT participants, May 7, 1980, National Institute For Occupational Safety And Health, Cincinnati, OH.
- (4) U.S. Dept. of Health, Education and Welfare, "NIOSH Manual of Analytical Methods"; Government Printing Office: Washington D.C., 1977.
- (5) Swallow, G. L., Annual AIHA Meeting, Los Angeles, 1978, and AIHA Accreditation News & Notes, Aug 1978, American Industrial Hygiene Assoc., Akron, OH.
- (6) Swallow, G. L., Laboratory Directors' Meeting, Houston, 1980, and AIHA Accreditation News & Notes, Aug 1980, American Industrial Hygiene Assoc., Akron, OH.
- (7) Klug, H. P.; Alexander, L. E. "X-Ray Diffraction Procedures", 2nd ed.; Wiley-Interscience: New York, 1974; p 524.
- (8) Chung, F. H. *J. Appl. Crystallogr.* **1975**, *8*, 17.
- (9) Bhargara, O. P.; Alexiou, A. S.; Meilach, H.; Hines, W. G. *Am. Lab.* **1979**, Sept, 27.
- (10) Anderson, P. L. *Am. Ind. Hyg. Assoc. J.* **1975**, *36*, 767.
- (11) Chung, F. H. *J. Appl. Crystallogr.* **1974**, *7*, 519.
- (12) Chung, F. H. *J. Appl. Crystallogr.* **1974**, *7*, 526.
- (13) Chung, F. H. *Adv. X-ray Anal.* **1974**, *17*, 106.
- (14) National Bureau of Standards, Monograph 25, "Standard X-Ray Diffraction Powder Patterns"; Government Printing Office: Washington D.C., 1971; p 3.
- (15) Chung, F. H. *Environ. Sci. Technol.* **1978**, *12*, 1208.

Received for review November 30, 1981. Revised manuscript received May 17, 1982. Accepted July 8, 1982.

## Persistent Organic Chemicals in Sewage Effluents. 2. Quantitative Determinations of Nonylphenols and Nonylphenol Ethoxylates by Glass Capillary Gas Chromatography

Euripides Stephanou<sup>†</sup> and Walter Giger\*

Swiss Federal Institute for Water Resources and Water Pollution Control (EAWAG), CH-8600 Dübendorf, Switzerland

■ Nonylphenols and nonylphenol ethoxylates with one and two oxyethylene groups have been quantitatively determined in the effluents of six mechanical-biological sewage treatment plants. In three plants total concentrations of nonylphenolic compounds in the effluents ranged from 36 to 202  $\mu\text{g/L}$ , representing from 0.5% to 2.3% of the total residual dissolved organic carbon. In three plants operated at low loading conditions nonylphenolic compounds were not detectable ( $<10 \mu\text{g/L}$ ). These compounds are believed to be refractory metabolites of nonionic surfactants of the nonylphenol polyethoxylate type. In particular, the nonylphenols must be considered as compounds of high toxicity to aquatic organisms.

### Introduction

In the 1950s the use of synthetic surface-active agents (also called surfactants) led to severe environmental problems manifested by foaming on surface waters. The cause of this problem was the nonbiodegradability of tetrapropylenebenzenesulfonates, which were at that time the most popular synthetic surfactants in commercial detergents for household and industrial use. The introduction of more biodegradable surfactants like the linear alkylbenzenesulfonates has eliminated or considerably reduced the problems of foaming. Many studies have been conducted on the biodegradation of surfactants both in the laboratory and in full-scale sewage treatment plants (1-4). At present, regulatory activities are based on the observation of the disappearance of the parent surfactant molecules although it is known that metabolic products of higher persistence can be formed.

Alkylphenol polyethoxylates are increasingly popular nonionic surfactants, which in 1974 had an estimated market share of 18% of the total synthetic surfactants in Europe (5). In 1975 approximately 360 000 t (metric tons) were produced in the U.S. and Europe (6). The biodegradability of this surfactant class was disputed for some time, but presently the alkylphenol polyethoxylates are accepted as biodegradable detergents (6, 7). Many analytical procedures have been developed for the determination of anionic, nonionic, and cationic surfactant types (for recent reviews see ref 8 and 9). The majority of the studies on biodegradation and occurrence of such compounds in wastewaters, treatment effluents, and surface waters were conducted by measuring total amounts of the parent surfactant chemicals. In a number of investigations more specific methods were applied by which metabolic products were also detected. Difficult analytical problems were encountered when trace amounts in sewage effluents and natural waters had to be determined (8, 9). Gas chromatography/mass spectrometry (GC/MS) has been of limited use for surfactant determinations because most of these chemicals are not directly amenable to GC analyses due to their insufficient volatilities. Exceptions

were the determinations of alkylbenzenesulfonates and their metabolites after desulfonation (2, 8) and of nonionic surfactants after ether cleavage (8). Gas chromatography has also been applied to the alkylphenol polyethoxylates (10), and most recently ethoxylated alkylphenols were analyzed by GC/MS (11).

In part 1 of this publication series we described the confident identifications of nonylphenols and nonylphenol ethoxylates in treated sewage effluents by the use of glass capillary GC/MS (12). In this paper we present quantitative determinations of nonylphenols (NP), nonylphenol monoethoxylates (NP1), and nonylphenol diethoxylates (NP2) in secondary effluents of mechanical-biological sewage treatment plants and discuss the origin and the environmental significance of these water pollutants.

### Experimental Section

**Materials.** Acetone, methanol, and pentane were of "nanograde" quality (Mallinckrodt, St. Louis, MO) and were used without further purification. Methylene chloride was freshly distilled from the "technical" grade material (Fluka, Buchs, Switzerland). The reference nonylphenol ethoxylate Marlophen 83 was provided by Chemische Werke Hüls, Marl, Germany. According to the manufacturer, Marlophen 83 contains an average number of 3.15 oxyethylene groups. 2,4,6-Tribromophenol and 4-nonylphenol were used as received from the supplier (Fluka). Sodium sulfate and cotton were preextracted with methylene chloride. Sodium sulfate was dried and further purified by baking at 800 °C overnight. Silica (Kieselgel-40, 70-230 mesh, Merck, Darmstadt, Germany) was activated at 250 °C overnight.

**Samples and Reference Solutions.** Secondary effluent samples were collected by grab and 24-h composite sampling from several mechanical-biological treatment plants in the Zürich area. Sampling dates were from August 1980 to February 1981. Aqueous solutions of 4-nonylphenol and Marlophen 83 were prepared by dissolving 1-1.5 mg of these chemicals in 1 L of doubly distilled water.

The internal standard, 2,4,6-tribromophenol (TBP), was prepared in acetone at a precisely known concentration in the range 3-5 mg/mL. Aliquots of 3 or 4  $\mu\text{L}$  of the standard solution were added to the extracts with a 5- $\mu\text{L}$  syringe.

**Extraction and Isolation.** Two different solvent extraction techniques were applied: (A) batch extraction in a separatory funnel and (B) continuous liquid-liquid extraction. (A): Aqueous samples of 200 mL were extracted three times with 20-mL portions of methylene chloride in a 250-mL separatory funnel. Even at neutral pH severe emulsions hindered the partitioning of the sewage effluent samples. The combined extracts were dried with sodium sulfate (sometimes up to 40 g because of the emulsions) and filtered through a plug of cotton into 100-mL pear-shaped flasks. (B): A continuous liquid-liquid extraction unit for organic solvents heavier than water was applied. Figure 1 shows the design of this apparatus. Water sam-

<sup>†</sup>Present address: Department of Civil Engineering, Stanford University, Stanford, CA 94305.

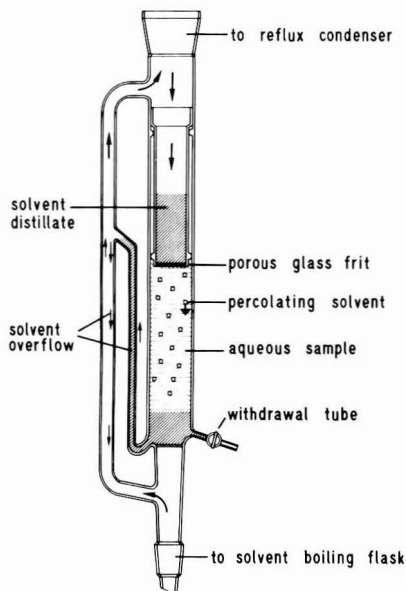


**Figure 1.** Schematic of continuous liquid-liquid extraction apparatus for solvents heavier than water.

ples of 250 mL were extracted with 150 mL of methylene chloride for 2 h. By passing through a porous frit (no. 0), the condensed solvent was dispersed into small droplets, which then percolated through the aqueous sample. No emulsion problems were encountered with this procedure.

The extracts were concentrated to 1–2 mL by employing a Kuderna-Danish evaporator with a three-ball Snyder column. The extracts were then subject to column chromatography on silica. Glass columns (1.0 cm i.d. × 20 cm) were filled with 5 mL of silica that had been deactivated with 15% (w/w) water. After application of the samples the columns were first eluted with 40 mL of pentane and then with 35 mL of methylene chloride containing 1% (v/v) methanol. The pentane eluates were discarded. The methylene chloride eluates were concentrated to 0.5–0.2 mL in Kuderna-Danish evaporators after adding TBP as an internal standard.

**Analytical Instruments and Procedures.** Gas chromatography (GC) was performed on a Carlo Erba apparatus (Model 2150) equipped with a flame ionization detector (FID). An injection port with septum flushing was used (Model 76, Brechbühler, Urdorf, Switzerland). The glass capillary columns (15 m × 0.3 mm) were kindly supplied by K. and G. Grob. The column had been deactivated by persilylation (13) and coated with immobilized OV-73 (14). Aliquots of 1–2  $\mu$ L of the methylene chloride extracts were injected without stream splitting onto the column at ambient temperature. The injector temperature was 250 °C. After 30 s the split valve was opened, allowing the septum and injection port to be purged at a flow rate of approximately 10 mL/min. After the elution of the solvent, the oven temperature was raised at 2 °C/min from 50 to 280 °C. Hydrogen was used as the carrier gas with a head pressure of 0.5 atm. Electronic integration of the gas chromatographic peak areas was performed with a digital integrator (Minigrator, Spectra Physics).

A Finnigan mass spectrometer (Model 4021C) with an INCOS 2000 data system was used for mass spectrometric

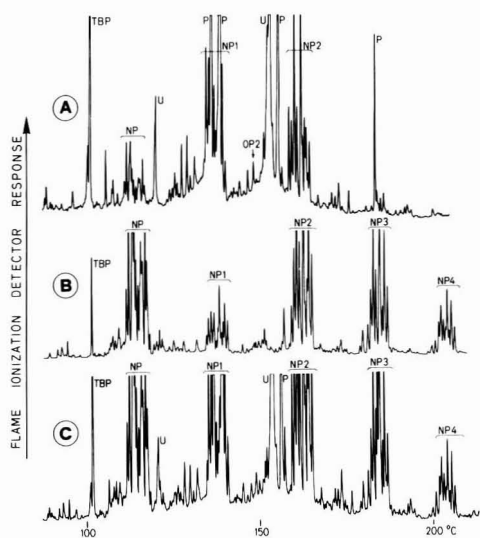


**Figure 2.** Glass capillary gas chromatograms: (A) extract of secondary sewage effluent; (B) reference mixture of nonylphenol and Marlophen 83; (C) coinjection of A and B. NP =  $H_{19}C_9-C_6H_4-OH$ ; NP1–4 =  $H_{19}C_9C_6H_4O(CH_2CH_2O)_n-CH_2CH_2OH$  ( $n = 1, 2, 3, 4$ ); OP2 =  $H_{17}C_8-C_6H_4OCH_2CH_2OCH_2CH_2OH$ ; TBP = 2,4,6-tribromophenol; P = phthalate; U = unknown.

identifications. A Carlo Erba gas chromatograph (Model 4160) was connected to the mass spectrometer. The glass capillary GC column was directly coupled to the ion source by a fused silica capillary. Helium was used for carrier gas with a back pressure of 0.8 atm. Gas chromatographic columns and procedures were as described above for the GC analyses.

Infrared absorption spectra were obtained from films formed by evaporation of methylene chloride solutions on sodium chloride plates. A Perkin-Elmer infrared spectrometer (Model 297) was used. Ultraviolet absorption spectra were measured from pentane solutions on a Beckman Spectrometer (Model 25).

## Results

**Qualitative Identifications.** Trace A of Figure 2 shows a typical gas chromatogram recorded by flame ionization detection. The sample analyzed was an extract of the effluent from an activated sludge wastewater treatment plant in Zürich. As indicated by GC/MS investigation, the three peak groups assigned NP, NP1, and NP2 comprise compounds with molecular ions of  $m/z$  220, 264, and 308, respectively, corresponding to the molecular masses of nonylphenols (NP), nonylphenol monoethoxylates (NP1), and nonylphenol diethoxylates (NP2) (for structural formulas see caption to Figure 2). The gas chromatogram B of Figure 2 was obtained from a reference mixture containing the commercial products 4-nonylphenol and Marlophen 83.

4-Nonylphenol is a technical product that has been manufactured from tripropylene and phenol (6). Therefore, it is a complex mixture of isomeric compounds with differently branched structures of the nonyl side chains. The first eluting peak group in Figure 2B represents the NP mixture as separated by the glass capillary GC used in this investigation. The complex NP mixture was only partly resolved into individual component peaks. All major NP peaks are attributed to the para-substituted com-

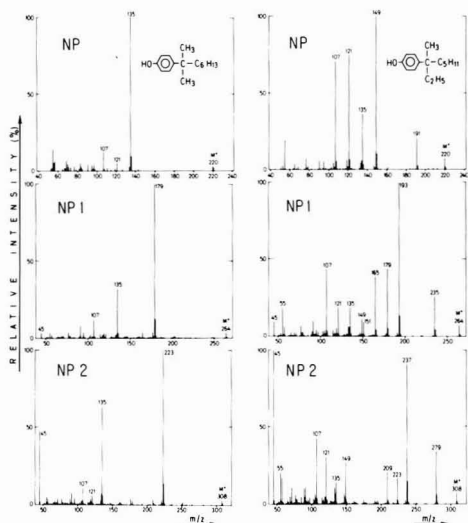


**Figure 3.** Typical mass spectra of 4-nonylphenols and 4-nonylphenol ethoxylates extracted from secondary sewage effluent.

pounds. The technical grade 4-nonylphenol also contains approximately 10% ortho-substituted compounds, which should have significantly shorter retention times than the para-isomers (15).

Nonylphenol polyethoxylates, like Marlophen 83, are manufactured by reacting ethylene oxide with 4-nonylphenol (6). Thus, similar complex mixtures of isomeric compound with differently branched nonyl side chains appear for each group of compounds with a distinct length of the polyoxyethylene side chains. In fact, the pattern of the GC signal is closely repeated with some loss of resolution with increasing number of oxyethylene groups. Very similar fingerprints of the peak groups NP, NP1, and NP2 can be observed in the chromatogram of the secondary sewage effluent extract (see Figure 2A). A coinjection of a sewage extract with the reference mixture provided evidence for the confident structural assignments for these peaks, as shown by trace C in Figure 2. The nonylphenols and nonylphenol ethoxylates in sewage effluents were further identified by the fragmentation patterns of their mass spectra, of which a detailed description has been presented elsewhere (12). Six typical mass spectra are plotted in Figure 3. The most significant mass spectral features are briefly summarized as follows:

One of the NP isomers (in the left column of Figure 3) yields a base peak at  $m/z$  135 and only low intensities of the other ions. This is because of the favored rupture of the benzylic bond in the nonyl side chain leading to a loss of  $C_6H_{13}$  (85 amu) from the molecular ion. Olefin elimination from the primary benzyl ion probably produces the significant abundance of  $m/z$  107. Hence, it is inferred that this NP compound has an  $\alpha,\alpha$ -dimethyl structure in the nonyl side chain. Only little information can be deduced about the structure of the hexyl substituent at the  $\alpha$  carbon. The low intensity of the  $m/z$  57 peak indicates the absence of a terminal tertiary butyl group. The mass spectrum of the other NP isomer (in the right column of Figure 3) shows high relative abundances of the fragment ions  $m/z$  107, 121, 135, 149, and also 191 corresponding to  $(M - C_2H_5)^+$ . Ions of  $m/z$  149 due to  $(M - C_6H_{11})^+$  produce the base peak. From this fragmentation pattern it is suggested that this compound has an  $\alpha$ -ethyl- $\alpha$ -methyl-substituted nonyl side chain. Further information

about the precise structure of the remaining pentyl substituent could not be obtained. In the mass spectra of NP1 and NP2 in the left column of Figure 3, the base peaks at  $m/z$  179 and 223 are attributed to the addition of one (44 amu) and two oxyethylene groups (88 amu), corresponding to  $m/z$  135 in NP. The presence of  $m/z$  135 can be rationalized by a loss of the oxyethylene side chain and a hydrogen transfer to the phenolic ions. Similarly, in the mass spectra of NP1 and NP2 in the right column of Figure 3, the homologous ion series of  $m/z$  151 + 14n and 209 + 14n, including the base peaks of  $m/z$  193 and 237, can be explained by the addition of oxyethylene groups to the 4-nonylphenol molecules. Other typical features in the mass spectra of the ethoxylated phenols are the abundant  $m/z$  45 ions in NP1 and NP2. These ions are assigned to  $CH_2CH_2OH^+$  species. With increasing length of the oxyethylene side chain the intensity of the  $m/z$  45 peak drastically increases and eventually becomes the base peak.

In several samples octylphenol diethoxylate (OP2 in Figure 2A) could also be tentatively identified. Its mass spectrum is analogous to the mass spectrum of 4-(1,1,3,3-tetramethylbutyl)phenol triethoxylate published by Sheldon and Hites (16).

The presence of alkylphenol ethoxylates in the sewage extracts was further confirmed by absorption spectra. Absorption bands at 276 and 282 nm were observed in the UV spectrum of the sewage extract and in a solution of Marlophen 83. Their IR spectra showed aromatic bands at 1640, 1570, and 1500  $cm^{-1}$  and an aryl ether band at 1270  $cm^{-1}$ .

**Quantitative Determinations.** The gas chromatograms of Figure 2 show that TBP was suitable as an internal standard for the quantitative determination of NP, NP1, NP2. The calibration for these quantitative determinations presented some difficulties because of no pure isomers of these chemicals were available. Marlophen 83, which was used as reference material, is not only a mixture of isomers but also of molecules with different oxyethylene chain lengths (see Figure 2B). For the determination of one group (NP, NP1 to NP5) the peak areas of the various isomers had to be integrated and added up. The relative distribution of NP1 to NP5 in Marlophen 83 was determined by assuming equal FID and overall GC response sensitivities for these molecules and neglecting the approximately 10% ortho-substituted components that are presented in technical nonylphenols. The following distribution was found: NP1, 14%; NP2, 42%; NP3, 30%; NP4, 12%; NP5, 2%. These results differ from the information given by the manufacturer, but they might be slightly biased by varying detection sensitivities of the flame ionization detector. Response factors with respect to TBP were 0.14 for NP and 0.38 for NP1 to NP5. For more reliable calibrations isolation or synthesis of nonylphenol ethoxylates with different oxyethylene chain lengths would be necessary.

Good recovery efficiencies were obtained by both extraction procedures (see Table I). The manual shaking method, however, was practically difficult because of severe emulsion formations. Therefore, the use of a continuous extractor (see Figure 1) was introduced with which even better recoveries were achieved. A continuous steam distillation extraction apparatus as used for our qualitative analyses (12) was also tested. Insufficient recoveries for ethoxylated nonylphenols, however, prevented the application of this otherwise very convenient extraction procedure.

Table I. Recovery Efficiencies for Nonylphenols and Nonylphenol Ethoxyates

compound	recovery, % <sup>a</sup>	
	A	B
nonylphenols (NP)	87 ± 4	101 ± 4
nonylphenol monoethoxyates (NP1)	86 ± 7	87 ± 3
nonylphenol diethoxyates (NP2)	79 ± 8	93 ± 5
nonylphenol triethoxyates (NP3)	85 ± 8	90 ± 10

<sup>a</sup> (A) manual batch extraction; (B) continuous extraction. Mean ± relative standard deviation for triplicate analyses.

For the determination of NP, NP1, and NP2 in secondary sewage effluents it was necessary to include a silica chromatography as a cleanup procedure to remove non-polar compounds (like aliphatic hydrocarbons) and carboxylic acids. Both compound classes interfered with the determination of NP chemicals. In many samples phthalate esters coeluted with NP1 isomers (see Figure 2). These contaminations were not removed by our procedure and often hampered the determinations of NP1. The detection limit of our determination method was estimated to be 10 µg/L each for NP, NP1, and NP2.

Effluents from six sewage treatment plants of the Glatt Valley in the canton of Zürich were studied. We have detected the persistent nonylphenolic compounds NP, NP1, and NP2 in the effluents of three plants (see Table II). In some effluent samples NP3 compounds were tentatively identified. Concentrations of 36–202 µg of the sum of nonylphenol derivatives per liter of effluent were found. These summed concentrations were also calculated as relative contributions to the total dissolved organic carbon (DOC) levels in these effluents. The nonylphenolic compounds accounted for 0.6–2.3% of the carbon measured as DOC. No NP, NP1, or NP2 could be detected in the three other sewage treatment plants.

### Discussion

The procedure employed in this study enabled confident structural assignments and quantitative determinations of NP, NP1, and NP2 in biologically treated sewage effluents. The application of glass capillary GC/MS allowed the elucidation of the basic molecular structures of the individual compounds, although no complete structural assignments could be made. Gas chromatography with flame ionization detection was well suited for the quantitative determinations. The specificity of our technique contrasts sharply to most methods that are applied for the determinations of surfactants in wastewater effluents and receiving waters. Total amounts of nonionic detergents are usually determined by the so-called Wickbold method, in which nonionic surfactants are isolated by stripping into ethyl acetate and determined after precipitation with a modified Dragendorff reagent. When these collective

values are determined at the low levels encountered in treated sewage effluents and surface waters, the results have to be interpreted with caution because the structures of the collectively determined compounds are not precisely known and the method may precipitate molecules other than ionic detergents. Even the more specific methods like thin-layer chromatography or high-performance liquid chromatography lack sufficient structural information and tend to be encumbered with interfering substances when they are applied to real sewage and water samples. Glass capillary GC techniques similar to ours have allowed the qualitative determination of alkylphenol ethoxyates with up to 13 oxyethylene groups (3, 17). In primary treated sewage samples we could qualitatively identify nonylphenol polyethoxyates with 7–12 oxyethylene groups after applying the isolation procedures described in this paper.

It should be noted that the Wickbold method is limited to alkylphenol ethoxyates with more than five oxyethylene groups, because the shorter chain compounds are not precipitated by the modified Dragendorff reagent. Thus, investigations using the Wickbold method were not able to detect the molecules described in this report.

Regarding the origins of the nonylphenol derivatives, it can be safely inferred that NP1 and NP2 were refractory metabolites of nonylphenol polyethoxyates with longer oxyethylene chains, which are widely used as nonionic detergents. Technical mixtures averaging approximately ten oxyethylene groups are very popular surfactants and are employed in a great variety of commercial products. Several authors have investigated the biodegradation of alkylphenol polyethoxyates in laboratory studies (3, 4). In these studies metabolites containing one or two residual oxyethylene groups were found to accumulate in the effluents of laboratory-scale activated sludge systems. Therefore, the occurrence of NP1 and NP2 in secondary sewage effluents can be explained by the refractory nature of these metabolites. Commercial products like Marlophen 83 with short oxyethylene chain lengths are of limited use as detergents because of their low water solubilities. Consequently they are not expected to widely occur as primary pollutants in wastewaters.

Alkylphenols without oxyethylene groups have thus far not been reported from biodegradation studies. Nevertheless, it seems probable that NP in secondary sewage effluents are also metabolites from nonylphenol polyethoxyates. The vast majority of NP are manufactured as raw materials for the production of polyoxyethylene derivatives, although some application as additives and plasticizers are also known. Nonylphenol is a major component in the pesticide formulation Matacil, which is used to fight spruce budworms in Canada (18, 19). However, we are not aware of any NP application in Switzerland that could cause their presence in secondary sewage effluents.

One interesting result of our investigation was that NP, NP1, and NP2 were found in the effluents of three sewage

Table II. Concentrations of Nonylphenols and Nonylphenol Ethoxyates in Secondary Sewage Effluents

sewage treatment plant	concn, µg/L <sup>a</sup>				DOC, mg C/L <sup>b</sup>	rel amt, % <sup>c</sup>	no. of determinations
	NP	NP1	NP2	total			
Dübendorf	10–35	83–133	13–70	78–202	6.4–12.9	0.6–2.3	9
Opfikon	nd–17	70–133	31–67	137–181	5.0–15.1	0.8–2.1	2
Zürich	10–23	24–52	nd–50	36–125	4.6–6.3	0.5–2.1	3
Bülach	}	nd	nd	nd	5.4–6.2	nd	3
Fällanden					5.4–7.2		3
Niederglatt					3.2		1

<sup>a</sup> nd: not determinable, i.e., below detection limit of 10 µg/L. <sup>b</sup> DOC: dissolved organic carbon. <sup>c</sup> Sum of NP, NP1, and NP2 calculated as percentage of DOC.

Table III. Toxicity to Aquatic Fauna of Nonylphenol Polyethoxylates and Nonylphenols

nonylphenol polyethoxylates <sup>a</sup>	no effect level, mg/L				ref
	<i>Pseudomonas</i>	<i>Scenedesmus</i>	<i>Colpoda</i>	<i>Daphnia</i>	
30	1000	5000	250	> 10000	
20	1000	125	250	1000	
10	1000	31	31	10	20
7	63-500	16	31	10	
6	500	10	16	5	
4	50	6	5	5	
	lethal thresholds (96 h, LC <sub>50</sub> ), mg/L				
	shrimp	salmon	fingerling rainbow trout	fingerling brook trout	ref
nonylphenol	0.30	0.13-0.19	0.230	0.145	19

<sup>a</sup> Average number of oxyethylene groups.

treatment plants and were not detectable in the effluents from three other plants (Table II). The wastewater treatment plants of Dübendorf, Opfikon, Zürich, Bülach, and Fällanden are conventional mechanical-biological activated sludge plants with decreasing loading rates in the listed order. The plant at Niederglatt is a two-stage activated sludge process. The treatment plants of Fällanden, Bülach, and Niederglatt produce a nitrified effluent throughout the year. The Zürich plant produces a partially nitrified effluent during the summer months. The plants of Dübendorf and Opfikon do not nitrify at all. These differences in loading conditions of the activated sludge processes (EAWAG, internal report) could bring about the different concentrations of NP compounds in the various effluents. On the other hand, the plants in Zürich, Dübendorf, and Opfikon generally receive wastewaters with greater contributions from industrial sources, including wastewaters from food industries and catering services. Such differences in the origins of the raw wastewaters could cause varying levels of nonionic detergents in the influents to the treatment plants. Further investigations determining the compositions of the influents and the effluents at the different plants would be needed to clarify this question. At present, however, no analytical method is available to specifically determine nonionic detergents of the alkylphenol polyethoxylate type in wastewaters. The pathways and the kinetics of the microbial degradation of alkyl phenol polyethoxylates are currently being studied in detail at our institute (17). The results of this investigation should help to gain more insight into the behavior of these nonionic detergents during biological sewage treatment.

It is desirable to assess the impact on the quality of the receiving waters by the findings presented in this paper. For that purpose the available information on the toxicity to the aquatic fauna is reviewed in Table III. Nonylphenol polyethoxylates with varying oxyethylene numbers have been extensively studied (20) because of their wide use as nonionic surfactants. All the chemicals investigated were technical products containing mixtures of compounds with different lengths of the oxyethylene side chains. The values in Table III clearly show that the toxicities generally increase with shorter oxyethylene side chains. The toxicity thresholds of NP1 and NP2 can be estimated to be similar or smaller than for the mixture with nonylphenol tetraethoxylates ( $n = 4$ ) as major components.

The high toxicity of nonylphenol was discovered in a study on the toxic effects of the pesticides formulation Matacil (18), which was composed of the active pesticide aminocarb (22%), nonylphenol (51%), and a diluent oil 585 (27%). This investigation revealed that nonylphenol

was by no means an "inert ingredient" of the formulation. In fact, much of the toxicity of the formulation was due to nonylphenol. An additional investigation confirmed that alkylphenols, particularly those with alkyl chains ranging from six to twelve carbon atoms, are highly toxic to aquatic fauna (19).

In the light of these toxicity data, the results reported in this paper are of considerable concern with respect to possible harmful effects to the aquatic fauna. In the case of the alkylphenol polyethoxylate surfactants, relatively harmless chemicals are transformed in the biological sewage treatment to refractory metabolites that are more toxic than the original chemicals. This situation warrants further studies on the sources and behavior of alkylphenols and alkylphenol ethoxylates in sewage treatment and in natural waters. Such investigations will be carried out at our institute in the near future.

#### Acknowledgments

We thank K. and G. Grob for supplying capillary columns and valuable advice, C. Jaques and C. Schaffner for technical assistance, and T. Conrad, K. Stadler, and R. Geiser for very helpful discussions. We are indebted to J. Graydon, W. Gujer, and R. Schwarzenbach for reviewing the manuscript.

#### Literature Cited

- (1) Swisher, R. D. "Surfactant Biodegradation"; Marcel Dekker: New York, 1970.
- (2) Leidner, H.; Gloor, R.; Wuhrmann, K. *Tenside Deterg.* **1976**, *13*, 122.
- (3) Geiser, R. Ph.D. Thesis, No. 6678, Swiss Federal Institute of Technology, Zürich, Switzerland, 1980.
- (4) Schöberl, P.; Kunkel, E.; Espeter, K. *Tenside Deterg.* **1981**, *18*, 64.
- (5) Environmental Resources Ltd., "Cleaning and Conditioning Agents. Their Impact on the Environment"; Graham and Trotman: London, 1977.
- (6) Wirth, W. *Tenside Deterg.* **1975**, *12*, 245.
- (7) Berth, P.; Heidrich, J.; Jakobi, G. *Tenside Deterg.* **1980**, *17*, 228.
- (8) Llenado, R. A.; Jamieson, R. A. *Anal. Chem.* **1981**, *53*, 174R.
- (9) Kunkel, E. *Tenside Deterg.* **1981**, *18*, 301.
- (10) Favretto, L.; Stancher, B.; Tunis, F. *Analyst* **1978**, *103*, 955.
- (11) Szymanowski, J.; Szweczyk, H.; Hepter, J. *Tenside Deterg.* **1981**, *18*, 333.
- (12) Giger, W.; Stephanou, E.; Schaffner, C. *Chemosphere* **1981**, *10*, 1253.
- (13) Grob, K. *J. High Resolut. Chromatogr. Chromatogr. Commun.* **1980**, *3*, 493.
- (14) Grob, K.; Grob, G. *J. High Resolut. Chromatogr. Chromatogr. Commun.* **1981**, *4*, 491.
- (15) Gerhardt, W. *Tenside Deterg.* **1979**, *16*, 247.



- (16) Sheldon, L. S.; Hites, R. A. *Sci. Total Environ.* 1979, 11, 279.
- (17) Conrad, T.; Stadler, K., EAWAG, private communication, 1981.
- (18) McLeese, D. W.; Zitko, V.; Metcalfe, C. D.; Sergeant, D. B. *Chemosphere* 1980, 9, 79.
- (19) McLeese, D. W.; Zitko, V.; Sergeant, D. B.; Burrige L.; Metcalfe, C. D. *Chemosphere* 1981, 10, 723.
- (20) Janicke, W.; Bringmann, G.; Kühn, R. *Gesund.-Ing.* 1969, 90, 133.

Received for review February 17, 1982. Accepted July 1, 1982. This work was supported by the Swiss Department of Commerce (Project COST 64 b). E.S. was recipient of a fellowship from the H. Schmid Foundation.

## Determination of Naphtho[2,1,8-*qra*]naphthacene in Soots

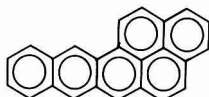
Akio Yasuhara,\* Masatoshi Morita, and Kellchiro Fuwa

Division of Chemistry and Physics, National Institute for Environmental Studies, Yatabe, Tsukuba-gun, Ibaraki 305, Japan

■ Naphtho[2,1,8-*qra*]naphthacene, a strongly carcinogenic substance, was detected in soots both by gas chromatography-mass spectrometry (GC/MS) and high-performance liquid chromatography-fluorescence spectrometry (HPLC/FLS). Detection limits of this compound were subnanograms in GC/MS and around 10 pg in HPLC/FLS. A soot sample collected at the chimney of a public garbage furnace contained naphtho[2,1,8-*qra*]naphthacene at the level of parts per million.

### Introduction

Polynuclear aromatic hydrocarbons (PAHs) have been studied for a long time because of their carcinogenicities. PAHs are adsorbed on airborne particulate matter of a specific size, one that aids their penetration of the human respiratory system. Among PAHs, benzo[*a*]pyrene is very famous for its strong carcinogenicity. Lots of attention has been paid to a correlation between molecular structure and carcinogenic activity. It was interesting whether a higher homologue, of benzo[*a*]pyrene, naphtho[2,1,8-*qra*]naphthacene (I), whose alternate names are naphtho[2,3-



Naphtho[2,1,8-*qra*]naphthacene (I)

*a*]pyrene and 2,3-naphtho-1,2-pyrene, is carcinogenic. Cook and Hewett (1) prepared I, and studied the toxicity. Their result, that tumors were not observed after applying I to mice for 8 months, agreed with the prediction from Pullman's theory (2). However, Lacassagne et al. (3) described carcinogenicity of I with results which showed that 8 of 17 mice developed sarcomas at the site of injection and 1 mouse a pulmonary adenoma after 160-295 days from the subcutaneous injection of 0.6 mg of I once a month for 3 months. Furthermore, Buu-Hoi and Hien (4) reported that only I was definitely carcinogenic of many naphthacene derivatives and that I showed the highest activity to induce microsomal xoxazolamine hydroxylase. Another investigator also verified the strong carcinogenicity of I experimentally (5). Modified hypotheses have been proposed for the correlation between carcinogenicity and physicochemical properties of PAHs including I (5-12).

Sawicki et al. (13, 14) showed the possibility of the existence of many unknown PAHs including I in airborne particulate matter by low-temperature fluorescence of the samples after treatment with tetramethylammonium hydroxide solution and by direct fluorescence analysis on thin-layer chromatograms without any identifications.

Recently, Pierce and Katz (15) reported the detection of I in atmospheric aerosols by a combination of thin-layer chromatography and fluorescence spectrometry, but no other reports have appeared in environmental analyses since. Because the separation capability of thin-layer chromatography is limited for a complex mixture of PAHs, the identification of I in environmental samples seemed to be made by recently advanced HPLC/FLS and GC/MS techniques.

This paper describes the determination of I in soots, which are one of the most important origins for airborne particulate matter, by gas chromatography-mass spectrometry and high performance liquid chromatography-fluorescence spectrometry.

### Experimental Section

**Synthesis of Naphtho[2,1,8-*qra*]naphthacene (I).** 1,2-(*o*-Phthaloyl)pyrene (3.59 g), which was prepared from pyrene according to the literature (16), was extracted from a Soxhlet apparatus into a suspended solution of LiAlH<sub>4</sub> (4.95 g) in boiling tetrahydrofuran (350 mL) for 17 h. The excess hydride was decomposed with moist ether (50 mL), and then 6 M HCl solution (50 mL) was added. After the mixture was refluxed for 30 min to complete the decomposition, the aqueous layer was separated from the organic one and extracted several times with benzene. The combined organic layer was concentrated to dryness under reduced pressure after drying on anhydrous potassium carbonate. Deep red crystals of I (2.63 g) were obtained by a recrystallization of the crude product from benzene, yield 80.4%. These crystals were dissolved in boiling xylene and rapidly passed through short column of alumina (Merck) with heat in order to eliminate trace amounts of contaminants. The filtrate was recrystallized from xylene to give deep orange leaflets of I: mp 273-275 °C (lit. mp (1) 273 °C); IR (KBr disk) 3040, 900, 880, 840, 825, 745, 740, 690, 480 cm<sup>-1</sup>. Anal. Calcd. for C<sub>24</sub>H<sub>14</sub>: C, 95.33; H, 4.67. Found: C, 95.12; H, 4.71.

**Extraction of PAHs in Soot Samples.** Soot was collected at the lower part of the chimney of a public garbage furnace where a heavy oil has been used. Solvent-extractable matters were extracted with boiling benzene (200 mL) for 24 h from the soot (1.83 g). The extracts were concentrated, and the precipitated matter was filtered. The filtrate was directly analyzed without separation.

Another soot sample was obtained at a bottom of a chimney on a home furnace where firewood was burnt every day. Organic materials were extracted by the same method as described above from this soot (13.57 g). The extract was chromatographed on alumina (Merck, activity I, 30 g). The first fraction, eluted with hexane (300 mL),

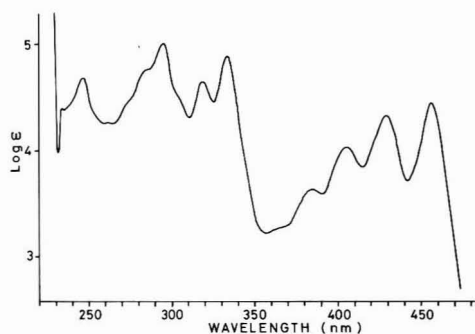


Figure 1. Ultraviolet and visible absorption spectrum of I in tetrahydrofuran.

contained mainly aliphatic hydrocarbons. All PAHs were involved in the second fraction, eluted with benzene (500 mL). The second fraction was concentrated and separated further by preparative thin-layer chromatography using silica gel plate and a 1:1 benzene/hexane solvent. The part corresponding to I was scratched off, and PAHs were extracted with ethyl ether. All solvents used were of pesticide grade and redistilled before use.

**Gas Chromatography-Mass Spectrometry (GS/MS).** Mass spectra were measured by using a JEOL Model JMS-DX 300 mass spectrometer connected with a HP 5710A gas chromatograph and a JEOL JMA-3500 mass data analysis system. Gas chromatographic conditions were as follows: column, 1% OV-1 (1 m  $\times$  3 mm i.d.); column temperature, 200  $^{\circ}$ C for 2 min followed by an increase to 310  $^{\circ}$ C at a rate of 8  $^{\circ}$ C/min; injection temperature, 350  $^{\circ}$ C; helium flow rate, 18 mL/min. Mass-spectrometric conditions were as follows: ion source temperature, 310  $^{\circ}$ C; ion source pressure,  $1 \times 10^{-6}$  torr; ionizing current, 300  $\mu$ A; ionizing energy, 70 eV; accelerating voltage, 3 kV; scan range,  $m/z$  100-400; scan speed, 1.5 s/scan; repetition time, 3.0 s.

**High-Performance Liquid Chromatography-Fluorescence Spectrometry (HPLC/FLS).** A Waters Model 7000A high-performance liquid chromatograph was used with a Hitachi 650-10LC fluorescence detector. The operating conditions were as follows: column,  $\mu$ Bondapak  $C_{18}$  (1/8 in.  $\times$  1 ft); solvent, 80:20 acetonitrile/water; flow rate, 2.0 mL/min; excitation wavelengths, 294.4 or 335.0 nm (slit width, 10 nm); emission wavelengths, 463.2 nm (slit width, 10 nm).

### Results and Discussion

A standard sample of I was prepared by a synthesis involving a new final step that was better than previous methods (1, 17, 18) for mildness of reaction condition. The ultraviolet and visible absorption spectrum of I was measured in tetrahydrofuran and is shown in Figure 1. The UV spectrum was slightly different from the ones observed by other authors (17-20) because the solvent was different. Fluorescence excitation and emission spectra of I were measured in tetrahydrofuran and are shown in Figure 2. The wavelengths of excitation or emission maxima are similar to those reported (14, 15) but their relative intensities are different. The mass spectrum of I is shown in Figure 3. Molecular and double-charged ions are prominently observed, being a characteristic pattern of PAHs. The extraction process was followed by the method described previously (15). Contamination in extraction and fractionation processes was not observed, while rather rapid decomposition was observed on the thin-layer

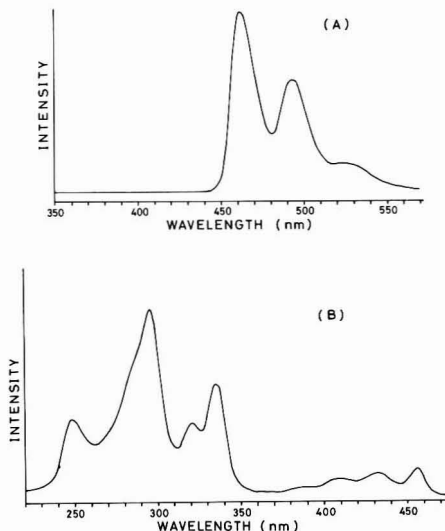


Figure 2. Fluorescence emission spectrum (A, excitation wavelength of 294.4 nm) and excitation spectrum (B, emission wavelength of 463.2 nm) of I.

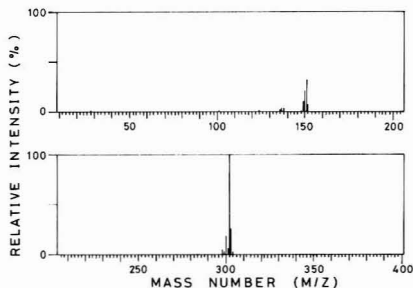
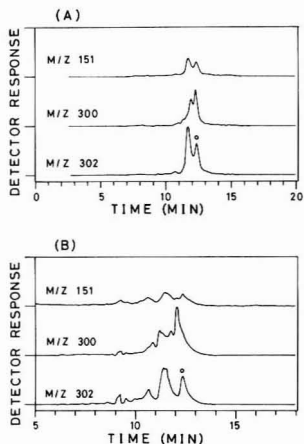


Figure 3. Mass spectrum of I.

chromatograph plate by use UV irradiation. Therefore, it is recommended that extraction and fractionation processes be operated under protection from strong light and that the solution containing I be stored under as low temperature as possible.

Combination of separation technique by GC and selective detection by MS is extremely effective for the determination of I even in the presence of various PAHs. Mass chromatography was carried out at  $m/z$  302, 300, and 151 for identification. Typical mass chromatograms are shown in Figure 4. A total current chromatogram was useless for the analysis because an exact peak due to I was completely concealed by many predominant peaks. The strong peak appearing at retention time 12.14 min in the mass chromatogram of  $m/z$  302 was due to I. It was confirmed with peak enhancement by spiking a standard sample. Also, mass spectra at the retention time corresponding to that of I agreed with the mass spectrum of a standard as shown in Figure 5.

An ion of  $m/z$  302 can come from  $C_{24}H_{14}$  (mol wt 302) and  $C_{24}H_{12}$  (mol wt 300) species. For this reason the mass chromatogram at  $m/z$  300 was also measured. The major peak in the mass chromatogram at  $m/z$  300 was assigned to coronene. Therefore, the peak of the same retention time as that of coronene in the mass chromatogram at  $m/z$  302 was ascribed to coronene. Another small peak in the



**Figure 4.** Mass chromatograms of the extracts from soot samples: (A) soot from the public garbage furnace; (B) soot from the home furnace. Peaks marked O correspond to I.

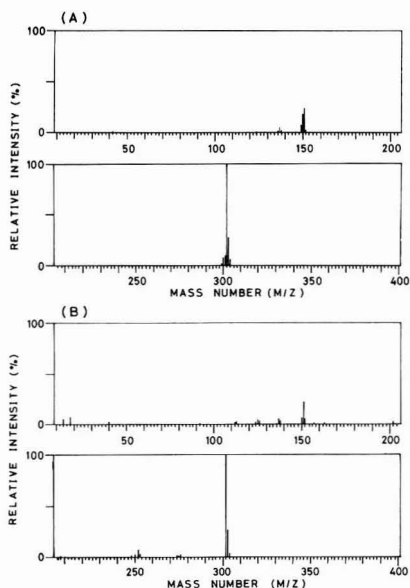


**Figure 5.** Mass spectra obtained with extracts from soot samples: (A) soot from the public garbage furnace; (B) soot from the home furnace.

*m/z* 302 mass chromatogram was thought to be one of the equal molecular weight isomers of I. Pierce and Katz (15) detected four hexacyclic compounds having the same molecular formulas of  $C_{24}H_{14}$  in the extracts from airborne particulate matter. In this study, only two  $C_{24}H_{14}$  species were observed in garbage soot. The detection limit of I by GC/MS was subnanograms in the standard sample, and the relative standard deviation was around 10%.

HPLC/FLS was used for further confirmation. HPLC using reverse-phase column has been known to show high resolution for analysis of PAHs and fluorescence spectrometry has high selectivity and sensitivity. A similar condition in the analysis of benzo[a]pyrene was used. The detection limit was estimated by using 294- or 335-nm excitation wavelengths and a 463-nm emission wavelength. Both excitation wavelengths gave practically the same sensitivity, and the detection limit was estimated to be 1

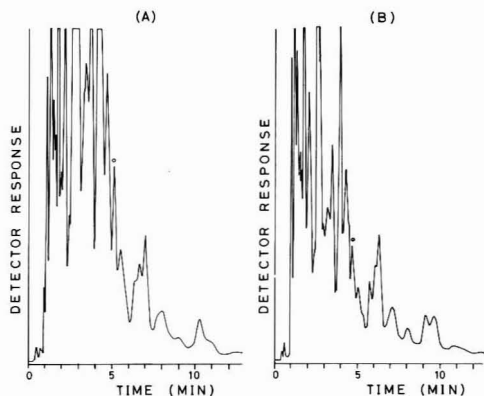


**Figure 6.** High-performance liquid chromatograms of soot extracts from the public garbage furnace with a fluorescence detection of 463 nm: (A) excitation wavelength of 294 nm; (B) excitation wavelength of 335 nm. Peaks marked O correspond to I.

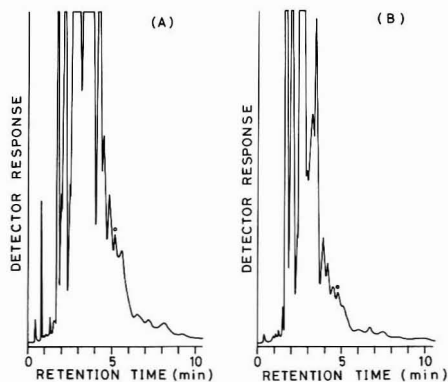


**Figure 7.** High-performance liquid chromatograms of soot extracts from the home furnace with the fluorescence detection of 463 nm: (A) excitation wavelength of 294 nm; (B) excitation wavelength of 335 nm. Peaks marked O correspond to I.

pg for pure standard sample with  $S/N = 2$  as the detection limit. Figures 6 and 7 show the chromatograms of soot samples obtained with 294 and 335 nm excitation wavelengths. Although both chromatograms gave similar patterns, the use of a 335-nm excitation wavelength seemed superior to that of 294 nm because the peak height ratio of other material to I was smaller in the 335-nm than the 294-nm chromatogram. Peak assignment and quantification were made by the standard addition method.

Analytical results by HPLC/FLS (excitation wavelengths, 335 nm) were 14.9  $\mu\text{g/g}$  for soot from the public garbage furnace and 0.15  $\mu\text{g/g}$  for soot from the home furnace. For the exact determination of I, further extensive work is necessary.

Pierce and Katz reported the concentrations (5.1 and 1.9  $\mu\text{g/g}$ ) in airborne particulate matters by TLC/FLS. In our attempt to determine I in a dust on an air-conditioner filter set up in a biotron, which is a special germless building for animal experiments, the level of I was no more than 0.2  $\mu\text{g/g}$ . The difference may be due to the difference of sample and/or the difference of analytical method.

It is worthy to note that the chromatogram is not simple even with the high resolution ( $N = 4500$ ) by HPLC and selective fluorescence spectrometric detection. There may be some danger of overestimation when TLC is employed

instead of HPLC because the resolution of TLC is inferior to HPLC.

The existence of I in soot was verified both by GC/MS and HPLC/FLS methods. Since soot is one of the source of environmental contamination by PAHs, further investigation is necessary to establish a routine analytical procedure and to estimate its concentration in the environment.

**Acknowledgments**

We thank Naoki Furuta for measuring standard fluorescence excitation and emission spectra of I.

**Literature Cited**

(1) Cook, J. W.; Hewett, C. L. *J. Chem. Soc.* 1933, 398.  
 (2) Pullman, A. *Ann. Chim.* 1947, 2, 5.  
 (3) Lacassagne, A.; Buu-Hoi, N. P.; Zajdela, F. C. R. *Hebd. Seances Acad. Sci.* 1960, 250, 3547.  
 (4) Buu-Hoi, N. P.; Hien, D. Z. *Naturforsch., B* 1967, B22, 532.  
 (5) Herndon, W. C. *Trans. N.Y. Acad. Sci.* 1974, 36, 200.  
 (6) Hoffman, F. *Theor. Chim. Acta* 1969, 15, 393.

(7) Scribner, J. D. *Cancer Res.* 1969, 29, 2120.  
 (8) Sung, S. C. R. *Hebd. Seances Acad. Sci., Ser. D* 1972, 274, 1597.  
 (9) Popp, F. A. *Arch. Geschwulstforsch.* 1977, 47, 97.  
 (10) Berger, G. D.; Smith, I. A.; Seybold, P. G.; Serve, M. P. *Tetrahedron Lett.* 1978, 231.  
 (11) Smith, I. A.; Berger, G. D.; Seybold, P. G.; Serve, M. P. *Cancer Res.* 1978, 38, 2968.  
 (12) Norden, B.; Edlund, U.; Wold, S. *Acta Chem. Scand., Ser. B* 1978, B32, 602.  
 (13) Sawicki, E.; Johnson, H. *Microchem. J.* 1964, 8, 85.  
 (14) Sawicki, E.; Stanley, T. W.; Johnson, H. *Microchem. J.* 1964, 8, 257.  
 (15) Pierce, R. C.; Katz, M. *Anal. Chem.* 1975, 47, 1743.  
 (16) Vollmann, H.; Becker, H.; Corell, M.; Streeck, H. *Justus Liebigs Ann. Chem.* 1937, 531, 1.  
 (17) Clar, E. *Ber. Deut. Chem. Ges.* 1936, 69, 1671.  
 (18) Clar, E.; Willicks, W. *Chem. Ber.* 1956, 89, 743.  
 (19) Clar, E. *J. Chem. Soc.* 1949, 2168.  
 (20) Boggiano, B.; Clar, E. *J. Chem. Soc.* 1957, 2681.

Received for review April 1, 1982. Accepted July 22, 1982.

## Removal and Recovery of Arsenious Oxide from Flue Gases. A Pilot Study of the Activated Carbon Process

Roger L. Player

Mount Isa Mines Ltd., Mount Isa, Queensland 4825, Australia

Hulbert J. Wouterlood\*

CSIRO Division of Fossil Fuels, North Ryde, New South Wales 2113, Australia

■ Absorption of arsenious oxide vapors by activated carbon was studied in a pilot unit linked to an industrial furnace. The unit was designed for a flow of 10 (N)m<sup>3</sup>/h and an uptake of 1.62 kg of arsenious oxide. The results confirmed the findings of the laboratory investigation; the arsenic content of flue gas was reduced by 99.94% without cooling the gas. The carbon could be regenerated by purging with nitrogen gas at about 400 °C. Arsenic was recovered as pure, saleable arsenolite (As<sub>2</sub>O<sub>3</sub>). However, the pilot-plant studies indicated that the following problems could arise in a full-scale plant: (1) combustion of the activated carbon by oxygen in the incoming gas; (2) blockage of the absorption columns by dust in the incoming gas; (3) formation of sulfuric acid in the condenser. However, insufficient data were available to assess secondary chemical reactions and/or corrosion of the columns and condenser by sulfuric acid.

### 1. Introduction

One of the problems encountered in high-temperature metallurgical processes is the safe disposal of the heavy-metal impurities originating from ores and concentrates. Removal of particulate matter is often not sufficient as some substances have an appreciable volatility at the temperature of the flue gas. An important example of the latter category is found in the smelting of arsenic-containing sulfide ores. At typical gas temperatures (~200 °C) only about 10% of the arsenious oxide present in the flue gas can be removed as solid, together with other particulate matter; the remainder occurs in the vapor state and must be removed by methods other than baghouses or electrostatic precipitators.

An efficient method of arsenic removal to meet the increasingly stringent statutory regulations is economically attractive because it would obviate the need for stockpiling of ores with a high arsenic content but otherwise suitable properties for smelting.

Previous laboratory investigations (1) showed that activated carbon was the most promising material for absorbing arsenious oxide from hot flue gas (150–200 °C) without the need for lowering the gas temperature drastically. Flue gas cooling would effectively remove arsenic by condensation but would have a deleterious effect on the performance of the stack. Moreover, arsenious oxide could be recovered easily, and in a pure form, by heating the saturated carbon to about 400 °C and purging with an inert gas.

Following the success of the laboratory experiments (1), a pilot unit with a packed-bed absorber was built to evaluate the absorption process under industrial conditions. The rig was operated at a large smelter at intervals over 2 years for a total operating time of 4938 h. This paper reports the results obtained with the pilot unit and their application in the design of a full-scale plant.

### 2. Pilot Unit

**2.1 Design Considerations.** On the basis of the results of the laboratory-scale tests (1), the following features were considered to be essential or desirable: (1) a gas residence time in the column of 6 s, as in the laboratory investigation; (2) a column diameter of 152 mm, which is large enough to eliminate wall effects; (3) an arbitrary height of 914 mm to permit variation of bed depth and thus residence time, independent of flow rate; (4) a system of two columns, chosen in view of the long absorption time, whereby one

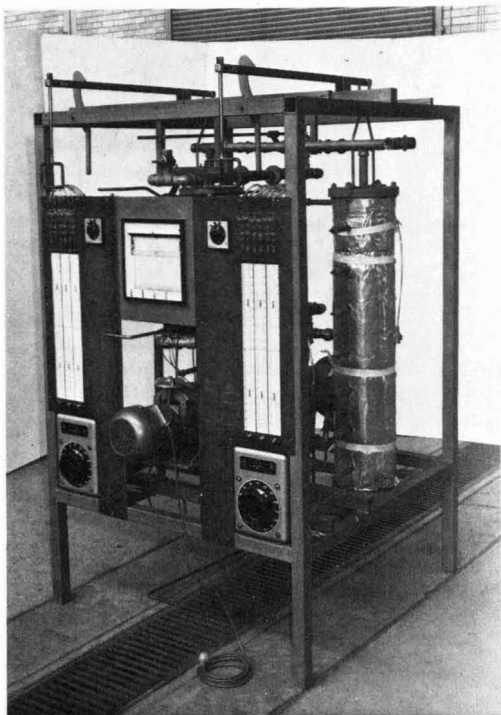


Figure 1. Front view of pilot plant under construction.

column could be purged while the other column was absorbing; (5) operating temperatures of 200 °C during absorption and 400 °C during desorption, as in the laboratory experiments; (6) facilities to monitor the inlet pressure to the column and the pressure drop over the length of the bed; (7) observation of the changes in weight of the columns during absorption and desorption with an accuracy of about 10 g; (8) reversal of gas flow during desorption to minimize the risk of a premature breakthrough of arsenious oxide in the next absorption cycle; (9) facilities for regeneration either with clean gas from the absorber column or with cylinder gas, e.g., nitrogen; (10) a condenser for recovery of the arsenious oxide liberated during desorption.

With the chosen dimensions, the area of the column is 182 cm<sup>2</sup> and the volume 0.016 68 m<sup>3</sup>. A residence time of 6 s then yields a superficial gas velocity of 15.24 cm/s and thus a volumetric flow of 0.1668 (N)m<sup>3</sup>/min ((N)m<sup>3</sup> = m<sup>3</sup> at standard temperature and pressure). At a bulk density of 485 g/L, 8.09 kg of carbon is required to fill one column. An uptake of arsenious oxide equal to 20% of the weight of the column packing could be expected, i.e., 1.62 kg. With reasonable values for gas flows and for arsenic loadings, it was calculated that the column packing would perform for as long as 45 days before becoming saturated.

**2.2 Construction Details.** The pilot plant (Figures 1 and 2) consisted of two mild steel columns supported side by side in a framework. Between them was a condenser featuring a water-cooled shell and a four-blade rotary scraper driven by an electric motor via a variable-speed transmission. The condenser unit was set at an angle to facilitate gravity movement of solid arsenious oxide toward the catchpot.

A system of ganged valves operated by levers at the front of the plant enabled the simultaneous admission of ar-

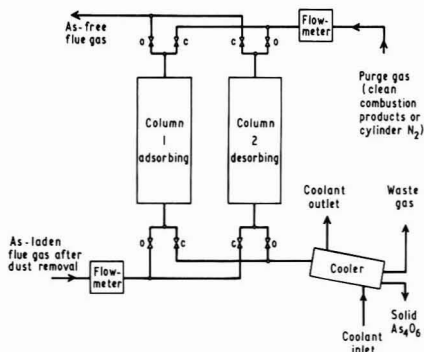


Figure 2. Flowsheet of pilot unit.

senic-bearing flue gas to the bottom of one column and purge gas to the top of the other column, and vice versa. In this way one column could function as absorber while the other was being regenerated. The exit gas from the latter was taken to the condenser, from which solid arsenious oxide could be collected.

Each column was provided with seven thermocouples at 15-cm vertical intervals and ports for withdrawal of gas and/or solid samples. A multiport valve was incorporated to monitor the gas pressure in the inlet and the outlet of the column, as well as the pressure drop over the bed. In this way impending blockages could be detected early.

Independent temperature control of each column provided for operation to 400 °C. Temperatures in the columns were monitored on a 12-point potentiometric recorder. Gas flows were measured by calibrated dual-range orifice meters with manometers on the front panel. Each column could be detached from the pipework and lifted onto a scale by means of a lever. All pipework was equipped with Pyrotex heating elements and lagged to prevent condensation of solids.

Oxygen in the flue gas was monitored by means of a paramagnetic oxygen analyzer. An infrared gas analyzer was used to measure sulfur dioxide concentrations in the effluent gas from the condenser.

**2.3 Testing.** Full-scale testing of the pilot unit before transport to the test location would have required the production of large volumes of arsenic-bearing gas, and this was deemed undesirable.

The efficacy of the scraper-cooler was assessed in the laboratory by a simulated desorption procedure using naphthalene as a model compound. One column was employed as a source of vapor by filling it with a mixture of 9 kg of Yallourn brown coal char (-6.5 + 1.5 mm) and 1.2 kg of crude flaked naphthalene. Air was supplied to the top of the column (in the "purge" mode) to give a flow of 2.1-2.5 (N)m<sup>3</sup>/h.

Naphthalene was released steadily at a temperature of 65 °C into a gas flow of 2.5 (N)m<sup>3</sup>/h. Desorption was monitored by weighing the column. Naphthalene was recovered continuously as a well-crystallized white product, indicating that no metal from the scraper-cooler was entrained.

The scraper became very noisy when solid material had condensed on the walls of the cooler. The blades were reground to provide more clearance and a relief at the trailing edge. This improved the performance. It was later found that the best way to operate the scraper was in short bursts (2 min) at maximum speed (400 rpm) every 2 h.

Dummy runs were carried out to test the temperature controllers, to ensure that the heating system was adequate

Table I. Experimental Conditions

run	carbon	column temp, °C		Absorption			As <sub>4</sub> O <sub>6</sub> in column after absn, %	
		av	range	flow rate, (N)m <sup>3</sup> /min	vol of gas treated, (N)m <sup>3</sup>	duration, h	av	max
		2	A <sup>a</sup>	157.0	141-179	0.170	8364	820
3	A	173.6	151-187	0.128	5267	686	14.8	21.7
4	A	159.2	157-163	0.130	5476	702	13.5	21.9
5	G <sup>b</sup>	151.2	132-161	0.135	3224	398	8.2	31.2
6	H <sup>c</sup>	161.2		0.110	3610	547	10.6	17.2

run	column temp, °C		Desorption			As <sub>4</sub> O <sub>6</sub> in column after absn, %		
	av	range	flow rate, (N)m <sup>3</sup> /h	vol of purge gas, (N)m <sup>3</sup>	duration, h	av As <sub>4</sub> O <sub>6</sub> in purge gas, g/(N)m <sup>3</sup>	av	max
	2	379.3	232-440	0.080	30.7	384	42.4	1.3
3	367.8	299-426	0.185	32.5	176		7.9	11.5
4	354.1	224-419	0.185	44.8	242		1.6	6.9
5	390.0		0.230	144.0	626		8.5	12.5

<sup>a</sup> Made from Victorian brown coal, of medium activity, surface area 900 m<sup>2</sup>/g. <sup>b</sup> A high-grade carbon made from Victorian brown coal. <sup>c</sup> A medium-activity carbon, surface area 625 m<sup>2</sup>/g.

and to ascertain the temperature distribution in the columns.

**2.4 Installation in an Industrial Situation.** Initially, the pilot unit was connected to the outlet of the induced draught fan of a large industrial furnace via a cyclone, to remove coarse grit, and a cylindrical filter (10 cm in diameter, 30 cm long) packed with glass wool, to remove fine dust. The cyclone, filter, and associated pipework were maintained at the temperature of the flue gas by external heaters. The outlet gas from the unit was returned to the flue by two blowers connected in series.

After the second run the unit was relocated to obtain a more suitable sampling point, closer to the waste heat boilers, where the oxygen content of the flue gas was lower.

**2.5 Operation.** Once the pilot unit had been connected to the flue gas and absorption had begun, arsenious oxide concentrations in inlet and outlet gas were measured intermittently during each 8-h shift (see section 3.12). Temperatures at the seven locations in the column were recorded continuously. Absorption was continued until rising concentrations of arsenious oxide in the outlet gas indicated a distinct breakthrough. At various stages during the absorption phase, samples of carbon were taken from each sampling port and analyzed for arsenic. These amounts were plotted to give loading profiles. From the final profile the width of the absorption front at breakthrough was determined.

A similar procedure was followed during desorption. During each shift the arsenious oxide collected in the condenser was weighed, and the volume of purge gas was measured. From these data the arsenious oxide loading of the purge gas was calculated. Desorption was continued until no more arsenious oxide could be collected from the condenser. The carbon was then sampled and analyzed as in the absorption runs.

### 3. Results

Six absorption and five desorption runs were conducted under the conditions described in Table I. A short description of each run, together with the principal results, is given below.

**3.1 First Run.** Uncontrolled ignition of the carbon bed occurred several times. During ignition, the temperature of the bed exceeded 500 °C, resulting in loss of carbon and desorption of arsenious oxide. Although no arsenious oxide

Table II. Arsenious Oxide Content of Column after Second Absorption

sampling pt	As <sub>4</sub> O <sub>6</sub> , %	SO <sub>4</sub> <sup>2-</sup> , %	total S, %	temp, °C
1 (top)	<0.66			179
2	1.27	0.5	0.71	176 <sup>b</sup>
3	14.4	0.3	0.50	167
4	18.7	0.2	0.36	153
5	22.2	0.2	0.33	146
6	22.0	0.3	0.44	142 <sup>b</sup>
7 (bottom)	14.9 <sup>a</sup>	1.2	1.3	141

<sup>a</sup> The carbon charge in this section was contaminated with flue dust. <sup>b</sup> Calculated from temperature plot.

was collected in the condenser during desorption, when the column was dismantled, a deposit of large crystals of arsenious oxide was found inside the base of the column and on the gas distributor. This run confirmed that arsenious oxide can be absorbed by activated carbon from flue gas at 130-190 °C and can be desorbed at 360-450 °C with nitrogen as purge gas. It also demonstrated the need to keep low oxygen levels in the flue gas.

**3.2 Second Absorption Run.** The arsenic loading profile at the end of the run is given in Table II. A mass balance over the column indicated a total arsenious oxide content of 1166 g.

**3.3 Second Desorption Run.** The calculated amount of arsenious oxide removed by the purge gas (1073 g) represents a 92% recovery of the amount absorbed during the first phase of the run (1166 g). The calculated amount left in the column (93 g) agrees reasonably well with the amount (106 g) estimated from the average arsenious oxide content of the column after desorption (1.32%).

At the start of the desorption, high levels of sulfur dioxide (in excess of 20% v/v) were measured in the purge gas leaving the condenser, indicating that SO<sub>2</sub> as well as As<sub>4</sub>O<sub>6</sub> was absorbed on the carbon. The concentration decreased to zero in approximately 130 h (Figure 3).

**3.4 Third Absorption Run.** Temperature gradients in the column and fluctuations in column temperature with time were reduced by changes to the inlet filtering system and associated pipework and heaters.

The column arsenic levels at the end of this run were much lower than in the second absorption run. No com-

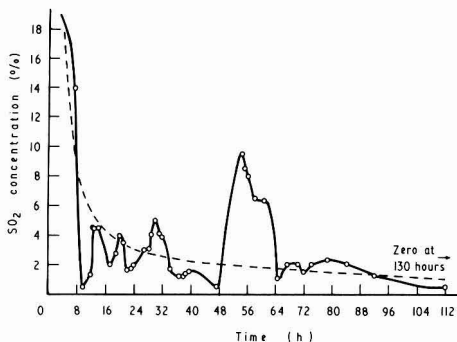


Figure 3. Desorption of sulfur dioxide: (—) daily variations; (---) mean value.

Table III. Arsenious Oxide Concentration in Column after Desorption (%)

position	3rd desorption	4th desorption
1 (top)		
2	3.6	0.44
3	8.8	0.46
4	7.4	6.9
5	8.2	0.33
6	11.5	0.61
7 (bottom)	8.3	0.40

bustion occurred. The width of the absorption front was again found to be of the order of 0.5 m. Column  $\text{SO}_4^{2-}$  levels were higher throughout the column than in previous runs (6.75% on average).

In the new location combustion of the charge did not recur, but new problems were encountered with dust buildup on the inlet filters.

**3.5 Third Desorption Run.** The arsenic levels remaining in the column after desorption were high, as only part of the arsenious oxide had been removed (see Table III). Desorbed arsenious oxide blocked the outlet pipe and prevented most of the oxide from reaching the condenser. The arsenic in the column was distributed more evenly throughout the carbon. Maintaining negative pressure throughout the column was difficult, as the pressure drop was large.

Water and sulfuric acid desorbed rapidly at 150–200 °C. Their desorption was completed after about 24 h, and the resulting acid solution was then removed from the condenser. This run demonstrated the need to redesign the condenser system.

**3.6 Fourth Absorption Run.** Arsenic levels in the column were slightly higher than for the third absorption run but lower than in the second run. No combustion occurred. The absorption front was about 0.2 m wide. The column was operated as a packed bed, being filled to the top and constrained by stainless steel mesh. Again the  $\text{SO}_4^{2-}$  levels were very high (6.29%). The results of this run did not differ very much from those obtained in the third absorption run.

**3.7 Fourth Desorption Run.** Most of the arsenious oxide condensed as dust in the first condenser, with some large crystals lying on the dust. Some oxide was captured in the second stage and a small amount escaped to the KOH solution in the bubbler. Once again it was difficult to maintain negative pressure throughout the column.

The residual arsenic loadings (Table III) are very low. The only reading in excess of 0.6% is from the center of

Table IV. Effect of Washing Arsenic-Laden Carbon

	$\text{SO}_4^{2-}$ , %	$\text{As}_2\text{O}_3$ , %
before	4.82	13.3
after	1.18	14.3

the column (6.9%). Carbon in this area may have been contaminated with condensed arsenious oxide from the side sampling points, which were not heated. The increase in the yield of arsenious oxide compared to the previous run reflects improvements made in the condenser system.

**3.8 Fifth Absorption Run.** The column was again operated as a packed bed. The run was terminated after a prolonged fire occurred, resulting in the loss of about 20% of the carbon charge. This was attributed to the use of high-grade carbon with higher reactivity.

The arsenic levels in the carbon at the end of the run were the highest observed so far. When the column was doused with water (in the course of extinguishing the fire) it was found that the arsenic level had increased somewhat but coadsorbed sulfate was removed, as is shown in Table IV. This run confirmed that the oxygen content of the incoming gas is critical when carbons of high activity are used.

**3.9 Fifth Desorption Run.** The condensing system for this run consisted of a small screw conveyor with a water-cooled copper coil around it at the inlet end. The gas was withdrawn from the lowest sampling point on the column itself. The arsenious oxide crystals were formed on the walls of the condenser and were swept along its length until they fell into a glass collecting vessel. This run confirmed that the design of the original condenser system, when properly proportioned, is the most suitable for full-scale operation.

**3.10 Sixth Absorption Run.** This run proved that other carbons of medium activity can also absorb well, although with reduced capacity. The experimental work was terminated at this stage, and no desorption of arsenic from the sixth absorption cycle was carried out.

**3.11 Measurement of Pressure-Drop Characteristics.** Carbon A, with a particle size range of 2–5 mm, was used in these measurements. Both laboratory tests at room temperature and plant tests at 160–180 °C were carried out. When the present laboratory measurements are compared with those reported in the first part of this investigation (1), it must be borne in mind that the particle size range used in the latter tests was somewhat wider (2–6 mm).

For a given superficial linear velocity, the pressure drop in the plant tests is greater than that in the laboratory tests. This is caused by (a) the increase in measurement temperature and (b) the gradual blocking of the base of the column by dust in the flue gas.

Calculation showed that an increase in temperature from 0 to 200 °C causes an increase in pressure drop of about 15%. The results of the measurements are given in Figure 4. It was found that those for the plant tests could be expressed by the empirical relationship

$$\Delta p/L = 11.4 \times v^{1.2}$$

where  $\Delta p$  = pressure drop over bed (kPa),  $L$  = bed depth (m), and  $v$  = superficial linear velocity (m/s).

**3.12 Measurement of Arsenic Concentration.** Arsenic concentrations in flue gas were measured by withdrawing a known volume of gas from the flue via a filter (kept at 170–180 °C) to remove all particulate matter. The gas was then passed through a known volume of 10% potassium hydroxide solution. Arsenic was determined in

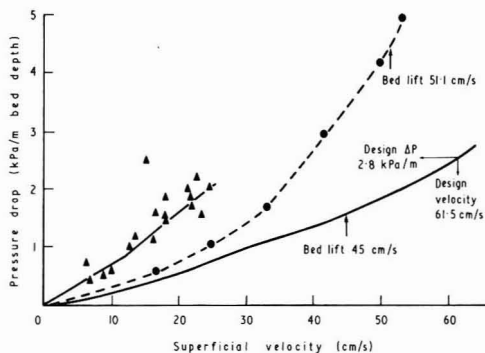


**Figure 4.** Pressure drop across the carbon bed: (—) earlier CSIRO laboratory tests (ref 1, room temperature, particle size 2–6 mm); (●) laboratory tests (room temperature, particle size 2–5 mm); (▲) plant tests (at 160–180 °C, particle size 2–5 mm).

the solution by iodometric titration. The detection limit of the method was 0.1 mg/(Nm<sup>3</sup>). Arsenic was also determined from time to time in carbon samples taken from various locations in the column.

#### 4. Discussion

**4.1 Absorption.** The saturation level of arsenious oxide absorbed on carbon A in the presence of flue gas was about 22% at temperatures in the range 130–190 °C. The corresponding figure for carbon G (of higher activity) was 31.2%, and that for carbon H (of lower activity) was 17.2%. A similar increase in arsenic absorption with surface area had been observed in the laboratory investigation with other carbons (1). The results obtained with carbon A are lower than those found in the laboratory tests, viz., 25.9% with a dry gas mixture and 24.5% with gas saturated with water vapor at room temperature. This is understandable because flue gases usually contain substantial quantities of water vapor from moisture in coal and combustion of hydrocarbons. Another reason for the lower arsenic loadings is that much higher flow rates were used than in the laboratory tests, and therefore equilibrium conditions were not reached.

The width of the absorption front ranged from 0.25 to 0.5 m, with a gradual decrease in concentration from the base upward. In the range of variables studied, the front width was not influenced by flow rate or temperature.

It was found that as the temperature of the column increased, the average and maximum arsenic levels decreased. The best temperature range appeared to be 150–160 °C. Gas flow rate did not affect the arsenic loading profile greatly.

The finding of the earlier investigation that the carbon charge was equally effective in subsequent cycles was confirmed.

Simultaneous adsorption of SO<sub>2</sub> occurred to a marked extent (about 6–7%). About 60–70% of total sulfur was present as sulfate. It was possible to remove this from the column at the end of the absorption period by washing with water, without affecting the absorbed arsenious oxide (Table IV).

**4.2 Desorption.** The concentration of the absorbed arsenious oxide could be reduced to about 0.65% by purging with nitrogen gas at 360–450 °C. This is rather better than was obtained in the laboratory tests, probably because of the higher temperature in the pilot plant. The concentration in the purge gas was found to vary considerably owing to the difficulty of maintaining a given flow rate and temperature at the inlet to the condenser. A

mean value of 47.3 g of As<sub>2</sub>O<sub>3</sub>/m<sup>3</sup> was found.

The effects of desorption temperature and gas flow rate on the desorption breakthrough and the concentration of arsenious oxide in the purge gas require further investigation. It was found, however, that as long as the temperature is kept above 300 °C desorption is fast. Higher gas flow rates do not appear to increase the rate of desorption.

Many difficulties were experienced in recovering condensed arsenious oxide. The scraper-cooler originally installed in the pilot plant was too large. Its holding capacity prevented frequent collection and weighing of the arsenious oxide required for studying the desorption quantitatively. Various condensers were tried, both air and water cooled, but all were prone to blocking by condensed arsenious oxide. Finally a smaller version of the original scraper-cooler idea was used in the form of a small screw feeder, one end of which was cooled by an external cooling coil. This has worked satisfactorily.

The appearance of the final product varied considerably, from well-formed, transparent crystals up to 6 mm thick to a dirty grey-brown powder contaminated with carbon and heavy-metal sulfates. X-ray diffraction and X-ray fluorescence analysis confirmed that arsenolite was the only phase in most samples. Purity was found to be very high, 99–99.5%.

When the flue gas contained little water vapor during the absorption period, sulfur was desorbed in the form of SO<sub>2</sub> only. The initial concentration in the purge gas was about 20%, dropping to zero in 130 h (Figure 3). When water vapor had been present, water and sulfuric acid desorbed rapidly at 150–200 °C for the first 24 h.

**4.3 Effect of Dust on Column Operation.** At the original location of the column—downstream from the dust collectors on the waste heat boilers—the dust concentration were low. A cyclone and glass wool filter, changed once or twice per 8-h shift, was sufficient to remove the remaining dust. At the final location, however, ahead of the dust collectors, the cyclone was followed by two bag filters in parallel. These rapidly became blocked and constant cleaning was required to maintain the flow. Considerable amounts of dust collected at the base of the column and about 15 cm into the carbon. While this had little effect on arsenic capacity, it increased the column pressure drop and created difficulties in desorption. Removal of this dust was required before desorption to prevent contamination of the product arsenolite. Moreover, the dust is hot and can readily ignite, thus causing problems in the control of overheating.

Absorption of arsenious oxide did not cause an increase in column pressure drop, as no such increase was found when the dust burden of the incoming gas was low.

**4.4 Effect of Oxygen Content of Flue Gas.** This is the most significant problem associated with any activated carbon adsorption process. In the early stages of the pilot-plant work there were problems with uncontrollable combustion of carbon in the column. This caused bed temperatures of over 500 °C, desorption of previously absorbed arsenious oxide, and loss of carbon. The fires could be attributed to (1) an unexpectedly high oxygen content in the flue gas (about 9%), largely the result of leaks in the ducting system, and (2) an influx of atmospheric air during cleaning of the inlet filter. It was also possible that the carbon bed had become contaminated with small amounts of unburned hydrocarbons from the reverberatory furnace operation.

When the pilot plant was moved to its new location, the oxygen level in the flue gas was much lower (1–4%), but



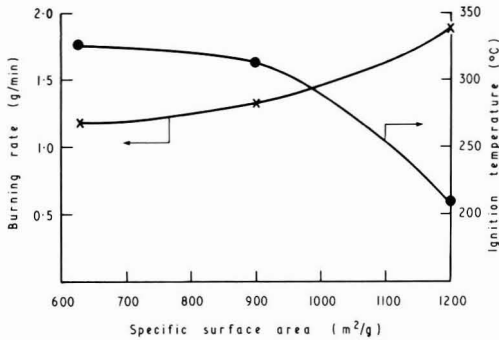


Figure 5. Carbon ignition temperature and burning rate.

peaks in the oxygen level to about 7%, arising from air admitted during charging of the furnace and when collapses of the furnace bricks occur, could possibly start a fire. It is not possible, therefore, to use cleaned flue gas from the absorber column as a purge gas for desorption unless the oxygen content remains very low throughout.

Moreover, it was further found that more highly activated carbons had a lower ignition temperature and a higher burning rate (see Figure 5). Carbon A appeared to be the most suitable compromise and was cheaper. Oxygen levels below about 7% appeared safe for this type of carbon at normal absorption temperatures.

It was found that in the absence of column fires, carbon consumption by the absorptions process was negligible.

### 5. Design of a Full-Scale Plant

Preliminary design calculations were made after completion of the first part of the investigation (1). As more data were acquired during the operation of the pilot plant, this initial design was updated several times. Some factors that have an important bearing on the design are discussed below.

**5.1 Linear Gas Velocity.** One of the key points in the design is the choice of superficial linear gas velocity for a given carbon. Low values result in very wide, shallow columns in which it is difficult to distribute the gas evenly. High values necessitate narrow, tall columns, which create a large pressure drop. This in turn calls for high fan power, which is costly. There is also the danger of fluidization of the bed when the linear velocity is high. It was found that it was easiest to operate the column as a packed bed. A value of 0.6 m/s was therefore considered a good compromise between these conflicting requirements. This corresponds to a pressure drop of 6.3 kPa/m (see section 3.11).

**5.2 Temperature.** The chosen operating temperature of 160 °C is also a compromise. When the temperature of the inlet gas is high and the absorption process is adapted to that temperature, the operation of the stack is optimized but at the cost of decreased absorption and increased risk of column fires (for a given level of oxygen in the incoming gas). When the inlet temperature is decreased, the latter factors are improved but at the cost of decreased buoyancy of the plume from the stack.

**5.3 Activated Carbons.** The choice of grade of activated carbon is a compromise between high surface area types (~1200 m<sup>2</sup>/g), which have a greater absorptive capacity for arsenic but are more liable to ignite (higher burning rate and lower ignition temperature), and those with a lower surface area (e.g., 600 m<sup>2</sup>/g), which are more tolerant toward oxygen although their absorptive capacity

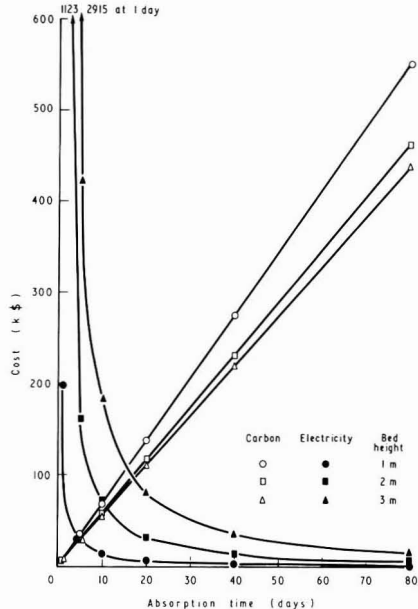


Figure 6. Carbon and electricity costs.

is smaller. Carbon A would seem to fulfill the requirements for large-scale operation.

**5.4 Dust Level of Incoming Gas.** While it was shown in the pilot plant operation that dust had little effect on the arsenic capacity of the column, it does increase the pressure drop. It also creates problems during desorption, and as it often ignites readily it can give rise to overheating problems. It is therefore imperative that a large-scale plant be operated after an efficient electrostatic precipitator or baghouse.

**5.5 Simultaneous Absorption of Sulfur Dioxide.** With sufficient water in the inlet gas, the coadsorbed sulfur dioxide and oxygen will produce sulfuric acid. During desorption a strong solution of H<sub>2</sub>SO<sub>4</sub> is accumulated in the condenser. The necessary equipment must be installed to neutralize this liquid, e.g., by reaction with limestone slurry. There is also the danger of corrosion of mild steel and a further reaction of the hydrogen thus released with arsenious oxide to form arsine. At present insufficient data are available to determine under which conditions these reactions occur.

**5.6 Scale-up Calculations.** In the final design calculations the following parameters were considered: (1) those determined by the plant to be detoxified, viz., flow rate and arsenic loading of the flue gas; (2) those determined by the absorption plant, viz., height and arsenic concentration of the front zone of the column, saturation concentration of the rest of the column, and density of the absorbent carbon.

It is assumed that three columns will be used: two for absorption and one for desorption, in keeping with current practice in similar active-carbon installations for other purposes (2).

On the basis of these input data, column characteristics such as diameter, quantity of carbon, pressure drop, and fan power were calculated as functions of the independent variables, absorption time, and column height.

Most of the major capital costs are virtually independent of column size. These include site preparation, structures, ducts, fans, valves, heaters, sealing and insulation, and the

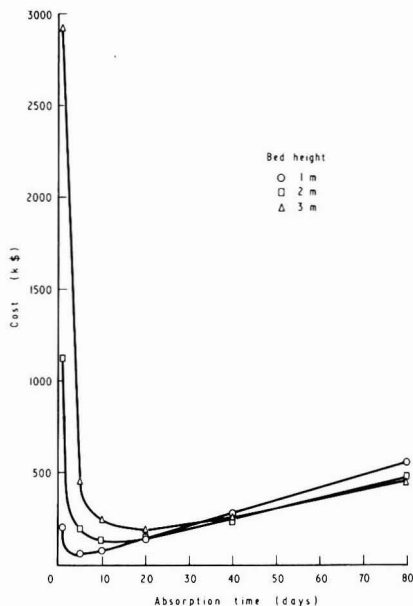


Figure 7. Variable fraction of total cost.

desorption plant. The capital cost of the carbon, however, is a function of absorption time and column height (see Figure 6).

The highest single operating cost is the fan power. Its relationship to absorption time and column height is also shown in Figure 6. Other major operating costs include heating, operating labor, and maintenance.

The total cost per annum thus consists of a more or less constant amount plus the sum of carbon and electricity costs as function of absorption time and column height. This relationship is given in Figure 7.

It can be seen that the cost of carbon increases linearly with absorption time, while that of power is proportional to (absorption time)<sup>-1.2</sup>. This stems from the use of the empirical relationship of pressure drop and linear velocity. Summation of these two costs results in a minimum in the curve for total cost (Figure 7). The cost is seen to rise rapidly for absorption times shorter than 5 or 10 days, whereas the increase is only gradual for times greater than 20 days.

## 6. Conclusions

(1) The process of absorption on activated carbon was used to reduce the content of arsenious oxide vapor in dust-free flue gas to 0.06% of its initial value without cooling the gas. Absorption proceeded excellently at 150–160 °C.

(2) Carbon loadings of 13–20% As<sub>4</sub>O<sub>6</sub> were obtained in the pilot plant compared to about 25% in laboratory tests. The concentration varied throughout the column.

(3) The absorption front in the carbon bed was about 0.5 m wide.

(4) The absorption process was affected by (i) carbon grade—a medium surface area (~900 m<sup>2</sup>/g) is the optimum with respect to all properties; (ii) coadsorption of SO<sub>2</sub>—when water vapor and oxygen are present, SO<sub>2</sub> is oxidized to SO<sub>3</sub> and forms sulfuric acid; (iii) temperature—higher concentrations of arsenious oxide in the column are promoted by lower temperatures.

(5) Oxygen levels in the flue gas must be kept below 7% to reduce the possibility of carbon ignition during the absorption cycle.

(6) Desorption to approximately 0.7% As<sub>4</sub>O<sub>6</sub> was possible.

(7) Nitrogen and carbon dioxide were suitable desorbing gases. Cleaned flue gas could only be used if it had a very low oxygen content (say 0.5% continuously). The cleaned flue gas encountered in the present studies (ca. 9% O<sub>2</sub>) caused combustion of the absorbing carbon at desorption temperatures of 350–450 °C.

(8) The desorbed arsenolite was of high quality (99.5% As<sub>4</sub>O<sub>6</sub>) if the inlet gas was dust-free. It was collected in a form that is directly saleable.

(9) Those costs related to size show a minimum for absorption times from 5 to 20 days.

## Acknowledgments

Thanks are due to the company on whose behalf this research was carried out and to the members of its staff involved in this project. We are also greatly indebted to K. McG. Bowling for many helpful discussions.

## Literature Cited

- (1) Wouterlood, H. J.; Bowling, K. McG. *Environ. Sci. Technol.* **1979**, *13*, 93–97.
- (2) Kiyoura, R.; Munidasa, M. *Proc. Int. Clean Air Congr. 2nd* **1970**, 842–850.

Received for review January 4, 1982. Revised manuscript received June 25, 1982. Accepted July 20, 1982.

## Development and Evaluation of Sunlight Actinometers

David Dullin and Theodore Mill\*

Physical Organic Chemistry Department, SRI International, Menlo Park, California 94025

■ We have developed and used two binary chemical actinometers for sunlight measurements from 300 to 370 nm that have the great advantage of possessing adjustable quantum yields to provide half-lives ranging from a few minutes to several weeks in sunlight. One actinometer is the known *p*-nitroanisole (PNA)/pyridine (pyr) system in water, the half-life of which in sunlight can be varied from a few minutes to 12 h by changing the concentration of the pyridine. The other actinometer is *p*-nitroacetophenone (PNAP)/pyr, which has a half-life in sunlight ranging from several hours to 2 months and also can be adjusted by varying the concentration of pyr. Both systems are well behaved kinetically and have quantum yields invariant with wavelength from 313 to 366 nm. Neither PNA nor PNAP is volatile from water or readily sorbed, and each is easily analyzed by UV or HPLC. For PNA/pyr,  $\phi = 0.44[\text{pyr}] + 0.00028$  and for PNAP/pyr,  $\phi = 0.0169[\text{pyr}]$ .

### Introduction

The Toxic Substances Control Act of 1976 (PL 94-469) requires that the U.S. Environmental Protection Agency (EPA) evaluate all new chemicals for their possible adverse effects on the environment before manufacture and use are permitted. The act also provides that the manufacturers of new chemicals provide the EPA with laboratory and other test data on the fate and effects of specific chemicals that may constitute a possible hazard to a biological population. To be useful to the EPA, test data must be developed under conditions that allow meaningful interpretation in the context of environmental transport and transformation processes.

Laboratory test methods or protocols have now been developed for a variety of kinetic and equilibrium fate processes believed to be important in aquatic, atmospheric, and soil systems (1, 2); other protocols are still being developed.

The photolysis protocols are designed to provide approximate or accurate rate constants for photolysis over a range of sunlight conditions commonly found in aquatic systems. However, application of the kinetic data derived from photolysis under one set of sunlight conditions to a wide range of sunlight conditions requires the use of one or more standard actinometers to monitor and integrate the variable solar irradiance during the photolysis period, which may last from a few minutes to several weeks (1). This study was conducted to explore, develop, and evaluate actinometers suitable for use in the sunlight photolysis protocols.

### Background

**General Considerations.** Estimation of the rate constant for photolysis in sunlight ( $k_{pE}$ ) of a specific chemical in dilute aqueous solution requires information about the absorption spectrum of the chemical, the quantum yield of the process ( $\phi$ , the efficiency), and the intensity of sunlight as a function of wavelength, latitude, season, and, perhaps, time of day (1, 3). Laboratory measurements give estimates of  $\phi$  at selected wavelengths, and solar irradiance data are available for all regular variations in the sun's zenith and declination. Thus, in principle,  $k_{pE}$  can be estimated from laboratory measurements. However, lab-

oratory measurements for  $\phi$  are time-consuming, require special equipment, and can be complicated by a variety of factors; estimates of  $k_{pE}$  made in this way sometimes are subject to significant errors, although in many cases the estimates agree closely with measurements made in direct sunlight (4, 5).

Estimates of  $k_{pE}$  and  $\phi$  can also be made by direct exposure of solutions of a chemical to sunlight providing the solar irradiance is monitored in some way to account for all of the variations induced by weather, diurnal cycling, and seasonal changes (for long exposures). One way to do this is to simultaneously expose another chemical (actinometer) that has a known value of  $\phi$  that is invariant with wavelength. Ideally, the chemical and actinometer should have similar absorption spectra and should be exposed for the same time period to ensure accurate integration of the solar irradiance available to the chemical. At the time this work began, no actinometers were available for use in sunlight for periods of days or weeks; laboratory actinometers such as *o*-nitrobenzaldehyde (5) typically have high values of  $\phi$  (>0.5) and have half-lives in sunlight of a few minutes.

**Kinetics of Environmental Photolysis.** The upper atmosphere cuts off solar irradiance at about 290 nm (Figure 1); therefore, chemicals in the terrestrial environment can absorb photons only at this or longer wavelengths. In general the specific photochemical process that occurs cannot be predicted, although some useful generalizations have been made (6, 7).

Kinetic relations governing light absorption and reaction in dilute solutions of chemicals in water have been discussed previously by Mabey et al. (1) and Zepp (8).

In sunlight, the rate constant for photolysis ( $k_{pE}$ ) is given by

$$d[C]/dt = 2.3r\phi\sum L_{\lambda}\epsilon_{\lambda}[C] = k_{pE}[C] \quad (1)$$

where  $\epsilon_{\lambda}$  and  $L_{\lambda}$  are the extinction coefficient and solar irradiance, respectively, at wavelength  $\lambda$ ,  $\phi$  is the quantum yield, which is assumed to be wavelength independent, and  $r$  is a reaction parameter characteristic of the system. Integration of eq 1 gives

$$\ln [C_0]/[C_t] = k_{pE}t \quad (2)$$

where  $[C_0]$  and  $[C_t]$  refer to concentrations at time zero and  $t$ .

Equation 2 may be used to estimate  $k_{pE}$  by using laboratory measurements of  $\phi$  and  $\epsilon_{\lambda}$  and tables of  $L_{\lambda}$  values to give values of  $k_{pE}$  for clear weather conditions. Equation 2 also can be used to estimate  $k_{pE}$  if losses of the chemical (C) and actinometer (A) are followed while both are exposed to sunlight; simple regression of  $\ln (A_0/A_t)$  vs.  $\ln (C_0/C_t)$  gives the slope  $S$ , from which the average or an environmental quantum yield for photolysis of the chemical ( $\phi_{cE}$ ) can be estimated from the outdoor experiment by using the relation

$$\phi_{cE} = \phi_a \left[ \frac{1 \sum L_{\lambda}\epsilon_{\lambda}^a}{S \sum L_{\lambda}\epsilon_{\lambda}^c} \right] \quad (3)$$

where superscripts a and c refer to actinometer and chemical, respectively. Once  $\phi_{cE}$  is known, eq 2 can be used

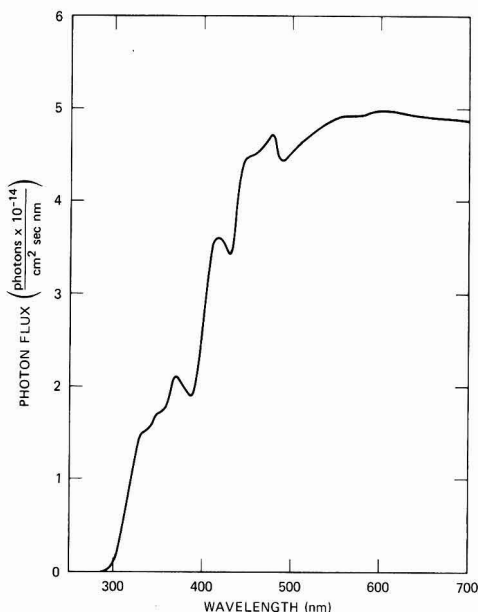


Figure 1. Solar irradiance as a function of wavelength.

to estimate  $k_{pE}$  at other latitudes and seasons in clear weather.

Equation 3 assumes that the ratio of the light absorbed by the chemical and the actinometer are constant over changes in seasons, latitudes, and sky conditions. This assumption is quite good if  $\lambda \geq 350$  nm but is increasingly in error as  $\lambda$  approaches 300 nm because the difference between intensities of sunlight near 300 and  $\geq 350$  nm increases in winter and under cloud cover.

Another problem that arises from using eq 3 is the need to interpolate values of  $L_\lambda$  that are usually listed for a single date in each season (1, 8) to the values of  $L_\lambda$  on the date of the experiment (and perhaps under cloud cover). Simple linear interpolation between seasonal values probably is accurate enough for this purpose. We estimate that  $L_\lambda$  will have a maximum error of 15% from the true value.

Finally, we must emphasize that  $\phi_{cE}$  estimated in this way is a quantum yield averaged over all wavelengths; regardless of whether the value is in good agreement with a measurement of  $\phi_c$  in a narrow wavelength interval, it does represent a "real" value applicable to exposure to the sun. In some cases, the value of  $\phi$  estimated in this way is more useful than the value measured in the laboratory, either because  $\phi$  is not constant with wavelength or because of special optical problems that can occur on photolysis in the laboratory but not in sunlight.

**Properties of Sunlight Actinometers.** For measuring sunlight intensity, chemical actinometry offers several advantages over instrumental methods, the most important being that the proper actinometer can integrate solar flux during the time and weather conditions experienced by the test chemical. Moreover the actinometer can conform to the same geometry as that of the test chemical.

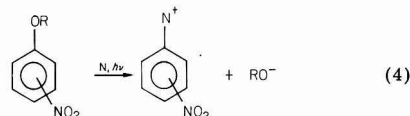
Listed below are several criteria for chemical and spectral properties that we believe should be given high priority in selecting actinometers for use in sunlight. An ideal sunlight actinometer should (a) absorb light moderately and uniformly in the near UV but be relatively stable in room light, (b) have a quantum yield that is temperature and wavelength independent, (c) have a

quantum yield that is independent of the concentration of the actinometer, (d) have an adjustable half-life between 0.1 and 30 days, (e) have photolysis products that do not interfere with photolysis, either chemically or spectrally, (f) be readily analyzed by conventional methods, (g) be very stable in water in the dark, (h) be moderately soluble and nonvolatile in water.

The adjustable half-life or quantum yield is perhaps the most unusual but most useful feature for a sunlight actinometer. In practice the half-life or quantum yield would be varied by changing the composition of the actinometer solution in some way to bracket the half-life of the test chemical and ensure that both actinometer and chemical were exposed to the same levels of sunlight.

The most promising approach to developing an actinometer with an adjustable half-life lies in finding suitable bimolecular photoreactions that are therefore amenable to changes in  $\phi$  with changes in the concentration of one (usually photoinert) reactant. Photonucleophilic substitutions constitute one important class of these reactions (9, 10).

In general, among substituted benzenes and naphthalenes,  $\text{NO}_2$  substitution activates loss of OR (10); see eq 4, where  $\text{N} = \text{N}_3^-$ ,  $\text{MeNH}_2$ ,  $\text{HO}^-$ ,  $\text{R}_1\text{R}_2\text{NH}$ ,  $\text{C}_6\text{H}_5\text{N}$ ; OR =



OMe,  $\text{OSO}_3^-$ . Many of these reactions follow the relation

$$\phi = k_p[\text{N}] \quad (5)$$

### Experimental Procedures

**Chemicals.** All chemicals came from commercial sources and were used without further purifications because analyses by HPLC revealed only trace impurities in the samples.

**Preparation of Reaction Solutions.** All glassware used was routinely baked overnight at 580 °C. Solutions of chemicals were prepared in pure water obtained from a Milli-Q water purification system. The filter-sterilized water obtained typically shows greater than 18 mho cm resistivity and less than  $1 \mu\text{g mL}^{-1}$  total organic carbon, which is the detectable limit.

Reaction solutions were usually prepared from a stock solution of the chemical in acetonitrile. An aliquot of this solution was diluted with an amount of water to give a 1% or 0.1% acetonitrile in water solution. Preparation of the stock solution and subsequent dilutions were made to obtain the desired concentrations.

**Laboratory Photolyses.** Reaction mixtures of the chemical (4 mL) were placed either in 12-mm o.d. borosilicate (Pyrex 7740) or 11.9-mm o.d. quartz tubes and photolyzed on a merry-go-round reactor (MGRR) (Ace Glass). The irradiance source was a Hanovia 450-W medium-pressure Hg lamp contained in a borosilicate immersion well. The distance between the irradiance source and tubes was about 10 cm. The reaction temperature was the ambient operating temperature of the system ( $\sim 26$  °C).

The photolyses were carried out by using several different filter systems, which were placed between the Hg lamp and the reaction mixtures. In all laboratory photolyses, the borosilicate glass immersion well (8-mm total glass path length) served as a filter to screen out all light below 290 nm. The 313 and 366 nm filter systems are

Table I. Photolysis of PNA/pyr at 313 nm and 26 °C<sup>a,b</sup> in Pyrex

time, min	10 <sup>4</sup> [PNA], M
0	7.90
30	4.98
50	3.50
75	2.38
120	1.24
150	0.77

<sup>a</sup>  $k_p = 1.54 \times 10^{-2} \text{ min}^{-1}$ ;  $t_{1/2} = 44.9 \text{ min}$ . <sup>b</sup> [pyr] = 0.0124 M;  $\phi(313) = 5.7 \times 10^{-3}$ .

described by Calvert and Pitts (6). Sample tubes were removed from the MGRR at appropriate times and analyzed at the end of each experiment. We calculated  $\phi$  from the photolysis rate constant  $k_p$  as described previously (1, 6, 8).

**Actinometry with *o*-Nitrobenzaldehyde.** The photochemical system was calibrated at 313 and at 366 nm by using the *o*-nitrobenzaldehyde actinometer system (6). In these calibration experiments, a solution of approximately  $1 \times 10^{-2} \text{ M}$  *o*-nitrobenzaldehyde in acetonitrile was photolyzed in borosilicate or quartz tubes for reaction times as long as 16 min at either wavelength in the MGRR. The solutions were analyzed for starting aldehyde by using reverse-phase HPLC with 50% acetonitrile in water as eluent. The light incident on the tubes was then calculated according to the method of Calvert and Pitts (6) by using a quantum yield for *o*-nitrobenzaldehyde photolysis of 0.505. We calculated that at 313 nm  $I_0$  varies from  $2.5 \times 10^{-6}$  to  $3.5 \times 10^{-6} \text{ einstein s}^{-1} \text{ L}^{-1}$  and at 366 nm varied from  $6.73 \times 10^{-6}$  to  $8.18 \times 10^{-6} \text{ einstein s}^{-1} \text{ L}^{-1}$ .

**Sunlight Photolyses.** Outdoor photolyses were carried out with pure water solutions of each chemical. Photolyzed solutions were placed in a location free of excessive reflections from walls and windows and without morning and afternoon shadows. We used 12-mm o.d. borosilicate or 11.9-mm o.d. quartz tubes held in a rack at a 45° angle to the horizon for PNA and PNAP samples and at 60° to the horizon for all other samples. The tubes were made from the same glass stock used in the laboratory photolyses. Rate constants were evaluated in the same way as laboratory photolyses rate constants.

**Analyses.** Most analyses were performed by HPLC on a Waters Associates chromatograph (Model 6000A pump, MV6K injector, and a M440 absorbance detector). Separations were made with a 30 cm  $\times$  4 mm  $\mu$ Bondapak C<sub>18</sub> column (reverse phase). The solvent eluent composition, UV detector wavelength, and internal standard (the internal standard in all cases *p*-nitrotoluene, if any, are given in the following table. Peak areas in the HPLC traces were determined on a Spectro-Physics Autolab Minigrator.

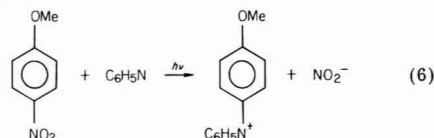
	mobile phase	flow rate, mL/min	detector, wavelength, nm
<i>p</i> -nitroanisole	50/50 CH <sub>3</sub> CN/H <sub>2</sub> O	2	300
<i>p</i> -nitroacetophenone	50/50 CH <sub>3</sub> CN/H <sub>2</sub> O	2	288
dibenzothio-phenone	75/25 CH <sub>3</sub> CN/H <sub>2</sub> O	2	244

**Data Treatment.** First-order rate constants were estimated from the regression ln ( $C_0/C_t$ ) vs. time by using standard linear regression programs available in many small calculators, including the HP-97 Stat Pac. The

special case of  $C_t = C_0$  was not used to avoid forcing the origin through zero. The slope of the regression is  $k_p$ .

## Results

***p*-Nitroanisole/Pyridine Actinometer.** One potentially useful reaction involves pyridine (pyr) substitution on *p*-nitroanisole (PNA) first described by Letsinger et al. (11) (eq 6). When the reactants are irradiated in water



with light  $\geq 300 \text{ nm}$ , the reaction proceeds cleanly over 10 half-lives to give the single product. Oxygen does not affect the reaction, nor are secondary reactions of either  $\text{NO}_2^-$  or *p*-pyridinium anisole reported. The reaction slows slightly with increasing temperature, indicating a small negative activation energy ( $-3 \text{ kcal/mol}$ ).

The UV spectrum of PNA shows a maximum at 314 nm ( $\log \epsilon = 4.04$ ); pyr absorbs much more weakly, with a maximum at 250 nm ( $\log \epsilon = 3.48$ ). Consequently, even high concentrations of pyr do not absorb significant fractions of sunlight.

Our experiments used concentrations ratios of PNA:pyr of 1:10 to 1:1000 to maintain a large excess of pyr over PNA throughout the reaction and to ensure a reasonable approximation to pseudo-first-order kinetics. However, water was found to compete with pyr at the lowest pyr concentration used. Table I summarizes some typical experimental data for PNA with 0.0124 M pyr. The reaction was well behaved over two half-lives, with a half-life of 45 min. For this reaction, the quantum yield was calculated to be  $5.7 \times 10^{-3}$ .

The effect of varying concentrations of pyr on the value of  $\phi$  at 313 and 366 nm is summarized in Table II. The most important features of the data are (1) the constant value of  $\phi$  at 313 and 366 nm at three concentrations of pyr, (2) the linear relation between  $k_p$  or  $\phi$  over a 20-fold change in pyr concentration, and (3) the competitive photoreaction of PNA with water. The range of reactivity observed here is equivalent to 15 min to 4 h for PNA/pyr exposed to bright summer sunlight. The data in Table III correlate with the relationship

$$\phi_{\text{obsd}} = 0.44[\text{PYR}] + 0.00028 \quad (7)$$

We performed several experiments to measure the rate constant for photolysis of PNA in sunlight ( $k_{\text{PE}}$ ) using PNA solutions in quartz tubes mounted at 60° from the horizon. These values and corresponding half-lives are listed in Table III. PNA/pyr or PNA in water alone is a fast actinometer with half-lives ranging from 12 h under overcast conditions with little or no pyr to as little as 13 min in clear weather with 0.01 M pyr.

Table IV lists values of the half-life of PNA for all four seasons over a range of [pyr], calculated by using eq 1.  $\phi$  values were measured at 313 and 366 nm and combined with the sum of  $L_{\lambda 6\lambda}$  for absorption of PNA from 299–430 nm.  $L_{\lambda}$  values were taken from Mabey et al. (1). These data are plotted in Figure 2 for convenient reference in selecting a value of [pyr] to give a desired half-life of PNA.

The reader should note that all values of  $t_{1/2(\text{E})}$  in Table IV have been divided by 2.2 to convert them from values applicable to a flat water body (for which  $L_{\lambda}$  applies) to cylindrical tubes exposed to scattered light on all sides. We have compared the rates of photolysis of aqueous solutions of PNA/pyr, PNAP/pyr, and Rose bengal in open

**Table II. Rate of Photolysis of PNA/pyr as a Function of pyr Concentration at 366<sup>a</sup> and 313 nm at 27 °C**

10 <sup>5</sup> [PNA], M	[pyr], M	10 <sup>3</sup> k <sub>p</sub> , h <sup>-1</sup> <sup>a</sup>	t <sub>1/2</sub> , h	10 <sup>4</sup> φ <sub>PNA</sub> <sup>a,b</sup> (366)	10 <sup>4</sup> φ <sub>PNA</sub> <sup>b,c</sup> (313)
1.0	0	0.47 ± 0.004	15	2.9	
1.0	1.0 × 10 <sup>-4</sup>	0.42 ± 0.009	17	2.7	2.4
0.79	1.24 × 10 <sup>-3</sup>	1.20 ± 0.022	5.0	9.0	
0.79	3.31 × 10 <sup>-3</sup>	2.44 ± 0.039	2.84	17	15
0.79	1.24 × 10 <sup>-2</sup>	9.24 ± 0.120	0.750	57	57

<sup>a</sup> At 366 nm. <sup>b</sup> φ<sub>PNA</sub> values are ±12%.

**Table III. Photolysis of PNA/pyr in Sunlight<sup>d</sup>**

10 <sup>4</sup> - [pyr], M	sky, date <sup>b</sup>	10 <sup>3</sup> k <sub>pE</sub> , min <sup>-1</sup>	t <sub>1/2(E)</sub> , h (min)
0	PC, 8:30-4:00 A29	0.22 ± 0.046	5.2
0	Cl, 11:00-4:00 J23	0.47 ± 0.012	2.4
1.00 <sup>c</sup>	OC, 9:20-4:30 A23	0.093 ± 0.011	12.4
1.00 <sup>c</sup>	Cl, 9:20-4:30 A25	0.27 ± 0.01	4.3
12.4	PC, 10:00-1:00 J4	0.90 ± 0.01	1.3
124	Cl, 2:00-3:00 M22	5.11 ± 0.17	0.22 (13)
124	PC, 10:18-11:00 J3	4.34 ± 0.04	0.26 (16)
124	OC, 10:40-11:00 J12	1.63 ± 0.04	0.70 (42)
124	Cl, 1:40-2:00 J12	2.63 ± 0.066	0.44 (26)
124	PC, 3:00-3:15 J12	3.30 ± 0.083	0.35 (21)

<sup>a</sup> [PNA] = 0.79 × 10<sup>-5</sup> M in 10-cm quartz tubes unless otherwise noted. <sup>b</sup> Sky: Cl = clear, OC = overcast, PC = partly cloudy. Date: daylight hours, April (A), May (M), or June (J), date. <sup>c</sup> [PNA] = 1.00 × 10<sup>-5</sup> M.

**Table IV. Calculated Half-Life of PNA in Tubes as a Function of [pyr] in Sunlight at lat 40 °C<sup>a</sup>**

10 <sup>4</sup> [pyr], M	t <sub>1/2</sub> , h			
	spring	summer	fall	winter
0	12.0	5.9	11.6	24.7
1.00	10.4	5.2	10.1	21.5
2.00	9.2	4.6	8.9	19.0
4.00	7.5	3.7	7.2	15.4
8.00	5.4	2.7	5.3	11.2
16.00	3.5	1.7	3.4	7.2
32.00	2.1	1.0	2.0	4.2
64.00	1.1	0.56	1.1	2.3
128.00	0.56	0.29	0.55	1.2

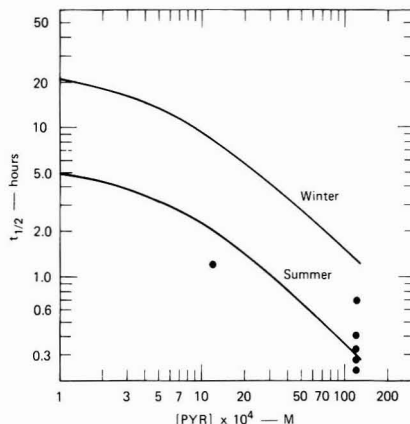
<sup>a</sup> t<sub>1/2</sub> = ln 2 / 2.2 φ<sub>T</sub> Σ ε<sub>λ</sub> L λ where φ<sub>T</sub> = φ<sub>pyr</sub> + 0.00028.

dishes with those in quartz tubes (at 60° from the horizon) and find a fairly consistent factor of 2.2-3, depending on the action spectrum of the solution, for the ratio of rates in dish to tube.

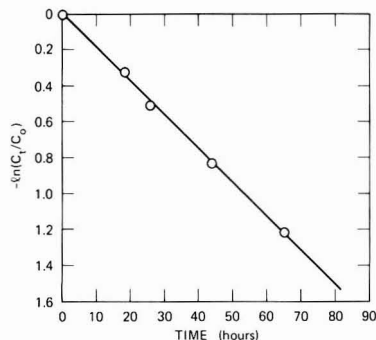
**p-Nitroacetophenone (PNAP)/pyr Actinometer.** PNA/pyr is a variable quantum yield actinometer useful for short-term sunlight experiments of under 12 hours. We screened several aromatic ketones as possible long term actinometers and found that p-nitroacetophenone (PNAP) is very stable to photolysis in water with a half-life of over 5 months. Photonucleophilic substitution by pyridine on PNAP is facile, and this combination forms the basis for a second variable quantum yield actinometer with a much larger range of half-lives than PNA/pyr. The spectrum of PNAP exhibits a maximum at 275 nm (log ε = 4.17), with a tail extending into the solar region.

Table V summarizes the results of several experiments we performed to measure quantum yield dependence on wavelength, temperature, and [pyr] for photolysis of the PNAP/pyr system. The results show that φ is the same at 313 and 366 nm and the change in φ with [pyr] is linear over a 20-fold change in [pyr]. The relation between [pyr] and φ is given by the equation (r = 0.999)

$$\phi = 0.0169[\text{pyr}] \quad (8)$$



**Figure 2. Calculated half-life on PNA in sunlight as a function of [pyr] at lat 40°; (●) experimental results. Values are for tube measurements.**



**Figure 3. Photolysis of PNAP with 2.48 × 10<sup>-2</sup> M pyr at 313 nm.**

**Table V. Photolysis of PNAP/pyr in Water at 313 and 366 nm and 25 and 43 °C<sup>a</sup>**

10 <sup>3</sup> [pyr] <sub>0</sub> , M	10 <sup>3</sup> k <sub>p</sub> , h <sup>-1</sup>	10 <sup>5</sup> - φ(313 nm)	10 <sup>5</sup> - φ(366 nm)
1.25	0.77 ± 0.036	3.6 <sup>b</sup>	
4.29	1.71 ± 0.037	8.0 <sup>b</sup>	
9.06	3.21 ± 0.19	15 <sup>b</sup>	
12.4	9.17 ± 0.92	21 <sup>b</sup>	
14.1	5.34 ± 0.07	25 <sup>b</sup>	
24.9	9.20 ± 0.15	43 <sup>b</sup>	44 <sup>b</sup>
24.9 <sup>c</sup>	15.7 ± 0.15	38 <sup>c</sup>	

<sup>a</sup> [PNAP]<sub>0</sub> = 1.0 × 10<sup>-5</sup> M. <sup>b</sup> 25 °C. <sup>c</sup> 43 °C.

Essentially no change in φ occurred when the temperature was increased from 25 to 43 °C. In each experiment, PNAP exhibited good first-order kinetics to 75% conversion, as shown in Figure 3.

We performed one series of experiments in summer sunlight using quartz tubes with a constant PNAP con-

Table VI. Photolysis of PNAP/pyr in Summer Sunlight<sup>a</sup>

10 <sup>2</sup> [pyr], M	k <sub>pE</sub> , day <sup>-1</sup>	t <sub>1/2</sub> , days	
		measd	calcd
1.60	0.18	3.8	2.7
3.38	0.39	1.8	1.4
6.09	0.71	0.97	0.90
7.84	0.88	0.78	0.70
9.70	1.07	0.64	0.55

<sup>a</sup> [PNAP] = 2 × 10<sup>-5</sup> M; clear weather in July.

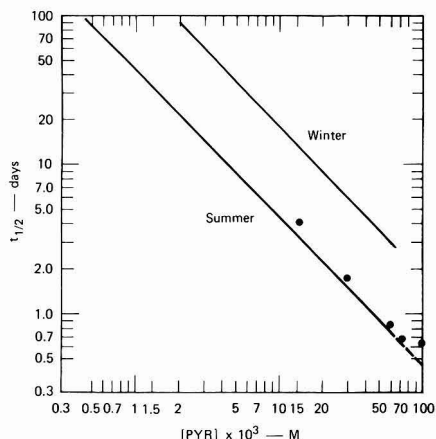
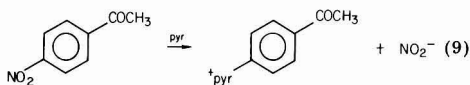


Figure 4. Calculated half-life of PNAP in sunlight as a function of [pyr] at lat 40°; (●) experimental points. Values are for tube measurements.

centration but varying pyr over a 6-fold range to measure k<sub>pE</sub> and t<sub>1/2(E)</sub>. We also calculated k<sub>pE</sub> and t<sub>1/2(E)</sub> for photolysis of PNAP as function of [pyr] at lat 40° in summer, by using eq 1, the values of φ in Table V, and the values of L<sub>λ</sub> for the interval 299–430 nm. Table VI summarizes the results. For convenience half-lives for PNAP as a function of [pyr] are plotted in Figure 4 for summer and winter.

Attempts to characterize the products from the reaction have met with only limited success. We have shown by HPLC that 1 equiv of NO<sub>3</sub><sup>-</sup> ion is formed on photolysis, apparently via oxidation of first-formed NO<sub>2</sub> ion. This result, if confirmed, points to a process analogous to that found for PNA with pyridine, in which a nitro group is displaced to form the pyridinium salt (eq 9). We have



not yet succeeded in isolating this product. The excellent kinetic behavior exhibited by PNA and PNAP indicates that these products do not interfere with the photochemical processes of interest.

**Evaluation of PNAP/pyr Actinometer in Sunlight.** To evaluate the photolysis screening protocols using an actinometer, we selected dibenzothiophene (DBT) as a test chemical and simultaneously exposed aqueous solutions of DBT and PNAP/pyr to sunlight in quartz tubes for periods as long as 240 h (10 days elapsed time). The PNAP/pyr actinometer was adjusted to give a half-life of close to 4 days under late summer clear sky conditions; the initial [pyr] was 0.022 M. In previous studies in this laboratory (5) DBT had a quantum yield in water of 5 × 10<sup>-4</sup>

Table VII. Sunlight Photolysis of PNAP and DBT<sup>a</sup>

time, days	10 <sup>5</sup> [PNAP], M <sup>b</sup>	10 <sup>6</sup> [DBT], M
0	2.00	2.60
2	1.34	1.68
4	0.842	1.13
6	0.578	0.707
10	0.288	0.479

k<sub>pE</sub> = 0.19 day<sup>-1</sup>      k<sub>pE</sub> = 0.16 day<sup>-1</sup>

<sup>a</sup> In quartz tubes.    <sup>b</sup> [pyr] = 0.022 M.

Table VIII. Theoretical Sunlight Absorption Values for DBT and PNAP at lat 40°

Σ L <sub>λ</sub> ε <sub>λ</sub> , day <sup>-1</sup>	DBT	PNAP/pyr
k <sub>p</sub>	0.17	0.19
summer	189	412
spring	87.7	201
midexperiment (May 14, 1981)	117 <sup>a</sup>	262

<sup>a</sup> Absorption values are weighted averages for summer and spring.

at 313 nm [t<sub>1/2(E)</sub> = 6 days (borosilicate)].

Table VII summarizes analytical results for DBT and PNAP/pyr and gives values of k<sub>pE</sub> for each chemical. In quartz, both DBT and PNAP have half-lives of about 4 days. Thus the actinometer served as a useful monitor of the changing sunlight intensity during exposure of DBT.

The quantum yield for DBT was calculated from eq 3; a regression slope of 1.107 (r = 0.997) was obtained from ln ([PNAP]<sub>0</sub>/[PNAP]<sub>t</sub>) vs. ln ([DBT]<sub>0</sub>/[DBT]<sub>t</sub>) and used in eq 3, with values of sunlight absorbance calculated from the UV spectrum of each chemical and L<sub>λ</sub> values of Mabey et al. (1). A quantum yield of 3.8 × 10<sup>-4</sup> for PNAP was obtained from eq 8. Relevant data are given in Table VIII.

The quantum yield for DBT in sunlight was estimated as 7.5 × 10<sup>-4</sup>, which agrees fairly well with the value measured at 313 nm in this laboratory 3 years ago (5).

### Conclusions

We believe that the PNA/pyr and PNAP/pyr actinometers will prove to be valuable tools for estimating accurate values of quantum yields for photolysis of chemicals in water. Although we have emphasized the need for and application of these actinometers for sunlight measurements, they are also useful in the laboratory where φ is measured at a single wavelength, usually 313 or 366 nm. In this application, the adjustable quantum yield and low sensitivity to room light also offer great advantages over conventional actinometers, which typically require handling in darkened rooms and short exposure times (6).

Work is continuing in this laboratory to evaluate these actinometers for sunlight measurements of φ<sub>pE</sub> for several different chemicals. Results will be reported in later papers.

### Acknowledgments

John Davenport and John Winterle made many helpful suggestions during the course of this work.

### Literature Cited

- Mabey, W. R.; Mill, T.; Hendry, D. G. In "Test Protocols for Environmental Processes: Photolysis in Water"; EPA Final Report EPA 600/3-82-022, 1982; pp 49–102.
- Fed. Regist. 1979, 16240–16292.
- Zepp, R. G.; Cline, D. M. *Environ. Sci. Technol.* 1977, 11, 359.
- Zepp, R. G.; Schlotzhauer, P. F. *Chemosphere* 1981, 10, 479.

- (5) Mill, T.; Mabey, W. R.; Baraze, A.; Lan, B. *Chemosphere* 1981, 10, 1281.  
 (6) Calvert, J. G.; Pitts, J. N. "Photochemistry"; Wiley: New York, 1967.  
 (7) Turro, N. J. "Modern Molecular Photochemistry"; Benjamin/Cummings: Menlo Park, CA, 1978.  
 (8) Zepp, R. G. *Environ. Sci. Technol.* 1978, 12, 327.  
 (9) Letsinger, R. L.; Colb, A. L. *J. Am. Chem. Soc.* 1972, 94, 3665.  
 (10) Cornelisse, J.; Havinga, E. *Chem. Rev.* 1975, 75, 353.  
 (11) Letsinger, R. L.; Ramsay, O. B.; McCain, J. H. *J. Am. Chem. Soc.* 1965, 87, 2945.

- (12) Dulin, D.; Winterle, J.; Mabey, W.; Tse, D.; Mill, T., SRI unpublished results, 1981-1982.

Received for review February 1, 1982. Accepted August 2, 1982. This work was supported by subcontract T-6416-7197-030 from Battelle Columbus Laboratories and EPA Contract 68-01-6325. Although the research described in this article has been funded wholly or in part by the U.S. Environmental Protection Agency through Contract 68-01-6325 to SRI International, it has not been subjected to the agency's required peer and policy review and therefore does not necessarily reflect the views of the Agency, and no official endorsement should be inferred.

## Entrapment of Zinc and Other Trace Elements in a Rapidly Flushed Industrialized Harbor

Scott A. Sinex and George R. Helz\*

Department of Chemistry, University of Maryland, College Park, Maryland 20742

■ Baltimore Harbor possesses an unusual three-layer circulation system that causes its water to be renewed at about 10% per day. Despite this rapid flushing, very fine grained argillaceous sediments accumulate in its upper reaches and appear to trap effectively trace-element contaminants such as zinc. Accumulated anthropogenic zinc in Harbor sediments is estimated to be  $(21-62) \times 10^3$  Mg, and the historic discharge of anthropogenic zinc is estimated to be about  $42 \times 10^3$  Mg. In places, zinc has been mixed to depths greater than 3 m below the sediment-water interface. In recent decades, about  $0.9 \times 10^6$  Mg/year of sediment in the Harbor has been displaced by dredging, and this activity has probably contributed to the plowing of contaminants into the Harbor bottom.

### Introduction

Baltimore Harbor, in the Patapsco subestuary of the Chesapeake Bay system, is well-known to many estuarine scientists because of its unusual three-layer circulation (1, 2). This causes water in the Harbor to be renewed at a rate of about 10% per day (3). It would be reasonable to expect that contaminants from the numerous industrial sources fringing the harbor would be rapidly transported into the main stem of Chesapeake Bay by the rapid flushing. However, previous studies of trace elements in the sediments from the main stem of the Bay provided little evidence for this (4). Therefore, we have become interested in the dynamics of contaminant transport in the Harbor. In this paper some geochemical data on Harbor sediments will be presented. Particular use will be made of zinc as an indicator of where contaminated materials are being deposited.

### Sample and Locality Information

A total of 13 gravity cores and 22 surface grab samples were collected from Baltimore Harbor during May and June 1981. The plastic core liners had a diameter of 7 cm. Earlier work found this size core to have minimal compaction and foreshortening on collection (5). The locations are shown in Figure 1A. Samples from two deep cores near Fort McHenry in the Harbor were obtained from the Maryland State Highway Administration.

Baltimore Harbor is located on the drowned Pleistocene Valley of the Patapsco River, which is a small tributary to the Chesapeake Bay. Because the fresh water inflow

of the Patapsco River is small, a circulation pattern is developed and controlled by the density or salinity distribution in the adjacent Chesapeake Bay (1, 2). Fresh water inflow occurs at the surface and saline water inflow occurs near the bottom (Figure 1B). Outflow of intermediate salinity water occurs at middepth. This constitutes the major mechanism for exchange or renewal of water in the Harbor (1).

Carpenter (3) established the water renewal rate by observing the effect of acid waste discharges on alkalinity in the Harbor. This rate yields a complete turnover of Harbor water in about 10 days. Earlier estimates of 110 days by Garland (6) using tidal exchange were shown to be wrong. The effect of the three-layer circulation system has probably been enhanced over the last 75 years due to deepening of the channel into the Harbor (7).

Dredging in Baltimore Harbor began in the early 1800s and by 1836 was a federal government operation. By 1852 a complete channel from Fort McHenry to the deep water of the main Bay was completed (8). Gross and Cronin (9) estimated that  $1.2 \times 10^8$  m<sup>3</sup> of materials were dredged from Baltimore Harbor between 1925 and 1975. Disposal records are limited; however, most of the disposal was overboard into sites near the operations. Records of the Baltimore Department of Public Works show that in the 1940s most disposal was done at a site outside the Harbor, slightly south of station A (Figure 1A).

With Gross and Cronin's (9) estimate, converted to an average annual rate of dredging ( $2.4 \times 10^6$  m<sup>3</sup>/year), and with assumption that this dredged material contains 70% water and has a density of 1.25 Mg/m<sup>3</sup> (10), the dry weight of material dredged from Baltimore Harbor was  $0.9 \times 10^6$  Mg/year. This number is an estimate for approximately the last 50 years and on a year-to-year basis varied considerably. This average dry weight of dredged material is comparable to the suspended sediment discharge of the Susquehanna River, which was  $0.9 \times 10^6$  Mg/year for the period 1966-1976, excluding major floods (11). Not all of the Harbor dredged material was deposited in the main Bay, especially in more recent years when disposal sites within the Harbor have been used.

Gottschalk (8) presented evidence that high rates of siltation have occurred in the upper Harbor especially near the mouth of the Patapsco River. This area was navigable 200 years ago, but today it is a marsh. This siltation problem was caused by uncontrolled erosion occurring



Table I. Reproducibility and Accuracy of Lithium Metaborate Fusion Method ( $\mu\text{g/g}$  except Where %)

	Al	Si	Ti	V	Cr	Mn	Fe	Co	Ni	Zn
NRC BCSS-1										
this study ( $n^a = 9$ )	5.5%	31%	0.35%	92	110	190	2.9%	18	55	110
%CV <sup>b</sup>	2	4	4	8	5	7	5	27	5	7
NRC	6.3%	31%	0.44%	93	123	229	3.3%	11	55	119
95% TL <sup>c</sup>	$\pm 0.22$	$\pm 0.47$	$\pm 0.01$	$\pm 5$	$\pm 14$	$\pm 15$	$\pm 0.10$	$\pm 2$	$\pm 4$	$\pm 12$
NBS SRM-1646										
this study ( $n^a = 10$ )	5.4%	30%	0.36%	89	72	270	3.0%	19	31	120
%CV <sup>b</sup>	5	4	10	11	2	6	5	21	16	7
NBS	6.3%	(31%) <sup>d</sup>	(0.51)	88	76	375	3.4%	11	32	138
95% TL <sup>c</sup>	$\pm 0.20$			$\pm 10$	$\pm 3$	$\pm 20$	$\pm 0.10$	$\pm 1.3$	$\pm 3$	$\pm 6$

<sup>a</sup> Number of replicates. <sup>b</sup> Coefficient of variation (%) =  $100\sigma/\text{mean}$ . <sup>c</sup> 95% tolerance limits. <sup>d</sup> Not certified.

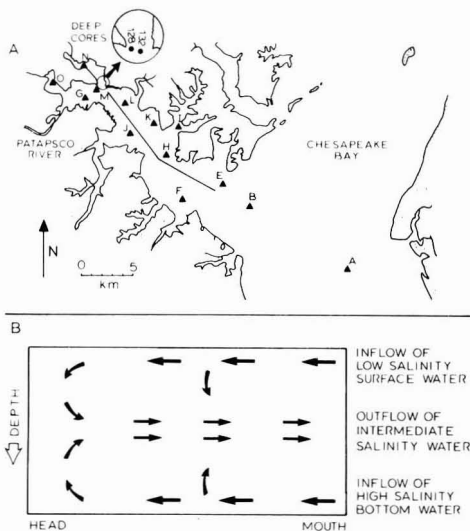


Figure 1. (A) Location of gravity cores ( $\blacktriangle$ ) and surface grab sample traverse ( $\times$ ) in Baltimore Harbor; (B) three-layer circulation pattern adopted from ref 1-3.

during early land clearing. Bathymetric charts from 1849, 1861, and 1892, when compared to modern charts, show little net deposition in the main stem of the Patapsco subestuary seaward of station M (Figure 1A). However, deepening in channel areas due to dredging operations is evident in these charts.

#### Materials and Methods

The cores were sectioned into 2-cm intervals. These and the surface samples were dried at  $105^\circ\text{C}$ , ground with a mullite mortar and pestle, and stored. For analysis, 200 mg of each sample was fused with 1 g of lithium metaborate for 15 min at  $950^\circ\text{C}$ . The resulting solutions, produced after dissolving the borate glass bead in 5%  $\text{HNO}_3$ , were analyzed by DC plasma emission spectrometry. Further details concerning the analytical methodology can be found elsewhere (12, 13).

Reproducibility and accuracy were evaluated by analyzing standard sediment samples. Results for the Canadian National Research Council (NRC) certified marine sediment, BCSS-1, and the U.S. National Bureau of Standards (NBS) certified estuarine sediment, SRM-1646, are given in Table I. The NBS SRM-1646 is a sediment collected from the Chesapeake Bay near the mouth of the York River in Virginia.

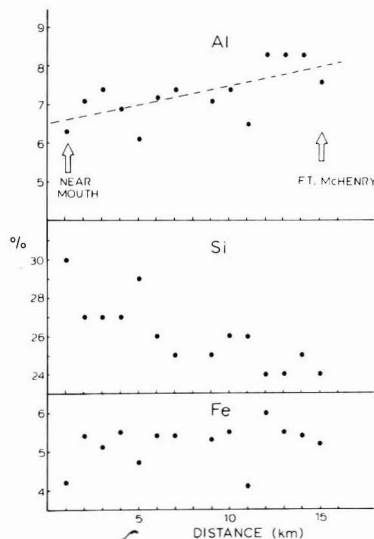


Figure 2. Distribution of Al, Si, and Fe in channel going into Baltimore Harbor. Location of traverse shown in Figure 1. Distance scale refers to 0 km at mouth and 15 km at head of harbor.

As judged by the coefficients of variation in Table I, reproducibility is better than  $\pm 10\%$  for all elements except Co. Recovery of the certified concentrations in the NRC BCSS-1 standard was within the 95% tolerance levels for Si, V, Cr, Ni, and Zn. In the case of Al, Ti, Mn, and Fe, recovery ranged from 80% to 88%, probably reflecting incomplete fusion of refractory phases in the sample. Recovery for the NBS SRM-1646 was very similar to the NRC standard, except for Ti, Mn, and Zn, which were 71%, 72%, and 87%, respectively. Cobalt values are systematically high and poorly reproducible due to a large blank correction. The high blank may be caused by a combination of contaminated  $\text{LiBO}_2$  and high signal background at the wavelength used (340.5 nm).

#### Surficial and Temporal Distributions

The data for the core samples are given in Table II. Five samples from each core were analyzed; these were selected from the top, bottom, and three equally spaced intermediate points. In about half the cores most elements show no systematic change with depth, i.e., the concentrations vary but do so erratically, with lower values overlying higher values in some cases. This suggests that the sediments of the Harbor have been profoundly disturbed over the years by such processes as propellor wash and dredging. The levels of metals in the Harbor sediment are

Table II. Data for Gravity Cores in Baltimore Harbor (Al, Si, Ti, and Fe Are %; Others Are  $\mu\text{g/g}$ )

core/depth, cm	Al	Si	Ti	V	Cr	Mn	Fe	Co	Ni	Zn
A/0-2	8.8	25.0	0.40	170.0	100.0	1900.0	4.6	51.0	94.0	310.0
A/24-26	10.3	25.0	0.40	180.0	120.0	2800.0	4.8	70.0	100.0	440.0
A/50-52	10.8	25.0	0.40	180.0	120.0	1400.0	4.7	63.0	99.0	410.0
A/74-76	11.2	24.0	0.40	180.0	92.0	1000.0	4.4	60.0	88.0	240.0
A/98-100	9.6	26.0	0.39	180.0	93.0	920.0	4.4	49.0	81.0	210.0
B/0-2	7.1	28.0	0.34	130.0	150.0	1600.0	4.6	37.0	58.0	340.0
B/22-24	8.2	28.0	0.34	140.0	84.0	940.0	4.4	26.0	44.0	120.0
B/42-44	8.1	28.0	0.34	130.0	83.0	840.0	4.3	19.0	43.0	120.0
B/62-64	8.0	29.0	0.34	130.0	85.0	900.0	4.3	27.0	46.0	120.0
B/84-86	8.3	29.0	0.33	130.0	89.0	850.0	4.4	22.0	45.0	120.0
E/0-2	6.9	23.0	0.32	190.0	190.0	710.0	5.8	50.0	69.0	780.0
E/18-20	7.4	26.0	0.35	110.0	77.0	750.0	3.8	27.0	47.0	120.0
E/36-38	7.1	25.0	0.33	120.0	76.0	800.0	3.8	28.0	39.0	120.0
E/56-58	7.0	26.0	0.32	110.0	75.0	740.0	3.8	24.0	41.0	110.0
E/76-78	7.1	27.0	0.32	130.0	71.0	660.0	3.7	33.0	39.0	110.0
F/0-2	7.9	22.0	0.45	330.0	230.0	970.0	6.0	45.0	69.0	540.0
F/18-20	8.1	23.0	0.38	200.0	160.0	1100.0	5.2	42.0	58.0	470.0
F/38-40	8.3	22.0	0.36	150.0	120.0	1300.0	4.6	31.0	55.0	350.0
F/56-58	8.2	23.0	0.40	160.0	130.0	710.0	4.6	40.0	70.0	410.0
F/74-76	7.8	23.0	0.36	130.0	100.0	990.0	4.5	30.0	51.0	220.0
G/0-2	9.5	26.0	0.42	180.0	390.0	510.0	4.9	44.0	81.0	470.0
G/24-26	9.7	26.0	0.44	180.0	320.0	470.0	5.1	39.0	78.0	400.0
G/46-48	9.0	28.0	0.43	170.0	270.0	490.0	4.9	45.0	79.0	440.0
G/68-70	8.4	29.0	0.46	190.0	330.0	500.0	4.7	49.0	86.0	590.0
G/94-96	7.5	29.0	0.44	170.0	330.0	430.0	4.6	47.0	69.0	460.0
H/0-2	7.9	22.0	0.42	250.0	330.0	1600.0	6.0	53.0	69.0	630.0
H/20-22	5.9	23.0	0.39	320.0	480.0	400.0	8.0	48.0	66.0	1100.0
H/40-42	8.5	24.0	0.34	200.0	370.0	600.0	6.0	28.0	100.0	1100.0
H/60-62	9.2	26.0	0.40	170.0	110.0	1200.0	4.7	46.0	62.0	130.0
H/80-82	8.5	26.0	0.37	160.0	93.0	900.0	4.5	42.0	50.0	120.0
I/0-2	8.5	20.0	0.58	420.0	570.0	550.0	6.9	46.0	83.0	900.0
I/26-28	8.4	22.0	0.47	230.0	240.0	580.0	6.9	45.0	54.0	400.0
I/52-54	8.1	17.0	0.53	380.0	870.0	440.0	13.0	44.0	60.0	1500.0
I/78-80	6.6	29.0	0.46	130.0	140.0	270.0	2.8	34.0	48.0	120.0
I108-110	10.6	23.0	0.42	160.0	160.0	550.0	4.6	47.0	79.0	140.0
J/0-2	8.1	21.0	0.60	450.0	580.0	520.0	7.0	44.0	84.0	980.0
J/26-28	8.2	24.0	0.46	230.0	210.0	590.0	6.8	34.0	58.0	380.0
J/52-54	7.1	18.0	0.54	350.0	910.0	470.0	14.0	46.0	79.0	1300.0
J/78-80	9.3	25.0	0.40	170.0	470.0	560.0	4.9	43.0	87.0	380.0
J106-108	10.1	26.0	0.41	170.0	170.0	510.0	4.7	38.0	84.0	160.0
K/0-2	7.1	25.0	0.43	220.0	460.0	630.0	5.3	24.0	69.0	650.0
K/18-20	7.6	23.0	0.40	200.0	530.0	890.0	6.3	29.0	62.0	780.0
K/36-38	7.4	25.0	0.36	150.0	170.0	1200.0	5.1	14.0	53.0	340.0
K/54-56	7.1	25.0	0.36	130.0	130.0	1200.0	4.5	17.0	58.0	210.0
K/72-74	8.1	27.0	0.36	130.0	150.0	1100.0	4.8	15.0	57.0	280.0
L/0-2	7.8	24.0	0.41	240.0	460.0	730.0	5.8	47.0	86.0	850.0
L/24-26	7.5	24.0	0.43	250.0	530.0	640.0	6.1	41.0	80.0	970.0
L/50-52	7.7	24.0	0.42	250.0	570.0	610.0	6.3	48.0	86.0	1100.0
L/74-76	8.4	25.0	0.35	160.0	390.0	390.0	5.0	43.0	90.0	840.0
L/98-100	9.3	26.0	0.37	160.0	250.0	420.0	4.5	47.0	84.0	380.0
M/0-2	7.4	23.0	0.36	190.0	690.0	620.0	4.8	47.0	85.0	630.0
M/26-28	8.3	25.0	0.38	210.0	560.0	450.0	5.0	44.0	110.0	740.0
M/52-54	8.7	25.0	0.36	150.0	310.0	390.0	4.5	42.0	90.0	430.0
M/78-80	7.4	21.0	0.33	210.0	1400.0	280.0	5.8	34.0	81.0	1200.0
M106-108	7.1	20.0	0.33	160.0	1800.0	310.0	6.3	41.0	88.0	1100.0
N/0-2	7.3	23.0	0.37	140.0	2000.0	530.0	4.5	18.0	75.0	840.0
N/22-24	6.7	24.0	0.38	140.0	1900.0	560.0	4.5	16.0	86.0	790.0
N/44-46	6.4	22.0	0.38	150.0	1800.0	550.0	4.4	15.0	81.0	820.0
N/66-68	5.9	24.0	0.40	83.0	180.0	420.0	3.8	3.0	76.0	110.0
N/86-88	5.5	24.0	0.40	87.0	220.0	450.0	3.6	6.0	70.0	130.0
O/0-2	6.8	22.0	0.39	140.0	320.0	500.0	4.0	14.0	99.0	560.0
O/16-18	7.8	21.0	0.42	160.0	270.0	1500.0	4.3	19.0	110.0	400.0
O/32-34	6.6	25.0	0.39	140.0	270.0	710.0	4.4	17.0	110.0	490.0
O/48-50	5.9	25.0	0.39	150.0	290.0	830.0	4.6	16.0	100.0	350.0
O/64-66	5.5	28.0	0.39	150.0	260.0	770.0	4.4	19.0	81.0	280.0

high compared to Chesapeake Bay sediment.

The surface samples, which are from the channel that runs the length of the Harbor, show gradation toward more argillaceous sediment headward from the mouth (Figure 2). The Al content increases from approximately 6% at the mouth to 8% or greater in the inner reaches. The Si content shows a decrease into the Harbor, while Fe has a fairly constant concentration throughout. This trend to-

ward more argillaceous compositions in the headward direction is opposite to the pattern expected in a body of water receiving sediment from a tributary at its head. The latter would contain its coarsest sediments near its head (14). Consequently an offshore source for at least part of the Baltimore Harbor sediments is suggested.

The trend in increasing Al with distance into the Harbor agrees with the physical sedimentological data. Palmer

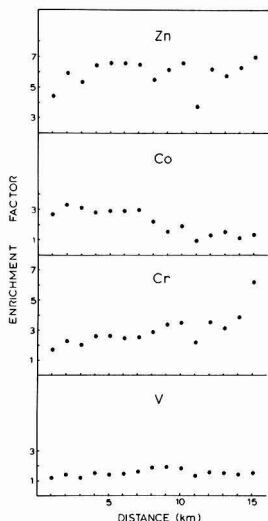


**Figure 3.** Enrichment factors for V, Cr, Co, and Zn in Baltimore Harbor surface channel samples. Location of traverse shown in Figure 1. Distance scale refers to 0 km at mouth and 15 km at head of Harbor.

(15) found the upper third of the Harbor to have >60% clay-sized material; coarser material was found further seaward. More recent unpublished sedimentological data from the Maryland Geological Survey on samples collected simultaneously with ours (16) also indicate the fine-grained nature of upper Harbor sediments. The fast flushing rate of the Harbor undoubtedly facilitates transport of suspended material from the Bay into the Harbor, where it can be deposited, especially in the upper reaches. However, Harris et al. (17) report that metal ratios (Pb/Fe, Cu/Fe, Sn/Fe) for northern Bay sediments are similar to those found in the Harbor, indicating that exchange between the Bay and the Harbor probably occurs in both directions. Dredge spoil disposal might be partly or even wholly responsible for transfer of Harbor material into the Bay.

A convenient device for discussing geochemical trends and making comparisons between different geographical areas is the enrichment factor, EF (4). This will be defined here as

$$EF = (X/Al)_{\text{sediment}} / (X/Al)_{\text{av shale}}$$

where X/Al is the ratio of the concentration of element X to Al. Aluminum was chosen as the element of normalization because natural sources vastly dominate its input. Turekian and Wedepohl's (18) average shale data are used as a reference level because of the argillaceous nature of the Harbor sediments. Since trace elements tend to be preferentially associated with the fine grained, clay fraction of estuarine sediments, use of the enrichment factor partly eliminates fluctuations in trace-element concentrations caused by grain size variations. Thus, it becomes easier to distinguish contaminated sediments from uncontaminated ones.

In Baltimore Harbor, there is a large amount of enrichment of Cr, Co, and Zn usually found down the length of the cores. The other elements investigated in this study (Ti, Mn, Fe, Ni) show minimal enrichment. Vanadium does show some enrichment in certain areas. The enrichment can be seen in the channel samples from the Harbor mouth to the inner Harbor near Fort McHenry (Figure 3). Four different patterns emerge: (1) Vanadium

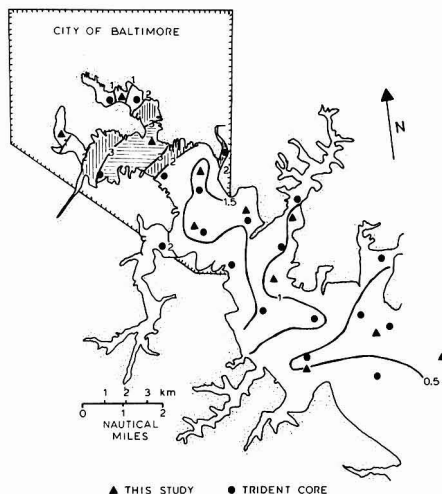


**Figure 4.** Depth in meters to 200 µg/g zinc isopleth (see text for explanation; Trident core data from ref 19).

shows no enrichment in the channel; core samples closer to shore, however, do show some enrichment. (2) Chromium shows increasing enrichment up the Harbor. (3) Cobalt shows decreasing enrichment up the Harbor. (4) Finally, Zn shows enrichment throughout the Harbor.

Zinc is the most persistently enriched element of those studied. Although the Zn concentrations vary erratically in the upper portions of many cores (see Table II), the lower most samples usually contain less than 200 µg/g. Based on Cantillo's (12) study of the main Bay, <200 µg/g seems also to be a reasonable background level for the main stem of Chesapeake Bay. Based on the high enrichment factors for Zn and the fact that Zn concentrations decline to <200 µg/g at depth, it seems likely that the surface sediments of Baltimore Harbor have been pervasively contaminated with zinc by human activities.

From the data from 13 cores from this study and 18 cores from an earlier study (19) the depth to the 200 µg/g isopleth can be estimated, either by interpolation between data or, in cases where it lies slightly below the bottom sample, by extrapolation. However, if the extrapolated depth of the 200 µg/g isopleth was more than half the core's length below the bottom sample, then the core was rejected. The depth in meters to the 200 µg/g Zn isopleth is shown in Figure 4. The most obvious feature is the massive area of contamination (>3 m) in the inner reaches of the Harbor near Fort McHenry. The wedge of contamination slowly thins in a seaward direction. The contaminated zone is less than half of a meter at the Harbor mouth.

It is of particular interest that the thick layer of contaminated sediment in the upper part of the Harbor is not simply an indicator of the thickness of sediments accumulated in that region since the time that contamination began. Figure 5 shows the Zn profiles from cores 128 and 132. At the site of core 128, outside the channel, the historic change in water depth is not known, but a net accumulation of sediments has very likely occurred. On the other hand, at the site of core 132, in the channel, a net removal rather than accumulation of sediment has occurred. This removal was caused by dredging of the channel, first to about 10 m (in 1890) and then to about 12 m (in 1920). Yet high concentrations of Zn are observed as far as 3 m below the modern, artificial channel depth.

Table III. Lower Limits for the Zinc Inventory in the Patapsco Subestuary

thickness, <sup>a</sup> m	outcrop area, 10 <sup>6</sup> m <sup>2</sup>	vol, <sup>b</sup> 10 <sup>6</sup> m <sup>3</sup>	dry mass, <sup>c</sup> 10 <sup>12</sup> g	zinc concn, <sup>d</sup> 10 <sup>-6</sup> g/g	total zinc, 10 <sup>9</sup> g	anthro- pogenic zinc, <sup>e</sup> 10 <sup>9</sup> g
0-0.5	10.9	2.7	1.00	450	0.5	0.3
0.5-1.0	29.2	21.9	8.10	1400 <sup>f</sup>	11.3	9.7
1.0-1.5	16.2	20.3	7.51	750	5.6	4.1
1.5-2.0	11.9	20.8	7.70	630	4.9	3.3
2.0-3.0	4.7	11.8	4.37	625	2.7	1.9
>3.0	3.8	13.3	4.92	620	3.1	2.1
total	76.7	90.8	33.60		28.1	21.4

<sup>a</sup> Thickness of contaminated sediments in Figure 4, defined as the depth to the 200 µg/g zinc isopleth. <sup>b</sup> Obtained by multiplying outcrop area by the midpoint of the thickness range. Where the thickness exceeded 3 m, a thickness of 3.5 m was assumed. <sup>c</sup> Based on a density of 0.37 g of dry mass/cm<sup>3</sup>; this corresponds to an assumed water content of 70%. <sup>d</sup> Average of all core data (this work and ref 19). <sup>e</sup> Anthropogenic zinc. This is based on the assumption that the natural zinc concentration would be 200 µg/g. <sup>f</sup> The high zinc concentration for the 0.5-1.0 interval is caused by a highly enriched zone around the Sparrows Point steel mill.

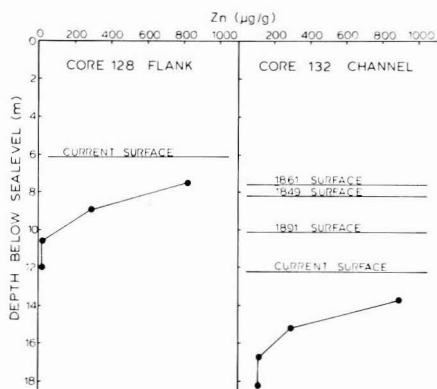


Figure 5. Comparison of Zn levels in two deep cores. At site 128, located outside the channel, moderate sediment accumulation has probably occurred, while at site 132, in the channel, net removal of sediment by dredging has occurred. Historical depths to the sediment surface at site 128 are shown based on U.S. Coastal and Geodetic Survey charts.

The Zn profiles are quite similar at both sites. It is likely that continual maintenance dredging of the channel, followed by overboard disposal of spoil on the flanks, followed in turn by transport of sediments back into the channel, has homogenized the sediments laterally to some extent and caused zinc to be mixed downward into the bottom.

### Discussion

The results suggest that the upper part of the Patapsco subestuary is apparently trapping aluminum-rich fine sediment derived from offshore sources. This finding helps account for the unusually high rate of deposition of silt and clay in the Harbor, as described by Gottschalk (8) and Garland (6). To achieve a flushing rate of 10% per day, it is necessary that  $1.6 \times 10^{13}$  L of water, a volume equivalent to roughly half the average annual-flow of the Susquehanna River, pass through the Patapsco subestuary each year (20). If this much water deposited 10 mg of silt and clay from each liter, then the annual accumulation would be  $1.6 \times 10^{11}$  g (equal to  $4.4 \times 10^5$  m<sup>3</sup>, assuming the sediments contain 70% water). This amount of sediment is nearly the same as the actual accumulation estimated by Gottschalk (8) and Garland (6). Since some of the annual accumulation is surely derived from the Patapsco watershed, 10 mg/L is an upper limit on the concentration of sediment that must be supplied in the water from offshore sources. It is reasonable to suppose that the high

rate of silt and clay deposition in the Patapsco subestuary scavenges contaminants such as zinc, causing them to be trapped with the sediments inside the Patapsco.

The efficiency of the Patapsco subestuary for retaining zinc can be estimated from a zinc budget. An inventory of the zinc in the sediments of the Harbor is presented in Table III, which is based on the data in Figure 4. The inevitable assumptions involved in estimates of this type were all made in a manner that could bias the results in the direction of underestimation. Thus the volume and mass of contaminated sediments and the masses of total and anthropogenic zinc in Table III may be regarded as minimum estimates.

Of the total area of the Patapsco (117 km<sup>2</sup>), about 35% lies in tributary embayments where there are no core data. In Table III, these areas were neglected, which is tantamount to assuming that they are free of contaminated sediments. Alternatively, if it were assumed that they contained contaminated sediments in an amount proportional to their area, then the estimate of the total volume of contaminated sediments in Table III would be raised to  $140 \times 10^6$  m<sup>3</sup>. Similarly, in converting from volume to mass in Table III, it was assumed that the sediments contained 70% water and thus had a density of 0.37 g of dry mass/cm<sup>3</sup>. A water content of 70% is essentially the upper limit observed by us in a number of Chesapeake Bay cores. If one assumed a water content of only 50%, which seems to be a lower limit for modern, fine-grained sediments in the Chesapeake region, then the density would be 0.71 g of dry mass/cm<sup>3</sup>, and the estimate of the dry mass of contaminated sediments would be roughly twice that given in Table III. Finally, the 200 µg/g zinc concentration, which was adopted here as the boundary between contaminated and uncontaminated sediments, may be unreasonably high. A case could be made for placing the boundary at about 120 µg of zinc/g. This lower boundary would have only a small effect in the estimated volume of contaminated sediment and on the mass of total zinc. However, the mass of zinc ascribed to anthropogenic sources would increase about 12% because less of the total zinc would be assigned to natural sources.

Taking these uncertainties into account, the actual volume of contaminated sediments in the Patapsco subestuary probably lies in the range  $(91-140) \times 10^6$  m<sup>3</sup>. The actual mass of this sediment probably lies in the range  $(34-99) \times 10^{12}$  g. The total zinc in this sediment is likely to be between  $28 \times 10^9$  and  $82 \times 10^9$  g, and the anthropogenic zinc is likely to be between  $21 \times 10^9$  g and  $62 \times 10^9$  g.

This inventory of anthropogenic zinc can be compared with the annual input from anthropogenic sources (20). As

of 1970, approximately  $0.65 \times 10^9$  g/year of zinc was being introduced into the Harbor, of which about 85% came from industrial discharges and sewage treatment plants. Most of the remaining 15% was from the atmosphere and probably had mainly an anthropogenic origin.

Unfortunately, the manner in which this flux has changed with time is not known. However, one way to model the historical change would be to assume that the zinc discharges grew in proportion to population in the Baltimore metropolitan area. Census data for the period 1880–1970 show that this population grew exponentially, with a doubling time of 38 years. If anthropogenic zinc discharges grew in the same fashion, then the integrated anthropogenic zinc influx from precolonial times up to 1970 would be

$$\text{total anthropogenic zinc} = \frac{(1970 \text{ flux})(38)}{\ln 2} = 36 \times 10^9 \text{ g}$$

If the rate were as much as 50% smaller, then unreasonably large zinc fluxes in the early 19th century would be implied. On the other hand, a growth rate more than 50% larger would imply a very rapid rise in discharges in recent decades. The major markets for zinc have not changed much in recent decades, and national zinc consumption has grown slowly (21), so assumption of a rapid rise in the discharge rate to Baltimore Harbor cannot be justified. If it is further assumed that growth in industrial activity during 1970–1980 was offset by pollution abatement measures, yielding a constant zinc discharge rate, then the estimated anthropogenic zinc discharged up to 1980 then becomes  $42 \times 10^9$  g.

This estimate of the total influx of anthropogenic zinc falls midway between the minimum and maximum estimates of anthropogenic zinc contained within the Patapsco sediments. Thus these estimates are consistent with the hypothesis that all of the anthropogenic zinc historically discharged to Baltimore Harbor still resides in the sediments of the Harbor. This hypothesis accounts for the earlier observation (4) that, except for dredge spoil disposal sites, little zinc appears to have escaped the Harbor to contaminate the sediments of the main stem of Chesapeake Bay. However, it is clear that the uncertainties in the budget estimates are large enough that loss of perhaps as much as two-thirds of the historic zinc input cannot be precluded.

### Conclusion

Although the rapid flushing of Baltimore Harbor creates an opportunity for rapid transport of contaminants into the main stem of Chesapeake Bay, it also creates opportunity for entrapment of contaminants within the Harbor by sorption on fine particles that are imported from the Bay. In the case of zinc, the latter process is apparently the dominant one. A substantial fraction of the total anthropogenic zinc historically discharged to the Harbor may still reside there.

Because of shipping activities, dredging, and the hydraulic response of sediments to instabilities created by dredging, the sediments of Baltimore Harbor have been

churned for decades. Observable consequences of this have been plowing of contaminants to considerable depths below the sediment surface and creation of erratic vertical profiles in which highly contaminated sediments in some cases are overlain by less contaminated material.

### Acknowledgments

Special thanks are expressed to Chris Masterson for help with sample preparation and to Randy Kerhin and the Maryland Geological Survey for collecting the samples and supplying old navigational charts. We also thank M. Nichols for reviewing the manuscript.

### Literature Cited

- (1) Cameron, W. M.; Pritchard, D. W. In "The Sea"; Hill, M. N., Ed.; Wiley: New York, 1963; Vol. 2, pp 306–324.
- (2) Officer, C. B. "Physical Oceanography of Estuaries and Associated Coastal Waters"; Wiley: New York, 1976; p 350.
- (3) Carpenter, J. H. Proc. 33rd Ann. Conf. Maryland-Delaware Water Sewage Assoc., 1960; pp 67–78.
- (4) Sinex, S. A.; Helz, G. R. *Environ. Geol.* 1981, 3, 315.
- (5) Bricker, O. P., U.S. Geological Survey, personal communication, 1982.
- (6) Garland, C. F. "A Study of Water Quality in Baltimore Harbor"; Chesapeake Biol. Lab. Publ. 96, University of Maryland Natural Resources Inst., 1952.
- (7) Schubel, J. R.; Hirschberg, D. J.; Pritchard, D. W.; Gross, M. G. "A General Assessment of Selected Dredging/Disposal Options for Three Federal Dredging Projects in Upper Chesapeake Bay"; Special Report 40, Marine Sci. Res. Center, SUNY, Stony Brook, NY, 1980.
- (8) Gottschalk, L. C. *Soil Conserv.* 1944, 10, 3.
- (9) Gross, M. G.; Cronin, W. B. In "Ocean Dumping and Marine Pollution"; Palmer, H. D., Gross, M. G., Eds.; Dowden, Hutchinson, Ross: Stroudsbrugh, PA, 1979; pp 131–145.
- (10) Biggs, R. B. *Mar. Geol.* 1970, 9, 187.
- (11) Gross, M. G.; Karweit, M.; Cronin, W. B.; Schubel, J. R. *Estuaries* 1978, 1, 106.
- (12) Cantillo, A. Y. Ph.D. Thesis, University of Maryland, College Park, MD, 1982.
- (13) Sinex, S. A.; Cantillo, A. Y.; Helz, G. R. *Anal. Chem.* 1980, 52, 2342.
- (14) Wright, L. D. In "Coastal Sedimentary Environments"; Davis, R. A., Ed.; Springer-Verlag: New York, 1978; pp 5–68.
- (15) Palmer, H. D. In "Upper Bay Survey—Technical Report", Westinghouse Elec. Corp., Oceanic Division, 1975; Vol. 11, pp 4-1 to 4-33.
- (16) Kerhin, R. MD Geol. Survey, unpublished data, 1981.
- (17) Harris, R.; Nichols, M.; Thompson, G.; Banacki, J.; Vadas, G. "Heavy Metal Inventory in Suspended Sediment and Fluid Mud of Chesapeake Bay"; Virginia Inst. of Mar. Sci. Spec. Rept. No. 99, 1980.
- (18) Turekian, K. K.; Wedepohl, K. H. *Geol. Soc. Am. Bull.* 1961, 72, 175.
- (19) "Evaluation of the Problem Posed by In-Place Pollutants in Baltimore Harbor and Recommendation of Corrective Action"; EPA-440/5-77-015A & B, 1977.
- (20) Helz, G. R. *Geochim. Cosmochim. Acta* 1976, 40, 573.
- (21) U.S. Bureau of Mines, Minerals Facts and Problems, *Bull. U.S., Bur. Mines* 1970, 650, 1291.

Received for review March 30, 1982. Accepted July 15, 1982. This work was supported by the U.S. Environmental Protection Agency (Grant No. R805954).

## NOTES

### Mutagenicity of SRC-II Coal Liquefaction Wastewater Treatment Residues

Georg Keleti,\* Joseph Bern, Maurice A. Shapfro, William P. Gulledge, and George T. Moore

Industrial Environmental Health Sciences, Graduate School of Public Health,  
University of Pittsburgh, Pittsburgh, Pennsylvania 15261

■ A first screen bioassay of an SRC-II coal liquefaction residual and three sludges resulting from treatment of the wastewater from the process was conducted by using the *Salmonella*/microsome (Ames test) method for detecting mutagenic activity. All of the residuals exhibited some mutagenicity, with those labeled as "vacuum bottoms" having 700 times greater specific mutagenic activity (revertants/milligram) than fresh clarifier sludge and 5600 times greater mutagenic activity than aged digester sludge in the first sample set. Organic fractions of each of the tested materials, produced by increasing polar solvent extraction, were also measured for mutagenicity. The toluene and hexane fractions of clarifier sludge as compared to digested sludge, which contains the bulk of the polycyclic aromatic hydrocarbons, showed little or no reduction in mutagenic activity. The other organic extract fractions showed great reduction in activity and in some cases complete elimination of the mutagenic fractions when the sludge has been digested.

#### Introduction

Initial investigations of untreated coal conversion products and residuals (1-3) emanating from coal liquefaction operations indicated that they have the potential to generate large quantities of mutagens and potential carcinogens. While engineering controls designed to minimize occupational exposure to dangerous materials in demonstration and commercial scale coal liquefaction applications are available, those materials contained in effluents discharged to the environment may present hazards. Researchers at the Pacific Northwest Laboratory (4) have identified the heavy distillate fraction (greater than 550 °F boiling point) produced by solvent-refined coal (SRC-II) technology as possessing high mutagenic activity and animal carcinogenicity. Since these polycyclic aromatic hydrocarbons (PAHs), polycyclic aromatic amines (PAAs), and nitrogen heterocyclics (NPAHs) associated with animal carcinogenicity may be present in SRC-II residuals, it is deemed necessary to define their potential health impacts.

The SRC-II system is basically a noncatalytic direct hydrogenation process designed to convert high-sulfur and high-ash coal into clean burning fuel. Phase separation and product cleaning operations of the system require large volumes of process water. It is estimated that to produce 600 barrels/day of liquid fuel at one proposed demonstration plant, approximately 7.5 million gallons of process water per day will be required. Approximately 1 million gallons of this process wastewater are to be treated at one such proposed demonstration plant (5).

Residuals tested in this investigation were produced at a pilot-scale SRC-II installation located at Fort Lewis, WA.

Unit processes at this facility include coal liquefaction and wastewater treatment. The water treatment system involves oil separation, flocculation with alum to remove suspended colloidal particles, biological treatment with activated sludge, and biosludge digestion (see Figure 1). Three semisolid, or sludge, residuals are generated: (1) alum sludge; (2) clarifier sludge—the fresh biosludge settling out in the clarification of treated wastewater; (3) digester sludge—treated biosludge, the residue remaining after aerobic digestion has taken place.

Raw coal conversion wastewaters have exhibited mutagenic activity in reported microbial mutagenicity assays (6-7). However, there is a paucity of knowledge regarding the mutagenic character of fractions that are removed from coal liquefaction wastewaters during treatment. Since these must be disposed, there is a critical need to develop information that would permit the characterization of the sludges generated. These data are essential for determining the degree of sludge treatment required and precautions to be taken when handling these residuals at the conversion facility.

Testing of individual components in coal conversion wastes, where thousands of compounds may be present, is a practical impossibility (8). Consequently, testing the whole effluent and certain fractions based on chemical similarities of organic constituents has been the usual investigative tool. Mutagenicity bioassays of coal conversion products and residuals based on research conducted at the Oak Ridge National Laboratory have been reported by Epler et al. (9). An ongoing project at Pacific Northwest Laboratory (4) includes microbial and cell transformation mutagenicity bioassays and animal carcinogenicity tests on SRC-II liquid products from the Fort Lewis, WA, pilot plant. Reported results of the three test methods were in agreement in identifying the neutral fraction, containing most of the PAHs, as the most mutagenically active component. Warshawsky et al. (10) conducted Ames tests on a group of residuals resulting from coal gasification and liquefaction. Schoeny et al. (11) reported on extension of the aforementioned study that characterized powdered coal, wastewater from a hydrogenation process, and some coal conversion waste streams. In the above two studies, vacuum bottoms, a solid residual, were found to exhibit high mutagenic activity. Brand et al. (7) describe a project that traces the mutagenic and toxic properties of raw coal conversion wastewaters and partially treated wastewater streams in a pilot-size treatment unit. In the Brand et al. (7) study, the raw wastewater was found to be mutagenic. All mutagenic activity seemed to have been removed from the intermediate wastewater streams after pH adjustment and removal of lime sludge. Development of a data base to establish the mutagenic character of biosludge is of importance because of the large sludge volumes expected

**Table I. Operating Conditions of the Hydrogenator and Coal Feedstock to an SRC-II Pilot Plant for the Samples Tested (16)**

sample set	hydrogenator operating conditions		pilot plant mode	coal feedstock	ash content, %
	P, psig	T, °F			
1936 vacuum bottoms	2100	800	SRC-II	Powhattan 6	24.03
1937 clarifier sludge <sup>a</sup>	2000	825	SRC-II	Kentucky 9, 14	
1938 biosludge <sup>a</sup>	2000	825	SRC-II	Kentucky 9, 14	
2277 vacuum bottoms	2100	825	SRC-II	Powhattan 6	2.3
2280 alum sludge	2000	825	SRC-II	Powhattan 6	
2278 clarifier sludge	2000	825	SRC-II	Powhattan 6	
2279 biosludge	2000	825	SRC-II	Powhattan 6	

<sup>a</sup> As all water wastes from plant operating areas are collected in a large surge reservoir (storage tank), the feed to the wastewater treatment plant reflects the wastewaters produced by the plant during the preceding period of days, weeks, and/or months. Operating conditions listed above correspond to those maintained during the week prior to sampling and are generally representative.

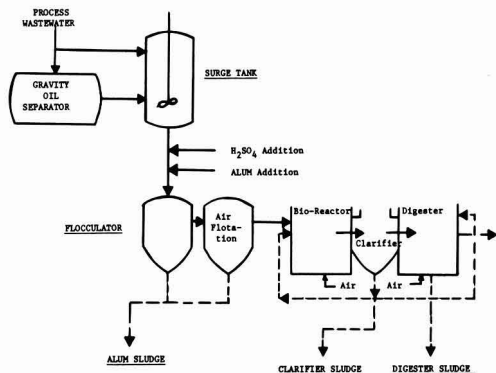


**Figure 1.** Ft. Lewis SRC wastewater treatment system block diagram.

to be generated at full-scale coal conversion plants.

In the investigation reported in this paper, we used the Ames *Salmonella* histidine-reversion system (12) to determine the mutagenic activity of SRC-II coal liquefaction wastewater treatment residues and one potential solid waste emanating from the conversion process. Additional mutagenicity data were developed by testing organic fractions generated by a serial solvent extraction method, described by Warshawsky (10), using increasingly polar organic solvents. This was done in an attempt to determine the most mutagenically active fractions of the whole materials.

### Materials and Methods

**Samples.** Source of test samples was the SRC-II pilot-scale coal liquefaction and wastewater treatment plant operated by the Pittsburgh and Midway Coal Mining Company for the Department of Energy (DOE) at Fort Lewis, WA. Table I lists the hydrogenation reactor operating conditions, ash content, and coal feedstock used when the samples were collected. It must be recognized that the listed conditions may bear little relationship to the process as it may finally be implemented in demonstration and/or commercial plants. Also, the residues tested may not be representative of those generated by similar experimental operations.

All sludge residuals generated by the wastewater treatment pilot plant were tested. The samples included (1) an alum sludge, (2) clarifier sludge, and (3) digested biosludge, which is the aerobically digested clarifier sludge. A coal liquefaction solid waste (vacuum bottoms) was

assayed to provide a comparison with mutagenic activity displayed by the wastewater treatment effluents.

**Sample Preparation. A. Vacuum Bottoms (Samples 1936 and 2277).** Approximately 20 mg of the solid material was suspended in 20 mL of dimethyl sulfoxide ( $\text{Me}_2\text{SO}$ ) by stirring for 24 h. All of the solid material went into suspension. The extract was sterilized by autoclaving at 121 °C for 5 min.

A serial organic extraction protocol, described by Warshawsky et al. (10) in which solid residuals are extracted by using increasingly polar solvents (hexane, toluene, methylene chloride, and acetonitrile) was utilized. Resulting extracts were taken to dryness by evaporation under nitrogen, weighed, and suspended in  $\text{Me}_2\text{SO}$ . The remaining insoluble residue was also suspended in  $\text{Me}_2\text{SO}$ .

**B. Alum, Clarifier, and Digested Biosludge (Samples 1937, 1938, and 2278–2280).** The sludges were filtered to separate the liquid and solid phases. Subsequent mutagenicity tests were conducted on the filtrate. Because the test results of the filtrate samples were negative, in later tests the whole sample was sterilized, as previously described, and agitated prior to dispensing in order to obtain a uniform distribution of solids in the aliquot used for testing.

**Mutagenicity Testing.** Whole sludges, a  $\text{Me}_2\text{SO}$  suspension of the vacuum bottoms, and organic solvent extract fractions plus the residue remaining after serial solvent extractions were tested for mutagenicity by the plate incorporation method as described by Ames et al. (12) using bacterial tester strains supplied by B. N. Ames, Department of Biochemistry, University of California at Berkeley. The whole sludges (aqueous and solid fractions) were tested at increasing volumes from 5 to 1000  $\mu\text{L}$ . Solvent extracts were assayed over a 3 log (concentration) range up to the limit imposed by toxicity of the sample to the tester strains.

The whole samples were tested, with and without Arachlor 1254 induced rat liver microsomes mixtures (S9) in five tester strains (*Salmonella typhimurium* TA98, TA100, TA1535, TA1537, and TA1538). In the mutagenicity assays of the whole materials, which were the first series to be run, tester strain TA1535 with and without S9 and TA1535 with S9 did not yield positive results when exposed to the highly mutagenic vacuum bottoms. Consequently, only the remaining strains (TA98, TA100, and TA1538) were used with the test employing microsomal activation. In addition, since all Ames tests conducted without microsomal activation were negative, such testing was discontinued.

Positive mutagen control tests were conducted to confirm viability and dose-response relationships of the tester

Table II. Mutagenicity Assay Test Results: Dose ( $\mu\text{g}$ ),<sup>f</sup> Revertants ( $\text{his}^+$ )<sup>g</sup> per Plate (rev/pl) and Mutagenicity Ratio (MR)<sup>h</sup> for Tester Strains

test materials	TA98 (+S9)			TA100 (+S9)			TA1538 (+S9)		
	$\mu\text{g}$	rev/pl	MR	$\mu\text{g}$	rev/pl	MR	$\mu\text{g}$	rev/pl	MR
1936 vacuum bottoms <sup>a</sup>									
whole	250	750	13.2	150	355	2.4	250	250	5.4
hexane fraction	75	945	16.6	75	462	3.1	75	497	10.8
toluene fraction	500	2245	39.4	100	555	3.7	75	617	13.4
methylene chloride fraction	250	680	13.6	250	336	2.5	250	345	7.5
acetonitrile fraction	75	1455	25.5	150	540	3.0	150	442	9.6
residue	100	145	2.5				250	114	2.5
2277 vacuum bottoms <sup>b</sup>									
whole	100	1137	21.4	- <sup>i</sup>	-	-	100	337	7.7
hexane fraction	150	484	15.6	-	-	-	100	169	5.3
toluene fraction	100	1361	44.0	-	-	-	100	292	9.1
methylene chloride fraction	100	705	13.8	-	-	-	100	304	8.7
acetonitrile fraction	75	1015	19.9	-	-	-	100	921	23.0
residue	100	122	2.0	-	-	-	-	-	-
2280 alum sludge <sup>b</sup>									
whole	10 <sup>c</sup>	175	3.0	-	-	-	-	-	-
hexane fraction	-	-	-	-	-	-	-	-	-
toluene fraction	-	-	-	-	-	-	-	-	-
methylene chloride fraction	100	296	5.1	-	-	-	75	109	2.2
acetonitrile fraction	100	200	4.5	-	-	-	50	111	2.2
residue	-	-	-	-	-	-	250	118	3.1
1937 clarifier sludge <sup>d</sup>									
whole	75 <sup>c</sup>	333	5.8	-	-	-	75 <sup>c</sup>	265	5.8
hexane fraction	75	150	3.9	-	-	-	-	-	-
toluene fraction	75	150	3.9	-	-	-	250	235	5.6
methylene chloride fraction	100	190	5.0	-	-	-	75	316	7.5
acetonitrile fraction	75	1180	31.0	-	-	-	75	315	7.5
residue	-	-	-	-	-	-	-	-	-
2278 clarifier sludge <sup>b</sup>									
whole	100 <sup>c</sup>	151	3.8	-	-	-	-	-	-
hexane fraction	-	-	-	-	-	-	-	-	-
toluene fraction	-	-	-	-	-	-	-	-	-
methylene chloride fraction	50	102	2.4	-	-	-	-	-	-
acetonitrile fraction	-	-	-	-	-	-	75	66	2.1
residue	-	-	-	-	-	-	250	165	5.3
1938 digester sludge <sup>d</sup>									
whole	500 <sup>c</sup>	296	6.2	1000 <sup>c</sup>	300	2.4	400 <sup>c</sup>	105	3.1
hexane fraction	250	113	2.6	-	-	-	-	-	-
toluene fraction	100	147	2.8	-	-	-	75	80	2.4
methylene chloride fraction	-	-	-	-	-	-	100	101	3.0
acetonitrile fraction	-	-	-	-	-	-	-	-	-
residue	-	-	-	-	-	-	250	128	3.8
2279 digester sludge <sup>b</sup>									
whole	50 <sup>c</sup>	104	2.8	-	-	-	-	-	-
hexane fraction	-	-	-	-	-	-	-	-	-
toluene fraction	25	125	2.4	-	-	-	-	-	-
methylene chloride fraction	75	109	2.5	-	-	-	100	107	3.4
acetonitrile fraction	-	-	-	-	-	-	-	-	-
residue	250	112	2.5	-	-	-	-	-	-

control  $\bar{X} \pm \text{std dev}^d$   
 no. of plates (N)<sup>e</sup>

	TA98(+S9)	TA100(+S9)	TA1538(+S9)
$\bar{X} \pm \text{std dev}^d$	46 $\pm$ 16	149 $\pm$ 39	39 $\pm$ 14
no. of plates (N) <sup>e</sup>	41	24	33

<sup>a</sup> First sample lot. <sup>b</sup> Second sample lot. <sup>c</sup> Whole sludge dose in  $\mu\text{L}$  (mg). <sup>d</sup>  $\bar{X} \pm \text{sd}$ , grand mean and standard deviation of spontaneous revertants on control plates rounded to nearest integer. <sup>e</sup> N: number of control plates for all bioassays. <sup>f</sup> Dose (in  $\mu\text{L}$  for whole sludge samples,  $\mu\text{g}$  for all others) at which the highest number of revertants were observed. <sup>g</sup> Number of histidine<sup>+</sup> revertants counted on each plate. <sup>h</sup> Mutagenicity ratio (MR) = revertants on test plates (spontaneous + induced revertants)/revertants on negative control plates (spontaneous revertants). <sup>i</sup> (-) is a negative result.

strains. A single plate-four spot method was developed in which a negative control and three concentrations of diffusible positive chemical mutagens were spot-tested on one plate. Positive chemical mutagens used for reversion confirmation included the following: daunomycin for TA98, N-methyl-N'-nitro-N-nitrosoguanidine (MNNG) for TA100 and TA1535, and 9-aminoacridine for TA1537, all without microsomal activation; 2-aminofluorene validated TA98, TA100, and TA1538, all with S9 microsomes added. Titrations determining optimum volume of liver supernatant added to the S9 mix (0.1 mL of liver supernatant/mL of cofactors) were run on each fresh batch of

microsomes by using tester strain TA98 with 2-aminofluorene as the positive mutagen. Routine sterility and toxicity checks were also run by using tester strain TA1537. Deviations from the original Ames method (12) for performing mutagenicity assays included (a) revertant counts after 48- and 72-h incubation periods instead of 48 h only, (b) 30-min preincubation in a water bath at 37 °C where microsomal activation was included, (c) the order of addition for plate assay by using the preincubation procedure was altered to 0.5 mL of sterile double-distilled (DD) water, aliquot of test sample, tester strain, and 0.5 mL of S9 mix, and after preincubation, 2.5 mL (instead



Table III. Specific Mutagenicity of Tested Coal Conversion Residuals and Wastewater Treatment Sludges

test sample	sample no.	organic solvent extract fractions											
		whole		hexane		toluene		methylene chloride		acetonitrile		residue	
		rev/mg <sup>a</sup>	r <sup>d</sup>	rev/mg	r	rev/mg	r	rev/mg	r	rev/mg	r	rev/mg	r
vacuum bottoms	1936	2875 <sup>a</sup>	0.963	11600	0.971	3695	0.956	2365	0.974	20330	0.918	560	0.828
	2277	11095 <sup>a</sup>	0.985	2567	0.881	12200	0.982	5552	0.931	9578	0.866	-	-
alum sludge	NS <sup>c</sup>												
	2280	7705	0.678	- <sup>b</sup>	-	-	-	1987	0.916	1295	0.959	-	-
clarifier sludge	1937	4.050	0.987	1268	0.918	1290	0.880	1349	0.965	14720	0.994	-	-
	2278	0.932	0.912	-	-	-	-	960	0.721	-	-	-	-
digester sludge	1938	0.530	0.985	236	0.873	984	0.978	-	-	-	-	-	-
	2279	1.273	0.911	-	-	2803	0.980	868	0.999	-	-	247	0.792

<sup>a</sup> Weight of 1 mg = 1  $\mu$ L of sludge (aqueous & solid phases). <sup>b</sup> (-) negative result in the Ames bioassay. <sup>c</sup> NS No sample available in this lot. <sup>d</sup> r: correlation coefficient of a linear regression of the portion of the dose-response curve before toxicity to the tester strain is exhibited.

of 2.0 mL) of molten top agar was added prior to pouring.

### Results and Discussion

Criteria used by Ames et al. (12) to define a positive result in the bioassay for mutagenic activity include (a) 2-fold or greater increase in the number of revertants exposed to the test material over spontaneous reversion rates, (b) for compounds of low mutagenicity, a reproducible dose-response relationship, and (c) repeatability, added by Epler (13), i.e., a confirmation of the positive result by running the test again after a 2-week period as a requirement.

Bioassays were conducted on the whole materials with and without microsomal activation. Test results were uniformly negative where microsomal activation was not included in the test protocol. This agrees with reports by Epler et al. (9), Warshawsky et al. (10), Rao et al. (14), and Schoeny et al. (11) of tests on coal conversion products and residues. All subsequent tests of the organic solvent extract fractions and the second lot of samples (2277-2280) included microsomal activation.

In all previously reported mutagenicity testing of coal conversion and combustion products using the Ames technique, the most sensitive tester strain, i.e., that showing the greatest number of histidine revertants over a spontaneous reversion rate, has been the R-plasmid carrying strain TA98 with S9. Test results for all seven materials and their fractions displayed in Table II confirm this phenomenon. In one test, tester strain TA1538 with S9 indicated a marginal positive result while the TA98 with S9 was negative. This result may be due to variability in the materials being fractionated. The highest levels of mutagenic activity found in the tested substances and their organic solvent fractions are consistently represented by the TA98 with S9 results. Table II tabulates the highest number of revertants counted, the dose at which this occurred, and the mutagenicity ratio (highest number of revertants divided by the number of spontaneous per plate) of each tested material.

Table III lists the specific mutagenic activity (revertants/milligram, rev/mg) for each of the whole test materials and their organic solvent extract fractions when TA98 with S9 was used as the indicator organism. Regression analyses were employed to determine the specific mutagenic activity; only the nontoxic portion of the dose-response curves was included in the calculations.

Mutagenicity tests on the filtrate of the sludges yielded negative results, both in the presence and absence of microsomal activation. This may be due to extremely low (below the sensitivity level of the Ames test) concentrations of mutagenic constituents in the aqueous fraction of the

sludge. Low solubility of the mutagenic compounds in water may account for the low concentration. Mutagenic polycyclic aromatic hydrocarbons and aromatic amines may be present in the sludges in the form of strongly bonded adsorbed particles on the solids fractions.

The results obtained when assaying the whole sludges must be converted to gravimetric units in order to compare specific mutagenicity of each of the tested materials. Specific gravity of the sludge is assumed to be equal to that of the water. The effect of any error in this assumption would be negligible due to the very low proportion of solids in the sludges, i.e., 0.58% for the clarifier sludge and 0.134% for the digester sludge. Consequently, the weight of 1  $\mu$ L of sludge is considered to be 1 mg.

When compared the specific mutagenicity of the three whole samples in the first lot shows the vacuum bottoms (1936) to be almost 700 times that of the clarifier sludge (1937), 2875:4.05 rev/mg, and 5600 times greater than the digester sludge (1938), 2875:0.53 rev/mg.

Mutagenicity of the clarifier sludge (1937) was approximately 8 times that of the digester sludge (1938), 4.05:0.53 rev/mg.

The second sample lot shows a different trend. In this case the digester sludge (2279) displayed a higher mutagenic activity than the clarifier sludge (2278), 1.273:0.932 rev/mg. Mutagenicity ratio of the second digester sludge was a 2.8 as compared to a 6.2-fold increase in gross revertants over background.

The second set of sludge samples (2278-2280) appear to have a significantly different mutagenic character. The first clarifier sludge tested (1937, 4.050 rev/mg) exhibited 4 times greater mutagenic activity than the second set sample (2278, 0.932 rev/mg). Mutagenicity characteristics show an opposite situation when comparing the digester sludges in the two sample sets, with the second sample exhibiting the higher specific mutagenic activity, 1.273 (2279) to 0.530 (1938) rev/mg.

A comparison of the change in mutagenic activity displayed by the various organic solvent extract fractions of the fresh (clarifier) and aged (digested) sludge is of interest. Figure 2 shows, in graphic form, the mutagenicity assay results for four organic solvent fractions and the residue of the first sample group sludges (1937 and 1938). Results for whole material tests are also shown. Toluene fractions extracted from clarifier and digester sludges show almost no reduction (no change in the slope of the curves) in mutagenic activity. Hexane fractions show some reduction, but the digested sludge still exhibits a positive Ames bioassay. The acetonitrile and methylene chloride fractions were reduced sufficiently in mutagenicity to display a negative response in the digested sludge solids. This is

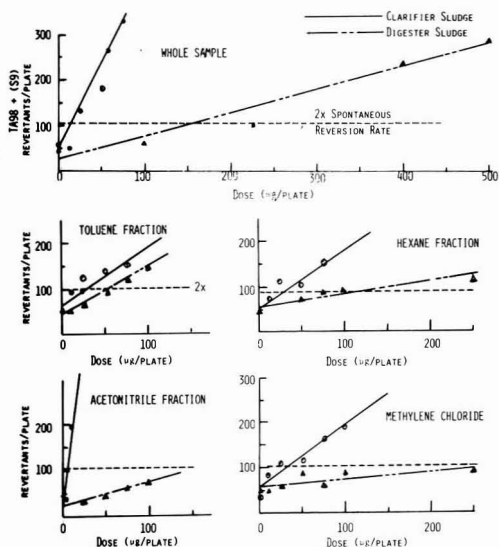


Figure 2. Comparative mutagenicity of clarifier and digester sludges and their organic solvent fractions.

in keeping with theoretical expectations, as set forth by Chambers et al. (15), that PAHs present in the methylene chloride and acetonitrile extract fractions are amenable to oxidative metabolism. The toluene fraction and the hexane extract are not transformed to the same extent.

There is a critical lack of data on residuals regarding factors affecting their composition, namely, (a) extent of oil removal from wastewater prior to treatment, i.e., there may or may not be oil removal by gravity separation, (b) feedstock coal identification and conversion process parameters, (c) relationship between the clarifier and digester sludge in a temporal sense, and (d) whether sludges come from the same test run of the hydrogenator and waste treatment plant. For this reason it is not possible to arrive, with any degree of confidence, at conclusions regarding comparative mutagenicity of the clarifier and digester sludges. What is evident is that potential mutagenicity of the wastes is highly dependent on the type of coal converted (bituminous or lignite) and conversion process (gasification or liquefaction) utilized.

Vacuum bottoms in both sample sets display considerable mutagenic activity (2875 and 11 095 rev/mg). Higher concentrations of polycyclic aromatic hydrocarbon compounds in the second sample lot, which were solubilized in the toluene fraction, might account for higher mutagenic activity of that sample 2277. Lower ash content also may have had some influence on this result.

#### Literature Cited

- (1) Rogashewski, P. J.; Koester, P. A.; Koralek, C. S.; Wetzel, P. S.; Shields, K. J. U.S. EPA Pub. No. EPA-600/7-78-091, 1978.
- (2) Budden, K. T.; Zieger, W. H. U.S. EPA Pub. No. EPA-600/7-78-019, 1978.
- (3) Braunstein, H. M. In "Environmental, Health and Control Aspects of Coal Conversion: An Informational Overview"; Braunstein, H. M., Copenhauer, E. D., Pfuender, H. A., Eds.; ORNL Pub. No. ORNL/EIS-94, Oak Ridge, TN, 1977.
- (4) Pelroy, R. A.; Cresto, J. T.; Peterson, M. R. Pacific Northwest Laboratory Pub. No. PNL-3189, Richland, WA, 1979.
- (5) U.S. DOE, "Solvent Refined Coal-II Demonstration Project at Fort Martin, West Virginia: Final Environmental Impact Statement"; U.S. DOE Pub. No. EIS-0069, 1981.
- (6) Epler, J. L.; Larimer, F. W.; Rao, T. K.; Nix, C. E.; Ho, T. *EHP, Environ. Health Perspect.* 1978, 27, 11-20.
- (7) Brand, J. I.; Klein, J. A.; Parkhurst, B. R.; Rao, T. K. 35th Annual Purdue Industrial Waste Conference, West Lafayette, IN, May 13-15, 1980.
- (8) Gehrs, C. W. ORNL Pub. No. ORNL-ESD-1194, 1977.
- (9) Epler, J. L.; Young, J. A.; Hardigree, A. A.; Rao, T. K.; Guerin, M. R.; Rubin, I. B.; Ho, T.; Clark, B. R. *Mutat. Res.* 1978, 57, 265-276.
- (10) Warshawsky, D.; Schoeny, R.; Hollingsworth, L.; Hund, M.; Moore, G. T. 20th Hanford Life Sciences Symposium, Richland, WA, October 19-23, 1980.
- (11) Schoeny, R.; Warshawsky, D.; Hollingsworth, L.; Hund, M.; Moore, G. T. *Environ. Mutagen.* 1981, 3, 181-195.
- (12) Ames, B. N.; McCann, J.; Yamasaki, E. *Mutat. Res.* 1975, 31, 347-363.
- (13) Epler, J. L.; Larimer, F. W.; Rao, T. K.; Burnett, E. M.; Griest, W. H. U.S. EPA Pub. No. EPA-600/2-80-057, 1980.
- (14) Rao, T. K.; Young, J. A.; Hardigree, A. A.; Winton, W.; Epler, J. A. *Mutat. Res.* 1978, 54, 185-191.
- (15) Chambers, C. W.; Tabak, H. H.; Kabler, P. W. *J. Water Pollut. Control Fed.* 1963, 35, 1517-1528.
- (16) Perussel, R., private communication, 1980.

Received for review November 5, 1981. Revised manuscript received May 21, 1982. Accepted July 19, 1982. This research was supported by DOE Contract No. DE AC22 80PC30337.

## ADDITIONS AND CORRECTIONS

1982, Volume 16

Michael A. Ribick,\* George R. Dubay, Jimmie D. Petty, David L. Stalling, and Christopher J. Schmitt: Toxaphene Residues in Fish: Identification, Quantification, and Confirmation at Part per Billion Levels.

Page 310. The second paragraph should conclude as follows: Bidleman et al. (10) found up to 0.13 ng/m<sup>3</sup> in air samples from Canadian Northwest Territories, and Munson (11) found up to 0.28 µg/L in Maryland rainwater.

Page 317. Reference 9 should read as follows: (9) Bidleman, T. F.; Olney, C. E. *Nature (London)* 1975, 257, 475.

# At Last!

## Research Results of Organometallic Chemistry at an Affordable Price!

# INTRODUCING

# ORGANOMETALLICS

**Edited By  
Dr. Dietmar Seyferth**

**PREMIERE ISSUE  
JANUARY 1982**

The American Chemical Society recognized a need for a definitive, international journal of organometallic chemistry – a quality journal to draw together the work of scientists worldwide and consolidate the literature in this highly active research field. A definitive, quality, international journal – that won't break your budget.

The new journal's name? **ORGANOMETALLICS.**

Edited by Dr. Dietmar Seyferth, **ORGANOMETALLICS** is for organic chemists, inorganic chemists, polymer chemists – all scientists needing the most current re-

search in organometallic chemistry.

Monthly issues will bring you Articles . . . Communications . . . and occasional reviews in all aspects of organometallic chemistry, including synthesis, structure and bonding, chemical reactivity and reaction mechanisms, and applica-

tions. And all at a fraction of the price you'd pay for comparable journals in this field.

So don't delay! Make sure your subscription starts with the very first issue of **ORGANOMETALLICS.** Use the coupon below or call **TOLL FREE (800) 424-6747** to enter your subscription today!

American Chemical Society

1155 Sixteenth Street, N.W. Washington, D.C. 20036 U.S.A.

Yes, please enter my introductory subscription to **ORGANOMETALLICS**, to begin publication January 1982, at the rate checked below:

	U.S.	Foreign Surface Postage Included	Foreign Air Freight Included
ACS Members	<input type="checkbox"/> \$ 20.00	<input type="checkbox"/> \$ 36.00	<input type="checkbox"/> \$ 84.00
ACS Student Members	<input type="checkbox"/> \$ 15.00	<input type="checkbox"/> \$ 31.00	<input type="checkbox"/> \$ 79.00
Nonmembers	<input type="checkbox"/> \$150.00	<input type="checkbox"/> \$166.00	<input type="checkbox"/> \$214.00

Payment enclosed. (Payable to American Chemical Society.)

Bill me  Bill company

Charge my  MasterCard  VISA

Card No. \_\_\_\_\_

Interbank No. \_\_\_\_\_ Expires \_\_\_\_\_  
(MasterCard only)

Signature \_\_\_\_\_

Name \_\_\_\_\_

Organization \_\_\_\_\_

Title \_\_\_\_\_

Home \_\_\_\_\_

Address  Business \_\_\_\_\_

City \_\_\_\_\_

State/Country \_\_\_\_\_ ZIP \_\_\_\_\_

Journal subscriptions start January 1982. Subscriptions at ACS member rates are for personal use only. Foreign payment must be made in U.S. currency, by international money order, UNESCO coupons, U.S. bank draft, or order through your subscription agency. Please allow 60 days for your first copy to be mailed.

1625T

WE LOOK TO THE FUTURE

## Biogas. AgipGiza is the company that transforms ecology into energy

**B**iomass, originally formed in nature by virtue of the capacity of vegetable organisms to store solar energy in the form of organic carbon, is an important source of renew-



able energy. "Derived" biomass, AgipGiza's principal sector of activity, is constituted of waste and by-products of agricultural, industrial and urban origin. The problems of ecological disposal to which these residues give rise, have been solved optimally with the use of purification plants that make it possible to

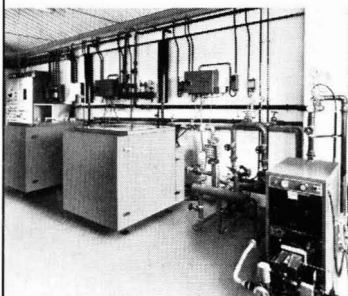
transform the cost of antipollution treat-

ment into the benefit of the production of biogas with a high energy content (70 percent methane). These installations use the process of anaerobic digestion, based on the action of special microorganisms which, in the absence of oxygen, transform into gas the organic substance contained in the waste. AgipGiza, a company owned jointly, in parity, by AgipNucleare and Giza Gi&Gi, was

set up for the purpose of designing, constructing and marketing plants, in Italy and abroad, for the anaerobic digestion of biomass.

AgipGiza's technology (which draws upon the process and microbiological experiments developed at the Eni research

laboratories) makes it possible to produce highly reliable and versatile installations which ensure high production yields. Thanks to the flexibility of the systems and processes utilized, AgipGiza is currently in a position to treat biomass of various origin:  urban sewage  effluents from food and tanning processes  manure from hog, cattle, sheep and bird breeding farms.



The company is constantly engaged in research and development work on new bioengineering solutions for broadening its areas of activity and making it possible to recover further valuable resources.

AgipGiza S.p.A.  
42100 Reggio Emilia  
Via Schwerin, 4  
Tel.: (0522) 45841  
Telex: 530034 Giza I



# AgipGiza

ENI Group

AgipNucleare Strategy for Energy Alternatives

CIRCLE 1 ON READER SERVICE CARD